INTERACTIONS BETWEEN OZONE POLLUTION AND FOREST ECOSYSTEMS

EDITED BY: Elena Paoletti, Silvano Fares and Zhaozhong Feng
PUBLISHED IN: Frontiers in Forests and Global Change

frontiers Research Topics

ISSN 1664-8714
ISBN 978-2-88966-603-4
DOI 10.3389/978-2-88966-603-4

About Frontiers

Frontiers is more than just an open-access publisher of scholarly articles: it is a pioneering approach to the world of academia, radically improving the way scholarly research is managed. The grand vision of Frontiers is a world where all people have an equal opportunity to seek, share and generate knowledge. Frontiers provides immediate and permanent online open access to all its publications, but this alone is not enough to realize our grand goals.

Frontiers Journal Series

The Frontiers Journal Series is a multi-tier and interdisciplinary set of open-access, online journals, promising a paradigm shift from the current review, selection and dissemination processes in academic publishing. All Frontiers journals are driven by researchers for researchers; therefore, they constitute a service to the scholarly community. At the same time, the Frontiers Journal Series operates on a revolutionary invention, the tiered publishing system, initially addressing specific communities of scholars, and gradually climbing up to broader public understanding, thus serving the interests of the lay society, too.

Dedication to Quality

Each Frontiers article is a landmark of the highest quality, thanks to genuinely collaborative interactions between authors and review editors, who include some of the world's best academicians. Research must be certified by peers before entering a stream of knowledge that may eventually reach the public - and shape society; therefore, Frontiers only applies the most rigorous and unbiased reviews.
Frontiers revolutionizes research publishing by freely delivering the most outstanding research, evaluated with no bias from both the academic and social point of view. By applying the most advanced information technologies, Frontiers is catapulting scholarly publishing into a new generation.

What are Frontiers Research Topics?

Frontiers Research Topics are very popular trademarks of the Frontiers Journals Series: they are collections of at least ten articles, all centered on a particular subject. With their unique mix of varied contributions from Original Research to Review Articles, Frontiers Research Topics unify the most influential researchers, the latest key findings and historical advances in a hot research area! Find out more on how to host your own Frontiers Research Topic or contribute to one as an author by contacting the Frontiers Editorial Office: frontiersin.org/about/contact

INTERACTIONS BETWEEN OZONE POLLUTION AND FOREST ECOSYSTEMS

Topic Editors:
Elena Paoletti, National Research Council (CNR), Italy
Silvano Fares, National Research Council (CNR), Italy
Zhaozhong Feng, Research Center for Eco-environmental Sciences (CAS), China

Citation: Paoletti, E., Fares, S., Feng, Z., eds. (2021). Interactions Between Ozone Pollution and Forest Ecosystems. Lausanne: Frontiers Media SA.
doi: 10.3389/978-2-88966-603-4

Table of Contents

frontiers
in Forests and Global Change

EDITORIAL
published: 11 February 2021
doi: 10.3389/ffgc.2020.604466

Editorial: Interactions Between Ozone Pollution and Forest Ecosystems

Elena Paoletti[1]*, Zhaozhong Feng[2], Silvano Fares[3], Pierre Sicard[4], Evgenios Agathokleous[2] and Alessandra De Marco[5]

[1] IRET-CNR, Sesto Fiorentino Firenze, Italy, [2] Key Laboratory of Agrometeorology of Jiangsu Province, Institute of Ecology, School of Applied Meteorology, Nanjing University of Information Science & Technology (NUIST), Nanjing, China, [3] National Research Council (CNR), Institute of BioEconomy (IBE), Rome, Italy, [4] ARGANS, Sophia Antipolis, France, [5] ENEA, CR Casaccia, Sustainability Department, Rome, Italy

Keywords: tropospheric O_3, forests, conference proceedings, editorial, special topic

Editorial on the Research Topic

Interactions between Ozone Pollution and Forest Ecosystems

OPEN ACCESS

Edited and reviewed by:
Jörg-Peter Schnitzler,
Helmholtz Zentrum
München, Germany

****Correspondence:***
Elena Paoletti
elena.paoletti@cnr.it

Specialty section:
This article was submitted to Forests and the Atmosphere, a section of the journal Frontiers in Forests and Global Change

Received: *09 September 2020*
Accepted: *28 September 2020*
Published: *11 February 2021*

Citation:
Paoletti E, Feng Z, Fares S, Sicard P, Agathokleous E and De Marco A (2021) Editorial: Interactions Between Ozone Pollution and Forest Ecosystems.
Front. For. Glob. Change 3:604466.
doi: 10.3389/ffgc.2020.604466

INTRODUCTION

Forests are a key element of landscape, carbon sink, biodiversity conservation, and human well-being. The major air pollutant nowadays affecting forest health and biodiversity worldwide is tropospheric ozone (O_3) (Li et al., 2017; Feng et al., 2019; Agathokleous et al., 2020). Progress has been achieved by controlling the emission of O_3 precursors in some areas of the world (Sicard et al., 2013; Paoletti et al., 2014). However, O_3 levels still reach potentially phytotoxic thresholds in many areas (Mills et al., 2018a; Sicard et al., 2020). Major gaps of knowledge in our understanding of O_3 and forest interactions exist. In particular, risk assessment, multifactorial responses, detoxification mechanisms, and the role of forest vegetation in cleaning urban air require further investigation (Paoletti et al., 2020).

This Research Topic of *Frontiers in Forests and Global Change*, Interactions between Ozone Pollution and Forest Ecosystems, presents eight original research articles that span the field of O_3 research on forests and give new insights based on novel results, thus providing a basis for further studies and potential reduction of the severity of O_3 impacts on forests.

Hoshika et al. developed stomatal-flux and exposure-based critical levels for O_3 risk assessment of biomass losses in two larch species (*Larix*), a genus of high forest value. They found that the critical levels for the larches were smaller than those for other forest tree species, suggesting a relatively high susceptibility of these larches. This research also revealed that the use of stomatal fluxes as the metric of dose resulted in no species-specific differences that were found using an exposure-based metric. Protection of forest productivity from negative impacts of O_3 requires species-specific critical levels that may be based on either O_3 concentrations or stomatal uptake accumulation over the growing season (Moura et al., 2018). Even though O_3 concentrations are more easily available, stomatal uptake, more biologically meaningful, is recommended in spite of the more complex calculation (Emberson et al., 2000; Paoletti and Manning, 2007). Stomatal-flux risk assessment may be carried out at different scales, e.g., leaf (Shang et al., 2017), ecosystem (Fares et al., 2013; Hoshika et al., 2017), regional (Anav et al., 2016; De Marco et al., 2020), or global (Mills et al., 2018b). Savi et al. investigated the relationship between stomatal O_3 fluxes and net ecosystem productivity (NEP), measured directly at the ecosystem level in a network of forest experimental sites with the eddy covariance technique, by the means of artificial neural networks. The analysis highlighted that O_3 effects over NEP are highly non-linear and site-specific. By isolating O_3 effects from other covarying environmental factors, negative effect on NEP were found in the order of 1 percent. These low but significant effects were correlated with meteorological variables showing that O_3 damage depends on weather conditions.

For a proper risk assessment, it is important to evaluate all environmental factors that may affect the ecosystem responses to O_3, such as nutrient (Zhang et al., 2018) and water availability (Hoshika et al., 2018). Hunová et al. evaluated O_3 concentrations, ambient NOx concentrations and meteorology in Czech mountain forests over the period 1992–2018. They found that both meteorology and air pollution are highly important in affecting day-to-day variability in O_3 concentrations in Czech forests. They applied a generalized additive model with semiparametric (penalized-spline-based) components to properly capture the non-linear responses that are typical of O_3 studies (Agathokleous et al., 2019) and are not captured by traditional linear regression approaches. Overall, there is an urgent need of using sophisticated statistical approaches for untangling the effects of O_3 from those of the co-occurring environmental factors. Multifactorial experiments will help to clarify the contribution of each factor. Sugai et al. investigated O_3 responses of larch in combination with soil salinization, an interaction that represents a potential concern for vegetation in many coastal areas (Calzone et al., 2019), and found that the responses were additive and did not exhibit significant interactive effects. Such additive responses are common in experiments where elevated O_3 is combined with other factors (e.g., Carriero et al., 2016; Yuan et al., 2017), and their identification and understanding may help developing a conceptual model of plant response to O_3 in a multi-factorial world.

Integrating plant detoxification processes into O_3 risk assessment is still a major challenge for O_3 research. Dusart et al. reviewed the great diversity of antioxidative systems, scattered in different cellular compartments, that are involved in foliar responses to O_3, in particular the Halliwell Asada Foyer cycle and phenolic compounds in cell wall, vacuole and chloroplasts. They pointed out that a better understanding of subcellular localization and transport would allow a more precise identification of the respective contribution of each compartment to the foliar defense system, and recommended more detoxification modeling efforts, similar to Tuzet et al. (2011).

The relevance of urban forests for human well-being and other services is continuously rising, and the selection of plant species that may improve air quality is thus of great interest (Samson et al., 2019). Plants may uptake Volatile Organic Compounds (VOC) emitted by anthropogenic activities. Araya et al. found several anthropogenic VOCs (e.g., toluene, styrene, xylenes, naphthalene, benzenes, and trichloroethene) in the leaves of two tree species in Santiago city (Chile), and *Liriodendron tulipifera* was more efficient than *Platanus* × *acerifolia* in the O_3 uptake. However, plants may also emit biogenic VOCs, e.g., isoprene and monoterpenes, which affect air quality and may contribute to O_3 formation (Sicard et al., 2018). Fitzky et al. reviewed the interplay of O_3 and urban vegetation shedding light on the complex photochemistry leading to O_3 production. BVOCs emitted by vegetation can be considered O_3 precursors especially in presence of anthropogenically emitted NO_X. The authors highlight differences along the rural-urban gradient affecting tropospheric O_3 concentrations. Grote et al. developed a new modeling approach for estimating abiotic and biotic stress-induced *de novo* emissions of BVOCs from plants. A function is proposed that describes the production of all stress-induced biogenic VOCs and scales with stress intensity. It is hypothesized that the response delay and the form of the function are specific for the production pathway and valid for stress induced by O_3 as well as wounding (herbivory). These results will help including biogenic VOC responses to stressors into modeling.

These articles were presented at the 2nd International Conference on "Ozone and Plant Ecosystems" that was held in Florence (Italy) in 2018. The next conference of this series was planned in 2020 but was postponed to May 2021 due to the COVID-19 pandemic (https://cyprus2021.com/). Interestingly, the lockdown following the pandemic resulted in a drastic improvement of the air quality, especially nitrogen dioxide (NO_2) levels, in many world areas (Zhang et al., 2020), while O_3 levels tended to increase in the cities (Sicard et al., 2020). Ozone is a unique air pollutant due to its high reactivity and the fact that is formed by reactions of precursors, including NO_2. This is why controlling O_3 pollution has resulted to be a serious challenge and justify why more research is still needed about the Interactions between Ozone Pollution and Forest Ecosystems.

AUTHOR CONTRIBUTIONS

EP, ZF, SF, PS, EA, and AD contributed to writing this Editorial of the Research Topic on Interactions between Ozone Pollution and Forest Ecosystems that they edited in 2019–2020. All authors contributed to the article and approved the submitted version.

FUNDING

This work was supported by the projects MOTTLES (LIFE15 ENV/IT/000183) and MITIMPACT (ALCOTRA 2016–2020).

REFERENCES

Agathokleous, E., Belz, R. G., Calatayud, V., De Marco, A., Hoshika, Y., Kitao, M., et al. (2019). Predicting the effect of ozone on vegetation via the linear non-threshold (LNT), threshold and hormetic dose-response models. *Sci. Total Environ.* 649, 61–74. doi: 10.1016/j.scitotenv.2018.08.264

Agathokleous, E., Feng, Z., Oksanen, E., Sicard, P., Wang, P., Saitanis, C. J., et al. (2020). Ozone affects plant, insect and soil microbial communities: a threat to terrestrial ecosystems and biodiversity. *Sci. Adv.* 6: eabc1176. doi: 10.1126/sciadv.abc1176

Anav, A., De Marco, A., Proietti, C., Alessandri, A., Dell'Aquila, A., Cionni, I., et al. (2016). Comparing concentration-based (AOT40) and stomatal uptake (PODy) metrics for ozone risk assessment to European forests. *Glob. Chang. Biol.* 22, 1608–1627. doi: 10.1111/gcb.13138

Calzone, A., Podda, A., Lorenzini, G., Maserti, B. E., Carrari, E., Deleanu, E., et al. (2019). Cross-talk between physiological and biochemical adjustments by *Punica granatum* cv. Dente di cavallo mitigates the effects of salinity and ozone stress. *Sci. Total Environ.* 656, 589–597. doi: 10.1016/j.scitotenv.2018.11.402

Carriero, G., Brunetti, C., Fares, S., Hayes, F., Hoshika, Y., Mills, G., et al. (2016). BVOC responses to realistic nitrogen fertilization and ozone exposure in silver birch. *Environ. Pollut.* 213, 988–995. doi: 10.1016/j.envpol.2015.12.047

De Marco, A., Anav, A., Sicard, P., Feng, Z., and Paoletti, E. (2020). High spatial resolution ozone risk assessment for Asian forests. *Environ. Res. Lett.* 15:104095. doi: 10.1088/1748-9326/abb501

Emberson, L. D., Ashmore, M. R., Cambridge, H. M., Simpson, D., and Tuovinen, J.-P. (2000). Modelling stomatal ozone flux across Europe. *Environmental Pollution* 109, 403–413. doi: 10.1016/S0269-7491(00)00043-9

Fares, S., Matteucci, G., Scarascia Mugnozza, G., Morani, A., Calfapietra, C., Salvatori, E., et al. (2013). Testing of models of stomatal ozone fluxes with field measurements in a mixed Mediterranean forest. *Atmos. Environ.* 67, 242–251. doi: 10.1016/j.atmosenv.2012.11.007

Feng, Z., De Marco, A., Anav, A., Gualtieri, M., Sicard, P., Tian, H., et al. (2019). Economic losses due to ozone impacts on human health, forest productivity and crop yield across China. *Environ. Int.* 131:104966. doi: 10.1016/j.envint.2019.104966

Hoshika, Y., Fares, S., Gruening, C., Goded, I., De Marco, A., Sicard, P., et al. (2017). Stomatal conductance models for ozone risk assessment at canopy level in two Mediterranean evergreen forests. *Agric. For. Meteorol.* 234, 212–221. doi: 10.1016/j.agrformet.2017.01.005

Hoshika, Y., Moura, B. B., and Paoletti, E. (2018). Ozone risk assessment in three oak species as affected by soil water availability. *Environ. Sci. Pollut. Res.* 25, 8125–8136. doi: 10.1007/s11356-017-9786-7

Li, P., Feng, Z., Catalayud, V., Yuan, X., Xu, Y., and Paoletti, E. (2017). A meta-analysis on growth, physiological, and biochemical responses of woody species to ground-level ozone highlights the role of plant functional types. *Plant Cell Environ.* 40, 2369–2380. doi: 10.1111/pce.13043

Mills, G., Pleijel, H., Malley, C. S., Sinha, B., Cooper, O. R., Schultz, M. G., et al. (2018a). Tropospheric Ozone Assessment Report: present-day tropospheric ozone distribution and trends relevant to vegetation. *Elementa Sci. Anthrop.* 6:47. doi: 10.1525/elementa.302

Mills, G., Sharps, K., Simpson, D., Pleijel, H., Broberg, M., Uddling, J., et al. (2018b).Ozone pollution will compromise efforts to increase global wheat production. *Glob. Chang. Biol.* 24, 3560–3574. doi: 10.1111/gcb.14157

Moura, B. B., Hoshika, Y., Ribeiro, R. V., and Paoletti, E. (2018). Exposure- and flux-based assessment of ozone risk in two sugarcane genotypes. *Atmos. Environ.* 176, 252–260. doi: 10.1016/j.atmosenv.2017.12.039

Paoletti, E., De Marco, A., Beddows, D. C. S., Harrison, R. M., and Manning, W. J. (2014). Ozone levels in European and USA cities are increasing more than at rural sites, while peak values are decreasing. *Environ. Pollut.* 192, 295–299. doi: 10.1016/j.envpol.2014.04.040

Paoletti, E., Feng, Z., De Marco, A., Hoshika, Y., Harmens, H., Agathokleous, E., et al. (2020). Challenges, gaps and opportunities in investigating the interactions of ozone pollution and plant ecosystems. *Sci. Total Environ.* 709:136188. doi: 10.1016/j.scitotenv.2019.136188

Paoletti, E., and Manning, W. J. (2007). Toward a biologically significant and usable standard for ozone that will also protect plants. *Environ. Pollut.* 150, 85–95. doi: 10.1016/j.envpol.2007.06.037

Samson, R., Moretti, M., Amorim, J. U., Branquinho, C., Fares, S., Morelli, F., et al. (2019). Towards an integrative approach to evaluate the environmental ecosystem services provided by urban forests. *J. For. Res.* 30, 1981–1996. doi: 10.1007/s11676-019-00916-x

Shang, B., Feng, Z. Z., Li, P., Yuan, X. Y., Xu, Y. S., and Calatayud, V. (2017). Ozone exposure- and flux-based response relationships with photosynthesis, leaf morphology and biomass in two poplar clones. *Sci. Total Enviro.* 603–604, 185–195. doi: 10.1016/j.scitotenv.2017.06.083

Sicard, P., Agathokleous, E., Araminiene, V., Carrari, E., Hoshika, Y., De Marco, A., et al. (2018). Should we see urban trees as effective solutions to reduce increasing ozone levels in cities? *Environ. Pollut.* 243, 163–176. doi: 10.1016/j.envpol.2018.08.049

Sicard, P., De Marco, A., Agathokleous, E., Feng, Z., Xu, X., Paoletti, E., et al. (2020). Amplified ozone pollution in cities during the COVID-19 lockdown. *Sci. Total Environ.* 735:139542. doi: 10.1016/j.scitotenv.2020.139542

Sicard, P., De Marco, A., Troussier, F., Renou, C., Vas, N., and Paoletti, E. (2013). Decrease in surface ozone concentrations at Mediterranean remote sites and increase in the cities. *Atmos. Environ.* 79, 705–715. doi: 10.1016/j.atmosenv.2013.07.042

Tuzet, A., Perrier, A., Loubet, B., and Cellier, P. (2011). Modelling ozone deposition fluxes: the relative roles of deposition and detoxification processes. *Agric. For. Meteorol.* 151, 480–492. doi: 10.1016/j.agrformet.2010.12.004

Yuan, X. Y., Shang, B., Xu, Y. S., Xin, Y., Tian, Y., Feng, Z. Z., et al. (2017). No significant interactions between nitrogen stimulation and ozone inhibition of isoprene emission in Cathay poplar. *Sci. Total Environ.* 601, 222–229.. doi: 10.1016/j.scitotenv.2017.05.138

Zhang, L., Hoshika, Y., Carrari, E., Badea, O., and Paoletti, E. (2018). Ozone risk assessment is affected by nutrient availability: evidence from a simulation experiment under free air controlled exposure (FACE). *Environ. Pollut.* 328, 812–822. doi: 10.1016/j.envpol.2018.03.102

Zhang, Z., Arshad, A., Zhang, C., Hussain, S., and Li, W. (2020). Unprecedented temporary reduction in global air pollution associated with COVID-19 forced confinement: a continental and city scale analysis. *Remote Sens.* 12:2420. doi: 10.3390/rs12152420

Conflict of Interest: The authors declare that the research was conducted in the absence of any commercial or financial relationships that could be construed as a potential conflict of interest.

frontiers in Forests and Global Change

ORIGINAL RESEARCH
published: 20 June 2019
doi: 10.3389/ffgc.2019.00031

What Are the Principal Factors Affecting Ambient Ozone Concentrations in Czech Mountain Forests?

Iva Hůnová[1,2]*, *Marek Brabec*[3,4] *and Marek Malý*[3,4]

[1] Ambient Air Quality Department, Czech Hydrometeorological Institute, Prague, Czechia, [2] Faculty of Science, Institute for Environmental Studies, Charles University, Prague, Czechia, [3] Department of Biostatistics, National Institute of Public Health, Prague, Czechia, [4] Department of Statistical Modeling, Institute of Computer Science of the Czech Academy of Sciences, Prague, Czechia

The aim of our study was to identify the factors substantially affecting day-to-day variability in O_3 concentrations in Czech mountain forests and to describe their influence in detailed, quantitative way. We examined the effects of meteorology and ambient NO_x recorded in regular long-term continuous monitoring at five mountain forest sites representing different regions, covering both polluted and relatively unpolluted areas over the time period of 1992–2018. To investigate the association between ambient O_3 concentrations on one hand, and precursor NO_x concentrations, and meteorology on the other hand, we used a generalized additive model, GAM, with semiparametric (penalized-spline-based) components to capture properly the possible departures from linearity that is not captured by traditional linear regression approaches. Our results revealed that the O_3 concentrations showed significant associations with all selected explanatory variables, i.e., air temperature, global solar radiation (GLRD), relative humidity, and NO_x. Apparently, both meteorology and air pollution are highly important for day-to-day O_3 concentrations, and this finding is consistent for all five rural sites, representing middle-elevated forested mountain areas in Central Europe. In addition to individual variables, we were able to detect interactions between three pairs of explanatory variables, namely temperature*GLRD, temperature*relative humidity, and GLRD*relative humidity. Moreover, we confirmed non-linear O_3 behavior toward all individual explanatory variables.

Keywords: ambient ozone, generalized additive model, NOx, meteorology, non-linear effects

Edited by:
Silvano Fares,
Council for Agricultural and Economics Research, Italy

Reviewed by:
Evgenios Agathokleous,
Nanjing University of Information Science and Technology, China
Diana Pitar,
National Institute for Research and Development in Forestry Marin Dracea (INCDS), Romania

***Correspondence:**
Iva Hůnová
iva.hunova@chmi.cz

Specialty section:
This article was submitted to Forests and the Atmosphere, a section of the journal Frontiers in Forests and Global Change

Received: *29 January 2019*
Accepted: *28 May 2019*
Published: *20 June 2019*

Citation:
Hůnová I, Brabec M and Malý M (2019) What Are the Principal Factors Affecting Ambient Ozone Concentrations in Czech Mountain Forests? Front. For. Glob. Change 2:31. doi: 10.3389/ffgc.2019.00031

INTRODUCTION

Ground-level ozone (O_3), an important constituent of the atmosphere (Prinn, 2003; Singh and Fabian, 2003; Monks et al., 2015), belongs among the major factors exerting negative impacts on forests (Ferretti et al., 2015; EEA, 2016), and remains a challenging problem for current and future timber production and the conservation of natural plant communities, including species diversity (Krupa et al., 2001). A range of impacts due to elevated O_3 exposures have been reported by numerous authors, from changes in biochemical processes in living organisms to macroscopic injuries (e.g., Roschina and Roschina, 2003; Cape, 2008; Paoletti et al., 2010, etc.), although the field evidence for the impact of O_3 on forests remains less clear (Manning, 2005; De Vries et al., 2014; Cailleret et al., 2018).

The chemistry of O_3 is very complex (Finlayson-Pitts and Pitts, 1997; Seinfeldt and Pandis, 1998). Ozone is a product of the photochemical reactions of precursors, i.e., nitrogen oxides (NO_x), volatile organic compounds (VOC), methane (CH_4), and carbon monoxide (CO). Meteorology is strongly involved in O_3 formation, with atmospheric stability, high atmospheric pressure, high solar radiation, and air temperature as factors promoting O_3 buildup (Kovač-Andrič et al., 2009; Wang et al., 2017; Pyrgou et al., 2018). Many processes—physical, chemical, and biological—affect the formation, transportation, and destruction of O_3 and thus the final O_3 concentrations (Colbeck and Mackenzie, 1994; Seinfeldt and Pandis, 1998; Fowler et al., 2009). Ozone formation in the highly non-linear O_3-VOC-NO_x system is not yet fully understood (Sillman, 1999; Carillo-Torres et al., 2017).

Trends in O_3 are difficult to detect due to its large interannual variability (Jonson et al., 2006). The ambient O_3 in Europe has significantly decreased, though not as much as expected with respect to sharp reduction in precursor emissions since the 1990s (Sicard et al., 2013; Paoletti et al., 2014; Colette et al., 2017). It appears that the negative O_3 trend throughout Europe due to European emission controls has been counteracted by tendencies related to climate warming and the hemispheric transportation of pollutants from the source regions, such as Southeast Asia (Yan et al., 2018). Climate variability generally regulates the interannual variability in European O_3, whereas the changes in anthropogenic precursor emissions predominantly influence O_3 trends (Yan et al., 2018).

In order to better understand O_3 behavior, it is of major concern to identify the factors that account for most of the day-to-day variability in O_3 concentrations. Numerous studies have been published tackling this issue from various perspectives, using different approaches, examining diverse variables and their measures (e.g., Duenas et al., 2002; Tarasova and Karpetchko, 2003; Abdul-Wahab et al., 2005; Özbay et al., 2011). Regression-based approaches—with the most often used multiple linear regression analysis—are commonly used for modeling O_3 concentrations as a response variable, and with meteorological characteristics and different ambient air pollutants as explaining variables (e.g., Abdul-Wahab et al., 2005; Sousa et al., 2006; Pavón-Domínguez et al., 2014).

Ambient ozone levels in Czech Republic are high (Hůnová and Bäumelt, 2018). Exposures over Czech forests exhibit high year-to year variability (Hůnová et al., 2019), nevertheless they consistently exceed the critical level of 5 ppm h AOT40F (UN/ECE, 2004) since 1994, with peak values reaching 38–39 ppm h at some sites in different years. In some mountain forests, such as in the Jizerske hory Mts., the O_3 exposures are similar as in highly polluted sites in South Europe and higher altitudes (Hůnová et al., 2016). The critical level of 5 ppm h AOT40F is usually exceeded early in the growing season, generally in May (Hůnová and Schreiberová, 2012). The highest O_3 exposures, indicated by AOT40F, are permanently measured in south Czech Republic, the region much less affected by clouds, and thus receiving higher global radiation loads during growing seasons (Hůnová et al., 2019). Existing studies on O_3 biological effects on Czech forests are equivocal (Šrámek et al., 2007, 2012; Hůnová et al., 2010, 2011; Zapletal et al., 2012; Vlasáková-Matoušková and Hůnová, 2015), however, and despite the high O_3 levels recorded, no serious damage attributable to O_3 has been reported so far.

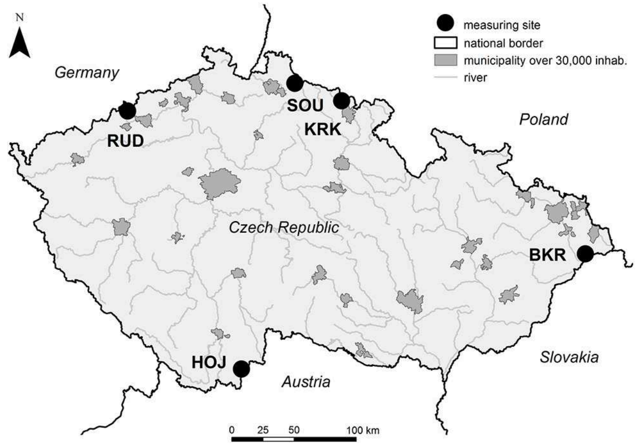

FIGURE 1 | Measuring sites in map (the map was created in ArcGIS 10.3, based on ZABAGED layers, i.e., the geographic base data of the Czech Republic, belonging to information systems of the public service).

The aim of our study is to explore selected factors substantially affecting the day-to-day variability of O_3 concentrations in Czech mountain forests. In the effort to decrease O_3 levels, it is truly of the utmost importance to know how meteorology and emission precursors influence ozone in a quantitative way.

METHODS

Sites and Period Under Review

We analyzed the observed data, recorded in regular long-term continuous monitoring at five mountain forest sites (**Figure 1**; **Table 1**) operated by the Czech Hydrometeorological Institute (CHMI). The sites under review are distributed unevenly across the territory of the Czech Republic (CR), and are situated in border mountains under different pollution loads: Krkonoše-Rýchory (KRK) and Souš (SOU) are situated in the northern CR; Rudolice v Horách (RUD) in the northwest CR, a region with cumulative major emission sources; Bílý Kříž (BKR) in the northeast CR in the highly polluted Silesia region; and Hojná Voda (HOJ) in the relatively unpolluted southern CR. All five measuring stations are situated in open areas. Nevertheless, in close vicinity of all these sites are extensive forested areas, covered predominantly by spruce forests (*Picea abies*). The KRK, BKR, and HOJ sites are roughly estimated to represent some tens to hundreds kilometers, whereas RUD and SOU sites represent somewhat less extensive regions, about several tens kilometers.

We examine the period of 1992–2018 (excluding days with missing ozone and/ or explanatory variables of our interest). This interval covers both the time with high emissions in the past (until 1998), and the "cleaner" period after profound socio-economic changes in Central Europe, including the CR, after the

TABLE 1 | Measuring sites - basic characteristics.

Site	Code	Mountain area	Classification	Altitude [m a. s. l.]
Krkonoše-Rýchory	KRK	Krkonoše	B/R/N-REG	1,001
Bílý Kříž	BKR	Beskydy	B/R/N-REG	890
Rudolice v Horách	RUD	Krušné hory	B/R/N-REG	840
Hojná Voda	HOJ	Novohradské hory	B/R/N-REG	818
Souš	SOU	Jizerské hory	B/R/N-REG	771

introduction of novel, more effective legislation for ambient air protection, and after the adoption of diverse countermeasures. From this 27-years record numerous data are missing, in different periods for individual sites. The NO_x ambient levels at four out of our five sites are available only until 2012. As a matter of fact, NO_x was monitored at Czech mountain sites only until 2012 (due to very low concentrations recorded in these areas previously), with the exception of BKR where NO_x monitoring continues. **Table S1** presents an overview of the numbers of daily data at disposal for our analysis.

Input Data: Ambient Air Quality and Meteorology

The input data were retrieved from ISKO, the Czech nationwide ambient air quality database (CHMI, 2018b). All data we used were based on real-time, continuous measurements, from which 1 h averages were routinely calculated and stored—as the basic primary data—in ISKO database. With regard to quality of the dataset used: (1) the ambient O_3 and NO_x concentrations were checked thoroughly for gross errors by a database procedure based on mathematical and statistical methods (CHMI, 2018a), whereas (2) meteorology data, considered as support data, were checked only based on logic. The input data for all five sites run by the CHMI were measured by well-established, standardized methods as follows.

Ambient Ozone

We used the daily mean O_3 concentrations calculated from 1 h measurements, from the continuous, year-round, nationwide ambient air quality network. The measurement method was UV absorbance, the EC reference method (EC, 2008); the O_3 analyzers used were TEI-M49, manufactured by Thermo Environmental Instruments Inc., based in Franklin, Massachusetts, U.S. The sampling equipment was changed in 2015 to TAPI T-400, manufactured by Teledyne Advanced Pollution Instrumentation, Inc., based in San Diego, California, U.S. Standard QA/QC procedures in accordance with EU legislation (EC, 2008) were applied.

Nitrogen Oxides

We used the daily mean NO_x concentrations calculated from 1 h measurements, from the continuous, year-round, nationwide ambient air quality network. The measurement method was chemiluminescence, the EC reference method (EC, 2008); the NOx analyzers used were TEI–M42, manufactured by Thermo Environmental Instruments Inc., based in Franklin, Massachusetts, U.S. The sampling equipment was changed in 2015 to TAPI T-200, manufactured by Teledyne Advanced Pollution Instrumentation, Inc., based in San Diego, California, U.S. Standard QA/QC procedures in accordance with EU legislation (EC, 2008) were applied.

Meteorology

Meteorology monitored continuously with a 1 h time resolution was used. Namely, we used the daily mean air temperature, daily mean relative humidity, and daily global solar radiation (GLRD). The temperature in this paper is given in Kelvines [K]—this unit is used in our nation-wide database to avoid negative numbers, as negative numbers are exclusively assigned to error codes. Ambient air temperature in 2 m above ground and relative humidity were measured by Thies Clima HTT Compact, manufactured by Adolf Thies GmbH & Co., based in Gottingen, Germany. GLRD was measured by CMP sensors, manufactured by Kipp & Zonen B.V., based in Delft, The Netherlands. The meteorological variables were measured at the same sites and at the same hourly intervals as the air pollution variables.

Statistical Analysis

We have investigated the association between ambient O_3 concentrations on one hand, and precursor NO_x concentrations and meteorology on the other hand, using a generalized additive model, GAM (Wood, 2006). We accounted for NO_x as a proxy for ambient air pollution and a key player in O_3 chemistry. Unfortunately, VOCs as another key precursor group for O_3 formation could not be accounted for, as their concentrations are not recorded at the sites under review.

O_3 concentration was considered the dependent variable in the GAM model, whereas global solar radiation, air temperature, relative humidity, and NO_x concentrations were considered as explanatory variables. We worked with daily mean values calculated from primary 1 h values stored in a nationwide air-quality database. As the effects of some of these variables are known not to be linear, we used flexible GAM model formulation with semiparametric (penalized-spline-based) components to capture departures from linearity instead of forcing the relationship into the traditional but unrealistic linear (or log-linear) framework (Crawley, 2005). On the other hand, the GAM-retrieved relationships essentially reduce to linearity when the data do not support a non-linear relationship.

In order to maintain the comparability of results, the functional form of the GAM model is kept the same for all the sites we consider. Fitting was done separately for different sites (we stratified on site) so that we have site-specific parameters of the model with the same interpretation. For a given site, the GAM model is as follows:

$$\begin{aligned} Y_t = {} & \beta_0 + s_T\left(Temperature_t\right) + s_G\left(GLRD_t\right) + s_H\left(Humidity_t\right) \\ & + s_{NOX}\left(NOX_t\right) + s_{TG}\left(Temperature_t, GLRD_t\right) + s_{TH} \\ & \left(Temperature_t, Humidity_t\right) + s_{GH}\left(GLRD_t, Humidity_t\right) + \varepsilon_t \end{aligned}$$

where:

- *Y_t is the daily mean ozone concentration for day t (time is indexed by the number of days since the first day of the data),*

- *β is an unknown constant (intercept) to be estimated from the data*
- *$Temperature_t$ is the mean temperature for day t,*
- *$GLRD_t$ is the mean GLRD for day t,*
- *$Humidity_t$ is the mean relative humidity for day t,*
- *NOX_t is the mean NO_x concentration for day t,*
- *ε_t is the random error term. We adopt a working assumption of $\varepsilon_t \sim N(0,\sigma^2)\varepsilon_t \sim N\left(0,\sigma^2\right)$, which is a normal, zero mean, homoscedastic distribution of errors,*
- *S_T is an unknown univariate function (of temperature as an argument), of which the form is to be estimated from the data. We estimate it as a penalized spline (regularizing wiggliness via the penalization of the integral of the squared second derivative with respect to temperature). By that, we allow for potentially non-linear, smooth shapes of (marginal) dependence of O_3 on temperature,*
- *S_G is an unknown univariate function (of GLRD) to be estimated from the data as a penalized spline,*
- *S_H is an unknown univariate function (of Humidity) to be estimated from the data as a penalized spline,*
- *S_{NOX} is an unknown univariate function (of NO_x) to be estimated from the data as a penalized spline,*
- *S_{TG} is an unknown bivariate function (of Temperature and GLRD) to be estimated from the data as a tensor product penalized spline. This term allows us to investigate the possible interaction of Temperature and GLRD in influencing ozone concentration (i.e., departures from the simple additive effects of Temperature and GLRD). In other words, this effect enables us to investigate how the effect of Temperature is modified by GLRD (or, equivalently, how the effect of GLRD is modified by Temperature),*
- *S_{TH} is an unknown bivariate function (of Temperature and Humidity) to be estimated from the data as a tensor product penalized spline. This term corresponds to the Temperature*Humidity (parsimoniously formulated) interaction,*
- *S_{GH} is an unknown bivariate function (of GLRD and Humidity) to be estimated from the data as a tensor product penalized spline. This term corresponds to the GLRD*Humidity (parsimoniously formulated) interaction.*

All unknown model components are estimated simultaneously (the model is identified) by optimizing the penalized likelihood. Unknown penalty coefficients are obtained via generalized cross-validation. All modeling computations were done in R core (2008). Results with $p \leq 0.05$ are considered statistically significant. In graphs, the estimated spline functions are supplemented with 95% confidence intervals (constructed in pointwise fashion, so that they do not claim simultaneous coverage).

When estimating the model, we use all days with available data for a given station. From the model-fitting point of view, data are available when O_3 and all explanatory variables (temperature, GLRD, humidity, NO_x) are available. When at least one of these variables is missing, the day effectively appears as missing (i.e., it is not used in the fitting). Since different stations had missing days at different time-points, the model was estimated on a somehow different set of times, assuming that the ozone-to-explanatory-variables relationship is homogeneous in time.

TABLE 2 | Descriptive statistics for included variables at all five sites (calculated from daily data).

Site	Variable	*N*	25th perc	50th perc	75th perc
KRK	O_3 [ppb]	7,737	28.61	36.98	46.26
	NO_X [ppb]	6,368	2.98	4.41	6.77
	H [%]	6,764	72.17	84.15	92.20
	Temp [K]	6,708	272.10	279.26	286.33
	GLRD [W m^{-2}]	6,277	39.70	107.74	201.42
BKR	O_3 [ppb]	8,705	27.46	35.08	44.61
	NO_X [ppb]	8,735	2.19	3.11	4.60
	H [%]	7,037	77.13	91.00	98.00
	Temp [K]	7,098	272.88	279.77	285.89
	GLRD [W m^{-2}]	6,188	31.08	95.44	182.90
RUD	O_3 [ppb]	8,115	25.98	33.74	42.39
	NO_X [ppb]	6,118	4.52	6.74	10.40
	H [%]	7,435	78.08	90.21	98.42
	Temp [K]	7,645	273.24	279.43	285.21
	GLRD [W m^{-2}]	7,187	50.27	119.50	213.00
HOJ	O_3 [ppb]	8,409	26.32	33.45	41.96
	NO_X [ppb]	6,405	2.43	3.34	4.94
	H [%]	7,847	71.13	82.96	91.29
	Temp [K]	8,079	273.69	280.20	286.21
	GLRD [W m^{-2}]	7,752	48.80	106.35	193.10
SOU	O_3 [ppb]	8,945	24.65	31.94	40.03
	NO_X [ppb]	7,030	3.29	4.79	7.14
	H [%]	7,454	82.17	90.88	95.96
	Temp [K]	7,673	273.64	280.13	286.89
	GLRD [W m^{-2}]	7,987	31.69	92.69	183.54

RESULTS

Table 2 presents an overview of descriptive statistics calculated from the mean daily values for all considered variables at all five measuring sites. **Figures 2**, **3** present the dynamics in the response variable (given as annual median values of respective variable), i.e., ambient O_3 concentrations, and explanatory variables: air temperature, GLRD, relative humidity, and ambient NO_x concentrations at all five sites under review. Though we used data over the 1992–2018 time period in our model, the dynamics in the variables (**Figures 2**, **3**) are shown only for 1996–2016 due to the fact that at the beginning of measuring period, many data are missing, which would misrepresent the annual median in graphs. The GAM model, however, can cope with the missing data automatically (assuming homogeneity of the O_3 relationship to the explanatory variables in time and missing at random, or the MAR mechanism (Little and Rubin, 2002). The year-to-year variability in O_3 is high; the median concentrations at individual sites range between 28 and 45 ppb with clear peaks at some sites in 2003 and 2006. In spite of a clear decrease in NO_x concentrations, the ambient O_3 levels apparently do not decrease accordingly. Annual median temperatures ranged between 277.5

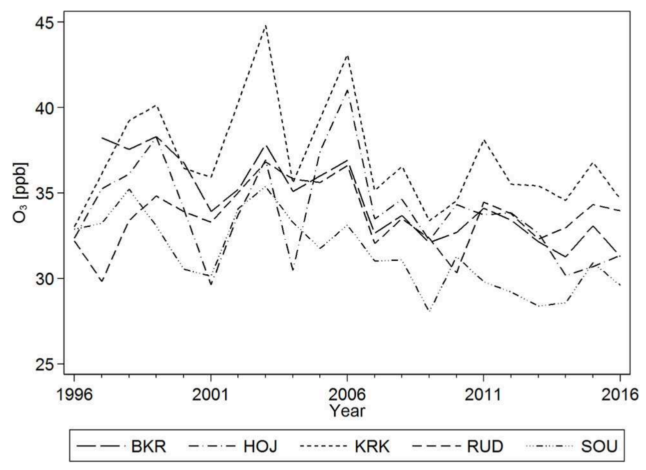

FIGURE 2 | Trend in annual median ambient O_3 levels.

and 282 K, GLRD between 74 and 200 W m^{-2}, and relative humidity between 74 and 98%.

The day-to-day variability in ambient O_3 concentrations is well described by a model including the additive effects of air temperature, GLRD, relative humidity, and ambient NO_x concentration, and the interactions of air temperature*GLRD, air temperature*relative humidity, and GLRD*relative humidity (**Figures 4–10**). Though **Figures 4–10** show the smooth terms with 95% confidence intervals from GAM model only for one site, namely BKR, the models for other four sites are looking quite similar. The relationship between O_3 expected value and temperature (**Figure 4**) shows higher O_3 values not only with higher temperatures, but, surprisingly, also with lower temperatures below 273.15 K (i.e., 0°C). Likely explanation for this finding rests in the fact that, mountain stations the data from which we analyze, are frequently above the inversion cloud layer in winter time, and receive high solar radiation capable of splitting the NO_2, a precursor molecule to O_3. Consequently, O_3 is recorded also in conditions of simultaneous low temperatures and high solar radiation, though O_3 levels are not that high as in summer when much higher temperatures promote O_3 formation reactions. The expected ozone value increases with increasing GLRD, though at some point the curve shows a plateau or even a slight decline (the decline is not significant, however, since it is outweighed by the increased variability) for higher GLRD values (**Figure 5**). Ozone concentration increases with decreasing relative humidity (**Figure 6**), right in line with physically-based intuition. The expected ozone value reaches its peak much more quickly than it decreases and shows a local maximum at about ambient NO_x concentration 3 ppb (**Figure 7**). Apart from the significant relationship between the response variable and individual explanatory variables, we also detected significant interactions between the three pairs of explanatory variables. **Figure 8** shows the complex effect of interactions of air temperature*GLRD upon the expected ambient O_3 concentration. Ozone evidently increases not only with increasing temperature and GLRD, which is a well-known fact, but also, surprisingly, with increasing GLRD at low temperatures. The dividing line is apparently around the ambient air temperature 280 K (i.e., 7°C). The ambient O_3 concentration generally increases with increasing temperature and decreasing humidity (**Figure 9**), whereas effect of interactions of relative humidity*GLRD upon expected ambient O_3 concentration appears less straightforward (**Figure 10**). We can see a sharp increase of O_3 concentrations with decreasing relative air humidity at a GLRD around 250 W m^{-2}, whereas above that GLRD value, O_3 decreases.

The marginal effects of all selected explanatory variables are significant, but they differ in the strength of their effects upon ozone. All variables and their selected interactions are highly significant ($p < 0.001$) for all five sites, with a minor exception for the interaction of GLRD*relative humidity for the KRK site, which is not significant, and for the BKR site with the p-value slightly less than the significance level of 0.05. The approximate significance of smooth terms is summarized in **Table 3**. At the KRK site, situated in the unpolluted top of the Krkonoše Mountains, influenced only by the long-range transport of air pollutants, all explanatory variables show similar strength, which also applies for interactions, which show a similar though lesser strength, as compared to the individual explanatory variables. A very similar pattern, though with a somewhat higher strength of relative humidity and lesser strength of air temperature, is obvious for the HOJ site, situated in the Novohradské hory Mountains, in the unpolluted (with regard to primary emissions and anthropogenic precursors of ambient ozone) south of the Czech Republic at the Austrian border. Ambient NO_x concentrations have a greater effect at sites representing more polluted regions. This holds true for the RUD site, situated at the Krusne hory mountain plateau and influenced by nearby large emission sources down in the valley (Bridges et al., 2002); for the SOU site, influenced by car exhaust from the nearby local road; and for the BKR site, influenced by emission sources in the polluted Silesian region (both on the Czech and the Polish sides of the border). The deviance explained for the individual sites is high, and ranges between 74.3% for the BKR and 63.4% for the SOU sites.

DISCUSSION

Complex Atmospheric Chemistry of O_3

Numerous studies examining O_3 chemistry, meteorology, and precursor emissions in Europe and North America, in different field research programs conducted under diverse geographical and climatic conditions, as well as studies of the combination of ground-based ozone data and meteorological observations, have resulted in enhancement of our knowledge of photochemical processes under various tropospheric conditions (Solomon et al., 2000; Monks et al., 2015). Nevertheless, it remains a challenge to interpret ambient O_3 behavior, levels, and trends. Atmospheric chemistry resulting in O_3 formation and destruction is, as a matter of fact, extremely complex due to numerous factors influencing these processes, and hence, O_3 concentrations (Cape, 2008).

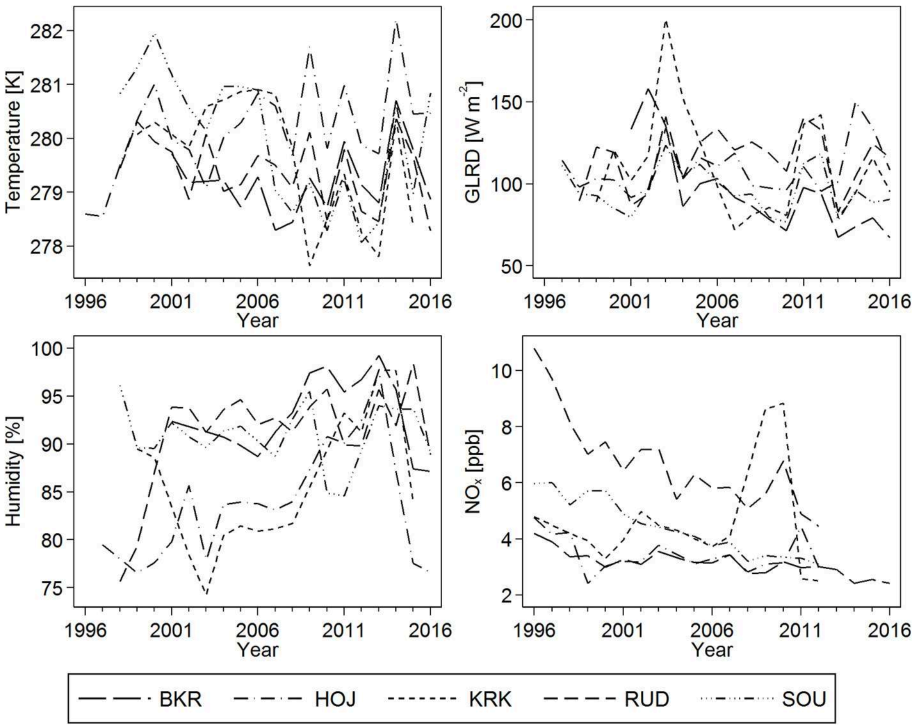

FIGURE 3 | Trends in annual median air temperature, GLRD, relative humidity, and ambient NO_X concentrations.

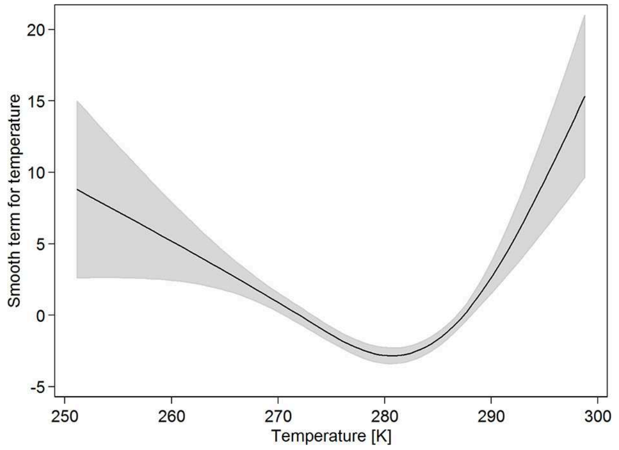

FIGURE 4 | Effect of air temperature upon expected ambient O_3 concentration, BKR site.

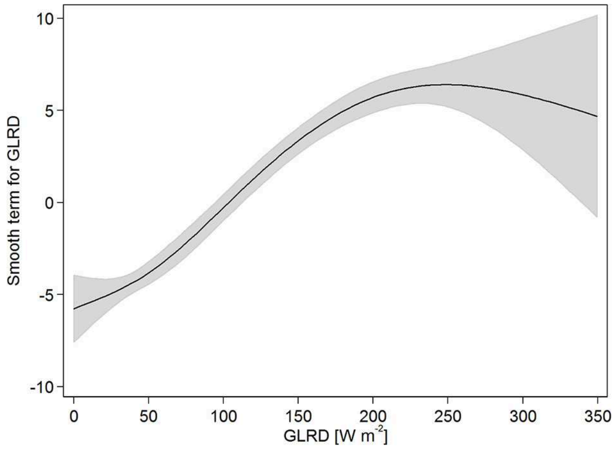

FIGURE 5 | Effect of GLRD upon expected ambient O_3 concentration, BKR site.

Meteorology is extremely important for O_3 formation. It affects O_3 concentrations not only directly (via horizontal advection, vertical diffusion, and photolysis rates), but also indirectly, by influencing the concentrations of its precursors and chemistry of its formation and destruction (Oikonomakis et al., 2018). O_3 has a temperature-dependent chemistry (Pusede et al., 2015), and temperature was used in some studies as a surrogate to indicate O_3 formation via the O_3-temperature association, both at individual measuring sites and on a greater regional scale (Oikonomakis et al., 2018). The O_3-temperature relationship originates in: (1) temperature-dependent biogenic VOC emissions, (2) thermal decomposition of PAN to HO_x and NO_x, (3) increased likelihood of favorable meteorological conditions for ozone formation (Abeleira and Farmer, 2017). However, there are major uncertainties in the mechanisms underlying the temperature-dependent changes in O_3 concentrations, their interactions, and relative contributions in rural and remote regions (Romer et al., 2018). Ozone chemistry

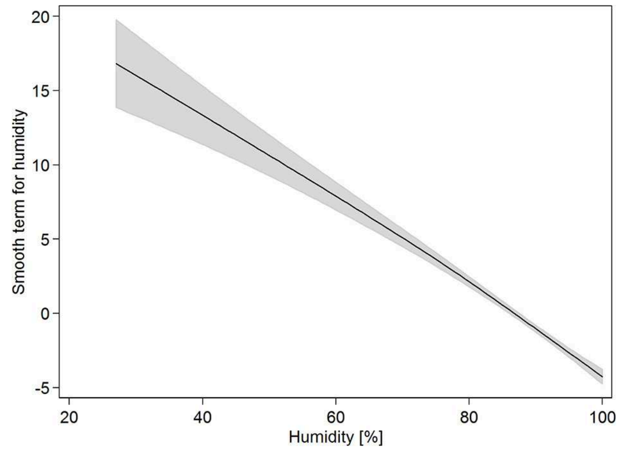

FIGURE 6 | Effect of relative humidity upon expected ambient O_3 concentration, BKR site.

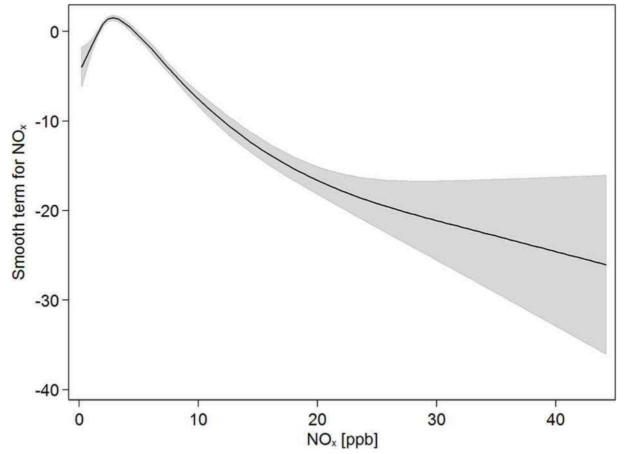

FIGURE 7 | Effect of ambient NO_X concentrations upon expected ambient O_3 concentration, BKR site.

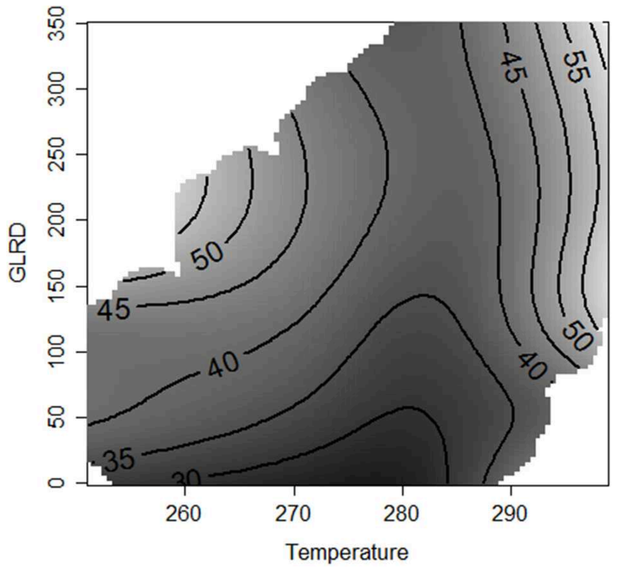

FIGURE 8 | Effect of interactions of air temperature*GLRD upon expected ambient O_3 concentration, BKR site.

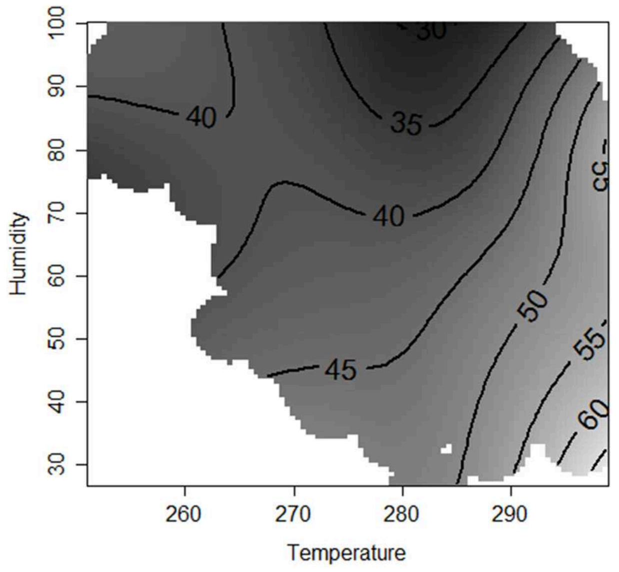

FIGURE 9 | Effect of interactions of air temperature*relative humidity upon expected ambient O_3 concentration, BKR site.

regimes are shifting as precursor emissions are changing (Abeleira and Farmer, 2017). Moreover, meteorology-dependent O_3 chemistry implicates the impact of ongoing climate change on O_3. Increasing temperature is expected to increase O_3 concentrations (Abeleira and Farmer, 2017). Additionally, the projected rise in global precursor emissions over the twenty-first century is also assumed to have a strong effect on O_3 throughout the world (Vingarzan, 2004). In contrast to temperature, field studies on GLRD influence on ground-level O_3 concentrations are scarce (Duenas et al., 2002). Though it is a well-known fact, that ambient O_3 is strongly dependent on GLRD (Finlayson-Pitts and Pitts, 1997; Seinfeldt and Pandis, 1998), some authors showed that solar radiation had a lower effect than expected upon O_3 concentrations as compared to more important effect of temperature (Abdul-Wahab and Al-Alawi, 2002).

The association between meteorological factors, precursor emissions, and O_3 daily variability might differ in urban and rural areas. Whereas the precursor emissions used to be much higher in urban areas, in rural regions the precursors are lower, in particular with respect to NO_x (Romer et al., 2018). Most papers on this issue examine the O_3 regime in urban areas (e.g., Duenas et al., 2002; Tan et al., 2018), whereas the papers on rural regions are less frequent (e.g., Pudasainee et al., 2006).

Strengths and Weaknesses of the GAM Model Used

Various statistical approaches to model O_3 dependence on meteorology and ambient air pollutants have been employed recently and have been reviewed by Thompson et al. (2001) and

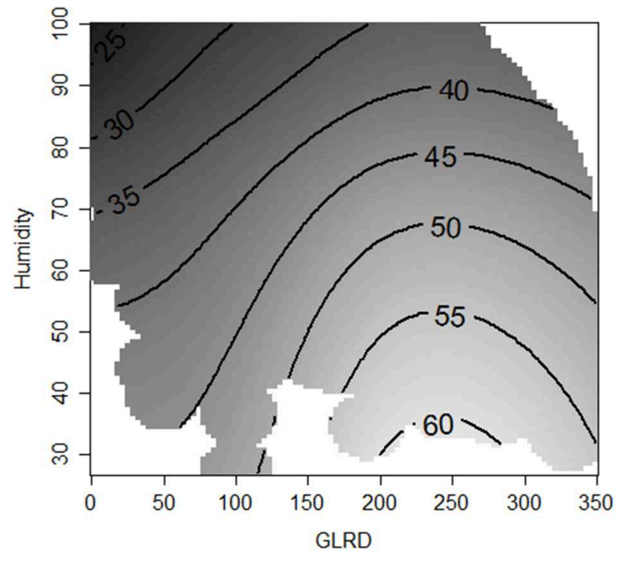

FIGURE 10 | Effect of interactions of GLRD*relative humidity upon expected ambient O_3 concentration, BKR site.

Schlink et al. (2003). The main objectives are O_3 forecasting, estimating O_3 time trends, and investigating the underlying processes based on observation data. The input data may vary widely both in terms of the variables considered, and in terms of observation scales in space and time (Thompson et al., 2001). The multiple linear regression method is frequently used (e.g., Abdul-Wahab et al., 2005; Sousa et al., 2006; Pavón-Domínguez et al., 2014), though it encounters serious difficulties when the independent variables are correlated with each other, i.e., when they exhibit multicollinearity (Al-Alawi et al., 2008). This is exactly the case of O_3, when e.g., the explanatory variables of temperature and GLRD are correlated. One method used to remove this multicollinearity is principal component analysis (PCA), selecting variables with high loadings to be used as predictors in a regression equation (e.g., Rajab et al., 2013). In our data (and moderate number of explanatory variables), collinearity is not a problem. The variance inflation factor, VIF (Rawlings et al., 1998), is smaller than 2.5 at all five sites. Even more importantly, O_3 formation and destruction are complex non-linear processes, and principal component regression cannot adequately model the non-linear relationship (Al-Alawi et al., 2008), and hence it cannot be used to retrieve true functional relationships, only linear (often hard-to-interpret) approximation. Neural networks and generalized additive models are recommended to address this issue, as they can handle non-linear associations and can be adapted easily to site-specific conditions (Schlink et al., 2003), but since they are used in a black-box style, they are much more useful for prediction than for analysis purposes.

Since we used a rather flexible class of statistical models (Generalized Additive Model with penalized spline components), we allow for a smooth relationship between O_3 and explanatory variables (temperature, GLRD, humidity, and NO_X). This class

TABLE 3 | Approximate significance of smooth terms.

	KRK			BKR			RUD			HOJ			SOU		
	F	**EDF**	***p*-value**	***F***	**EDF**	***p*-value**	***F***	**EDF**	***p*-value**	***F***	**EDF**	***p*-value**	***F***	**EDF**	***p*-value**
T	20.72	3.661	<0.001	30.07	3.638	<0.001	21.23	3.463	<0.001	15.73	3.999	<0.001	35.32	3.859	<0.001
GLRD	23.98	2.497	<0.001	84.85	3.691	<0.001	65.10	3.512	<0.001	53.24	3.796	<0.001	76.40	4.000	<0.001
I (T, GLRD)	5.47	12.451	<0.001	7.13	11.374	<0.001	2.56	7.811	<0.001	4.56	12.193	<0.001	10.286	8.269	<0.001
NO_X	32.44	4.89	<0.001	112.92	6.116	<0.001	195.53	5.190	<0.001	43.67	6.187	<0.001	110.13	7.029	<0.001
H	39.40	3.75	<0.001	150.63	1.738	<0.001	50.19	3.967	<0.001	64.09	1.879	<0.001	7.09	3.807	<0.001
I (T, H)	5.42	14.711	<0.001	8.14	8.748	<0.001	8.32	9.852	<0.001	7.54	7.786	<0.001	4.41	11.092	<0.001
I (GLRD, H)	2.21	3.859	0.054	2.53	4.150	<0.05	4.00	8.904	<0.001	14.86	10.904	<0.001	8.03	12.779	<0.001
Deviance explained		66.5%			74.3%			71.2%			66.3%			63.4%	

F, test statistics; EDF, equivalent degrees of freedom; I, interactions; T, temperature; GLRD, global solar radiation; H, relative humidity.

would not be ideal for relationships showing very sharp bends, sudden jumps at particular values of covariates, etc. From the physical and chemical backgrounds of O_3 behavior, however, we do not expect this sort of behavior and take GAM as a tool allowing for non-linearity in explanatory variables (unlike standard multiple regression, which insists on linearity, i.e., on the gradient with respect to a given explanatory variable being constant throughout its range). Since we use tensor product splines, we can also assess possible interactions in influences of certain pairs of explanatory variables (i.e., to assess whether their influence is simply additive or more complicated). Since we concentrate only on two-variable interactions, we can assess not only their overall significance (via the *p*-values of formalized hypothesis tests), but also display the interactions in graphical form (as contour plots showing how the mean ozone concentration depends on a pair of explanatory variables).

Volatile Organic Compounds Are Lacking in Our Model

The weak point of our model is the fact that the VOCs, an important O_3 precursor group, are not included in our model. This is due simply to the fact that the measured data are not available. There are no significant anthropogenic sources of VOCs near the five mountain sites under review; nevertheless, the surrounding forests are undoubtedly a major source of natural biogenic VOCs (further, BVOCs). BVOCs are a large group of organic chemicals including isoprene, terpenes, fatty acid derivates, benzenoids, phenylpropanoids, and amino acid derived metabolites (Esposito et al., 2016). They are emitted into the atmosphere by plants, and significantly affect its chemical composition and physical properties (Laothawornkitkul et al., 2009; Pinto et al., 2010), contributing substantially, among other effects, to the oxidizing capacity of the atmosphere through the recycling of hydroxyl radicals, OH (Lelieveld et al., 2008). Interestingly, on a global scale, BVOC emissions exceed by far those emitted due to anthropogenic activities (Seinfeldt and Pandis, 1998), and are more reactive (Holzinger et al., 2005). BVOCs belong among the key players in ambient O_3 chemistry in rural areas (Atkinson and Arey, 2003; Di Carlo et al., 2004).

We assume that natural BVOCs at the investigated sites are very important, as all five sites under review are situated in the close vicinity of vast forested areas, with a clear predominance of Norway spruce (*Picea abies*). It has been widely accepted that the vegetative emissions display large inter-species and inter-individual variability (Aydin et al., 2014). As compared to some other woody species, such as poplar or beech, spruce is a lower BVOC emitter (Bortsoukidis et al., 2014); however, it is still known to emit considerable amounts of reactive trace gases, and is considered particularly as an emitter of monoterpenes, such as α-pinene, β-pinene, limonene, and myrcene, whereas it is only a low isoprene emitter (Esposito et al., 2016; Jurán et al., 2017). Though some indicative information exists on BVOC emission for the CR (Zemankova and Brechler, 2010; Jurán et al., 2017), observation-based data in high time-resolution suitable for use in our model are lacking at present. Nevertheless, it would be very interesting in the future to include the data on BVOC concentration to observe how they influence our model.

Relevance of Our Results to Forests

On a long-term basis, ambient O_3 has been considered as a stress factor contributing to impairment of forest health status and its influence has been studied from different aspects. In spite of clear evidence of O_3 harmful effects observed in laboratory experiments, fumigation chambers, or FO_3X (Free air O_3 eXposure) experiments (Sandermann et al., 1997; Paoletti et al., 2017; Franz et al., 2018; Hoshika et al., 2018), the field evidence for impacts of O_3 exposure on tree growth is not that clear (De Vries et al., 2014; Cailleret et al., 2018). Moreover, observations in real stand conditions from numerous regions show that measured high O_3 exposures or modeled high O_3 stomatal flux do not correspond with unclear impacts on forest ecosystems (e.g., Ferretti et al., 2007; Matyssek et al., 2007; Waldner et al., 2007; Baumgarten et al., 2009).

European-wide assessment shows that, ambient O_3 exposures recorded at Czech background rural sites are medium in European context, being lower than in Southern Europe including Mediterranean, but higher than in Scandinavia, similar as in Germany and Switzerland (e.g., Waldner et al., 2007; Baumgarten et al., 2009; EEA, 2016). In our earlier work we assessed long-term time trends and spatial variability in ambient O_3 concentrations throughout the Czech Republic (Hůnová and Bäumelt, 2018), O_3 exposure over Czech forested areas (Hůnová and Schreiberová, 2012), compared different GIS methods to create a reliable O_3 and AOT40F map based on observed data (Hůnová et al., 2012), studied O_3 exposure, stomatal flux, and ozone injury on native vegetation in mountain forests (Hůnová et al., 2011; Vlasáková-Matoušková and Hůnová, 2015; Hůnová, 2017), and indicated the Czech forest regions which are stressed by permanent high O_3 exposures (Hůnová et al., 2019).

In present study we have investigated exclusively the O_3 behavior with respect to its day-to-day response to selected meteorology characteristics and NO_x precursors. Our results confirmed non-linear behavior of ambient O_3 not only to NO_x precursors, which is a well-known fact (Finlayson-Pitts and Pitts, 1997; Seinfeldt and Pandis, 1998), but also to meteorology, including all variables considered. Our results thus point out to certain deficiency of models investigating the underlying processes of O_3 formation based on measured data not considering this non-linear behavior toward ambient air temperature, GLRD, and relative humidity. This might be beneficial, for example, in modeling future scenarios for forested regions, accounting for changes in ambient O_3 toward local ambient air temperature, GLRD and relative humidity. Furthermore, our results indicated the necessity of considering not only individual explaining variables but also their interactions, such as the interactions of air temperature*GLRD, air temperature*relative humidity, and GLRD*relative humidity. This might be of high relevance in particular in context of global climate change (Bytnerowicz et al., 2007; Sicard et al., 2017). In this respect Czech Republic heads toward hotter and drier conditions (Hlásny et al., 2011; Trnka et al., 2015; Štěpánek et al., 2016), which is likely to affect future ambient O_3 concentrations.

The associations indicated by our study might enhance the models estimating potential future impacts of environmental/ climate changes on forests.

Ambient O_3 is, alongside with nitrogen deposition, considered on a long-term basis as an important factor affecting negatively European forests (EEA, 2016). Nevertheless, in recent years, this factor has been in Central Europe and elsewhere overshadowed by two other major threats for forests, namely unprecedented drought and unprecedented bark beetle outbreaks (Allen et al., 2010). Forests with compromised ecological stability, such as traditional forest monocultures in particular, are especially prone to large scale damage (Hlásny and Turčáni, 2013). This holds for most of the Czech forests, which can be classified as managed low-diversity ecosystems (Vacek et al., 2013), with decreased stand stability in respect to damages caused by natural abiotic agents (wind, snow, glaze, drought), biotic factors (insects including bark-beetle, pathogens), and also by anthropogenic effects, such as ambient air pollution. This adverse development is manifested by recent unprecedented salvage felling in Czech forests (Pajtík et al., 2018; Zahradník and Zahradníková, 2019). That present Czech forest decline is a result of a complex interplay of multiple factors was stressed by several recent observation-based studies (Kolár et al., 2015; Cienciala et al., 2016; Altman et al., 2017).

Czech forests in history were substantially changing in terms of area, species representation, and tree age. Presently, out of 26,664 km^2 of forested area representing some 34% of the Czech territory, Norway spruce (*Picea abies*), traditionally an important timber tree, is still a dominant species covering ca. 51% of the total forested area, following pine trees (*Pinus* spp.) cover 17%, beech (*Fagus sylvatica*) 8%, and oak (*Quercus* spp.) 7% (Ministry of Agriculture, 2015). Spruce is a somewhat ambiguous species with respect to O_3 sensitivity—it is assumed not to be especially sensitive in relation to visible injury but regarded as O_3-sensitive in relation to growth responses (UN/ECE, 2004). Nevertheless, we have to keep on mind that ambient air pollution is a factor affecting forests. We have already witnessed earlier that, predisposition of Norway spruce by air pollution (namely by high ambient SO_2 concentrations in the 1970s and 1980s) to stress from climatic events, such as drought and temperature changes, resulted in forest decline in Czech Republic (Vacek et al., 2015).

CONCLUSIONS

The generalized additive model confirmed that selected explanatory variables, i.e., air temperature, GLRD, relative humidity, and NO_x, significantly affect daily O_3 concentrations in Czech forests. Apparently, both meteorology and air pollution are highly influential on day-to-day O_3 concentrations, and this finding is consistent for all five rural sites representing middle-elevated forested mountain areas in Central Europe. We believe it would be of the utmost importance to include BVOCs in our analysis. Nevertheless, at present this is impossible, as the relevant data for BVOCs for these sites do not exist. Additionally, in contrast to a standard approach based on multiple linear regression used for similar studies, we were able to access non-linear relationships of various covariates to ozone, and also to characterize the interactions of the three pairs of explanatory variables, namely temperature*GLRD, temperature*relative humidity, and GLRD*relative humidity. We extracted functional relationship of various explanatory variables, demonstrating deficiencies of standardly used linear approximations. Local extrema visible in some of the bivariate relationships (O_3 to temperature or to NO_x) can, in addition to saturation (upper asymptote) visible in the relationship of O_3 to GLRD, easily distort quantification of covariate effects, e.g., to forests injury and/ or to smear out various climatic scenario comparisons based on standard linear approach. Non-linear relationships (qualitatively clear from the O_3 atmospheric chemistry) should be taken seriously also in real, observed data analysis. GAM methodology offers a powerful tool for this.

AUTHOR CONTRIBUTIONS

IH coordinated the study. IH, MB, and MM contributed to the conception and design of the study. MM organized the database and prepared the final version of **Figures 2–10**. MB performed the statistical analysis. IH wrote the first draft of the manuscript. All authors contributed to manuscript revision, read, and approved the submitted version.

FUNDING

This work was partially supported by the long-term strategic development financing of the Institute of Computer Science (Czech Republic RVO 67985807).

ACKNOWLEDGMENTS

We thank Erin Naillon for proofreading our manuscript and Jana Schovánková from the CHMI for preparing the **Figure 1**. We also appreciate the comments and suggestions of three reviewers, which enhanced our manuscript substantially.

SUPPLEMENTARY MATERIAL

The Supplementary Material for this article can be found online at: https://www.frontiersin.org/articles/10.3389/ffgc.2019.00031/full#supplementary-material

REFERENCES

Abdul-Wahab, S. A., and Al-Alawi, S. M. (2002). Assessment and prediction of tropospheric ozone concentration levels using artificial neural networks. *Environ. Model. Softw.* 17, 219–228. doi: 10.1016/S1364-8152(01)00077-9

Abdul-Wahab, S. A., Bakheit, C. S., and Al-Alawi, S. M. (2005). Principal component and multiple regression analysis in modelling of ground-level ozone and factors affecting its concentrations. *Environ. Model. Softw.* 20, 1263–1271. doi: 10.1016/j.envsoft.2004.09.001

Abeleira, A. J., and Farmer, D. K. (2017). Summer ozone in the northern Front Range metropolitan area: weekend-weekday effects, temperature dependences, and the impact of drought. *Atmos.Chem. Phys.* 17, 6517–6529. doi: 10.5194/acp-17-6517-2017

Al-Alawi, S. M., Abdul-Wahab, S. A., and Bakheit, C. B. (2008). Combining principal component regression and artificial neural networks for more accurate predictions of ground-level ozone. *Environ. Model. Softw.* 23, 396–403. doi: 10.1016/j.envsoft.2006.08.007

Allen, C. D., Macalady, A. K., Chenchouni, H., Bachelet, D., McDowell, N., Vennetier, M., et al. (2010). A global overview of drought and heat-induced tree mortality reveals emerging climate change risks for forests. *For. Ecol. Manage.* 259, 660–684. doi: 10.1016/j.foreco.2009.09.001

Altman, J., Fibich, P., Santruckova, H., Dolezal, J., Stepanek, P., Hunova, I., et al. (2017). Environmental factors exert strong control over the climate-growth relationships of Picea abies in Central Europe. *Sci. Total Environ.* 609, 506–516. doi: 10.1016/j.scitotenv.2017.07.134

Atkinson, R., and Arey, J. (2003). Gas-phase tropospheric chemistry of biogenic volatile organic compounds: a review. *Atmos. Environ.* 37 (Suppl. 2), S1972–S219. doi: 10.1016/S1352-2310(03)00391-1

Aydin, Y. M., Yaman, B., Koca, H., Dasdemir, O., Kara, M., Altiok, H., et al. (2014). Biogenic volatile organic compound (VOC) emissions from forested areas in Turkey: determination of specific emission rates for thirty-one tree species. *Sci. Total Environ.* 490, 239–253. doi: 10.1016/j.scitotenv.2014.04.132

Baumgarten, M., Huber, C., Buker, P., Emberson, L., Dietrich, H.-P., et al. (2009). Are Bavarian forests (southern Germany) at risk from ground-level ozone? Assessment using exposure and flux based ozone indices. *Environ. Pollut.* 157, 2091–2107. doi: 10.1016/j.envpol.2009.02.012

Bortsoukidis, E., Williams, J., Kesselmeier, J., Jacobi, S., and Bonn, B. (2014). From emissions to ambient mixing ratios: online seasonal field measurements of volatile organic compounds over a Norway spruce-dominated forest in central Germany. *Atmos.Chem. Phys.* 14, 6495–6510. doi: 10.5194/acp-14-6495-2014

Bridges, K. S., Jickells, T. D., Davies, T. D., Zeman, Z., and Hůnová, I. (2002). Aerosol, precipitation and cloud water chemistry observations on the Czech Krusne hory plateau adjacent to a heavily industrialised valley. *Atmos. Environ.* 36, 353–360. doi: 10.1016/S1352-2310(01)00388-0

Bytnerowicz, A., Omasa, K., and Paoletti, E. (2007). Integrated effects of air pollution and climate change on forests: a northern hemisphere perspective. *Environ. Pollut.* 147, 438–445. doi: 10.1016/j.envpol.2006.08.028

Cailleret, M., Ferretti, M., Gessler, A., Rigling, A., and Schaub, M. (2018). Ozone effects on European forest growth – towards an integrative approach. *J. Ecol.* 106, 1377–1389. doi: 10.1111/1365-2745.12941

Cape, J. N. (2008). Surface ozone concentrations and ecosystem health: past trends and a guide to future projections. *Sci. Total Environ.* 400, 257–269. doi: 10.1016/j.scitotenv.2008.06.025

Carillo-Torres, E. R., Hernández- Paniagua, I. Y., and Mendoza, A. (2017). Use of combined observational- and model- derived photochemical indicators to assess the O_3-NO_x-VOC system sensitivity in urban areas. *Atmosphere* 8:22. doi: 10.3390/atmos8020022

CHMI (Czech Hydrometeorological Institute) (2018a). *Tabular Survey 2017*. Prague: Czech Hydrometeorological Institute. Czech /English version. Avaliable online at: http://portal.chmi.cz/files/portal/docs/uoco/isko/tab_roc/2017_enh/index_GB.html

CHMI (Czech Hydrometeorological Institute) (2018b). *Air Pollution in the Czech Republic in 2017*. Prague: Czech Hydrometeorological Institute. Czech /English version. Avaliable online at: http://portal.chmi.cz/files/portal/docs/uoco/isko/grafroc/17groc/gr17cz/Obsah_CZ.html

Cienciala, E., Russ, R., Šantručková H., Altman, J., Kopáček, J., Hůnová, I., et al. (2016). Discerning environmental factors affecting current tree growth in Central Europe. *Sci. Total Environ.* 573, 541–554. doi: 10.1016/j.scitotenv.2016.08.115

Colbeck, I., and Mackenzie, A. R. (1994). *Air Pollution by Photochemical Oxidants*. Amsterdam: Elsevier.

Colette, A., Andersson, C., Manders, A., Mar, K., Mircea, M., Pay, M-T., et al. (2017). EURODELTA-Trends, a multi-model experiment of air quality hindcast in Europe over 1990−2010. *Geoscient. Model Dev.* 10, 3255–3276. doi: 10.5194/gmd-10-3255-2017

Crawley, M. J. (2005). *Statistics: An Introduction Using R.* London: John Wiley & Sons, Ltd.

De Vries, W., Dobbertin, M. H., Solberg, S., Van Dobben, H. F., and Schaub, M. (2014). Impacts of acid deposition, ozone exposure and weather conditions on forest ecosystems in Europe: an overview. *Plant Soil* 380, 1–45. doi: 10.1007/s11104-014-2056-2

Di Carlo, P., Brune, W. H., Martinez, M., Harder, H., Lesher, R., Ren, X., et al. (2004). Missing OH reactivity in a forest: evidence for unknown reactive biogenic VOCs. *Science* 304, 722–725. doi: 10.1126/science.1094392

Duenas, C., Fernández, M. C., Canete, S., Caarretero, J., and Liger, E. (2002). Assessment of ozone variations and meteorological effects in an urban area in the Mediterranean cost. *Sci. Total Environ.* 299, 97–113. doi: 10.1016/S0048-9697(02)00251-6

EC (2008). *Directive 2008/50/EC of the European Parliament and of the Council of 21 May 2008 on Ambient Air Quality and Cleaner Air for Europe.* OJEC L 152.

EEA (2016). *Air Quality in Europe – 2016 Report*. Luxembourg: European Environment Agency.

Esposito, R., Lusini, I., Večerová K., Holišová P., Pallozzi, E., Guidolotti, G., et al. (2016). Shoot-level terpenoids emission in Norway spruce (*Picea abies*) under natural field and manipulated laboratory conditions. *Plant Physiol. Biochem.* 108, 530–538. doi: 10.1016/j.plaphy.2016.08.019

Ferretti, M., Fagnano, M., Amoriello, T., Badiani, M., Ballarin-Denti A., Buffoni, A., et al. (2007). Measuring, modelling and testing ozone exposure, flux and effects on vegetation in southern European conditions – What does not work? A review from Italy. *Environ. Pollut.* 146, 648–658. doi: 10.1016/j.envpol.2006.05.012

Ferretti, M., Sanders, T., Michel, A., Calatayud, V., Cools, N., Gottardini, E., et al. (2015). *The Impact of Nitrogen Deposition and Ozone on the Sustainability of European Forests.* ICP Forests 2014 Executive Report, e-ISSN. 2198–6541.

Finlayson-Pitts, B. J., and Pitts, J. N Jr. (1997). Tropospheric air pollution: ozone, airborne toxics, polycyclic aromatic hydrocarbons, and particles. *Science* 276, 1046–1052. doi: 10.1126/science.276.5315.1045

Fowler, D., Pilegaard, K., Sutton, M. A., Ambus, P., Raivonen, M., Duyzer, J., Simposon, D., et al. (2009). Atmospheric composition change: ecosystems-Atmosphere interactions. *Atmos. Environ.* 43, 5193–5267. doi: 10.1016/j.atmosenv.2009.07.068

Franz, M., Alonso, R., Arneth, A., Buker, P., Elvira, S., Gerosa, G., et al. (2018). Evaluation of simulated ozone effects in forest ecosystems against biomass damage estimates from fumigation experiments. *Biogeosciences* 15, 6941–6957. doi: 10.5194/bg-15-6941-2018

Hlásny, T., Holuša, J., Štěpánek, P., Turčáni M, and Polčák, N. (2011). Expected impacts of climate change on forests: Czech Republic as a case study. *J. For. Sci.* 57, 422–431. doi: 10.17221/103/2010-JFS

Hlásny, T., and Turčáni, M. (2013). Persisting bark beetle outbreak indicates the unsustainability of secondary Norway spruce forests: case study from Central Europe. *Ann. For. Sci.* 70, 481–491. doi: 10.1007/s13595-013-0279-7

Holzinger, R., Lee, A., Paw, U. K. T., and Goldstein, A. H. (2005). Observations of oxidation products above a forest imply biogenic emissions of very reactive compounds. *Atmos.Chem. Phys.* 5, 67–75. doi: 10.5194/acp-5-67-2005

Hoshika, Y., Moura, B., and Paoletti, E. (2018). Ozone risk assessment in three oak species as affected by soil water availability. *Env. Sci. Pollut. Res.* 25, 8125–8136. doi: 10.1007/s11356-017-9786-7

Hůnová, I. (2017). Measurement of ground-level ozone in Czech mountain forests: what we have learnt from using diffusive samplers. *Eur. J. Environ. Sci.* 7, 125–129. doi: 10.14712/23361964.2017.11

Hůnová, I., and Bäumelt, V. (2018). Observation-based trends in ambient ozone in the Czech Republic over the past two decades. *Atmos. Environ.* 172, 157–167. doi: 10.1016/j.atmosenv.2017.10.039

Hůnová, I., Horálek, J., Schreiberová, M., and Zapletal, M. (2012). Ambient ozone exposure in Czech forests: a GIS-based approach to spatial distribution assessment. *Scient. World J.* 2012:123760. doi: 10.1100/2012/123760

Hůnová, I., Kurfürst, P., and Baláková L. (2019). Areas under high ozone and nitrogen loads are spatially disjunct in Czech forests. *Sci. Total Environ.* 656, 567–575. doi: 10.1016/j.scitotenv.2018.11.371

Hůnová, I., Matoušková L., Srněnský, R., and Koželková, K. (2011). Ozone influence on native vegetation in the Jizerske hory Mts. of the Czech Republic: results based on ozone exposure and ozone-induced visible symptoms. *Env. Monit. Assess.* 183, 501–515. doi: 10.1007/s10661-011-1935-8

Hůnová, I., Novotný, R., Uhlírová, H., Vráblík, T., Horálek, J., Lomský, B. et al. (2010). The impact of ambient ozone on mountain spruce forests in the Czech Republic as indicated by malondialdehyde. *Environ. Pollut.* 158, 2393–2401. doi: 10.1016/j.envpol.2010.04.006

Hůnová, I., and Schreiberová, M. (2012). Ambient ozone phytotoxic potential over the Czech forests as assessed by AOT40. *iFor. Biogeosci. Forestr.* 5, 153–162. doi: 10.3832/ifor0617-005

Hůnová, I., Stoklasová, P., Schovánková, J., and Kulasová, A. (2016). Spatial and temporal trends of ozone distribution in the Jizerské hory Mountains of the Czech Republic. *Env. Sci. Pollut. Res.* 23, 377–387. doi: 10.1007/s11356-015-5258-0

Jonson, J. E., Simpson, D., Fageerli, H., and Solberg, S. (2006). Can we explain the trends in European ozone levels? *Atmos.Chem. Phys.* 6, 51–66. doi: 10.5194/acp-6-51-2006

Jurán, S., Palozzi, E., Guidolotti, G., Fares, S., Sigut, L., Calfapietra, C., Alivernini, A. et al. (2017). Fluxes of biogenic volatile organic compounds above temperate Norway spruce forest of the Czech Republic. *Agricult. For. Meteorol.* 232, 500–513. doi: 10.1016/j.agrformet.2016.10.005

Kolár, T., Cermák, P., Oulehle, F, Trnka, M., Štěpánek, P., Cudlín, P. et al. (2015). Pollution control enhanced spruce growth in the "Black Triangle" near the Czech-Polish border. *Sci. Total Environ.* 538, 708–711. doi: 10.1016/j.scitotenv.2015.08.105

Kovač-Andrič, E., Brana, J., and Gvozdič, V. (2009). Impact of meteorological factors on ozone concentrations modelled by time series analysis and multivariate statistical methods. *Ecol. Inform.* 4, 117–122. doi: 10.1016/j.ecoinf.2009.01.002

Krupa, S., McGrath, M. T., Andersen, C. P., Booker, F. L., Burkey, K. O., Chappelka, A. H., et al. (2001). Ambient ozone and plant health. *Plant Dis.* 85, 4–12. doi: 10.1094/PDIS.2001.85.1.4

Laothawornkitkul, J., Taylor, J. E., Paul, N. D., and Hewit, C. N. (2009). Biogenic volatile organic compounds in the Earth system. *New Phytol.* 183, 27–51. doi: 10.1111/j.1469-8137.2009.02859.x

Lelieveld, J., Butler, T. M., Crowley, J. N., Dillon, T. J., Fischer, H., Ganzeveld, L., et al. (2008). Atmospheric oxidation capacity sustained by a tropical forest. *Nature* 452, 737–740. doi: 10.1038/nature06870

Little, R. J. A., and Rubin, D. B. (2002). *Statistical Analysis with Missing Data*. 2nd edn. New York, NY: Wiley. doi: 10.1002/9781119013563

Manning, W. J. (2005). Establishing a cause and effect relationship for ambient ozone exposure and tree growth in the forest: progress and an experimental approach. *Environ. Pollut.* 137, 443–454. doi: 10.1016/j.envpol.2005.01.031

Matyssek, R., Bytnerowicz, A., Karlsson, P.-E., Paoletti, E., Sanz, M., Schaub, M., et al. (2007). Promoting the O_3 flux concept for European forest trees. *Environ. Pollut.* 146, 587–607. doi: 10.1016/j.envpol.2006.11.011

Ministry of Agriculture (2015). *Information on Forests and Forestry in the Czech Republic by 2014*, Prague: Ministry of Agriculture of the Czech Republic.

Monks, P. S., Archibald, A. T., Colette, A., Cooper, O., Coyle, M., Derwent, R., et al. (2015). Tropospheric ozone and its precursors from the urban to the global scale from air quality to short-lived climate forcer. *Atmos. Chem. Phys.* 15, 8889–8973. doi: 10.5194/acp-15-8889-2015

Oikonomakis, E., Aksoyoglu, S., Ciarelli, G., Baltensperger, U., and Prevot, A. S. H. (2018). Low modeled ozone production suggests underestimation of precursor emissions (especially NOx) in Europe. *Atmos.Chem. Phys.* 18, 2175–2198. doi: 10.5194/acp-18-2175-2018

Özbay, B., Keskin, G. A., Dogruparmark, S. C., and Ayberk, S. (2011). Multivariate methods for ground-level ozone modeling. *Atmos. Res.* 102, 57–65. doi: 10.1016/j.atmosres.2011.06.005

Pajtík, J., Cihák, T., Konopka, B, Merganičová, K., and Fabiánek, P. (2018). Annual tree mortality and felling rates in the Czech Republic and Slovakia over three decades. *Centr. Eur. Forestr. J.* 64, 238–248. doi: 10.1515/forj-2017-0048

Paoletti, E., De Marco, A., Beddows, D. C. S., Harrison, R. M., and Manning, W. J. (2014). Ozone levels in European and USA cities are increasing more than at rural sites, while peak values are decreasing. *Environ. Pollut.* 192, 295–299. doi: 10.1016/j.envpol.2014.04.040

Paoletti, E., Materassi, A., Fasano, G., Hoshika, Y., Carriero, G., Silaghi, D., et al. (2017). A new-generation 3D ozone FACE (free Air Controlled Exposure). *Sci. Total Environ.* 575, 1407–1414. doi: 10.1016/j.scitotenv.2016.09.217

Paoletti, E., Schaub, M., Matyssek, R., Wieser, G., Augustaitis, A., Bastrup-Birk, A. M., et al. (2010). Advances of air pollution science: from forest decline to multiple-stress effects on forest ecosystem services. *Environ. Pollut.* 158, 1986–1989. doi: 10.1016/j.envpol.2009.11.023

Pavón-Domínguez, P., Jiménez-Hornero, F. J., and Gutiérrez de Ravé, E. (2014). Proposal for estimating ground-level ozone concentrations at urban areas based on multivariate statistical methods. *Atmos. Environ.* 90, 59–70. doi: 10.1016/j.atmosenv.2014.03.032

Pinto, D. M., Blande, J. D., Souza, S. R., Nerf, A.-M., and Holopainen, J. K. (2010). Plant Volatile Organic Compounds (VOCs) in Ozone (O3) polluted atmospheres: the ecological effects. *J. Chem. Ecol.* 36, 22–34. doi: 10.1007/s10886-009-9732-3

Prinn, R. G. (2003). "Ozone, hydroxyl radical, and oxidative capacity," in *The Atmosphere; Treatise in Geochemistry*, Vol. 4, eds R. F. Keeling, H. D. Holland, and K. K. Turekian (Oxford: Elsevier-Pergamon), 1–19.

Pudasainee, D., Sapkota, B., Shrestha, M. L., Kaga, A., Kondo, A., and Inoue, Y. (2006). Ground level ozone concentrations and its association with NO_x and meteorological parameters in Kathmandu valley, Nepal. *Atmos. Environ.* 40, 8081–8087. doi: 10.1016/j.atmosenv.2006.07.011

Pusede, S. E., Steiner, A. L., and Cohen, R. C. (2015). Temperature and recent trends in the chemistry of continental surface ozone. *Chem. Rev.* 115, 3898–3918. doi: 10.1021/cr5006815

Pyrgou, A., Hadjinicolau, P., and Santamouris, M. (2018). Enhanced near-surface ozuone under heatwave conditions in a Mediterranean island. *Sci. Rep.* 8:9191. doi: 10.1038/s41598-018-27590-z

R core (2008). *A Language and Environment for Statistical Computing*. Vienna: R Foundation for Statistical computing. Avaliable online at: http://www.R-project.org/ (accessed May 5, 2018).

Rajab, J. M., Matjafri, M. Z., and Lim, H. S. (2013). Combining multiple regression and principal component analysis for accurate predictions for column ozone in Peninsular Malaysia. *Atmos. Environ.* 71, 36–43. doi: 10.1016/j.atmosenv.2013.01.019

Rawlings, J. O., Pantula, S. G., and Dickey, D. A. (1998). *Applied Regression Analysis. A Research Tool,* 2nd Edn. New York, NY: Springer. doi: 10.1007/b98890

Romer, P. S., Duffey, K. C., Woolridge, P. J., Edgerton, E., Baumann, K., Feiner, P. A., et al. (2018). Effects of temperature-dependent NO_x emissions on continental ozone production. *Atmos.Chem. Phys.* 18, 2601–2614. doi: 10.5194/acp-18-2601-2018

Roschina, V. V., and Roschina, V. D. (2003). *Ozone and Plant Cell.* Dordrecht: Kluwer.

Sandermann, H., Wellburn, A. R., and Heath, R. L. (eds.) (1997). *Forest Decline and Ozone: A Comparison of Controlled Chambers and Field Experiments. Ecological Studies 127*. Berlin: Springer. doi: 10.1007/978-3-642-59233-1

Schlink, U., Dorling, S., Pelikan, E., Nunnari, G., Cawley, G., et al. (2003). A rigorous inter-comparison of ground-level ozone predictions. *Atmos. Environ.* 37, 3237–3253. doi: 10.1016/S1352-2310(03)00330-3

Seinfeldt, J. H., and Pandis, S. N. (1998). *Atmospheric Chemistry and Physics: From Air Pollution to Climate Change, 3rd Edn.* New York, NY: John Wiley & Sons.

Sicard, P., Anav, A., De Marco, A., and Paoletti, E. (2017). Projected global ground-level ozone impacts on vegetation under different emission and climate scenarios. *Atmos.Chem. Phys.* 17, 12177–12196. doi: 10.5194/acp-17-12177-2017

Sicard, P., De Marco, A., Troussier, F., Renou, C., Vas, N., and Paoletti, E. (2013). Decrease in surface ozone concentrations at Mediterranean remote sites and increase in the cities. *Atmos. Environ.* 79, 705–715. doi: 10.1016/j.atmosenv.2013.07.042

Sillman, S. (1999). The relation between ozone, NO_x and hydrocarbons in urban and polluted rural environments. *Atmos. Environ.* 33, 1821–1845. doi: 10.1016/S1352-2310(98)00345-8

Singh, O. N., and Fabian, P. (2003). *Atmospheric Ozone: A Millenium Issue. EGU Special Publication Series 1.* Berlin: Copernicus, 147.

Solomon, P., Cowling, E., Hidy, G., and Furiness, C. (2000). Comparison of scientific findings from major ozone field studies in North America and Europe. *Atmos. Environ.* 34, 1885–1920. doi: 10.1016/S1352-2310(99)00453-7

Sousa, S. I. V., Martins, F. G., Pereira, M. C., and Alvim-Ferraz, M. C. M. (2006). Prediction of ozone concentrations in Oporto city with statistical approaches. *Chemosphere* 64, 1141–1149. doi: 10.1016/j.chemosphere.2005.11.051

Šrámek, V., Novotný, R., Bednárová, M., and Uhlírová, H. (2007). Monitoring of ozone risk for forest in the Czech Republic: preliminary results. *Scient. World J.* 7, 78–83. doi: 10.1100/tsw.2007.84

Šrámek, V., Novotný, R., Vejpustková, M., Hůnová, I., and Uhlírová, H. (2012). Monitoring of ozone effects on the vitality and increment of Norway spruce and European beech in the Central European forests. *J. Environ. Monitor.* 14, 1696–1702. doi: 10.1039/c2em10964f

Štěpánek, P., Zahradníček, P., Farda, A., Skalák, P., Trnka, M., Meitner, J., et al. (2016). Projection of drought-inducing climate conditions in the Czech Republic according to Euro-CORDEX models. *Climate Res.* 70, 179–193. doi: 10.3354/cr01424

Tan, Z., Lu, K., Jiang, M., Su, R., and Dong, H., Zeng, L., et al. (2018). Exploring ozone pollution in Chengdu, southwestern China: a case study from radical chemistry to O_3-VOC-NO_x sensitivity. *Sci. Total Environ.* 636, 775–786. doi: 10.1016/j.scitotenv.2018.04.286

Tarasova, O. A., and Karpetchko, A.Y. (2003). Accounting for local meteorological effects in the ozone time-series of Lovozero (Kola Peninsula). *Atmos.Chem. Phys.* 3, 941–949. doi: 10.5194/acp-3-941-2003

Thompson, M. L., Reynolds, J., Cox, L. H., Guttorp, P., and Sampson, P. D. (2001). A review of statistical methods for the meteorological adjustment of tropospheric ozone. *Atmos. Environ.* 35, 617–630. doi: 10.1016/S1352-2310(00)00261-2

Trnka, M., Brázdil, R., Možný, M., Štěpánek, P., Dobrovolný, P., Zahradníček, P., et al. (2015). Soil moisture trends in the Czech republic between 1961 and 2012. *Int. J. Climatol.* 35, 3733–3747. doi: 10.1002/joc.4242

UN/ECE (2004). *Mapping Manual Revision. UN-ECE Convention on Long-Range Transboundary Air Pollution. Manual on the Methodologies and Criteria for Modelling and Mapping Critical Loads and Levels and Air Pollution Effects, Risks and Trends*. Avaliable online at: https://www.umweltbundesamt.de/publikationen/manual-on-methodologies-criteria-for-modelling

Vacek, S., Bílek, L., Schwarz, O., Hejcmanová, P., and Mikeska, M. (2013). Effect of air pollution on the health status of spruce stands. *Mt. Res. Dev.* 33, 40–50. doi: 10.1659/MRD-JOURNAL-D-12-00028.1

Vacek, S., Hůnová, I., Vacek, Z., Hejcmanová, P., Podrázský, V., Král, J., et al. (2015). Effects of air pollution and climatic factors on Norway spruce forests in the Orlické hory Mts. (Czech Republic), 1979–2014. *Eur. J. For. Res.* 134, 1127–1142. doi: 10.1007/s10342-015-0915-x

Vingarzan, R. (2004). A review of surface ozone background levels and trends. *Atmos. Environ.* 38, 3431–3442. doi: 10.1016/j.atmosenv.2004.03.030

Vlasáková-Matoušková, L., and Hůnová, I. (2015). Stomatal ozone flux and visible leaf injury in native juvenile trees of *Fagus sylvatica* L.: a field study from the Jizerske hory Mts., the Czech Republic. *Environ. Sci. Pollut. Res.* 22, 10034–10046. doi: 10.1007/s11356-015-4174-7

Waldner, P., Schaub, M., Graf Pannatier, E., Schmitt, M., Thimonier, A., and Walthert, L. (2007). Atmospheric deposition and ozone levels in Swiss forests: are critical values exceeded? *Environ. Monit. Assess.* 128, 5–17. doi: 10.1007/s10661-006-9411-6

Wang, T., Xue, L., Brimblecombe, P., Lam, Y. F., Li, L., and Zhang, L. (2017). Ozone pollution in China: A review of concentrations, meteorological influences, chemical precursors, and effects. *Sci. Total Environ.* 575, 1582–1596. doi: 10.1016/j.scitotenv.2016.10.081

Wood, S. N. (2006). *Generalized Additive Models: An Introduction With R*, London: Chapman and Hall/CRC. doi: 10.1201/9781420010404

Yan, Y., Pozzer, A., Ojha, N., Liu, J., and Lelieveld, J. (2018). Analysis of European ozone trends in the period 1995–2014. *Atmos.Chem. Phys.* 18, 5589–5605. doi: 10.5194/acp-18-5589-2018

Zahradník, P., and Zahradníková, M. (2019). Salvage felling in the Czech Republic's forests during the last twenty years. *Centr. Eur. Forestr. J.* 65, 12–20. doi: 10.2478/forj-2019-0008

Zapletal, M., Pretel, J., Chroust, P., Cudlín, P., Edwards-Jonášová, M., Urban, O., et al. (2012). The influence of climate change on stomatal ozone flux to a mountain Norway spruce forest. *Environ. Pollut.* 169, 267–273. doi: 10.1016/j.envpol.2012.05.008

Zemankova, K., and Brechler, J. (2010). Emissions of biogenic VOC from forest ecosystems in central Europe: estimation and comparison with anthropogenic emission inventory. *Environ. Pollut.* 158, 462–469. doi: 10.1016/j.envpol.2009.08.032

Conflict of Interest Statement: The authors declare that the research was conducted in the absence of any commercial or financial relationships that could be construed as a potential conflict of interest.

frontiers
in Forests and Global Change

ORIGINAL RESEARCH
published: 25 June 2019
doi: 10.3389/ffgc.2019.00026

A New Modeling Approach for Estimating Abiotic and Biotic Stress-Induced *de novo* Emissions of Biogenic Volatile Organic Compounds From Plants

Rüdiger Grote [1], Monica Sharma [2,3], Andrea Ghirardo [3] and Jörg-Peter Schnitzler [3]*

[1] Institute of Meteorology and Climate Research - Atmospheric Environmental Research, Karlsruhe Institute of Technology, Garmisch-Partenkirchen, Germany, [2] Faculty of Geosciences, Geoengineering and Mining, Technische Universität Bergakademie Freiberg, Freiberg, Germany, [3] Research Unit Environmental Simulation (EUS), Helmholtz Zentrum München, Munich, Germany

The emission of biogenic volatile organic compounds (BVOCs) is usually thought to depend on species-specific emission capacities that vary with seasonal and phenological conditions. Actual—so called constitutive—emissions are then calculated from prevailing temperature and radiation. However, various abiotic and biotic stressors such as ozone, extreme radiation and temperature conditions, as well as wounding e.g., from insect feeding, can lead to *de-novo* emissions of stress-induced BVOCs (sBVOCs) that may excel constitutive emissions by more than an order of magnitude. These emissions often have a considerable different compound composition and are short-lived but can prolong under continuous stress for quite some time. Thus, they may easily have a large impact on overall regional BVOC emissions. However, sBVOCs are generally not considered in models since up to date no consistent mechanism has been proposed. This manuscript suggests a new mechanism based on the finding that sBVOCs originate from a handful of biosynthetic pathways which synthesize compounds in the groups of monoterpenes, sesquiterpenes, and green leave volatiles, as well as methyl salicylate, ethanol/acetaldehyde, methanol/formaldehyde, and acetone. Isoprene is also considered but since it is often constitutively emitted, the specific role of stress induction is difficult to determine for this compound. A function is proposed that describes the production of all *de-novo* sBVOCs sufficiently well and scales with stress intensity. It is hypothesized that the response delay and the form of the function is specific for the production pathway and valid for ozone as well as wounding (herbivory) induced stress. Model parameters are then derived from pooled literature data based on a meta-analysis of suitable induction-response measurements of different plant species. The overall emission amount derives from the intensity and frequency of the stress impulse. We present a number of literature studies that are used to parameterize the new model as well as a selection of evaluations for single- and multiple-stress inductions. Furthermore, coupling and interaction with constitutive emission models as well as limitations and possible further developments are discussed.

Keywords: ozone impact, herbivory, wounding, oxidative stress, induced emissions, BVOCs, modeling

Edited by:
Silvano Fares,
Council for Agricultural and Economics Research, Italy

Reviewed by:
Steffen M. Noe,
Estonian University of Life Sciences, Estonia
Guy Schurgers,
University of Copenhagen, Denmark

***Correspondence:**
Rüdiger Grote
ruediger.grote@kit.edu

Specialty section:
This article was submitted to Forests and the Atmosphere, a section of the journal Frontiers in Forests and Global Change

Received: *06 March 2019*
Accepted: *20 May 2019*
Published: *25 June 2019*

Citation:
Grote R, Sharma M, Ghirardo A and Schnitzler J-P (2019) A New Modeling Approach for Estimating Abiotic and Biotic Stress-Induced de novo Emissions of Biogenic Volatile Organic Compounds From Plants. Front. For. Glob. Change 2:26. doi: 10.3389/ffgc.2019.00026

INTRODUCTION

Volatile organic compounds (VOCs) are important precursors for the formation of tropospheric ozone and secondary aerosols (Shallcross and Monks, 2000; Atkinson and Arey, 2003). Excessively high ozone concentrations in the lower atmosphere are representing a considerable threat to human health, causing yield losses in agriculture and forestry, and reduce carbon sequestration as well as other ecosystem services (Wilkinson et al., 2012; Lombardozzi et al., 2015; Silva et al., 2017). Secondary aerosols or fine and ultrafine particles are also causing pulmonary diseases, directly affect the radiation regime of the atmosphere, and are important cloud condensation nuclei (Riipinen et al., 2012; Shrivastava et al., 2017). A considerable share of VOCs originates from biogenic emissions (BVOCs) (Laothawornkitkul et al., 2009). Therefore, in order to evaluate the most efficient air pollution reduction strategies, it is important to know the quantity and composition of BVOC emissions from different plant sources and thus their spatial and temporal distribution.

BVOC emissions have been studied since the late 1980's and relationships between some main compounds and environmental conditions have been quantified for many plant species. This led to the general distinction between constitutive and induced emissions, assuming continuously developing boundary conditions to drive the first, and oxidative and mechanical stress to trigger the second (Litvak and Monson, 1998; Brilli et al., 2009; Ali et al., 2011; Joo et al., 2011; Jiang et al., 2016; Copolovici et al., 2017). Constitutive emissions are described based on genetically determined emission potentials and the ability to form compound-specific VOC storages in different types of plant tissues and organs. Various environmental conditions are responsible for the expression of this species-specific potential, from which temperature and radiation are the most important ones, both for short- and longer-term impacts. Water availability affects BVOC emission directly and indirectly and may act in different directions dependent on stress severity. CO_2 and nutrient availability do also change BVOC emission intensity but possible connections to production pathways are numerous and the exact mechanism is yet not fully elucidated (Grote et al., 2013).

In contrast, BVOC emissions may also occur as responses to specific stressors. Such stressors can be oxidative stress originating from excessive light, temperature and air pollutants, or mechanical stress such as biting, sucking, cutting, or wounding including abrasion due to wind movement (Haase et al., 2011) and membrane damages due to freeze/thaw cycles (Fall et al., 2001). Although the drivers can be abiotic or biotic, the plant internal signal cascades and thus the responses of plants are often similar (Iriti and Faoro, 2009). One of the reasons for this surprising fact is that the kind of provoked damages are often the same, i.e., destroyed or impaired membrane functions which causes changes in plasma trans-membrane potential and cytosolic Ca^{2+}concentration (Dicke and Baldwin, 2010). Another reason may be that the same substances that are used for repair of and protection against oxidative stress also serve for signaling in order to repel parasites or attract enemies of herbivores (Cape, 2008; Loreto and Schnitzler, 2010). In fact, many of the volatile terpenes that serve as antioxidative defenses, are also non-specific toxins active against a wide range of organisms (bacteria, fungi, plants, and animals) (Meena et al., 2017). Nevertheless, the large variety of the emitted compounds and the species-specific as well as stress-specific emission intensity results in a multitude of different possible blends (Kravitz et al., 2016).

Numerous structurally quite different molecules can be produced but oxygenated VOCs, and more specifically green leaf volatiles (GLVs), constitute a general element in most blends of induced emissions, in particular aldehydes, alcohols and acetates (Blande et al., 2014). The emission is generally proportional to the extent of wounding (Mithöfer et al., 2005; Niinemets et al., 2013; Portillo-Estrada et al., 2015) and occurs in attached or detached leaves. Other relevant sBVOCs are the C11 homoterpene dimethyl-nonatriene (DMNT) and the volatile benzoid methyl salicylate (MeSA). Emissions of DMNT have often been found in response to herbivore attack (e.g., Vuorinen et al., 2004b; Ibrahim et al., 2008; Tholl et al., 2011; Copolovici et al., 2014) but also as a response to ozone (Behnke et al., 2009; Carriero et al., 2016). Similarly, MeSA is often associated with ozone responses (e.g., Hartikainen et al., 2012; Cardoso-Gustavson et al., 2014; Li et al., 2017; Bison et al., 2018) but is similarly common in herbivore induced emission blends (Vuorinen et al., 2007; Kigathi et al., 2009). Since isoprene and terpenoids help to mitigate any kind of membrane damage, their production may be induced or upregulated in response to abiotic as well as biotic stress (Litvak et al., 1999; Prieme et al., 2000; Brilli et al., 2011; Achotegui-Castells et al., 2013; Faiola et al., 2015; Semiz et al., 2017; Kanagendran et al., 2018b; Visakorpi et al., 2018) but may also been downregulated in favor of GLVs (Brilli et al., 2009; Copolovici et al., 2017). The up-regulation of terpenoids have been found to increase the emissions by a factor of ∼10–20 in response to needle damages of feeding insects (Ghimire et al., 2017) as well as to bark beetle infestations (Amin et al., 2012, 2013).

Similar to constitutive emissions, induced compounds may be *de-novo* produced or released from storages when the diffusive resistance is decreased by wounding of any kind. In some plant species, storages in specific tissues occur from which volatiles can be released that reduce the attractiveness of tissues for herbivores and protect wounds from getting infected by microbes and fungi. As far as we know, not all stored compounds but only monoterpenes are released from such storages (Litvak and Monson, 1998; Clancy et al., 2016), possibly because of their antibiotic properties (e.g., Michelozzi, 1999). Therefore, most induced BVOCs are directly emitted after production but a clear differentiation between emissions from storages and *de-novo* production cannot be given, except if the emissions are directly related to increased resin flow (Baier et al., 2002; Eller et al., 2013). It should be noted that wounding includes cutting which is a widespread management activity in grasslands and forests. In fact, it is known that grasslands and pastures do release high amounts of GLVs after cutting which origin from *de-novo* production, in particular alcohols (Karl et al., 2001; Warneke et al., 2002; Davison et al., 2008). Therefore, it has been hypothesized that the large transient fluxes caused by cutting could be in the same order of magnitude as constitutive emissions from undisturbed pasture. Considering induced emissions thus would virtually double emission estimates from these ecosystems (Kirstine et al., 1998). Forest harvests and thinning are by definition much less frequent. Nevertheless, a thinning of half the trees in a Scots pine forests has triggered a monoterpene release from wounded tissue that was 40 times the constitutive emission rate (Schade and Goldstein, 2003).

Induced emissions from abiotic as well as biotic disturbances can thus be considered as extremely important as they can increase short- and medium term BVOC fluxes by at least one order of magnitude. They also have a different blend than emissions in undisturbed conditions. Nevertheless, there is currently no relationship implemented in emission models that account for induced emissions in response to air pollution, insect gradations, or mechanical disturbances although this issue has been recognized as important (Arneth and Niinemets, 2010). The only approach that we are aware of uses experimentally determined relations between stress-induced and constitutive emissions to quantify the impact of spruce aphids in the field (Bergström et al., 2014). A general model that relates induced emissions to stress severity and intensity is thus still missing. We therefore suggest a globally applicable approach that describes induced emission strength directly in dependence on environment and can be parameterized for different species. We hypothesize that all compounds synthesized by a specific pathway have the same dynamics (delay time between stress and emission and duration of emission after a single stress event) and only stress sensitivity depends on species. This enables to pool normalized data from various compounds and species for parametrization. We thus use experimental data obtained from a meta-analysis investigating ozone as well as herbivore-induced BVOC emission pattern. The new algorithm is then applied on three independent data sets that either use ozone or herbivores as stressors over a defined time period so that simulated and measured emissions could be compared for different compound emissions over the course of several days.

MODEL DEVELOPMENT AND PARAMETERIZATION

Due to a lack of clear indication of storage-related induced emissions and in order to keep the approach simple, we only consider compound releases that originate from *de-novo* synthesis. *De-novo* synthesis in response to wounding generally occurs within very short time periods after the induction event independent of the kind of induction. For example, maximum emission rates of acetaldehyde were reached within minutes after the start of the treatment (Portillo-Estrada et al., 2015). This type of behavior is well-represented with the so-called Fraser-Suzuki function (Equation 1) which has first been used to describe band shapes (Fraser and Suzuki, 1969) and is still popular for the representation of chemical responses (Stankovic et al., 2018).

$$\mathbf{E_i} = e^{\left[-\frac{\ln(2)}{Fdel_i^{2}}\left(\ln\left(\frac{Fdel_i(t-t_0)}{Fbr_i}\right)\right)^2\right]} \tag{1a}$$

$$\mathbf{E_i}' = \mathbf{E_i}\, Fsc\, \mathbf{NSE} \tag{1b}$$

E_i being the emission rate for the compound "I", *Fdel* and *Fbr* are parameters that define the delay of the exponential increase with time and the broadness of the function, respectively. *Fsc* is a species- and compound-specific scaling parameter that describes the maximum response per unit stress, and NSE is the number of stress events during a time interval ($t-t_0$). This implies that the emission response scales linearly with the experienced stress severity, which is an assumption that holds some pitfalls. Regarding ozone, Carriero et al. (2016) indeed describe a weak linear response of induced emissions. However, the response should be related to ozone uptake (Li et al., 2017) while there is not always a linear relation between uptake and ozone exposure. Thus, responses to exposure might change for example with stomatal acclimation or damage. Emission in response to herbivore damage is linearly related to damaged tissue (e.g., Niinemets et al., 2013) and an increasing number of individuals should be related to NSE, while differences in stress intensity—that might be related to the different kind of damages (such as sucking and biting)—are difficult to determine yet. The responsiveness of the function to changes of parameters is demonstrated in **Figure 1** (with *Fsc* set to 1 in all simulations). It demonstrates that small *Fbr* values result in left-skewed distributions that develop to into Gaussian distributions and increase their width when increasing. *Fdel* shifts the whole distribution to the right, accounting for response delays that occur in particular when emitted compounds need to be *de-novo* synthesized.

We assume that specific compounds are always produced in a similar way, respectively by a specific synthesis pathway, which enables representing the dynamics of this pathway generaly and refrain from species-specific parameterization. Thereby we differentiate between 12 compounds that are produced from 7 pathways (**Figure 2**). The indications of pathways are based on previous publications (Pare and Tumlinson, 1997; Kesselmeier and Staudt, 1999; Laothawornkitkul et al., 2009; Loreto and Schnitzler, 2010; Schnitzler et al., 2010; Tholl et al., 2011; Dudareva et al., 2013; McCormick et al., 2014b). If this assumption holds, the production of sBVOC emissions can be described with compound-specific emission parameters and the

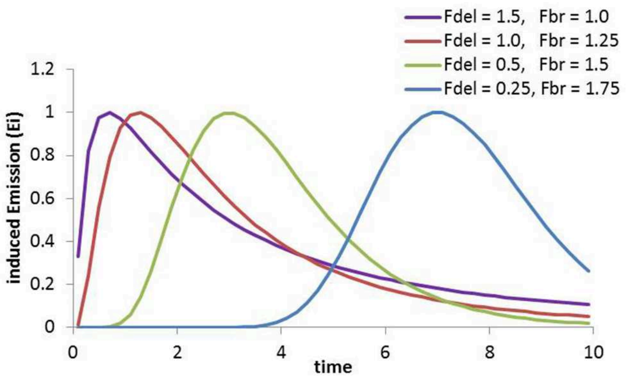

FIGURE 1 | Sensitivity of the Fraser-Suzuki function to changes in the parameters. The unit of time is not specific but a reasonable order of magnitude would be hours for the distributions shown.

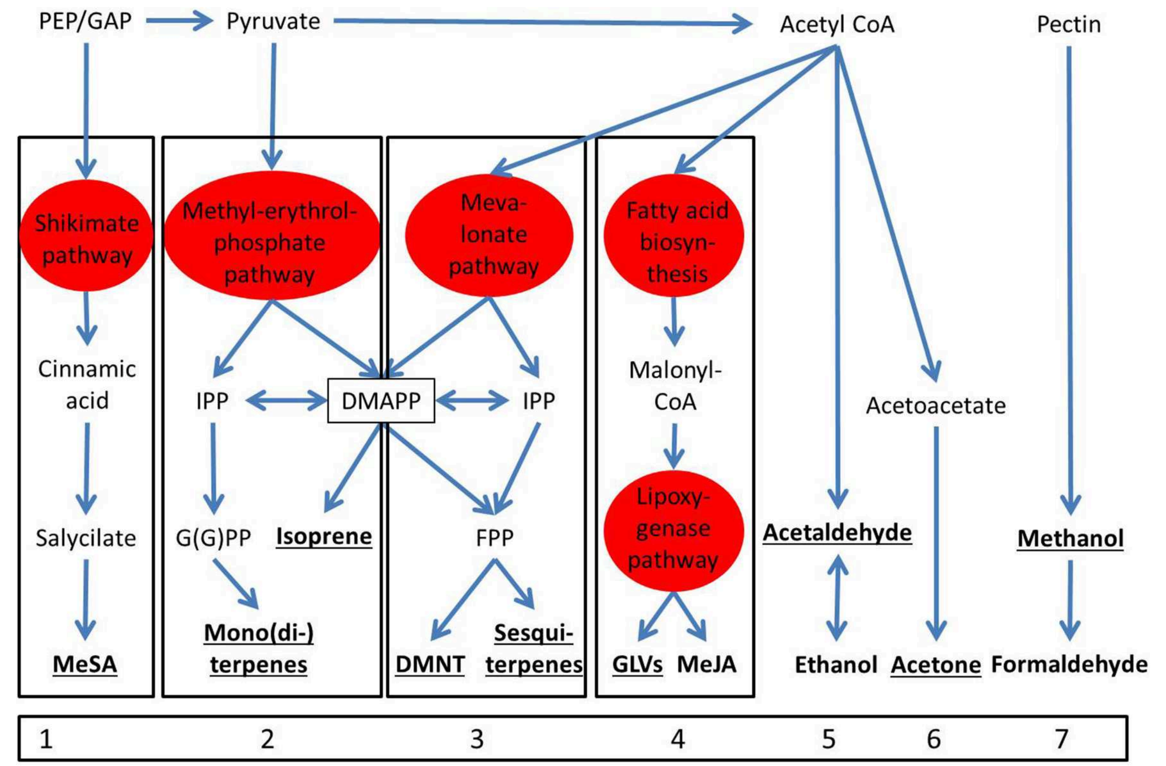

FIGURE 2 | Biosynthetic pathways of the major compounds that are emitted from induction (numbered 1–7). The potentially emitted compounds are indicated in bold letters from which those that are investigated here are underlined. Pathways that comprise several intermediate products are shown in red. (abbreviations: PEP, phenolenolpyruvate; GAP, glyceraldehyde 3-phosphate; MeSA, methyl salicylate; IPP, isopentenyl diphosphate; G(G)PP, geranylgeranyl pyrophosphate; DMAPP, dimethylallyl pyrophosphate; FPP, farnesyl pyrophosphate; DMNT, (*E*)-4,8-dimethyl-1,3,7-nonatriene; GLVs, green leaf volatiles; MeJA, methyl jasmonate). Despite their common components, the methylerythritol phosphate (MEP) and the mevalonate pathway (MVP) are distinguished because they are occurring in the plastids and in the cytosol, respectively.

intensity of the response is simply scaled with the parameter *Fsc*, including the option to be set to 0 in case a specific compound emission is below the detection threshold.

In order to parameterize the emission pattern of the different compounds we have collected data from 11 studies that are providing response patterns for 9 of the 12 compounds (MeSA, monoterpenes, DMNT, sesquiterpenes, GLVs, acetaldehyde, acetone, and methanol) from all of the seven pathways. From these studies, five use ozone as the inducing abiotic stress (Beauchamp et al., 2005; Behnke et al., 2009; Pazouki et al., 2016; Li et al., 2017; Acton et al., 2018), six others apply biotic stressors and one both (Kanagendran et al., 2018b). From the abiotic stress experiments, two have exposed experimental plants to real insects (Mengistu et al., 2014; Yli-Pirilä et al., 2016), while four studies use mechanical wounding (Brilli et al., 2011; Erb et al., 2015; Portillo-Estrada et al., 2015; Kanagendran et al., 2018b) and two studies applied methyl-jasmonate (Faiola et al., 2015; Jiang et al., 2017) to mimic herbivory. Data are extracted from the literature either directly using the Engauge digitizer 10.11 software or from presented graphs by determining the turning points of emission developments. These data have been normalized for stress intensity (setting the largest obtained emission rate as 1) and parameters of Equation 1 are defined for each of the investigated 9 compounds (using the solver tool in Excel, Microsoft Cooperation).

During the exploration of the data, we noticed that several compounds typically exhibit a bimodal emission pattern to one single stress event, i.e., monoterpenes, sesquiterpenes, GLVs, and methanol. The pattern is characterized by a fast response that peaks within the first 30 min after stress induction and is quickly fading thereafter. In parallel and without any further stress event, a slower response builds up within 5–15 h which needs ∼1–2 days to fade out. However, the pattern has not been observed in all investigations which might partly be related to methods that are too coarse to detect such fast responses (Behnke et al., 2009; Pazouki et al., 2016; Acton et al., 2018; Kanagendran et al., 2018a). In these cases, normally only the second peak is described in the publication. We considered the bimodal pattern by introducing a second emission term into Equation 1b:

$$\mathbf{E_j}' = \left(\mathbf{E_{fast\_j}}\, \boldsymbol{Fsc}_{\mathbf{fast\_j}} + \mathbf{E_{slow\_j}}\, \boldsymbol{Fsc}_{\boldsymbol{slow\_}\mathbf{j}} \mathbf{EA_j}'\right) \mathbf{NSE} \tag{2a}$$

$$\mathbf{EA_j}' = \mathbf{EA} + \alpha - \mu\mathbf{EA} \tag{2b}$$

E_{fast} and E_{slow} are calculated according to equation 1a with separately derived parameters for delay and broadness (*Fdel, Fbr*) (see **Table 1**). The indicator "j" represents the six compounds for which this differentiation is used (monoterpenes, sesquiterpenes, GLVs, MeSA, methanol, and DMNT). It should be noted, however, that only for monoterpenes, GLVs, and methanol (only in ozone-induced emissions) this pattern has actually observed simultaneously in one or more of the datasets. For sesquiterpenes, fast and slow responses originate from different datasets: for MeSA and DMNT only the slow response is backed by experimental data, and regarding DMNT the data are from one experimental source only (Behnke et al., 2009). While no short-term response has been recorded, the similarity of the response to that of methanol let us assume that a fast response might have occurred but gone unnoticed since the first measurements have been carried out after 3 h. Similarly, the currently used data sets for MeSA emissions seem to indicate that a fast induction response is minor or non-existent but other studies report strongly increased emissions only 1 h after stress exposure (Filella et al., 2006). Therefore, we decided to assume a short term response for both of these compounds too. The remaining three compounds show only fast responses derived from one single observation each, although a slow response cannot be excluded since the measurement might not have been long enough. Simulated mono- and bimodal responses for all investigated compound groups are presented in **Figure 3**, distinguished into data from herbivory and ozone stressed plants.

While the fast emission term is assumed to rely on available precursors, the slow emission term represents the intermediates supply from biosynthesis pathways that requires enzymatic reactions. Enzyme activity (EA) is regulated on biochemical level by fast activation/deactivation and on a protein level requiring a gene expression and respective protein biosynthesis. To represent the development of EA we assume a protein synthesis rate (α) that linearly increases enzyme activity during the period where stress events occur and a constant protein decomposition rate (μ). Both parameters are given per unit of time (e.g., 1 h). This approach is similar to the one developed for the build-up of isoprene synthase activity (Lehning et al., 2001) although widely simplified since no temperature dependency is implemented so far. Two further restrictions to the enzyme production term are applied: First, enzyme formation only starts after a threshold time period (*Td*) that accounts for a delay between stress application and signal recognition and processing. Again, we assume that this threshold period is compound specific and does not change with species or stress type. Second, while protein degradation is independent of the diurnal cycle, biosynthesis of the compounds only occurs in the model during the light phase, assuming that the biochemical precursors need to be supplied from photosynthetic intermediates and not from storages. The parameters *Td*, α, μ for all compounds as derived from experiments where stress was applied over a certain period of time (not as pulse) and which prolonged over several days (see below), are given in **Table 1**.

TABLE 1 | Parameter values for Equations (1) and (2) as estimated for different inducible compounds from published studies.

	Fast *Fdel*	*Fbr*	Slow *Fdel*	*Fbr*	*Td (h)*	α (h^{-1})	μ (h^{-1})
Acetaldehyde	0.7	0.02	–	–	–	–	–
Acetone	0.7	0.28	–	–	–	–	–
DMNT	1.0	0.7	0.4	4.0	6.0	0.3	0.3
GLVs	0.3	0.7	0.5	3.0	2.0	0.2	0.2
Isoprene	0.7	0.025	–	–	–	–	–
Methanol	0.7	0.8	0.55	5.0	nv	nv	nv
MeSA	0.8	0.8	0.5	3.0	7.0	0.2	0.4
Monoterpenes	1.4	1.0	0.7	3.0	6.0	0.5	0.25
Sesquiterpenes	1.0	0.7	0.45	3.5	8.0	0.2	0.2

nv, not validated and indicates that no data were available to define the dynamic properties of the slow response of induced emissions.

EVALUATION RESULTS

In order to evaluate the derived and parameterized function, we used three literature sources that provide emission responses to 5 h of ozone fumigation (Heiden et al., 1999) or 1.5–2 days of herbivore exposure (Ghirardo et al., 2012; McCormick et al., 2014a). Emissions of selective GLVs, monoterpenes, and sesquiterpenes were calculated before, during and after the respective induction signal that prolonged during a certain period (from the green to the red arrows in **Figures 4–6**). Since emissions from one signal are not faded out before the next signal occurs, emissions at a particular point in time may originate from several induction events if these events occur in shorter time intervals than complete fading is achieved. The overall emission strength is scaled with the *Fsc* parameter that is linearly related to a specific induction interval. The examples presented are simulated for a time interval of 1 h, a time resolution frequently used by mechanistic models. Since GLVs and monoterpene emissions were also observed before stress induction, these compounds are assumed to be emitted also constitutively. This fraction has therefore been separately calculated using Equation 1 and has been added into the sum of total emission displayed in **Figures 4**, **5**. Parameters for control emissions are adjusted to measurements and are: *Fdel* 1.5, *Fbr* 20, *Fsc* for GLV: 50, *Fsc* for MONO: 30 (**Figure 4**), 2 (**Figure 5**). Note that the broadness parameter is relatively large, leading to a function maximum toward the end of the day. The driver ($t-t_0$) is the daytime since sunrise and the emission is set to 0 during dark hours, reflecting the assumption that control emissions are directly related to photosynthesis. It should also be noted that parameters for enzyme kinetics (*Td*, α, μ) are not parameterized separately for each evaluation data set but are set independent from the plant species or the kind of stress.

DISCUSSION AND CONCLUSION

Despite a rather huge number of investigations regarding induced BVOCs, still only few data are available providing high resolution continuous measurements for the main emission types and compounds. Thus, our meta-analysis sometimes only

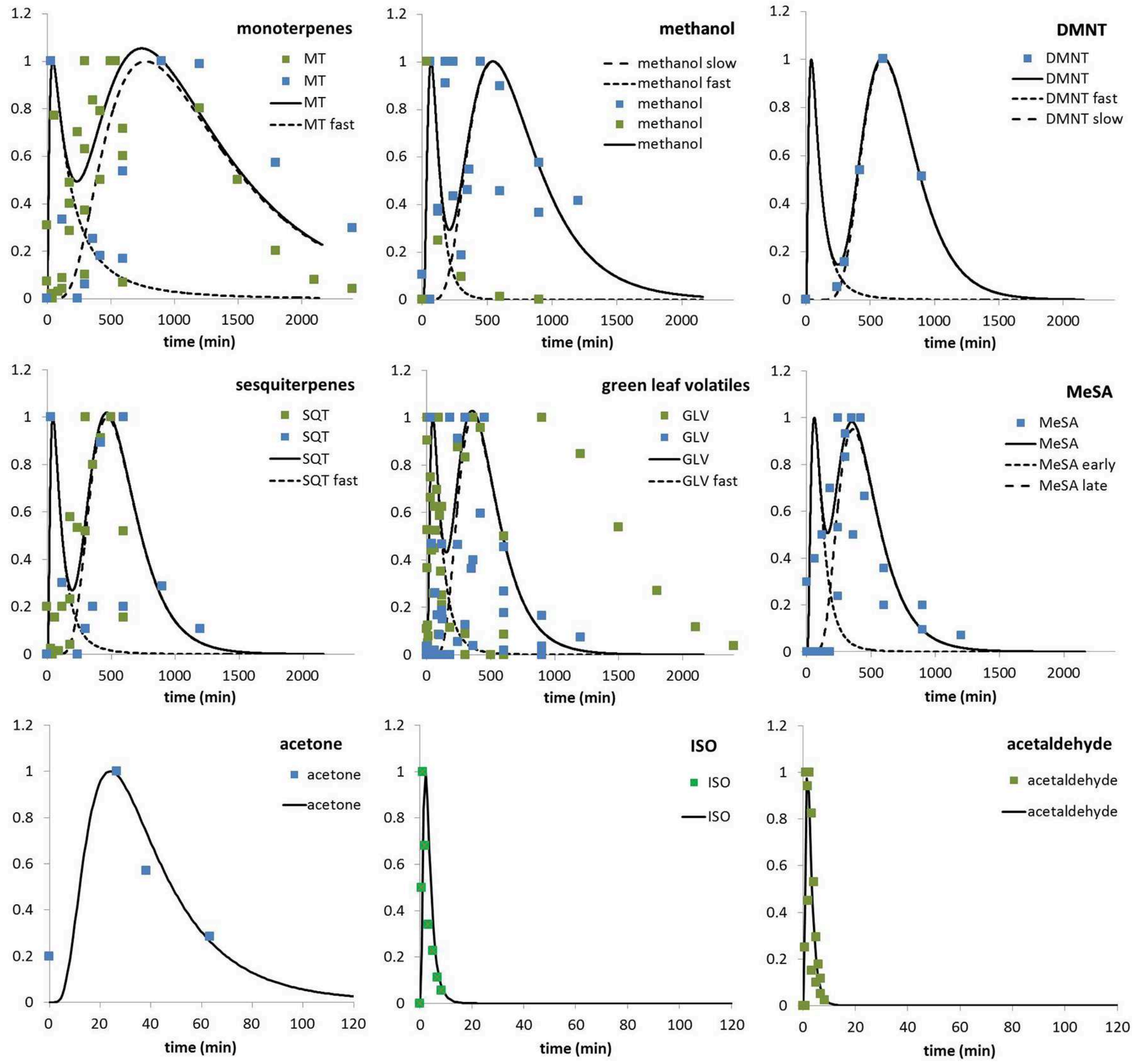

FIGURE 3 | Normalized temporal development of emissions in response to induced ozone (blue dots) and herbivory (green dots) stress as derived from 13 publications (5 for ozone, 7 for herbivory, and one for both). Lines are representing simulated transients of emissions. In case of bi-model developments, the single representations for slow and fast responses are separately normalized as indicated with broken lines. Compounds are sorted according to response time. It should be noted that the last row is given in a different temporal scale than the rows above. See text for literature sources.

yielded one or few datasets per compound group that not always covered a period necessary to determine short- as well as long-term responses. Nevertheless, it is interesting to note that the general pattern of immediate responses that are fueled by existing biochemical precursors in combination with responses that develop and decompose on an hourly time scale as proposed by Jiang et al. (2017) is persistent throughout the investigated plant species. It also seems to apply for ozone as well as herbivory-induced stress which supports the view that plant stress which reduces primary production simultaneously enhances secondary metabolic pathways (Iriti and Faoro, 2009) and that responses may have developed due to adaptive co-evolution (Vuorinen et al., 2004a). However, plant species might still only display either immediate or slow responses and specific volatile compounds within one compound group seem to show a rather large variability regarding reaction speed and decay of the emission rates. Accordingly, the data base for parameterization and possible further differentiation of compound groups should be elaborated when new data will become available. The precision of modeling might also be increased if the intensity of the stress events could be normalized, which particularly relates to methyl-jasmonate treatments where the induction is supposed to start at the time of spraying while the arrival time at sensitive sites in the leaves and the actually effective dose is not defined (Jiang et al., 2017). Similar, ozone treatments might differ in their effectiveness depending whether the ozone dose induces an acute or chronic response and on the physiological state of the plant, in particular regarding uptake resistance of stomata and mesophyll.

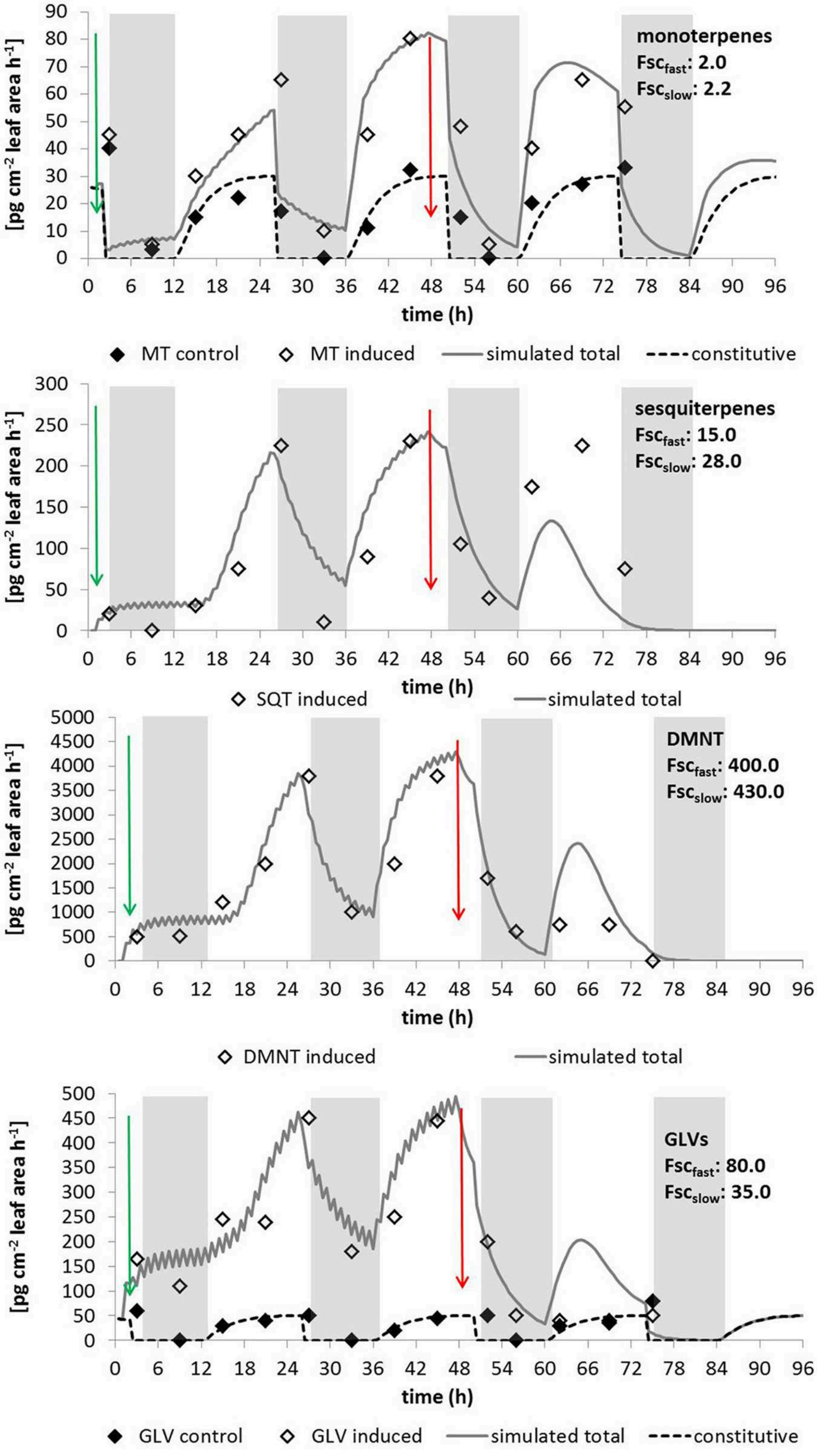

FIGURE 4 | Simulated and measured emissions of (from the top to the bottom) α-pinene, β-caryophyllene, DMNT, and the GLV hexenyl acetate which are typical representatives for the indicated emission types. Data are taken from McCormick et al. (2014a) measured at young poplar trees (*Populus nigra*) exposed to gypsy moth larvae (*Lymantria dispar*). Shaded areas denote dark periods without *de-novo* biosynthesis; green arrows show the start of the exposure to larvae and red arrows the end of larvae feeding. Indicated scaling parameters are given for 1-h induction cycles; for other parameters see text and **Table 1**.

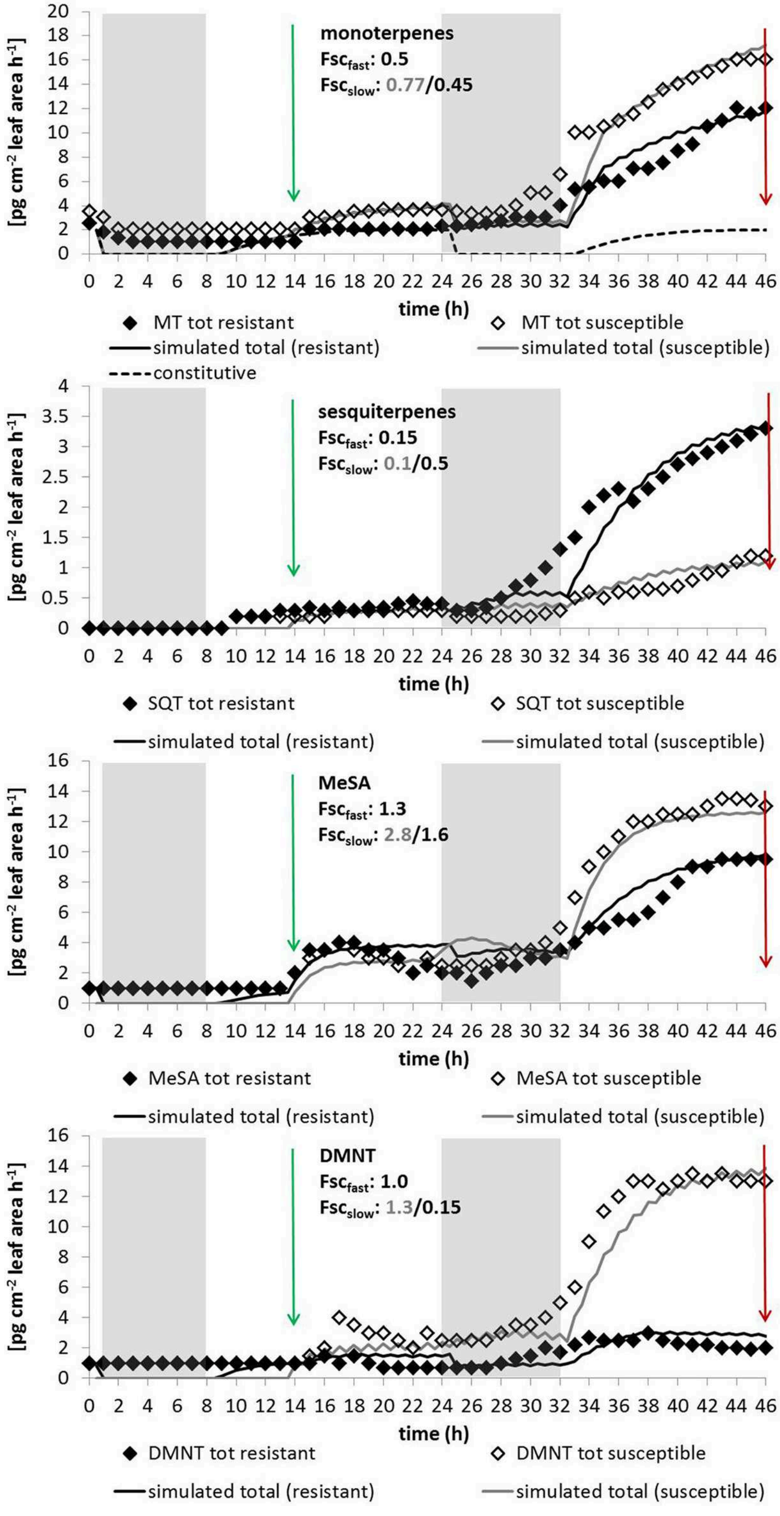

FIGURE 5 | Simulated and measured emissions of (from the top to the bottom) pooled monoterpenes and sesquiterpenes, as well as of MeSA and DMNT for plants that are susceptible (gray lines and open symbols) and tolerant (black lines and closed symbols) to caterpillar feeding. Data are taken from Ghirardo et al. (2012) measured on young oak seedlings (*Quercus robur*) exposed to larvae of *Tortrix viridana*. Shaded areas denote dark periods without *de-novo* biosynthesis; green arrows show the start of the larvae exposure and red arrows the end of larvae feeding. Indicated scaling parameters are given for 1-h induction cycles; for other parameters see **Table 1**.

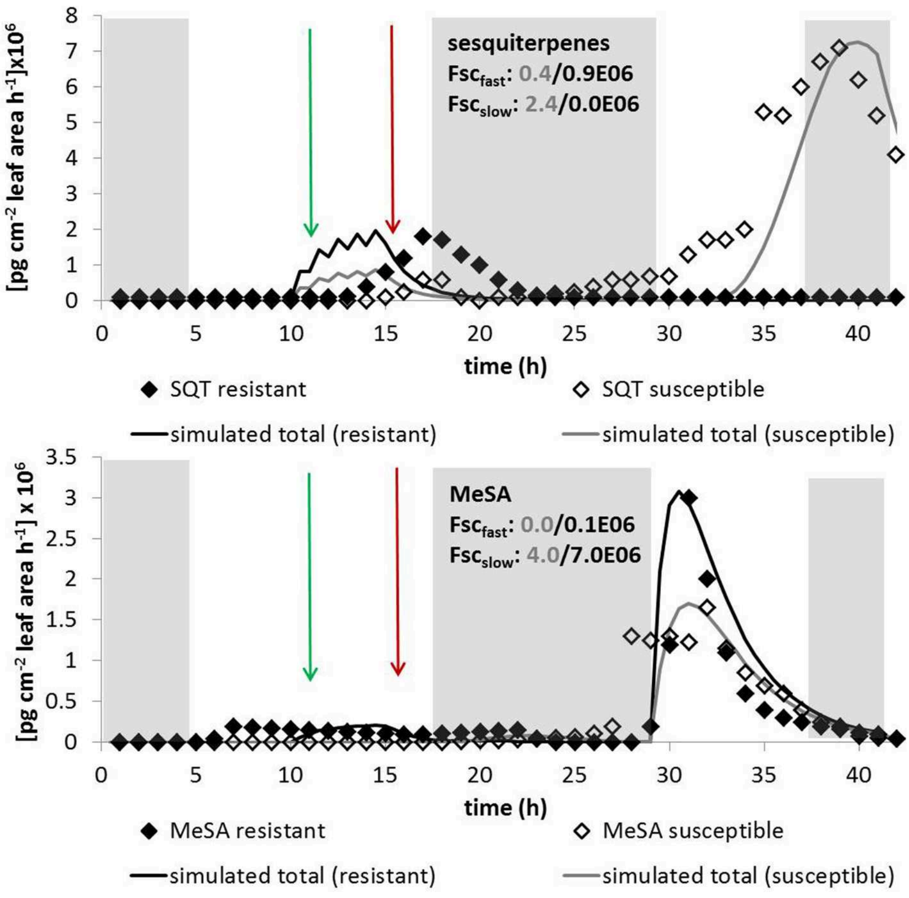

FIGURE 6 | Simulated and measured emissions of the sesquiterpene valencene (top) and MeSA (bottom) for susceptible (gray lines and open symbols) and stress tolerant variants (black lines and closed symbols). Data are taken from Heiden et al. (1999) measured at tobacco plants (*Nicotiana tabacum*) exposed to ozone. Shaded areas denote dark periods without *de-novo* biosynthesis; green arrows show the start and red arrows the end of the fumigation. Indicated scaling parameters are given for 1-h induction cycles; for other parameters see **Table 1**.

The latter point indicates a general link to ecosystem models since uptake resistance certainly depends on drought stress—an issue that often coincides with high ozone episodes as well as herbivore abundance.

Simple assumptions about the kinetics of enzyme formation and degradation with time only differentiating between night- and day-time dynamics enabled scaling of emission responses over several days. Simulations using the same parameters per emission type were in good accordance with measurements, independent from the kind of stress (caterpillar feeding or ozone fumigation). Remaining differences indicate that enzyme biosynthesis and hence the increase in biosynthetic capacity also occurs during nighttime explaining the start of slow-response emissions even before the light is switched on again (Heiden et al., 1999; Ghirardo et al., 2012). Also, the applied 1-h time step showed to lead to small oscillations of emissions originating from fast responses, indicating that a higher temporal resolution would be preferable. Nevertheless, the presented scaling procedure provides a mechanistic basis for further emission estimations at the stand- or ecosystem scale, considering total foliage area and stress abundance. In case of herbivore damage, the situation is more complicated since the leaf area is dynamically reduced during feeding, an effect that has to be considered during extended disturbance events. Also, the number of herbivores are difficult to estimate and develop dynamically, requiring a separate model approach (Pitt et al., 2007; Trnka et al., 2007; Pinkard et al., 2010; Battaglia et al., 2011).

It should be noted that the assumption of a constant effectiveness of induced emissions so that emission responses scale with stress severity might not always hold. This is because a continuous stress can trigger an adjustment of the plant so that the sensitivity to the stress decreases with time (Achotegui-Castells et al., 2015). The adjustment might include increased uptake resistances for air pollution or the production of compounds that are difficult to digest by herbivores. In addition, also BVOCs, i.e., mono- and sesquiterpenes can reduce the effectiveness of induced stressors as they can detoxify ozone already within the leaf (Vickers et al., 2009) and might directly repel herbivores or indirectly reduce their impact by attracting predators (Meena et al., 2017; Turlings and Erb, 2018). In general, very strong or prolonged induction is also likely to pose a feedback to stress-induced emissions since it decreases the amount of emitting tissue (i.e., by herbivore feeding) and damages the photosynthetic process (i.e., due to ozone) thus leading to supply limitation (Visakorpi et al., 2018). Such limitation may also be triggered by other stressors such as drought as has been demonstrated in a field study by Scott et al. (2019). In this case, specific site conditions and plant behavior would need to be considered for whole-ecosystem estimations.

We also acknowledge that an explicit dependence on temperature could serve the general applicability of the approach. It is obvious that the speed of biosynthesis and thus in particular the slow-response term should depend on this impact. However, available data and the practice to keep temperatures constant during experiments to concentrate on the exposure effect didn't allow to incorporate the temperature effect yet. The suggested model for sBVOC emissions is based on simple assumptions regarding the emission behavior of the most common compounds but also accounts for species-specific differences in stress sensitivity as well as stress severity and duration. It can be applied in addition to simulating constitutive emission without necessary interactions. Therefore in can easily be combined with temperature and light dependent models (Guenther, 1999; Niinemets et al., 1999; Monson et al., 2012; Grote et al., 2014). Consistency could be assured simply by using leaf area or biomass for scaling in both approaches. Coupled to ecosystem models, the approach could contribute to an improved ability to estimate climate change impacts on air chemistry by considering the secondary effects that originate from increased insect aggregations (Seidl et al., 2017) and ozone concentrations (Sicard et al., 2017).

The proposed model describes emission responses to oxidative and wounding stress by compound and stress severity. In addition, the strength of emission response seems to be species-specific although a comparison of experimental results is hampered due to different stress intensities applied. If it is assumed that the parameterization is independent of further environmental conditions and that stress intensity could be generally defined (e.g., as feeding intensity of one insect per time period), it should be possible to scale modeled emissions to the ecosystem level (e.g., based on estimates of insect number and activity). Such an endeavor, however, demands for future experiments with relevant plant species and insect-plant combinations as well as for large-scale field measurements for evaluation. For evaluation purposes, further processes such as the dynamic development of stress needs to be considered. This might be more easy for stress related to air pollution than to insect abundance and development, the latter requiring dynamic gradation models (Nedorezov and Sadykova, 2015). In addition, likely physiological adaptations or increased resource competition of herbivores might render the assumption of a linear stress-response relation invalid, which demands for further model refinements. Nevertheless, we suppose that despite these challenges the model could eventually contribute to the determination of full BVOC emission inventories.

DATA AVAILABILITY

The raw data supporting the conclusions of this manuscript will be made available by the authors, without undue reservation, to any qualified researcher.

AUTHOR CONTRIBUTIONS

RG has developed and parameterized the model while MS conducted the meta-analysis and extracted the data to be compared with model outputs. J-PS and AG contributed substantially to the model concept and design of the work and supported the use of data produced in their laboratory. All co-authors worked on the data analysis, wrote text passages, and critically revised the text.

ACKNOWLEDGMENTS

We acknowledge support by Deutsche Forschungsgemeinschaft and Open Access Publishing Fund of Karlsruhe Institute of Technology.

REFERENCES

Achotegui-Castells, A., Danti, R., Llusià, J., Rocca, G. D., Barberini, S., and Peñuelas, J. (2015). Strong induction of minor terpenes in Italian Cypress, *Cupressus sempervirens*, in response to infection by the fungus *Seiridium cardinale*. *J. Chem. Ecol.* 41, 224–243. doi: 10.1007/s10886-015-0554-1

Achotegui-Castells, A., Llusià, J., Hódar, J., and Peñuelas, J. (2013). Needle terpene concentrations and emissions of two coexisting subspecies of Scots pine attacked by the pine processionary moth (*Thaumetopoea pityocampa*). *Acta Physiol. Plantarum* 35, 3047–3058. doi: 10.1007/s11738-013-1337-3

Acton, W. J. F., Jud, W., Ghirardo, A., Wohlfahrt, G., Hewitt, C. N., Taylor, J. E., et al. (2018). The effect of ozone fumigation on the biogenic volatile organic compounds (BVOCs) emitted from *Brassica napus* above- and below-ground. *PLoS ONE* 13:e0208825. doi: 10.1371/journal.pone.0208825

Ali, J. G., Alborn, H. T., and Stelinski, L. L. (2011). Constitutive and induced subterranean plant volatiles attract both entomopathogenic and plant parasitic nematodes. *J. Ecol.* 99, 26–35. doi: 10.1111/j.1365-2745.2010.01758.x

Amin, H., Atkins, P. T., Russo, R. S., Brown, A. W., Sive, B., Hallar, A. G., et al. (2012). Effect of bark beetle infestation on secondary organic aerosol precursor emissions. *Environ. Sci. Technol.* 46, 5696–5703. doi: 10.1021/es204205m

Amin, H. S., Russo, R. S., Sive, B., Hoebeke, R. E., Dodson, C., McCubbin, I. B., et al. (2013). Monoterpene emissions from bark beetle infested Engelmann spruce trees. *Atmos. Environ.* 72, 130–133. doi: 10.1016/j.atmosenv.2013.02.025

Arneth, A., and Niinemets, Ü. (2010). Induced BVOCs: how to bug our models? *Trends Plant Sci.* 15, 118–125. doi: 10.1016/j.tplants.2009.12.004

Atkinson, R., and Arey, J. (2003). Gas-phase tropospheric chemistry of biogenic volatile organic compounds: a review. *Atmos. Environ.* 37, 197–219. doi: 10.1016/S1352-2310(03)00391-1

Baier, P., Führer, E., Kirisits, T., and Rosner, S. (2002). Defence reactions of Norway spruce against bark beetles an the associated fungus *Ceratocystis polonica* in secondary pure and mixed species stands. *Forest Ecol. Manage.* 159, 73–86. doi: 10.1016/S0378-1127(01)00711-3

Battaglia, M., Pinkard, E. A., Sands, P. J., Bruce, J. L., and Quentin, A. (2011). Modelling the impact of defoliation and leaf damage on forest plantation function and production. *Ecol. Modelling* 222, 3193–3202. doi: 10.1016/j.ecolmodel.2011.06.017

Beauchamp, J., Wisthaler, A., Hansel, A., Kleist, E., Miebach, M., Niinemets, Ü., et al. (2005). Ozone induced emissions of biogenic VOC from tobacco: relationships between ozone uptake and emission of LOX products. *Plant Cell Environ.* 28, 1334–1343. doi: 10.1111/j.1365-3040.2005.01383.x

Behnke, K., Kleist, E., Uerlings, R., Wildt, J., Rennenberg, H., and Schnitzler, J.-P. (2009). RNAi-mediated suppression of isoprene biosynthesis in hybrid poplar impacts ozone tolerance. *Tree Physiol.* 29, 725–736. doi: 10.1093/treephys/tpp009

Bergström, R., Hallquist, M., Simpson, D., Wildt, J., and Mentel, T. F. (2014). Biotic stress: a significant contributor to organic aerosol in Europe? *Atmos. Chem. Phys.* 14, 13643–13660. doi: 10.5194/acp-14-13643-2014

Bison, J. V., Cardoso-Gustavson, P., de Moraes, R. M., da Silva Pedrosa, G., Cruz, L. S., Freschi, L., et al. (2018). Volatile organic compounds and nitric oxide as responses of a Brazilian tropical species to ozone: the emission profile of young and mature leaves. *Environ. Sci. Pollut. Res.* 25, 3840–3848. doi: 10.1007/s11356-017-0744-1

Blande, J. D., Holopainen, J. K., and Niinemets, Ü. (2014). Plant volatiles in a polluted atmosphere: stress response and signal degradation. *Plant Cell Environ.* 37, 1892–1904. doi: 10.1111/pce.12352

Brilli, F., Ciccioli, P., Frattoni, M., Prestininzi, M., Spanedda, A. F., and Loreto, F. (2009). Constitutive and herbivore-induced monoterpenes emitted by *Populus × euroamericana* leaves are key volatiles that orient *Chrysomela populi* beetles. *Plant Cell Environ.* 32, 542–552. doi: 10.1111/j.1365-3040.2009.01948.x

Brilli, F., Ruuskanen, T. M., Schnitzhofer, R., Müller, M., Breitenlechner, M., Bittner, V., et al. (2011). Detection of plant volatiles after leaf wounding and darkening by proton transfer reaction "Time-of-Flight" mass spectrometry (PTR-TOF). *PLoS ONE* 6:e20419. doi: 10.1371%2Fjournal.pone.0020419

Cape, J. N. (2008). Interactions of forests with secondary air pollutants: some challenges for future research. *Environ. Pollut.* 155, 391–397. doi: 10.1016/j.envpol.2008.01.038

Cardoso-Gustavson, P., Bolsoni, V. P., de Oliveira, D. P., Guaratini, M. T., Aidar, M. P., Marabesi, M. A., et al. (2014). Ozone-induced responses in *Croton floribundus* spreng. *(Euphorbiaceae):* metabolic cross-talk between volatile oganic compounds and calcium oxalate crystal formation. *PLoS ONE* 9:e105072. doi: 10.1371/journal.pone.0105072

Carriero, G., Brunetti, C., Fares, S., Hayes, F., Hoshika, Y., Mills, G., et al. (2016). BVOC responses to realistic nitrogen fertilization and ozone exposure in silver birch. *Environ. Pollut.* 213, 988–995. doi: 10.1016/j.envpol.2015.12.047

Clancy, M. V., Zytynska, S. E., Senft, M., Weisser, W. W., and Schnitzler, J.-P. (2016). Chemotypic variation in terpenes emitted from storage pools influences early aphid colonisation on tansy. *Sci. Rep.* 6:38087. doi: 10.1038/srep38087

Copolovici, L., Kännaste, A., Remmel, T., and Niinemets, Ü. (2014). Volatile organic compound emissions from *Alnus glutinosa* under interacting drought and herbivory stresses. *Environ. Exp. Bot.* 100, 55–63. doi: 10.1016/j.envexpbot.2013.12.011

Copolovici, L., Pag, A., Kännaste, A., Bodescu, A., Tomescu, D., Copolovici, D., et al. (2017). Disproportionate photosynthetic decline and inverse relationship between constitutive and induced volatile emissions upon feeding of *Quercus robur* leaves by large larvae of gypsy moth (*Lymantria dispar*). *Environ. Exp. Bot.* 138, 184–192. doi: 10.1016/j.envexpbot.2017.03.014

Davison, B., Brunner, A., Ammann, C., Spirig, C., Jocher, M., and Neftel, A. (2008). Cut-induced VOC emissions from agricultural grasslands. *Plant Biol.* 10, 76–85. doi: 10.1055/s-2007-965043

Dicke, M., and Baldwin, I. T. (2010). The evolutionary context for herbivore-induced plant volatiles: beyond the 'cry for help'. *Trends Plant Sci.* 15, 167–175. doi: 10.1016/j.tplants.2009.12.002

Dudareva, N., Klempien, A., Muhlemann, J. K., and Kaplan, I. (2013). Biosynthesis, function and metabolic engineering of plant volatile organic compounds. *New Phytol.* 198, 16–32. doi: 10.1111/nph.12145

Eller, A. S. D., Harley, P., and Monson, R. K. (2013). Potential contribution of exposed resin to ecosystem emissions of monoterpenes. *Atmos. Environ.* 77, 440–444. doi: 10.1016/j.atmosenv.2013.05.028

Erb, M., Veyrat, N., Robert, C. A. M., Xu, H., Frey, M., Ton, J., et al. (2015). Indole is an essential herbivore-induced volatile priming signal in maize. *Nat. Commun.* 6:6273. doi: 10.1038/ncomms7273

Faiola, C. L., Jobson, B. T., and VanReken, T. M. (2015). Impacts of simulated herbivory on volatile organic compound emission profiles from coniferous plants. *Biogeosciences* 12, 527–547. doi: 10.5194/bg-12-527-2015

Fall, R., Karl, T., Jordon, A., and Lindinger, W. (2001). Biogenic C5VOCs: release from leaves after freeze-thaw wounding and occurrence in air at a high mountain observatory. *Atmos. Environ.* 35, 3905–3916. doi: 10.1016/S1352-2310(01)00141-8

Filella, I., Peñuelas, J., and Llusia, J. (2006). Dynamics of the enhanced emissions of monoterpenes and methyl salicylate, and decreased uptake of formaldehyde, by *Quercus ilex* leaves after application of jasmonic acid. *New Phytol.* 169, 135–144. doi: 10.1111/j.1469-8137.2005.01570.x

Fraser, R. D. B., and Suzuki, E. (1969). Resolution of overlapping bands. Functions for simulating band shapes. *Anal. Chem.* 41, 37–39. doi: 10.1021/ac60270a007

Ghimire, R. P., Kivimäenpää, M., Kasurinen, A., Häikiö, E., Holopainen, T., and Holopainen, J. K. (2017). Herbivore-induced BVOC emissions of Scots pine under warming, elevated ozone and increased nitrogen availability in an open-field exposure. *Agric. Forest Meteorol.* 242, 21–32. doi: 10.1016/j.agrformet.2017.04.008

Ghirardo, A., Heller, W., Fladung, M., Schnitzler, J.-P., and Schroeder, H. (2012). Function of defensive volatiles in pedunculate oak (*Quercus robur*) is tricked by the moth *Tortrix viridana*. *Plant Cell Environ.* 35, 2192–2207. doi: 10.1111/j.1365-3040.2012.02545.x

Grote, R., Monson, R., and Niinemets, Ü. (2013). "Leaf-level models of constitutive and stress-driven volatile organic compound emissions," in *Biology, Controls and Models of Tree Volatile Organic Compound Emission*, eds Ü. Niinemets and R. K. Monson (Dordrecht: Springer), 315–355.

Grote, R., Morfopoulos, C., Niinemets, Ü., Sun, Z., Keenan, T. F., Pacifico, F., et al. (2014). A fully integrated isoprenoid emissions model coupling emissions to photosynthetic characteristics. *Plant Cell Environ.* 37, 1965–1980. doi: 10.1111/pce.12326

Guenther, A. (1999). "Modeling biogenic volatile organic compound emissions to the atmosphere," in *Reactive Hydrocarbons in the Atmosphere*, ed C. N. Hewitt (San Diego, CA: Academic Press), 41–94.

Haase, K. B., Jordan, C., Mentis, E., Cottrell, L., Mayne, H. R., Talbot, R., et al. (2011). Changes in monoterpene mixing ratios during summer storms in rural New Hampshire (USA). *Atmos. Chem. Phys.* 11, 11465–11476. doi: 10.5194/acp-11-11465-2011

Hartikainen, K., Riikonen, J., Nerg, A. M., Kivimäenpää, M., Ahonen, V., Tervahauta, A., et al. (2012). Impact of elevated temperature and ozone on the emission of volatile organic compounds and gas exchange of silver birch (*Betula pendula* Roth). *Environ. Exp. Bot.* 84, 33–43. doi: 10.1016/j.envexpbot.2012.04.014

Heiden, A. C., Hoffmann, T., Kahl, J., Kley, D., Klockow, D., Langebartels, C., et al. (1999). Emission of volatile organic compounds from ozone-exposed plants. *Ecol. Appl.* 9, 1160–1167. doi: 10.2307/2641386

Ibrahim, M. A., Stewart-Jones, A., Pulkkinen, J., Poppy, G. M., and Holopainen, J. K. (2008). The influence of different nutrient levels on insect-induced plant volatiles in Bt and conventional oilseed rape plants. *Plant Biol.* 10, 97–107. doi: 10.1111/j.1438-8677.2007.00013.x

Iriti, M., and Faoro, F. (2009). Chemical diversity and defence metabolism: how plants cope with pathogens and ozone pollution. *Int. J. Mol. Sci.* 10, 3371–3399. doi: 10.3390/ijms10083371

Jiang, Y., Ye, J., Li, S., and Niinemets, Ü. (2017). Methyl jasmonate-induced emission of biogenic volatiles is biphasic in cucumber: a high-resolution analysis of dose dependence. *J. Exp. Bot.* 68, 4679–4694. doi: 10.1093/jxb/erx244

Jiang, Y., Ye, J., Veromann, L.-L., and Niinemets, Ü. (2016). Scaling of photosynthesis and constitutive and induced volatile emissions with severity of leaf infection by rust fungus (*Melampsora larici-populina*) in *Populus balsamifera var.* suaveolens. *Tree Physiol.* 36, 856–872. doi: 10.1093/treephys/tpw035

Joo, E., Dewulf, J., Amelynck, C., Schoon, N., Pokorska, O., Simpraga, M., et al. (2011). Constitutive versus heat and biotic stress induced BVOC emissions in *Pseudotsuga menziesii*. *Atmos. Environ.* 45, 3655–3662. doi: 10.1016/j.atmosenv.2011.04.048

Kanagendran, A., Pazouki, L., Bichele, R., Külheim, C., and Niinemets, Ü. (2018a). Temporal regulation of terpene synthase gene expression in *Eucalyptus globulus* leaves upon ozone and wounding stresses: relationships with stomatal ozone uptake and emission responses. *Environ. Exp. Bot.* 155, 552–565. doi: 10.1016/j.envexpbot.2018.08.002

Kanagendran, A., Pazouki, L., and Niinemets, Ü. (2018b). Differential regulation of volatile emission from *Eucalyptus globulus* leaves upon single and combined ozone and wounding treatments through recovery and relationships with ozone uptake. *Environ. Exp. Bot.* 145, 21–38. doi: 10.1016/j.envexpbot.2017.10.012

Karl, T., Guenther, A., Lindinger, C., Jordan, A., Fall, R., and Lindinger, W. (2001). Eddy covariance measurements of oxygenated volatile organic compound fluxes from crop harvesting using a redesigned proton-transfer-reaction mass spectrometer. *J. Geophys. Res.* 106, 24157–24167. doi: 10.1029/2000JD000112

Kesselmeier, J., and Staudt, M. (1999). Biogenic volatile organic compounds (VOC): an overview on emission, physiology and ecology. *J. Atmos. Chem.* 33, 23–88. doi: 10.1023/A:1006127516791

Kigathi, R. N., Unsicker, S. B., Reichelt, M., Kesselmeier, J., Gershenzon, J., and Weisser, W. W. (2009). Emission of volatile organic compounds after herbivory from *Trifolium pratense* (L.) under laboratory and field conditions. *J. Chem. Ecol.* 35, 1335–1348. doi: 10.1007/s10886-009-9716-3

Kirstine, W., Galbally, I., Ye, Y., and Hooper, M. (1998). Emissions of volatile organic compounds (primarily oxygenated species) from pasture. *J. Geophys. Res.* 103, 10605–10619. doi: 10.1029/97JD03753

Kravitz, B., Guenther, A. B., Gu, L., Karl, T., Kaser, L., Pallardy, S. G., et al. (2016). A new paradigm of quantifying ecosystem stress through chemical signatures. *Ecosphere* 7:e01559. doi: 10.1002/ecs2.1559

Laothawornkitkul, J., Taylor, J. E., Paul, N. D., and Hewitt, C. N. (2009). Biogenic volatile organic compounds in the Earth system. *New Phytol.* 183, 27–51. doi: 10.1111/j.1469-8137.2009.02859x

Lehning, A., Zimmer, W., Zimmer, I., and Schnitzler, J.-P. (2001). Modeling of annual variations of oak (*Quercus robur* L.) isoprene synthase activity to predict isoprene emission rates. *J. Geophys. Res.* 106, 3157–3166. doi: 10.1029/2000JD900631

Li, S., Harley, P. C., and Niinemets, Ü. (2017). Ozone-induced foliar damage and release of stress volatiles is highly dependent on stomatal openness and priming by low-level ozone exposure in *Phaseolus vulgaris*. *Plant Cell Environ.* 40, 1984–2003. doi: 10.1111/pce.13003

Litvak, M. E., Madronich, S., and Monson, R. K. (1999). Herbivore-induced monoterpene emissions from coniferous forest: potential impact on local tropospheric chemistry. *Ecol. Appl.* 9, 1147–1159. doi: 10.2307/2641385

Litvak, M. E., and Monson, R. K. (1998). Patterns of induced and constitutive monoterpene production in conifer needles in relation to insect herbivory. *Oecologia* 114, 531–540. doi: 10.1007/s004420050477

Lombardozzi, D., Levis, S., Bonan, G., Hess, P. G., and Sparks, J. P. (2015). The influence of chronic ozone exposure on global carbon and water cycles. *J. Clim.* 28, 292–305. doi: 10.1175/jcli-d-14-00223.1

Loreto, F., and Schnitzler, J.-P. (2010). Abiotic stresses and induced BVOCs. *Trends Plant Sci.* 115, 154–166. doi: 10.1016/j.tplants.2009.12.006

McCormick, A. C., Boeckler, G. A., Köllner, T. G., Gershenzon, J., and Unsicker, S. B. (2014a). The timing of herbivore-induced volatile emission in black poplar (*Populus nigra*) and the influence of herbivore age and identity affect the value of individual volatiles as cues for herbivore enemies. *BMC Plant Biol.* 14:304. doi: 10.1186/s12870-014-0304-5

McCormick, A. C., Irmisch, S., Reinecke, A., Boeckler, G. A., Veit, D., Reichelt, M., et al. (2014b). Herbivore-induced volatile emission in black poplar: regulation and role in attracting herbivore enemies. *Plant Cell Environ.* 37, 1909–1923. doi: 10.1111/pce.12287

Meena, R. K., Jangra, S., Wadhwa, Z., Wati, M., and Wati, L. (2017). Role of plant volatiles in defense and communication. *Int. J. Curr. Microbiol. App. Sci.* 6, 300–313. doi: 10.20546/ijcmas.2017.604.033

Mengistu, M. M., Kasurinen, A., Yli-Pirilä, P., Joutsensaari, J., Klemola, T., Holopainen, T., et al. (2014). Contrasting responses of silver birch VOC emissions to short- and long-term herbivory. *Tree Physiol.* 34, 241–252. doi: 10.1093/treephys/tpt127

Michelozzi, M. (1999). Defensive roles of terpenoid mixtures in conifers. *Acta Bot. Gallica* 146, 73–84. doi: 10.1080/12538078.1999.10515803

Mithöfer, A., Wanner, G., and Boland, W. (2005). Effects of feeding Spodoptera littoralis on Lima bean leaves. II. Continuous mechanical wounding resembling insect feeding is sufficient to elicit herbivory-related volatile emission. *Plant Physiol.* 137, 1160–1168. doi: 10.1104/pp.104.054460

Monson, R. K., Grote, R., Niinemets, Ü., and Schnitzler, J.-P. (2012). Modeling the isoprene emission rate from leaves. *New Phytol.* 195, 541–559. doi: 10.1111/j.1469-8137.2012.04204.x

Nedorezov, L. V., and Sadykova, D. L. (2015). Dynamics of larch bud moth populations: application of Moran – Ricker models with time lag. *Ecol. Modelling* 297, 26–32. doi: 10.1016/j.ecolmodel.2014.11.003

Niinemets, Ü., Kännaste, A., and Copolovici, L. (2013). Quantitative patterns between plant volatile emissions induced by biotic stresses and the degree of damage. *Front. Plant Sci.* 4:262. doi: 10.3389/fpls.2013.00262

Niinemets, Ü., Tenhunen, J. D., Harley, P. C., and Steinbrecher, R. (1999). A model of isoprene emission based on energetic requirements for isoprene synthesis and leaf photosynthetic properties for *Liquidambar* and *Quercus*. *Plant Cell Environ.* 22, 1319–1335. doi: 10.1046/j.1365-3040.1999.00505.x

Pare, P. W., and Tumlinson, J. H. (1997). *De novo* biosynthesis of volatiles induced by insect herbivory in cotton plants. *Plant Physiol.* 114, 1161–1167. doi: 10.1104/pp.114.4.1161

Pazouki, L., Kanagendran, A., Li, S., Kännaste, A., Memari, H. R., Bichele, R., et al. (2016). Mono- and sesquiterpene release from tomato (*Solanum lycopersicum*) leaves upon mild and severe heat stress and through recovery: from gene expression to emission responses. *Environ. Exp. Bot.* 132, 1–15. doi: 10.1016/j.envexpbot.2016.08.003

Pinkard, E. A., Battaglia, M., Bruce, J., Leriche, A., and Kriticos, D. J. (2010). Process-based modelling of the severity and impact of foliar pest attack on eucalypt plantation productivity under current and future climates. *Forest Ecol. Manage.* 259, 839–847. doi: 10.1016/j.foreco.2009.06.027

Pitt, J. P. W., Régnière, J., and Worner, S. (2007). Risk assessment of the gypsy moth, *Lymantria dispar* (L), in New Zealand based on phenology modelling. *Int. J. Biometeorol.* 51, 295–305. doi: 10.1007/s00484-006-0066-3

Portillo-Estrada, M., Kazantsev, T., Talts, E., Tosens, T., and Niinemets, Ü. (2015). Emission timetable and quantitative patterns of wound-induced volatiles across different leaf damage treatments in Aspen (*Populus Tremula*). *J. Chem. Ecol.* 41, 1105–1117. doi: 10.1007/s10886-015-0646-y

Prieme, A., Knudsen, T. B., Glasius, M., and Christensen, S. (2000). Herbivory by the weevil, *Strophosoma melanogrammum*, causes severalfold increase in emission of monoterpenes from young Norway spruce (*Picea abies*). *Atmos. Environ.* 34, 711–718. doi: 10.1016/S1352-2310(99)00357-X

Riipinen, I., Yli-Juuti, T., Pierce, J. R., Petaja, T., Worsnop, D. R., Kulmala, M., et al. (2012). The contribution of organics to atmospheric nanoparticle growth. *Nat. Geosci.* 5, 453–458. doi: 10.1038/ngeo1499

Schade, G. W., and Goldstein, A. H. (2003). Increase of monoterpene emissions from a pine plantation as a result of mechanical disturbances. *Geophys. Res. Lett.* 30, 1380–1383. doi: 10.1029/2002GL016138

Schnitzler, J.-P., Louis, S., Behnke, K., and Loivamäki, M. (2010). Poplar volatiles – biosynthesis, regulation and (eco)physiology of isoprene and stress-induced isoprenoids. *Plant Biol.* 12, 302–316. doi: 10.1111/j.1438-8677.2009.00284.x

Scott, E. R., Li, X., Kfoury, N., Morimoto, J., Han, W.-Y., Ahmed, S., et al. (2019). Interactive effects of drought severity and simulated herbivory on tea (*Camellia sinensis*) volatile and non-volatile metabolites. *Environ. Exp. Bot.* 157, 283–292. doi: 10.1016/j.envexpbot.2018.10.025

Seidl, R., Thom, D., Kautz, M., Martin-Benito, D., Peltoniemi, M., Vacchiano, G., et al. (2017). Forest disturbances under climate change. *Nat. Clim. Change* 7, 395–402. doi: 10.1038/nclimate3303

Semiz, G., Erbilgin, N., and Holopainen, J. K. (2017). *Hylobius abietis* L. feeding on the novel host *Pinus brutia* Ten. increases emission of volatile organic compounds. *J. Appl. Entomol.* 141, 133–140. doi: 10.1111/jen.12310

Shallcross, D. E., and Monks, P. S. (2000). New directions: a role for isoprene in biosphere–climate–chemistry feedbacks. *Atmos. Environ.* 34, 1659–1660. doi: 10.1016/S1352-2310(99)00483-5

Shrivastava, M., Cappa, C. D., Fan, J., Goldstein, A. H., Guenther, A. B., Jimenez, J. L., et al. (2017). Recent advances in understanding secondary organic aerosol: implications for global climate forcing. *Rev. Geophys.* 55, 509–559. doi: 10.1002/2016rg000540

Sicard, P., Anav, A., De Marco, A., and Paoletti, E. (2017). Projected global tropospheric ozone impacts on vegetation under different emission and climate scenarios. *Atmos. Chem. Phys.* 17, 12177–12196. doi: 10.5194/acp-17-12177-2017

Silva, R. A., West, J. J., Lamarque, J.-F., Shindell, D. T., Collins, W. J., Faluvegi, G., et al. (2017). Future global mortality from changes in air pollution attributable to climate change. *Nat. Clim. Change* 7, 647–651. doi: 10.1038/nclimate3354

Stankovic, B., Jovanovic, J., and Adnadjevic, B. (2018). Application of the Suzuki–Fraser function in modelling the non-isothermal dehydroxylation kinetics of fullerol. *React. Kinetics Mech. Catalysis* 123, 421–438. doi: 10.1007/s11144-018-1380-6

Tholl, D., Sohrabi, R., Huh, J. H., and Lee, S. (2011). The biochemistry of homoterpenes - common constituents of floral and herbivore-induced plant volatile bouquets. *Phytochemistry* 72, 1635–1646. doi: 10.1016/j.phytochem.2011.01.019

Trnka, M., Muska, F., Semeradova, D., Dubrovsky, M., Kocmankova, E., and Zalud, Z. (2007). European Corn Borer life stage model: regional estimates of pest development and spatial distribution under present and future climate. *Ecol. Modelling* 207, 61–84. doi: 10.1016/j.ecolmodel.2007.04.014

Turlings, T. C. J., and Erb, M. (2018). Tritrophic interactions mediated by herbivore-induced plant volatiles: mechanisms, ecological relevance, and application potential. *Annu. Rev. Entomol.* 63, 433–452. doi: 10.1146/annurev-ento-020117-043507

Vickers, C. E., Gershenzon, J., Lerdau, M. T., and Loreto, F. (2009). A unified mechanism of action for volatile isoprenoids in plant abiotic stress. *Nat. Chem. Biol.* 5, 283–291. doi: 10.1038/nchembio.158

Visakorpi, K., Gripenberg, S., Malhi, Y., Bolas, C., Oliveras, I., Harris, N., et al. (2018). Small-scale indirect plant responses to insect herbivory could have major impacts on canopy photosynthesis and isoprene emission. *New Phytol.* 220, 799–810. doi: 10.1111/nph.15338

Vuorinen, T., Nerg, A. M., and Holopainen, J. K. (2004a). Ozone exposure triggers the emission of herbivore-induced plant volatiles, but does not disturb tritrophic signalling. *Environ. Pollut.* 131, 305–311. doi: 10.1016/j.envpol.2004.02.027

Vuorinen, T., Nerg, A. M., Syrjälä, L., Peltonen, P., and Holopainen, J. (2007). *Epirrita autumnata* induced VOC emission of silver birch differ from emission induced by leaf fungal pathogen. *Arthropod Plant Interact.* 1, 159–165. doi: 10.1007/s11829-007-9013-4

Vuorinen, T., Reddy, G. V. P., Nerg, A.-M., and Holopainen, J. K. (2004b). Monoterpene and herbivore-induced emissions from cabbage plants grown at elevated atmospheric CO_2 concentration. *Atmos. Environ.* 38, 675–682. doi: 10.1016/j.atmosenv.2003.10.029

Warneke, C., Luxembourg, S. L., de Gouw, J. A., Rinne, H. J. I., Guenther, A. B., and Fall, R. (2002). Disjunct eddy covariance measurements of oxygenated volatile organic compounds fluxes from an alfalfa field before and after cutting. *J. Geophys. Res. Atmosph.* 107, ACH 6-1–ACH 6-10. doi: 10.1029/2001jd000594

Wilkinson, S., Mills, G., Illidge, R., and Davies, W. J. (2012). How is ozone pollution reducing our food supply? *J. Exp. Bot.* 63, 527–536. doi: 10.1093/jxb/err317

Yli-Pirilä, P., Copolovici, L., Kannaste, A., Noe, S., Blande, J. D., Mikkonen, S., et al. (2016). Herbivory by an outbreaking moth increases emissions of biogenic volatiles and leads to enhanced secondary organic aerosol formation capacity. *Environ. Sci. Technol.* 50, 11501–11510. doi: 10.1021/acs.est.6b02800

Conflict of Interest Statement: The authors declare that the research was conducted in the absence of any commercial or financial relationships that could be construed as a potential conflict of interest.

frontiers
in Forests and Global Change

ORIGINAL RESEARCH
published: 06 August 2019
doi: 10.3389/ffgc.2019.00042

Assessment of Anthropogenic Volatile Organic Compounds in Leaves of Two Urban Tree Species in Santiago de Chile

Mauricio Araya[1], Daniela Seelenfreund[2], Marianne Buscaglia[2], Barbara Peña-Ahumada[2], Javier Vera[1], Claudia Egas[3] and Margarita Préndez[3]*

[1] Departamento de Salud Ambiental, Instituto de Salud Pública de Chile, Santiago, Chile, [2] Laboratorio de Biología Molecular, Departamento de Bioquímica y Biología Molecular, Facultad de Ciencias Químicas y Farmacéuticas, Universidad de Chile, Santiago, Chile, [3] Laboratorio de Química de la Atmósfera y Radioquímica, Facultad de Ciencias Químicas y Farmacéuticas, Universidad de Chile, Santiago, Chile

Edited by:
Silvano Fares,
Council for Agricultural and Economics Research, Italy

Reviewed by:
Ana Maria Yáñez-Serrano,
University of Freiburg, Germany
Leonardo Montagnani,
Free University of Bozen-Bolzano, Italy

***Correspondence:**
Margarita Préndez
mprendez@ciq.uchile.cl

Specialty section:
This article was submitted to Forests and the Atmosphere, a section of the journal Frontiers in Forests and Global Change

Received: *01 February 2019*
Accepted: *16 July 2019*
Published: *06 August 2019*

Citation:
Araya M, Seelenfreund D, Buscaglia M, Peña-Ahumada B, Vera J, Egas C and Préndez M (2019) Assessment of Anthropogenic Volatile Organic Compounds in Leaves of Two Urban Tree Species in Santiago de Chile. Front. For. Glob. Change 2:42. doi: 10.3389/ffgc.2019.00042

Anthropogenic volatile organic compounds (AVOCs) represent the third largest contribution in gaseous emissions in the urban and peri-urban region of Santiago, the capital of Chile. Some of these compounds are toxic or mutagenic, cause serious damage to human health, and decrease plant growth and development. There is little international information related to atmospheric AVOCs in leaf content from trees exposed to specific sources of pollution, and to our knowledge, there is no research on this topic in Chile. The purpose of this work was to study the leaf content of AVOCs from the Organic Range of Gasoline (ORG: range 6–10 C) emitted by local traffic during the austral summer and spring seasons in leaves of two exotic tree species (*Liriodendron tulipifera* and *Platanus × acerifolia*). Leaf samples collected around 2 meters height above the ground were pulverized with a cryogenic mill and eleven chemical components were quantified (toluene, 1,2,4-trimethylbenzene (1,2,4-TMB), styrene, ethylbenzene, ortho, meta and para-xylenes, naphthalene, 1,3,5-trimethylbenzene (1,3,5-TMB), isopropylbenzene, and trichloroethene) using GC-MSD MSD. Benzene was detected but not quantified, because it was always under the quantification limit of the technique. Differences in concentrations were found for type of site exposure, season and tree species. The differences found in leaf content of AVOCs in *P. × acerifolia* exposed to vehicle traffic suggest that the concentration of these contaminants in leaves may be due to AVOC capturing. Considering the content of AVOCs in leaves and not in the whole individual tree, *L. tulipifera* presented a higher concentration of total AVOCs than *P. × acerifolia* for both seasons. The Prop-Equiv and OFP of *L. tulipifera* were very high in summer, being 13.6 and 14.8 times greater, respectively, than the corresponding values for *P. × acerifolia*.

Keywords: ecosystem services, ozone formation potential, vehicle emissions, Santiago de Chile, urban trees

INTRODUCTION

Anthropogenic volatile organic compounds (AVOCs) constitute the main precursors of tropospheric ozone, in conjunction with nitrogen oxide gaseous emissions from vehicles. Urban trees and forests provide multiple ecosystem services, including mitigation of air pollution by removing AVOCs. Fast-growing cities in developing countries are characterized by a disorganized spatial distribution, sprawling urban areas and increased vehicle traffic, which leads to poor air quality (Henríquez and Romero, 2019). Santiago, the capital of Chile, has a population of close to seven million inhabitants, where the large majority lives in areas with little vegetation, and only affluent neighborhoods in the northeast areas of the city have a close to adequate green infrastructure. Several factors contribute to high levels of air pollution in Santiago, including its dry and temperate region, location surrounded by mountains, a growing economy and densification of the city. Despite all technological improvements and policies developed since the 90's to tackle air pollution (MMA, 2016), the vehicle fleet and travel distances have progressively increased. On average, Santiago more than doubles the mean concentrations above the annual WHO recommendations (WHO, 2016), for both PM10 and PM2.5, especially during the autumn–winter period. Moreover, the Chilean normative for ozone (O_3) is exceeded several days in the eastern part of the city during the spring-summer season (Préndez et al., 2019).

Motor vehicles are important emitters of ozone precursors, including particulate matter and both organic and inorganic gases, such as NO_x. During the last years, Santiago has suffered a strong increase of the vehicle fleet. The period between 2014 and 2015 showed a growth rate of 2.71%, while in 2016 the city reached 4,960,946 vehicles, increasing 4% compared to 2015 (SINCA, 2017). Most vehicles (79.1%) corresponded to gasoline vehicles, 20.6% to diesel vehicles and only 0.3% corresponded to gas or electric vehicles (INE, 2018). Tropospheric O_3 is an important secondary urban air pollutant formed as a result of atmospheric reactions of volatile organic compounds (VOCs), anthropogenic and/or biogenic and nitrogen oxides ($NO_x = NO + NO_2$) (Atkinson, 2000; Kansal, 2009; Préndez et al., 2013a; Guo et al., 2016). The Metropolitan Region vehicles emit around 23,000 tons of NO_x per year (INE, 2018).

In urban areas, vehicle emissions (Shao et al., 2016; Li et al., 2017) are the main contributors to AVOCs. Fumes from liquid fuels containing aromatic compounds are emitted to the air; most of these aromatic compounds are added to gasoline for antiknock purposes, such as lead replacement (Karakitsios et al., 2007; Kountouriotis et al., 2014; Cui et al., 2018). In industrialized areas, high concentrations of AVOCs are mainly associated with petroleum refineries, petrochemical companies, petrol stations, commercial and industrial use of solvents, coal burning and even biomass burning (Karakitsios et al., 2007; Wang et al., 2015; Li et al., 2017).

Plants also emit VOCs; these biogenic VOCs (BVOCs) are an important source of some highly reactive pollutants derived from their eco-physiological functions (Kansal, 2009; Préndez et al., 2013a; Shao et al., 2016) that contribute to ozone formation. BVOCs include alkanes, alkenes, carbonyls, alcohols, esters, ethers, and acids (Kesselmeier and Staudt, 1999). The most important BVOCs are terpenes, the basic molecule of which is isoprene (2-methyl-1,3-butadiene, C_5H_8), and some monoterpenes.

The latest inventory of air pollutants in Santiago (Gramsch, 2014) revealed that emissions from VOCs corresponded to 97,028 t/year. Only 15% of the total VOCs correspond to BVOCs, which are mainly isoprene, monoterpenes and sesquiterpenes. Other gases are 2,3,2-MBO, methanol, acetone and CO. There is no specific information about benzene, toluene and xylenes (BTXs) or other benzene derivatives (Gramsch, 2014). To estimate the emissions from biogenic sources, the MEGAN2.1 program was used, including the latest improvements implemented in 2012 by the National Center for Atmospheric Research (Guenther et al., 2012). Préndez et al. (2019) experimentally quantified emissions of BVOCs from different urban tree species in Santiago, which corresponded mainly to terpenes (isoprene and monoterpenes).

Trees are an important part of the biomass of plants in urban settings and play an essential role in the population's quality of life. Several researchers in different continents, climates and socioeconomic conditions have reported the use of urban forests in the provision of ecosystem services. These forests cover the basic functions of the ecosystem, such as primary productivity (Costanza et al., 2007) and services, including the improvement of air quality (Escobedo et al., 2011), specially the removal of particulate matter (Dzierzanowski et al., 2011; Manes et al., 2016; Marando et al., 2016). Among these same functions, the advantage/disadvantage of emissions of BVOCs has been analyzed by Paoletti (2009), while Tallis et al. (2011) have shown that tree leaves can remove gases and aerosols from the atmosphere more efficiently than other surfaces. Therefore, a selection of species and an adequate location of urban vegetation can significantly improve air quality, not only by the direct effect on gases and atmospheric particulate matter, but also by generating local and regional ventilation (Hebbert and Webb, 2012). Therefore, the use of plants to improve air can be a cheaper, aesthetically pleasing, environmentally friendly, and sustainable process that can be used for a wide range of both organic and inorganic contaminants.

Globally, there is limited research on the likelihood of adsorption and/or absorption of atmospheric pollutants by tree leaves exposed to sources of pollution, specifically for AVOCs (Anyanwu and Kanu, 2006; Saphores and Li, 2012). To our knowledge, this information is non-existent in Chile. In the Metropolitan Region of Chile, where about one third of the population lives (around 7.1 million, INE, 2018), AVOCs represent the third source of gaseous emissions to the atmosphere after CO_2 and CO (Gramsch, 2014). In Santiago, green areas tend to be concentrated in the more affluent areas of the city (Romero, 2019).

Trees remove VOCs and AVOCs through processes defined by the anatomical structure of their leaves and complex physiological processes. As reported by Brilli et al. (2018), the mechanisms of removal and retention of VOCs by leaves include stomata absorption, where VOCs enter through the stomata and metabolic degradation occurs, and a non-stomata adsorption, where adsorption of VOCs may depend on the composition of the leaf cuticle (Wararat et al., 2014). Hydrophobic or lipophilic substances can be absorbed directly by the cuticle or diffuse into the leaf through the cuticle (Libbert, 1974; Niinemets et al., 2014), while hydrophilic compounds, like gaseous and liquid contaminants may be absorbed by the cuticle to some extent (Agarwal et al., 2018). VOCs in the atmosphere enter the intercellular space through the stomata, depending on the physicochemical parameters of each VOC. Some VOCs are metabolized (enzymatically or non-enzymatically) in the cytoplasm of mesophyll cells, facilitating further partitioning of VOCs into the cells, which appears as a process of "uptake" or "absorption" of VOCs by plants. The uptake of VOCs leads to changes in cell metabolism; for example, the accumulation of glycosides or redox potential increase (Matsui, 2016).

In addition to the cuticle and stomata that constitute barriers to gaseous diffusion, cell walls, membranes and mesophyll cells cause another type of resistance to gaseous diffusion. Mesophyllic resistance mostly depends on the solubility of gaseous pollutants, gas-liquid diffusion, and leaf size geometry, and are influenced by some environmental factors, such as wind speed (Khan and Abbasi, 2000).

Both BVOCs and AVOCs are precursors of tropospheric ozone. The theoretical contribution of ozone precursors can be calculated based on the Ozone Formation Potential (OFP). This OFP depends on the photochemical reactivity of the different VOCs with atmospheric OH radicals and other reactive species. A greater content of AVOCs in trees leaves is expected to remove more precursors that generate ozone in the urban environments, expressed in terms of propylene equivalents (Prop-equiv) and OFP, thereby improving air quality.

The aim of this work was to quantify the content of AVOCs emitted from motor vehicles in leaves from *Platanus* and *Liriodendrum* trees and evaluate their performance in terms of improving urban air quality, in relation to their proximity to vehicle emissions. The studied species were selected in a field context of the city of Santiago because they correspond to the most common trees lining main avenues with heavy vehicle traffic. Two locations with similar levels of vehicle emissions were selected and the leaf content of VOCs in two common exotic tree species was measured. In Santiago, *Platanus orientalis, P. occidentalis*, and *P.* × *acerifolia* are found, and these plane trees are common in the Vitacura commune. *Liriodendrum tulipifera* is common along streets with vehicle traffic in the La Florida commune.

MATERIALS AND METHODS

Sampling Sites

The Metropolitan Region (33.5°S, 70.8°W) is a closed basin between the Andes to the east and the Coastal Range to the west, the Chacabuco mountain range to the north, and the Cantillana mountain range to the south. The mountains surrounding the central valley reach altitudes between 1,000 and 6,000 m asl and the basin of the city has a gentle slope from west to east, from ∼450 m asl to over 1,000 m asl. During most of the year, the climate of the region is affected by synoptic systems, where the Southeast Pacific Subtropical Anticyclone is the dominant one. This anticyclone generates a persistent subsidence thermal inversion during the cold months, weak airflows, and semi-arid climatic conditions. Hence, ventilation at the basin is poor and mainly generated by local breeze systems. Wind intensity and direction vary seasonally, with a southwest regime being dominant throughout the year (Ulriksen, 1993). Four seasons are clearly distinguished: summer (December 21–March 21), autumn (March 21–June 21), winter (June 21–September 21), and spring (September 21–December 21).

Three sites of sampling sites were selected: two with similar high vehicle traffic and a third in an urban park, as explained below and shown in **Figure 1**. At the first site, samples of well-developed sunny leaves and directly exposed to high vehicle traffic (operational speed of 26.5 km/h, UOCT, 2019) were taken from twenty individuals of *L. tulipifera* ($n = 20$) along Vicuña Mackenna avenue (VM Avenue) in the La Florida commune. At the second site, and in similar conditions as the first site (operational speed of 29.5 km/h, UOCT, 2019) samples were taken from fourteen individuals of *Platanus* ($n = 14$) along Vitacura avenue (V Avenue), in the Vitacura commune. At both sites, the trees are in close proximity to a permanent flow of vehicles and exposed to fumes at a distance of <2 m. At the third site, well-developed sunny leaves were collected from twenty individuals of *L. tulipifera* ($n = 20$), located in an urban park called Parque Bicentenario (B Park), without internal motor vehicle traffic, located in the Vitacura commune. The same individuals were sampled in two campaigns carried out in the austral summer (February) and spring (November) of 2017. Each sampling campaign at each site took ∼6 h. In all cases, the selected leaves of each individual were collected in a height range of 1.7 and 2.5 meters all along the perimeter for each individual, until completing ∼30 g of foliar biomass, corresponding to around 40 leaves. All leaf samples were immediately frozen *in situ* in dry ice and stored at −20°C until analysis. This range of height corresponds to the criterion used for aerosol sampling for health purposes by the international monitoring (USEPA, 1989). From each sample of 30 g, a subset of 10 g leaf material was selected at random for chemical analysis.

Chemical Analysis

Leaf samples were milled using a cryogenic mill (CryoMill Retsch). Each sample of 2 g was placed in a 20 ml glass vial with PTFE/silicone septum. HS-SPME extraction was performed using a GC CombiPAL 80 Agilent, containing a fiber assembly with 65 μm Polydimethylsiloxane/Divinylbenzene (PDMS/DVB) coating (Supelco). Conditioning was performed according to the manufacturer's instructions, in the GC injection port at 250°C for 30 min prior to use. Extraction time of the analytes was 50 min at 70°C and temperature and desorption time was 5 min at 250°C at the injection port. A blank fiber experiment was carried out to ensure the absence of contaminants in the fiber.

Sample analysis was performed with an Agilent Technologies 7890A GC coupled with an Agilent technologies 5975C mass spectrometer (MS) in the selective ion monitoring (SIM) mode splitless injection onto a HP-5MS (30 m × 0.25 mm i.d, 0.25 μm film thickness); a capillary column was used

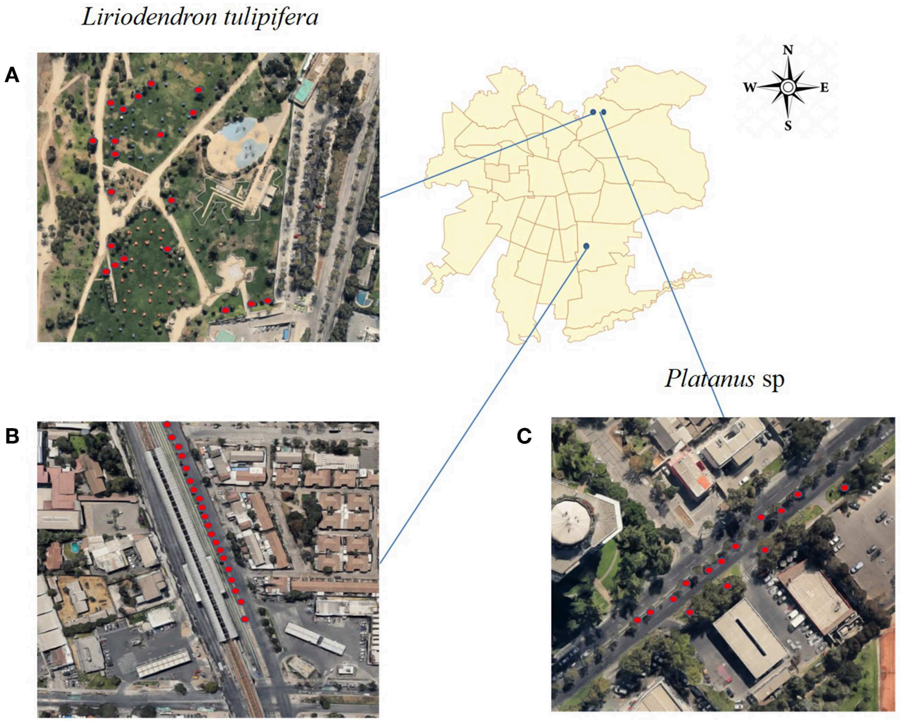

FIGURE 1 | Sampling sites in Santiago, Chile. **(A)** B Park (*L. tulipifera*); **(B)** VM Avenue (*L. tulipifera*); and **(C)** V Avenue (*Platanus* sp). Red dots identify individuals sampled at each site.

with a He flow 1 mL/min as carrier gas. The temperature of the injection port was set at 250°C and the temperature of the column was programmed at 35°C. The mass selective detector (MS) was used for mass spectral identification and quantification of the GC–HS-SPME components at a MS ionizations voltage of 70 eV. Eleven AVOCs were determined and quantified (styrene, 1,2,4-TMB, naphthalene, trichloroethene, 1,3,5-TMB, isopropylbenzene, ethylbenzene, toluene, and ortho, meta, para-xylenes) (standard provided by Chem Service) in the organic range of gasoline (ORG). An ααα-trifluorotoluene (standard provided by Supelco) internal standard was used. Quantification was performed by means of a calibration curve of nine concentration levels (in ng/g) of the leaf matrix.

Ozone Formation Potential (OFP)

In this work, we used the propylene equivalent concentration (Prop-Equiv) and the maximum incremental reactivity (MIR), as reported by Cai et al. (2010), Wu et al. (2017) and Kumar et al. (2018) to calculate OFP. The following equation was used to calculate the equivalent propylene concentration for each individual AVOC (Chameides et al., 1992):

$$\text{Prop} - \text{Equiv}_{(i)} = \text{conc}_{(i)} \times K_{OH(i)}/K_{OH(C3H6)} \tag{1}$$

where:

Prop-Equiv$_{(i)}$: Concentration of AVOC$_{(i)}$ on an OH-reactivity based scale normalized to the reactivity of C_3H_6, expressed in ppbC.

conc$_{(i)}$: Concentration of AVOC expressed in ppbC.

$K_{OH(i)}$: Rate constant for the reaction of compound i.*

$K_{OH(C3H6)}$: Rate constant for the reaction of C_3H_6 (propylene) with OH, respectively.

* As reported by Atkinson and Arey (2003).

The Ozone Formation Potential (OFP) for individual AVOC$_{(i)}$ using the MIR method (Carter, 1994), was defined by the following equation:

$$\text{OFP}_{(i)} = \text{conc}_{(i)} \times \text{MIR}_{\text{coeff}(i)} \tag{2}$$

where:

OFP$_{(i)}$: Ozone formation potential of individual AVOC$_i$, expressed in $\mu g/m^3$.

conc$_{(i)}$: Concentration of AVOC expressed in ppbC.

MIR$_{\text{coeff}(i)}$: Maximum incremental reactivity coefficient of compound$_i$, expressed in g O_3/g VOC.

Statistical Analysis

All analyses were performed using the Minitab 16 statistical software. Variables were tested for normality and homogeneity of variance, and transformations were made as necessary to meet the underlying statistical assumptions of the models used. A two-way analysis of variance (ANOVA) was used to test the main and interactive effects of species and seasons on AVOC emissions. The assertion of statistically significant differences between two groups of data (same species exposed to different sources of

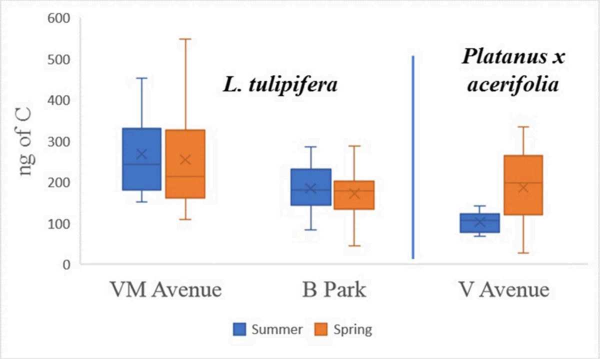

FIGURE 2 | Total concentrations of AVOCs leaf content in *L. tulipifera* and *Platanus x acerifolia* at the sampling sites VM Avenue, B Park, and V Avenue, both in summer and in spring. Concentrations are expressed as ng of C. In the boxes: *X* = arithmetic mean; horizontal line = median.

contamination and different species exposed to the same source) was supported by Fisher tests and *p*-value.

RESULTS

Variability of Total Concentration of AVOCs Leaf Content Due to the Pollution Source

The following AVOCs were quantified: toluene, 1,2,4-trimethylbenzene (1,2,4-TMB), styrene, ethylbenzene, ortho, meta, and para-xylenes, naphthalene, 1,3,5-trimethylbenzene (1,3,5-TMB), isopropylbenzene, and trichloroethene. Benzene was detected but not quantified, because it was always under the quantification limit of the technique. There were statistically significant differences between the total concentrations of AVOCs leaf content in leaves from *L. tulipifera* individuals exposed to high (VM Avenue) and low (B Park) emissions of vehicles. The mean values of total concentrations of AVOCs in summer were 267.9 ± 92.4 ng of C (153.6 ± 50.7 ng/g) and 184.7 ± 58.8 ng of C (102.5 ± 32.2 ng/g), respectively ($F_{obs} = 10.74$; *p*-value = 0.002). In spring, concentrations were 255.0 ± 127.9 ng of C (144.7 ± 70.1 ng/g) and 172.4 ± 52.6 ng of C (99.3 ± 28.7 ng/g), respectively ($F_{obs} = 7.17$; *p*-value = 0.011). Total concentrations of AVOCs content in leaves of *Platanus* individuals (V Avenue) exposed to high emissions of vehicles presented mean concentrations of 103.0 ± 24.1 ng of C (56.6 ± 13.1 ng/g) in summer and 186.7 ± 91.8 ng of C (103.0 ± 50.5 ng/g) in spring (**Figure 2**).

Figure 3 shows the leaf content of chemical compounds in individuals of *L. tulipifera* located along the high traffic VM Avenue and the low exposure B Park. The highest concentration was found for toluene in both seasons (summer and spring). Trichloroethene and isopropylbenzene were below detection limits at both sites and during both seasons, while 1,2,4-TMB levels were below detection limits in summer at the B Park. In most cases, a greater concentration of chemical species was observed in leaves sampled at the VM Avenue than at the B Park. There were statistically significant differences in toluene levels between VM avenue and B Park in summer, but not in spring. 1,2,4-TMB, styrene, xylenes and naphthalene show statistically significant differences between VM Avenue and B Park in both seasons ($F_{obs} > F_{cri}$, $p < 0.05$). 1,3,5-TMB shows statistically significant differences between VM Avenue and B Park in spring, but not in summer.

Seasonal Variability of Concentrations of AVOCs

Table 1 shows the statistical results of AVOCs in foliar material at the three sampling sites (VM Avenue, V Avenue and B Park) during the two seasons. Ethylbenzene (VM Avenue and B Park), toluene (VM Avenue), and trichloroethene (V Avenue) did not show statistically significant differences in samples for both seasons ($F_{obs} < F_{cri}$ and *p*-value > 0.05).

Figure 2 shows no variation in terms of total concentrations of AVOCs (ΣAVOCs), in each season for *L. tulipifera* from B Park ($F_{obs} = 2.80$; $F_{cri} = 4.10$; *p*-value = 0.103). A different behavior was observed for *L. tulipifera* from VM Avenue ($F_{obs} = 12.53$; *p*-value = 0.001) and for *Platanus* sp from V Avenue samples ($F_{obs} = 11.08$; *p*-value = 0.003), with greater total concentration of AVOCs in spring than in summer, mainly due to the low amount of ethylbenzene, toluene and xylene leaf content in summer (**Figure 2**).

Figure 4 shows the relative concentrations, in percentages of leaf content, of different AVOCs by leaves, when comparing the profiles of *L. tulipifera* at both sites in spring and summer. In summer, the main leaf content of chemical compounds along VM Avenue were toluene, styrene and 1,2,4-TMB, while at B park only toluene and styrene leaf content was quantified; 1,2,4-TMB and naphthalene were not detected in the foliar material.

There was a large heterogeneity of AVOCs in leaf content among *Platanus sp* samples collected in spring (see **Figure 4C**), which was not explained by the location of each individual along V Avenue. In order to determine if all *Platanus* trees sampled corresponded to the same species, a genetic analysis was performed. Therefore, the species or presence of *Platanus* hybrids was determined by analyzing the internal transcribed spacer (ITS) subregion of the nuclear rDNA cistron.

DNA extraction yields ranged between 90 and 220 ng/L and an amplicon of ∼650 bp was obtained for all samples. A single nucleotide polymorphism at the relative position 120 allowed discriminating between *P. orientalis* and the hybrid *P.* × *acerifolia*. This position is always "G" for *P. orientalis*, while a double signal of T or G is present in the hybrid *P.* × *acerifolia*. Analysis of 13 of the *Platanus* samples presented the "T" variant, defining their assignment to *P.* × *acerifolia*. Sample V7 did not amplify. Sample V14 presented five additional polymorphisms; however, the overall genetic profile was compatible with both *P. orientalis* and *P.* × *acerifolia*, and not indicative of *P. occidentalis* (**Figure 5**).

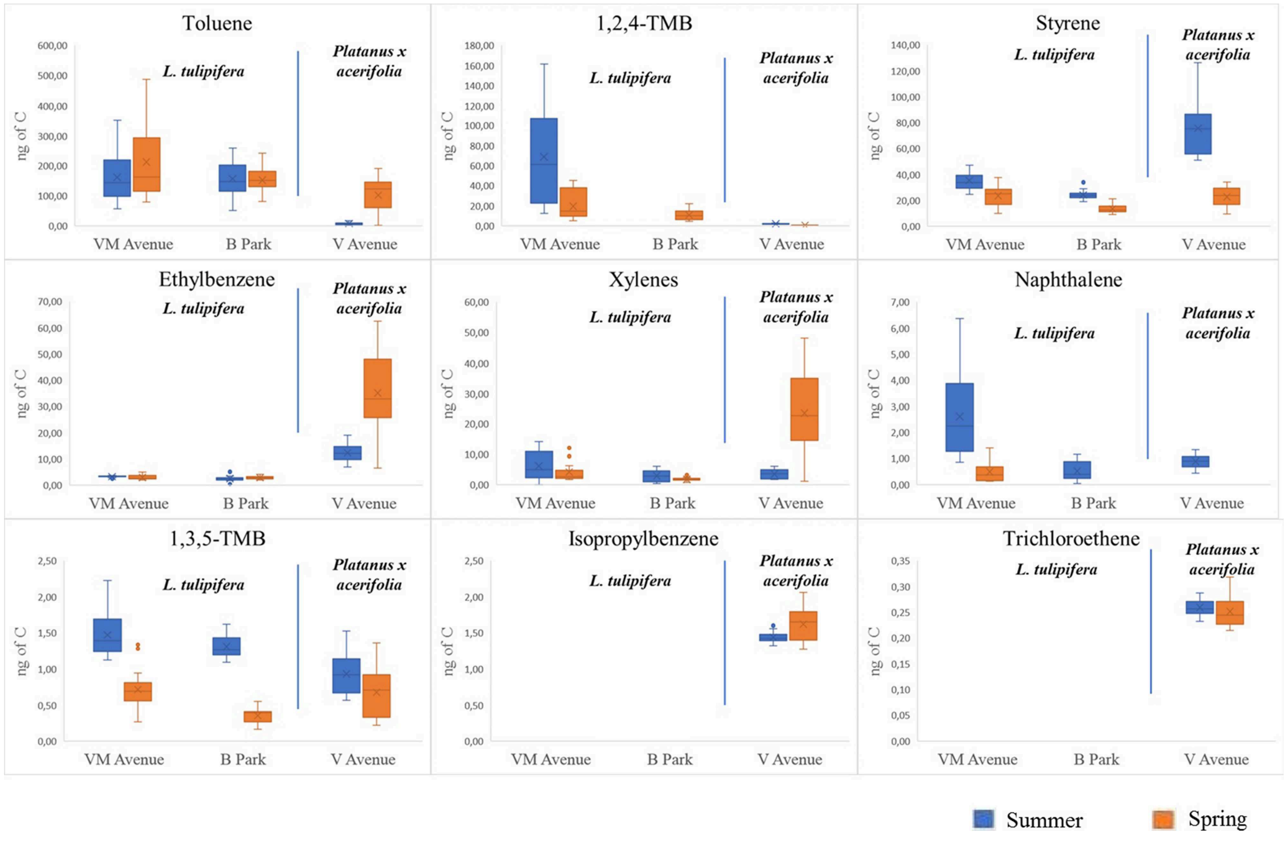

FIGURE 3 | Concentrations of individual AVOCs leaf content by the leaves of *L. tulipifera* and *Platanus x acerifolia* at the sampling sites VM Avenue, B Park, and V Avenue in both summer and spring. Concentrations are expressed as ng of C. In the boxes: *X* = arithmetic mean; horizontal line = median.

Ozone Formation Potential (OFP)

Table 2 shows the concentration of Prop-Equiv and the OFP calculated for AVOCs content in leaves from the studied sites in summer and spring. *L. tulipifera* individuals located at VM Avenue presented higher total and individual values, compared to *L. tulipifera* individuals located at B Park and the individuals of *P.* × *acerifolia* located at V Avenue (except for ethylbenzene and styrene). Additionally, the concentrations of Prop-Equiv and OFP for individuals sampled were higher in summer than in spring.

DISCUSSION

Many VOCs, including benzene, toluene and xylene are emitted by anthropogenic and biogenic sources. Annual global emissions of biogenic VOCs reported by Wiedinmyer et al. (2004) are mainly isoprene (250–750 TgC yr^{-1}), followed by methanol, various terpenes and very low concentrations of toluene (0.4–2 TgC yr^{-1}), in contrast to high toluene concentrations indicative of anthropogenic VOCs. Misztal et al. (2015) have reported that benzenoids from plants contribute in a similar proportion than AVOCs emitted by fossil fuels to atmospheric emissions in native forests located at the north and northeast regions of the United States. The proportion of BVOCs and AVOCs depends on climate conditions, urban development, plant cover and many other factors. Measurements of trace gas emissions of the small Mediterranean shrub *Halimium halimifolium* have revealed a broad range of BVOCs under controlled laboratory conditions, emitting terpenes, trimethylbenzene, ethylphenol, and toluene, indicating *de novo* BVOC biosynthesis of these compounds (Fasbender et al., 2018). Under field conditions, either in natural or urban settings, benzenoid emissions may vary significantly. In Santiago, Chile, a large city set in a temperate Mediterranean climate, AVOCs correspond to 85% of all VOCs emitted and only 15% are BVOCs (Gramsch, 2014). BVOCs are secondary metabolites that play an important role in the defense response to heat and drought, and complement other defense mechanisms, such as antioxidant enzymes (Tattini et al., 2015). *Platanus* × *acerifolia*, a high isoprene-emitting species, is frequently used as an ornamental plant in urban areas of the Mediterranean basin (Tattini et al., 2015) and other temperate regions exposed to the combined effect of high light, high temperature, and drought. *Liriodendrum tulipifera* is native to the United States and has been introduced in Chile because of its ornamental value and fast growth. The absorption mechanism and further degradation and metabolism of either AVOCs or BVOCs has not been studied in these two exotic arboreal species under the climate and pollution

TABLE 1 | Seasonal variability of selected AVOCs at the three sampling sites (VM Avenue, V Avenue, and B Park).

	Liriodendron tulipifera						***Platanus* × *acerifolia***		
	VM Avenue			**B Park**			**V Avenue**		
	Summer (mean ± SD in ng of C) (*n* = 20)	**Spring (mean ± SD in ng of C) (*n* = 20)**	**S/Sp ratio**	**Summer (mean ± SD in ng of C) (*n* = 20)**	**Spring (mean ± SD in ng of C) (*n* = 20)**	**S/Sp ratio**	**Summer (mean ± SD in ng of C) (*n* = 14)**	**Spring (mean ± SD in ng of C) (*n* = 14)**	**S/Sp ratio**
Ethylbenzene	3.3 ± 0.3	2.9 ± 0.8	1.1	2.5 ± 1.1	2.8 ± 0.6	0.9	12.4 ± 3.3	35.2 ± 15.7	0.4
Styrene	35.5 ± 6.5	23.5 ± 7.6	1.5	23.7 ± 2.5	13.5 ± 3.1	1.8	75.7 ± 20.8	22.8 ± 7.3	3.3
Toluene	161.1 ± 82	212.6 ± 123	0.8	156.4 ± 60	152.0 ± 40	1.0	6.9 ± 4.0	102.3 ± 59	0.1
1,3,5-TMB	1.5 ± 0.3	0.7 ± 0.3	2.1	1.3 ± 0.2	0.4 ± 0.1	3.7	0.9 ± 0.3	0.7 ± 0.4	1.4
1,2,4-TMB	68.7 ± 49	19.5 ± 14	3.5	<QL	10.7 ± 4.9	0.01	1.9 ± 0.3	0.5 ± 0.1	4.1
Xylenes	7.0 ± 4.2	4.1 ± 3.0	1.7	2.9 ± 1.8	1.8 ± 0.7	1.6	3.5 ± 1.5	23.5 ± 14.6	0.1
Naphthalene	2.6 ± 1.5	0.5 ± 0.4	5.3	0.5 ± 0.4	<QL	5.5	0.9 ± 0.2	<QL	9.5
Trichloroethene	<QL	<QL	1.0	<QL	<QL	1.0	0.3 ± 0.1	0.3 ± 0.1	1.0
Isopropylbenzene	<QL	<QL	1.0	<QL	<QL	1.0	1.4 ± 0.1	1.6 ± 0.1	0.9

Concentrations are expressed as ng of C.
n, number of samples; QL, quantification limit (0.10 ng of C).

conditions prevalent in Santiago, and was beyond the scope of this analysis.

Platanus sp

The *Platanus* individuals located on V Avenue presented greater content of ethylbenzene, toluene and xylenes in spring than in summer (S/Sp <1). The heterogeneity observed in concentrations of AVOC leaf content by the individual *Platanus* specimens was unexpected.

In Santiago, plane trees *P. orientalis, P. occidentalis*, and the hybrid *P.* × *acerifolia* are found. Due to the distinctly variable AVOC concentrations in samples from trees 1, 2, and 3 compared to samples from specimens 4 to 14, we hypothesized that the different trees might correspond to phenotypically similar, but genetically distinct *Platanus* accessions. Therefore, a genetic test that amplifies the nuclear ribosomal internal transcribed spacer (ITS) region allowed discriminating between the different *Platanus* species and the *P.* × *acerifolia* hybrid. This region of high copy number sequences is frequently utilized for phylogenetic analyses at the genus and species levels (Coleman, 2003), is inherited biparentally and useful to determine hybrid speciation (Álvarez and Wendel, 2003), and therefore, valuable in this study. The results of this analysis indicated that all sampled trees correspond to the *P.* × *acerifolia* hybrid and thus, the observed differences are not due to a differential genetic background. More details in **Supplementary Material**. At present, we lack an explanation for the observed differences in AVOC leaf content, except that individuals 1, 2, and 3 corresponded to older and larger trees. It is known that the emitted BVOCs vary according to development, as reported for other arboreal species (Préndez et al., 2013b); however, we did not expect to detect differences in AVOC leaf content depending on the age of individual trees. In hindsight, it is not unreasonable to speculate that age-related metabolic changes do not only modulate emissions, but may also affect AVOC content. Therefore, we cannot exclude active metabolic processes involving AVOC capturing.

The most common *Platanus* trees in Santiago are *P.* × *acerifolia*, and the samples analyzed correspond to this widely planted hybrid tree. Therefore, data obtained in this work is probably representative of AVOC leaf content by the bulk of *Platanus* trees in Santiago. Plane trees are one of the most common exotic trees, with a relative abundance of 2.3% at the city level (Hernández and Villaseñor, 2018), although all plane trees are planted along main avenues and hence, are one of the main urban species exposed to vehicle emissions.

Liriodendron tulipifera

We have not found reports on benzenoid emissions from or captured by *Liriodendron* in the literature. Our data indicate three concentration ranges in the leaf content of AVOCs of *L. tulipifera* (**Figure 3**): (1) toluene, 1,2,4 TMB and styrene (10–100 of ng of C); (2) ethylbenzene, xylenes, naphthalene and 1,3,5 trimethylbenzene (in the order of ng of C); (3) trichloroethane and isopropylbenzene were not quantified because they were below the detection limit of the technique used. All chemical compounds reported are present in emissions from vehicle traffic; however, vehicles are not the only source of these pollutants. For example, naphthalene is present in the combustion of tobacco and wood, manufacture of paints, varnishes and agents for leather tanning. Styrene is present in cigarette smoke, released by the use of photocopiers and the manufacturing industry at concentrations of 0.06–4.6 ppb in air. Xylenes are used in paints, varnishes, products that prevent corrosion, cleaning products and as solvents; xylene concentrations of 1–30 ppb are reported in air. Toluene is widely used in paint thinners, adhesives, paint varnishes and gasoline, at concentrations of 1–35 ppbv in air (ATSDR, 2019). For these reasons, the sampling was performed with leaves directly exposed to vehicle traffic at the V. Mackenna (VM Avenue) site.

FIGURE 4 | Concentration profiles of AVOCs, in relative percentages, for each sampling site in summer and spring: **(A)** VM Avenue (*L. tulipifera*), **(B)** B Park (*L. tulipifera*), and **(C)** V Avenue (*Platanus sp*).

The total concentration of AVOCs leaf content (**Figure 2**) by *L. tulipifera* on VM Avenue was statistically higher in summer and in spring than the corresponding concentrations found in the Bicentennial Park (B Park, low exposure to vehicle traffic), except that at B Park ethylbenzene and 1,2,4-TMB presented greater AVOC leaf content in spring than in summer. Toluene remained unchanged. AVOCs leaf content of *L. tulipifera* in B Park evidences a background level of pollution characteristic of urban activities, according to Kumar et al. (2018).

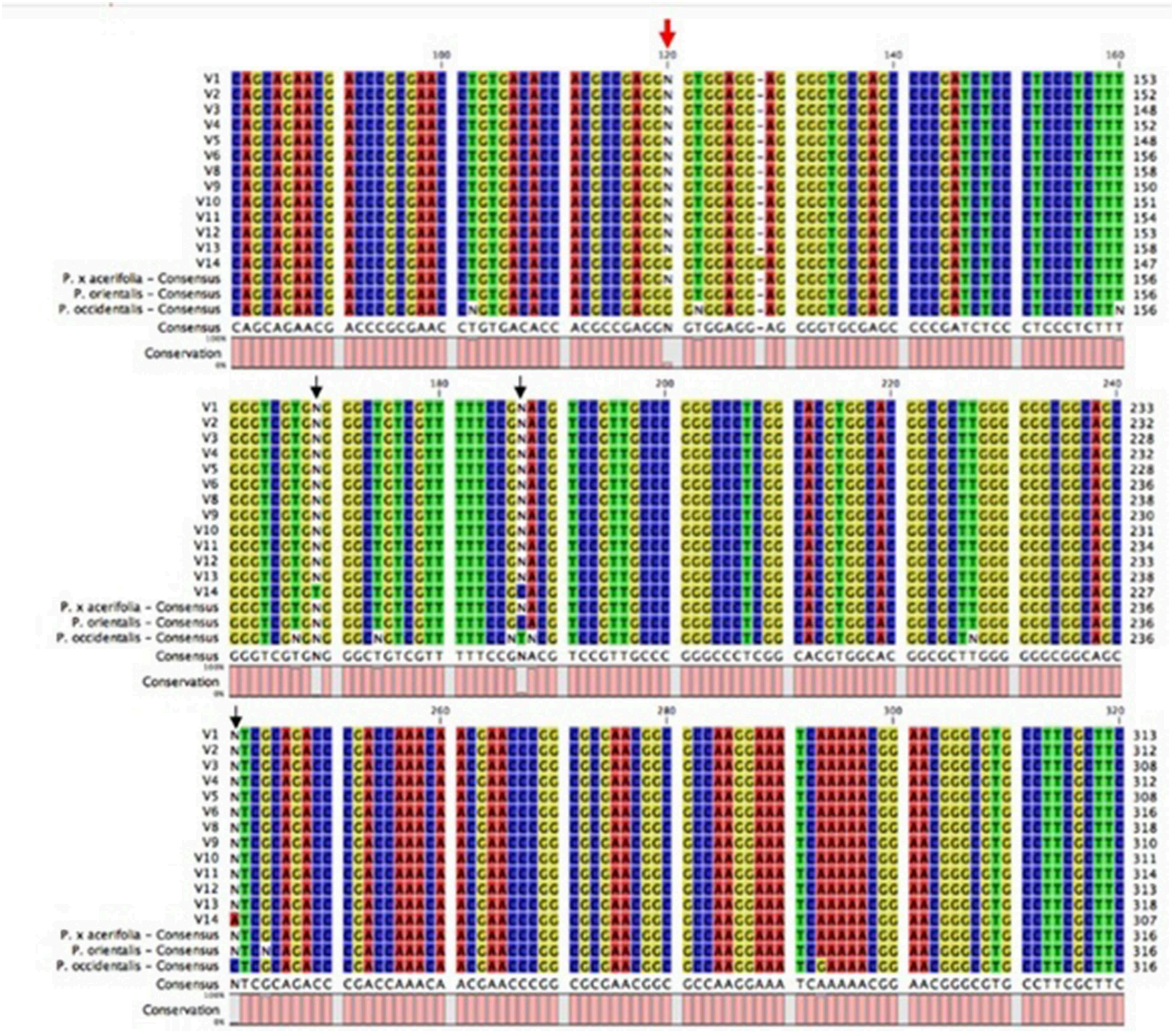

FIGURE 5 | Comparison of the ITS nuclear rDNA region from the *Platanus* samples and published *P.* × *acerifolia*, *P. orientalis*, and *P. occidentalis* consensus sequences. A red arrow at the relative position 120 shows the discriminating polymorphism. Small black arrows indicate other polymorphisms.

The standard deviations detected in spring were higher than in summer. According to Brilli et al. (2018), who studied the use of plants for improvement of indoor air quality, this could be due to the leaf content of VOCs through two mechanisms: stomatal absorption and cuticular adsorption, dependent on the process of greater vegetative growth that occurs in spring.

Toluene, 1,2,4-TMB and styrene presented the highest values for PFO and Prop-equiv (**Table 2**), which measure the contribution of different precursors to the atmosphere. The difference in benzenoid concentrations between the VM Avenue and B Park sites is related to different concentrations of ozone precursors present in leaves from each site, and therefore could indicate an eventual decrease of tropospheric ozone.

Interspecies Variability

A comparison of leaf content of the individual concentrations of AVOCs in both tree species near the source of pollution (**Figure 3**) showed a greater concentrations of ethylbenzene and xylenes (spring), styrene (summer), trichloroethene and isopropylbenzene (summer and spring) by *P.* × *acerifolia*, while *L. tulipifera* presented higher concentrations of toluene (spring), xylenes, naphthalene, 1,2,4-TMB, and 1,3,5-TMB (summer). No statistically significant differences were observed for styrene and 1,3,5-TMB by leaves in spring by both species.

Clear differences were observed in the AVOC leaf content profiles presented in **Figures 4A,C**: leaves collected in summer yielded mainly toluene, 1,2,4-TMB and styrene by *L. tulipifera*, and styrene and ethylbenzene by *P.* × *acerifolia*. In spring

TABLE 2 | Prop-equiv$_{(i)}$ concentration (ppbC) and OFP$_{(i)}$ (ppbC) of AVOCs at VM Avenue, B Park and V Avenue sites, for austral summer season, and austral spring.

	Prop-equiv$_{(i)}$, ppbC			**OFP$_{(i)}$, ppbC**		
	L. tulipifera		***P.* × *acerifolia***	***L. tulipifera***		***P.* × *acerifolia***
	VM Avenue	**B Park**	**V Avenue**	**VM Avenue**	**B Park**	**V Avenue**
AUSTRAL SUMMER SEASON						
Ethylbenzene	0.9	0.7	4.1	10.6	7.8	47.0
Toluene	42.9	34.1	1.5	803.1	137.9	28.3
Xylenes	6.2	2.6	2.1	80.4	29.5	31.5
1,3,5-TMB	3.2	2.8	2.0	17.2	15.1	10.8
1,2,4-TMB	86.5	0.1	2.3	620.9	0.8	16.3
Styrene	84.1	58.8	169.9	66.1	46.2	133.5
Naphthalene	2.3	0.5	0.8	8.9	1.9	3.2
Trichloroethene	0.0	0.0	0.0	0.0	0.0	0.2
Isopropylbenzene	0.0	0.0	0.4	0.2	0.2	3.7
Total AVOCs	226.2	99.6	183.2	1607.6	739.5	274.4
AUSTRAL SPRING SEASON						
Ethylbenzene	0.8	0.8	9.5	9.0	9.0	108.6
Toluene	46.4	34.8	22.3	867.1	650.5	416.8
Xylenes	3.2	1.7	16.6	43.2	23.6	207.1
1,3,5-TMB	1.6	0.8	1,6	8.6	4.3	8.6
1,2,4-TMB	24.7	13.4	0.7	177.2	95.9	4.9
Styrene	53.0	30.3	51.4	41.7	23.8	40.4
Naphthalene	0.5	0.1	0.1	1.9	0.3	0.3
Trichloroethene	0.0	0.0	0.4	0.0	0.0	0.2
Isopropylbenzene	0.0	0.0	0.4	0.2	0.2	3.7
Total AVOCs	130.1	81.7	102.5	1148.9	807.7	790.5

L. tulipifera leaves contained mainly toluene and styrene, while *P.* × *acerifolia* AVOC leaf content consisted mainly of toluene, ethylbenzene, xylenes and styrene. The differences in the response associated with AVOCs in leaves of *L. tulipifera* and *P.* × *acerifolia* may be related to the cuticular composition of the leaves of each species, affecting the adsorption of VOCs, as described by Wararat et al. (2014).

In terms of total concentrations of AVOCs (**Figure 2**), in summer *L. tulipifera* leaves contained 2.7 times more than *P.* × *acerifolia* leaves ($F_{obs} = 42.1$, p-value $= 7.03 \times 10^{-7}$) in terms of ng of C under field conditions with similar vehicle traffic. The same trend was observed in spring, when *L. tulipifera* leaves presented 1.4 times more AVOCs than *P.* × *acerifolia* leaves ($F_{obs} = 7.17$; p-value $= 0.011$), presenting statistically significant differences in all cases. It is important to point out that these results imply AVOC content at the level of leaf tissue, and that these values cannot be extrapolated directly to the performance of individual trees or species.

Prop-Equiv and OFP

We used the concentration values of Prop-Equiv and OFP to associate that greater AVOC content by leaves means lower generation of ozone in the urban environment.

Liriodendron tulipifera leaves presented a higher leaf content of total AVOCs than *Platanus* × *acerifolia* leaves in summer and spring. Even considering an eventual biogenic contribution of benzenoids by the studied species, it is possible to introduce the use of OFP and Prop-Equiv to estimate the decrease of ozone formation precursors in the atmosphere. In general, *L. tulipifera* showed a greater capacity to improve air quality than *P.* × *acerifolia*, presenting higher values in terms of total Prop-Equiv concentration (1.23 and 1.26 times for summer and spring, respectively) and total OFP (5.9 times in summer and 1.5 times in spring).

An important group of compounds for atmospheric chemistry is BTXs (benzene, toluene, and xylenes). In this work, benzene was not quantified because it was under the detection limits of the technique. However, concentrations of the TX compounds were high in the studied trees that were close to the source of pollution. Of note, the Prop-Equiv and OFP of *L. tulipifera* were very high in summer, being 13.6 and 14.8 times greater, respectively, than the corresponding values for *P.* × *acerifolia*. Therefore, when measuring the contribution of leaves, *L. tulipifera* contributes more to improving air quality than *P.* × *acerifolia*, because it decreases the amount of precursors that participate in the formation of tropospheric ozone.

CONCLUSION

Understanding how AVOCs contribute to environmental pollution is important in order to mitigate the effects of vehicle traffic and create more sustainable cities for the growing urban populations. The present study was performed under field conditions in an urban setting with a Mediterranean climate. The eastern part of Santiago showed high ozone concentrations during the spring-summer months. As a secondary pollutant, ozone reduction is closely linked to the decrease of its precursors: VOCs and NO_X. A natural way to reduce VOCs is to find urban tree species that efficiently remove these precursors from the atmosphere. To avoid the contribution of other chemical compound sources (range of aromatic components of gasoline), we studied the most common tree species directly exposed to vehicle traffic.

In this case, the study considered two species that are frequently planted along streets and avenues of the city: *L. tulipifera* and *P.* × *acerifolia*. The leaf content of AVOCs in these urban arboreal species was measured for the first time in Chile. To our knowledge, the emission of benzenoids by *L. tulipifera* has not been reported in the international literature. The large difference found between concentrations in leaves exposed to the high vehicle traffic of Av. Vicuña Mackenna (VM Avenue) and the low exposure to vehicle traffic in the Bicentennial Park (B Park), suggests that the values obtained for the B Park could correspond either to AVOCs or to emission of these compounds from the leaves.

The high values determined for Prop-equiv and OFP of 1,2,4 TMB, toluene, and styrene and their high content in leaves of *L. tulipifera,* showed that this tree has a higher potential than *P.* × *acerifolia* as a tool to cooperate with atmospheric decontamination processes in urban environments, as a first step to evaluate their decontamination potential. In order to extend these observations to the level of individual trees, the foliar surface of each tree has to be considered. Calculations of the Leaf Area Index (LAI) of individual trees and urban tree cover are in progress, in order to estimate the effective removal of AVOCs from vehicle emissions by different tree species in Santiago. Further steps will imply measurements of LAI in both species in order to compare their relative efficiency in the removal of AVOCs.

The two exotic species analyzed in this study are deciduous trees. During the austral winter, the main pollutant in Santiago corresponds to particulate matter, coincident with the season when these species lack leaves and therefore, do not contribute to the removal of this pollutant from urban air. However, during the austral spring, ozone is the main pollutant in Santiago. Under the studied field conditions, *P.* × *acerifolia* removes less AVOCs than *L. tulipifera,* measured in terms of leaf mass. Finding the most suitable arboreal species that are able to contribute to the improvement of the air quality of Santiago with criteria of sustainability will imply a long-term task.

AUTHOR CONTRIBUTIONS

MA: assembly and validation of the analytical technique, quantification of the chemical species absorbed in the leaves of the trees, discussion of results. DS: supervised and procured funding for genetic analyses and participated in the writing of the manuscript. MB: performed genetic analysis. BP-A: supervised genetic analysis and performed analysis of genetic data. JV: statistical support. CE: graphic and bibliographic support, discussion of results. MP: general design of the research and discussion of results and wrote the manuscript.

ACKNOWLEDGMENTS

Authors acknowledge project UREDES Consolidación-URC-026/17, VID, Universidad de Chile for financial support and thank reviewers for their useful comments and suggestions to improve this manuscript significantly.

SUPPLEMENTARY MATERIAL

The Supplementary Material for this article can be found online at: https://www.frontiersin.org/articles/10.3389/ffgc.2019.00042/full#supplementary-material

REFERENCES

Agarwal, P., Sarkar, M., Chakraborty, B., and Banerjee, T. (2018). "Phytoremediation of air pollutants: prospects and challenges," in *Phytomanagement of Polluted Sites: Market Opportunities in Sustainable Phytoremediation*, eds V. C. Pandey and K. Bauddh (Oxford, UK: Elsevier Inc.), 221–241. doi: 10.1016/B978-0-12-813912-7.00007-7

Álvarez, I., and Wendel, J. F. (2003). Ribosomal ITS sequences and plant phylogenetic inference. *Mol. Phylogenet. Evol.* 29, 417–434. doi: 10.1016/S1055-7903(03)00208-2

Anyanwu, E. C., and Kanu, I. (2006). The role of urban forest in the protection of human environmental in geographically prone unpredictable hostile weather conditions. *Int. J. Environ. Sci. Technol.* 3, 197–201. doi: 10.1007/BF03325926

Atkinson, R. (2000). Atmospheric chemistry of VOCs and NO_X. *Atmos. Environ.* 34, 2063–2101. doi: 10.1016/S1352-2310(99)00460-4

Atkinson, R., and Arey, J. (2003). Atmospheric degradation of volatile organic compounds. *Chem. Rev.* 103, 4605–4638. doi: 10.1021/cr0206420

ATSDR (2019). *Agency for Toxic Substances and Disease Registry*. Available online at: http://www.atsdr.cdc.gov (accessed April 28, 2019).

Brilli, F., Fares, S., Ghirardo, A., de Visser, P., Calatayud, V., Muñoz, A., et al. (2018). Plants for sustainable improvement of indoor air quality. *Trends Plant Sci.* 23, 507–512. doi: 10.1016/j.tplants.2018.03.004

Cai, C.-J., Geng, F.-H., Tie, X.-X., Yu, Q., Li, P., and Zhou, G.-Q. (2010). Characteristics of ambient volatile organic compounds (VOCs) measured in Shanghai, China. *Sensors* 10, 7843–7862. doi: 10.3390/s100807843

Carter, W. P. L. (1994). Development of ozone reactivity scales for volatile organic compounds. *Air Waste* 44, 881–899. doi: 10.1080/1073161X.1994.10467290

Chameides, W. L., Fehsfeld, F., Rodgers, M. O., Cardelino, C., Martinez, J., Parrish, D., et al. (1992). Ozone precursor relationships in the ambient atmosphere. *J. Geophys. Res.* 97, 6037–6055. doi: 10.1029/91JD03014

Coleman, A. W. (2003). ITS2 is a double-edged tool for eukaryote evolutionary comparisons. *Trends Genetics.* 19, 370–375. doi: 10.1016/S0168-9525(03)00118-5

Costanza, R., Fisher, B., Mulder, K., Liu, S., and Christopher, T. (2007). Biodiversity and ecosystem services: a multi-scale empirical study of the relationship between species richness and net primary production. *Ecol. Econ.* 61, 478–491. doi: 10.1016/j.ecolecon.2006.03.021

Cui, L., Wang, X. L., Ho, K. F., Gao, Y., Liu, C., Hang Ho, S. S., et al. (2018). Decrease of VOC emissions from vehicular emissions in Hong Kong from 2003 to 2015: results from a tunnel study. *Atmos. Environ.* 177, 64–74. doi: 10.1016/j.atmosenv.2018.01.020

Dzierzanowski, K., Popek, R., Gawronska, H., Sæbø, A., and Gawronski, S. W. (2011). Deposition of particulate matter of different size fractions on leaf surfaces and in waxes of urban forest species. *Int. J. Phytoremediation* 13, 1037–1046. doi: 10.1080/15226514.2011.552929

Escobedo, F. J., Kroeger, T., and Wagner, J. E. (2011). Urban forests and pollution mitigation: analyzing ecosystem services and disservices. *Environ. Pollut.* 159: 2078–2087. doi: 10.1016/j.envpol.2011.01.010

Fasbender, L., Yáñez-Serrano, A. M., Kreuzwieser, J., Dubbert, D., and Werner, C. (2018). Real-time carbon allocation into biogenic volatile organic compounds (BVOCs) and respiratory carbon dioxide (CO2) traced by PTR-TOF-MS, 13CO2 laser spectroscopy and 13C-pyruvate labelling. *PLoS ONE* 13:e0204398. doi: 10.1371/journal.pone.0204398

Gramsch, E. (2014). *Estudio "Actualización y sistematización del inventario de emisiones de contaminantes atmosféricos en la Región Metropolitana"*. Departamento de Física, Universidad de Santiago de Chile. Available online at: https://sustempo.com/website/wp-content/uploads/2015/07/Inventario-de-emisiones-RM_USACH_2014.pdf (accessed January 8, 2019).

Guenther, A.B., Jiang, X., Heald, C.L., Sakulyanontvittaya, T., Duhl, T., Emmons, L. K., et al. (2012). The model of emissions of gases and aerosols from nature version 2.1 (MEGAN2.1): an extended and updated framework for modeling biogenic emissions. *Geosci. Model Dev*. 5, 1471–1492. doi: 10.5194/gmd-5-1471-2012

Guo, H., Ling, Z. H., Cheng, H., Simpson, I., Lyu, X., Wang, X., et al. (2016). Tropospheric volatile organic compounds in China. *Sci. Total Environ.* 574, 1021–1043. doi: 10.1016/j.scitotenv.2016.09.116

Hebbert, M., and Webb, B. (2012). "Towards a liveable urban climate – lessons from Stuttgart," in *Liveable Cities: Urbanising World (ISOCARP 07)*, eds C. Gossop, and S. Nan (London; New York, NY: Routledge), 132–149 (Chapter 7).

Henríquez, C., and Romero, H. (2019). "Introduction," in *Urban Climates in Latin America*, eds C. Henríquez and H. Romero (Switzerland AG: Springer Nature), 1–14 (Chapter 1). doi: 10.1007/978-3-319-97013-4

Hernández, H. J., and Villaseñor, N. R. (2018). Twelve-year change in tree diversity and spatial segregation in the Mediterranean city of Santiago, Chile. *Urban Forestry and Urban Greening.* 29, 10–18. doi: 10.1016/j.ufug.2017.10.017

INE (2018). *Instituto Nacional de Estadísticas*. Available online at: http://www.ine.cl (accessed January 8, 2019).

Kansal, A. (2009). Sources and reactivity of NMHCs and VOCs in the atmosphere: a review. *J. Hazard. Mater*. 166, 17–26. doi: 10.1016/j.jhazmat.2008.11.048

Karakitsios, S. P., Delis, V. K., Kassomenos, P. A., and Pilidis, G. A. (2007). Contribution to ambient benzene concentrations in the vicinity of petrol stations: estimation of the associated health risk. *Atmos. Environ.* 41, 1889–1902. doi: 10.1016/j.atmosenv.2006.10.052

Kesselmeier, J., and Staudt, M. (1999). Biogenic volatile organic compouds (VOC): an overview on emission, physiology and ecology. *J. Atmos. Chem.* 33, 23–88. doi: 10.1023/A:1006127516791

Khan, F. I., and Abbasi, S. A. (2000). Attenuation of gaseous pollutants by greenbelts. *Environ. Monit. Assess.* 64, 457–475. doi: 10.1023/A:1006278000352

Kountouriotis, A., Aleiferis, P. G., and Charalambides, A. G. (2014). Numerical investigation of VOC levels in the area of petrol stations. *Sci. Total Environ.* 470, 1205–1224. doi: 10.1016/j.scitotenv.2013.10.064

Kumar, A., Singh, D., Kumar, K., Singh, B. B., and Kumar, J. V. (2018). Distribution of VOCs in urban and rural atmospheres of subtropical India: temporal variation, source attribution, ratios, OFP and risk assessment. *Sci. Total Environ.* 613–614, 492–501. doi: 10.1016/j.scitotenv.2017.09.096

Li, B., Ho, S. S. H., Xue, Y., Huang, Y., Wang, L., Cheng, Y., et al. (2017). Characterizations of volatile organic compounds (VOCs) from vehicular emissions at roadside environment: the first comprehensive study in Northwestern China. *Atmos. Environ.* 161, 1–12. doi: 10.1016/j.atmosenv.2017.04.029

Libbert, E. (1974). *Lehrbuch der Planzenphysiologie*. Jena, VEB Gustav Fischer Verlag.

Manes, F., Marando, F., Capotorti, G., Blasi, C., Salvatori, E., Fusaro, L., et al. (2016). Regulating ecosystem services of forests in ten Italian metropolitan cities: air quality improvement by PM10 and O_3 removal. *Ecol. Indic.* 67, 425–440. doi: 10.1016/j.ecolind.2016.03.009

Marando, F., Salvatori, E., Fusaro, L., and Manes, F. (2016). Removal of PM10 by forests as a nature-based solution for air quality improvement in the metropolitan city of Rome. *Forests.* 7:150. doi: 10.3390/f7070150

Matsui, K. (2016). Portion of plant airborne communication is endorsed by uptake and metabolism of volatile organic compounds. *Curr. Opin. Plant Biol.* 32, 24–30. doi: 10.1016/j.pbi.2016.05.005

Misztal, C.N., Hewitt, J., Wildt, J.D., Blande, A.S., Eller, D., Fares, S., et al. (2015). Atmospheric benzenoid emissions from plants rival those from fossil fuels. *Sci. Rep.* 5:12064. doi: 10.1038/srep12064

MMA (2016). *Informe Final para la Gestión de Episodios Críticos de Contaminación Atmosférica por Material Particulado Respirable (MP10), Periodo 2016. Secretaria Regional Ministerial (SEREMI) del Medio Ambiente, Región Metropolitana*. Ministerio del Medio Ambiente. Gobierno de Chile. Retrieved from: http://portal.mma.gob.cl/wp-content/uploads/2017/01/INFORME-_GEC_Fin-2016_EFA.pdf

Niinemets, Ü., Fares, S., Harley, P., and Jardine, K.J. (2014). Bidirectional exchange of biogenic volatils with vegetation: emission sources, reactions, breakdown and deposition. *Plant Cell Environ*. 37, 1790–1809. doi: 10.1111/pce.12322

Paoletti, E. (2009). Ozone and urban forests in Italy. *Environ. Pollu.* 157, 1506–1512. doi: 10.1016/j.envpol.2008.09.019

Préndez, M., Araya, M., Criollo, C., Egas, C., Farías, I., Fuentealba, R., et al. (2019). "Urban trees and its relationships with air pollution by particulate matter and ozone in Santiago de Chile," in *Chapter 8: Urban Climates in Latin America*, eds C. Henríquez, and H. Romero (Cham: Springer Nature Switzerland AG), 167–206. doi: 10.1007/978-3-319-97013-4_8

Préndez, M., Carvajal, V., Corada, K., Morales, J., Alarcón, F., and Peralta, H. (2013a). Biogenic volatile organic compounds from the urban forest of the Metropolitan Region, Chile. *Environ. Pollut*. 183, 143–150. doi: 10.1016/j.envpol.2013.04.003

Préndez, M., Corada, K., and Morales, J. (2013b). Emission factors of biogenic volatile organic compounds in various stages of growth present in the urban forest of the Metropolitan Region, Chile. *Res. J. Chem. Environ*. 17, 108–116. Available online at: https://www.scopus.com/inward/record.uri?eid=2-s2.0-84886913189&partnerID=40&md5=f20c25a3da64e278af06d56c7a513bc7

Romero, H. (2019). "Urban climates and the challenge of sustainable development of Chilean cities," in *Urban Climates in Latin America*, eds C. Henríquez, and H. Romero (Cham: Springer), 167–206. doi: 10.1007/978-3-319-97013-4_9

Saphores, J., and Li, W. (2012). Landscape and urban planning estimating the value of urban green areas: a hedonic pricing analysis of the single-family housing market in Los Angeles, CA. *Landsc. Urban Plan.* 104, 373–387. doi: 10.1016/j.landurbplan.2011.11.012

Shao, P., An, J., Xin, J., Wu, F., Wang, J., Ji, D., et al. (2016). Source apportionment of VOCs and the contribution to photochemical ozone formation during summer in the typical industrial area in the Yangtze River Delta, China. *Atmos. Res.* 176–177, 64–74. doi: 10.1016/j.atmosres.2016.02.015

SINCA (2017). *Sistema de Información Nacional de Calidad del Aire*. Gobierno de Chile. Available online at: http://sinca.mma.gob.cl/index.php/region/index/id/M (accessed December 10, 2019).

Tallis, M., Taylor, G., Sinnett, D., and Freer-Smith, P. (2011). Estimating the removal of atmospheric particulate pollution by the urban tree canopy of London, under current and future environments. *Landsc. Urban Plan.* 103,129–138. doi: 10.1016/j.landurbplan.2011.07.003

Tattini, M., Loreto, F., Fini, A., Guidi, L., Brunetti, C., Velikova, V., et al. (2015). Isoprenoids and phenylpropanoids are part of the antioxidant defense orchestrated daily by drought-stressed *Platanus* × *acerifolia* plants during Mediterranean summers. *New Phytol.* 207, 613–626. doi: 10.1111/nph.13380

Ulriksen, P. (1993). "Factores meteorológicos de la contaminación atmosférica de Santiago," in *Chapter 2: Contaminación Atmosférica de Santiago: Estado Actual y Soluciones*, eds H. Sandoval, M. Préndez, and P. Ulriksen (Santiago de Chile: Universidad de Chile y Comisión Especial de Descontaminación de la Región Metropolitana), 37–60.

UOCT (2019). *Operational Unit of Traffic Control, Ministry of Transport of Chile*. Available online at: http://www.mtt.gob.cl/pyd/uoct (accessed April 28, 2019).

USEPA (1989). *Network Design and Site Exposure Criteria for Nonmethane Organic Hydrocarbons. Office Air Quality Planning and Standards*, SYSAPP-89/138. Research Triangle Park, NC: United States Environmental Protection Agency.

Wang, H., Wang, Q., Chen, J., Chen, C., Huang, C., Qiao, L., et al. (2015). Do vehicular emissions dominate the source of C6-C8 aromatics in the megacity Shanghai of eastern China? *J. Environ. Sci.* 27, 290–297. doi: 10.1016/j.jes.2014.05.033

Wararat, S., Parinda, S., Sirintip, A., Polawat, K., Atcharaphan, W., Anuchit, S., et al. (2014). Uptake of toluene and ethylbenzene by plants: removal of volatile indoor air contaminants. *Ecotoxicol. Environ. Saf*. 102, 147–151. doi: 10.1016/j.ecoenv.2014.01.032

WHO (2016). *Ambient Air Pollution: A Global Assessment of Exposure and Burden Of Disease*. World Health Organization. Retrieved from: http://www.who.int/phe/health_topics/outdoorair/databases/cities/en/Z

Wiedinmyer, C., Guenther, A., Harley, P., Hewitt, N., Geron, C., Artaxo, P., et al. (2004). "Globals organic emissions from vegetation," in *Emissions of Atmospheric Trace Compounds*, eds C. Granier, P. Artaxo, and C. Reeves (Dordrecht: Kluwer Academic Publishers), 115–170. doi: 10.1007/978-1-4020-2167-1_4

Wu, W., Zhao, B., Wang, S., and Hao, J. (2017). Ozone and secondary organic aerosol formation potential from anthropogenic volatile organic compounds emissions in China. *J. Environ. Sci*. 53, 224–237. doi: 10.1016/j.jes.2016.03.025

Conflict of Interest Statement: The authors declare that the research was conducted in the absence of any commercial or financial relationships that could be construed as a potential conflict of interest.

frontiers
in Forests and Global Change

MINI REVIEW
published: 20 August 2019
doi: 10.3389/ffgc.2019.00045

Importance of Detoxification Processes in Ozone Risk Assessment: Need to Integrate the Cellular Compartmentation of Antioxidants?

*Nicolas Dusart, Anthony Gandin, Marie-Noëlle Vaultier, Ricardo Joffe, Mireille Cabané, Pierre Dizengremel and Yves Jolivet**

Université de Lorraine, AgroParisTech, Institut National de la Recherche Agronomique (INRA), UMR 1434 Silva, Nancy, France

Edited by:
Elena Paoletti,
Italian National Research Council (CNR), Italy

Reviewed by:
Marcela Regina Engela,
Institute of Botany São Paulo, Brazil
Lorenzo Cotrozzi,
University of Pisa, Italy

****Correspondence:***
Yves Jolivet
yves.jolivet@univ-lorraine.fr

Specialty section:
This article was submitted to Forests and the Atmosphere, a section of the journal Frontiers in Forests and Global Change

Received: *12 June 2019*
Accepted: *05 August 2019*
Published: *20 August 2019*

Citation:
Dusart N, Gandin A, Vaultier M-N, Joffe R, Cabané M, Dizengremel P and Jolivet Y (2019) Importance of Detoxification Processes in Ozone Risk Assessment: Need to Integrate the Cellular Compartmentation of Antioxidants? Front. For. Glob. Change 2:45. doi: 10.3389/ffgc.2019.00045

The correct integration of the detoxification processes in a risk assessment model for ozone damage on plants remains challenging. In particular, the intracellular compartmentation of antioxidant metabolites could play a role, since each compartment presents its own sensitivity to ROS and metabolite set. For each compartment, we tried to provide both qualitative and quantitative information on the metabolites present as well as the putative transporters implied. When they are known, the modifications caused by O_3 or oxidative stress are presented. Clearly, under O_3 exposure, integrative data which would allow to improve predictive models for O_3 risk assessment are missing.

Keywords: ozone, ROS, antioxidants, cellular compartmentation, risk assessment models

INTRODUCTION

Ozone (O_3) is a phytotoxic air pollutant known to negatively impact crop and forest productivity (Wittig et al., 2009; Jolivet et al., 2016; Li et al., 2017). In order to determine the critical level above which O_3 damage on plants occurs, the POD_Y (Phytotoxic Ozone Dose above a threshold flux of Y $nmol.m^{-2}.s^{-1}$) was derived from flux-based methods to improve dose-response relationships including the detoxifying capacity of leaf tissues (Musselman et al., 2006; Dizengremel et al., 2009). Flux-based models use a range of cut-off thresholds (Y) indicative of varying detoxification capacities. However, the considerable uncertainties to determine the contribution of each metabolite to the cellular antioxidant potential make the estimation of the threshold difficult to assess. This difficulty can be explained by the differences in concentrations and redox status of these metabolites between compartments. Here, we resumed recent highlights on the spatial distribution of the main defense metabolites to decipher their possible roles in response to O_3 and point out which importance the occurrence of this compartmentation might have in estimating the detoxification threshold.

DEAL WITH A DIVERSITY OF ANTIOXIDANT METABOLITES

Different classes of molecules serve as antioxidants amongst which ascorbate (AsA), glutathione (GSH), and phenolic compounds as flavonols are considered as the most ubiquitous according to their presence in several cell compartments (Foyer and Noctor, 2011; **Figure 1**), including vacuole and the extracellular space (Zhao and Dixon, 2009; Agati et al., 2012). Sugars such as

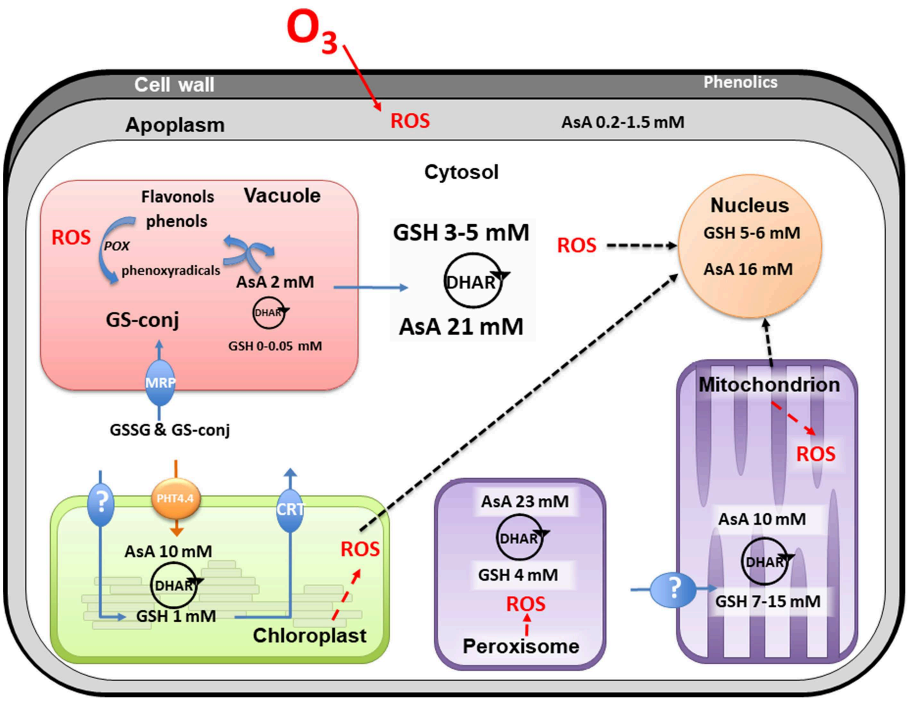

FIGURE 1 | Compartmentation of plant oxidative system. This non-exhaustive figure summarizes current knowledge from plant subcellular localization of antioxidants in non-stress conditions. In view of the multiplicity of all enzyme isoforms, the figure only mentions the presence of the HAF cycle in each compartment where the dehydroascorbate reductase (DHAR) has been characterized. AsA, total ascorbate; GSH, total glutathione; GSSG, glutathione disulphide; GS-conj, glutathione conjugates; HAF, Halliwell-Asada-Foyer; MRP, Multidrug Resistance associated Protein; CRT, Chloroquine Resistance Transporter; PHT, phosphate transporter; POX, phenol peroxidases; ROS, reactive oxygen species. See the text for references.

sucrose, RFOs (raffinose family oligosaccharides) and fructans are known to directly quench ROS in different organelles and thus contribute to antioxidant defense (Keunen et al., 2013). Another type are liphophilic antioxidants, such as α-tocopherol or carotenoids located in organelle membranes particularly in plastids (Das and Roychoudhury, 2014). Subcellular compartments also possess various enzymes able either to act as ROS scavengers or to support regeneration of the reduced form of the antioxidants (Noctor et al., 2018). The first group includes enzymes trapping the superoxide ion (such as superoxide dismutase, SODs) and hydrogen peroxide with catalases (specifically located in the peroxisome) or several peroxidases (AsA, GSH, or thioredoxin dependent) whose cell location has already been detailed in several reviews (Rouhier and Jacquot, 2005; Dos Santos and Rey, 2006; Mhamdi et al., 2010b; Rahantaniaina et al., 2013; Noctor et al., 2018). The second group, responsible for the regeneration of antioxidants, is ascribed to the close redox coupling of AsA and GSH pools *in vivo* (HAF as Halliwell Asada Foyer cycle). The presence of dehydroascorbate reductase (DHAR) seems to be sufficient to consider the presence and the functioning of the HAF cycle within a specific cell compartment (**Figure 1**; Rahantaniaina et al., 2013). It is also important to consider that the HAF cycle functioning needs to be linked with a correct enzyme regeneration through NAD(P)H reducing power, e.g., under O_3 stress (Dizengremel et al., 2008; Dghim et al., 2013), in cytosol as well as in organelles. *In fine*, detoxification results from the combined actions of all these mechanisms, which therefore explains the difficulty to choose key parameter(s) in modeling the detoxifying capacity of leaf tissues.

TOTAL POOL OF ANTIOXIDANTS: NOT SO SATISFYING

One major issue when considering the total pool of antioxidants is the difficulty to evaluate it as a whole, taking into account the diversity of the metabolites it contains. Indeed, the methods and kits used are disputable (Noctor et al., 2016). For example, in order to take into account the total antioxidant capacity in plants, some authors used the FRAP assay (ferric reducing ability of plasma given in micromoles of Fe^{2+} per gram in dry matter). However, the significance of the FRAP test is questionable since it takes antioxidants into consideration that do not necessarily react to the oxidative load generated by O_3 (Severino et al., 2007). To solve this issue, researches focused on specific metabolites considered as cue to explain differences in O_3 tolerance. AsA is one of the main examples of a potential factor in O_3 tolerance (Burkey et al., 2000; Conklin and Barth, 2004) at least for some species. To support this fact, studies with

AsA deficient mutants and clones (Conklin et al., 1996, 2000; Veljovic-Jovanovic et al., 2002) showed that low concentrations of AsA in the plant tissue limit O_3 tolerance. However, in numerous examples and particularly in ligneous species (e.g., *Populus* genotypes or *Quercus* sp.), differences in AsA content were not sufficient to explain the differences in O_3 tolerance (Dusart et al., 2019; Pellegrini et al., 2019). Other antioxidants such as GSH and/or phenolic compounds could play a more important role in some species or genotypes. In addition, changes at the leaf scale could hide more subtle changes at the scale of a cell compartment that is crucial for cell homeostasis. The redox state of each metabolite also varies, as some compartments differ from others with lower reduction states. Thus, the apoplast and vacuole were endowed with a lower level of reduction for AsA and GSH (Noctor and Foyer, 2016). In this respect, both the antioxidant content and the ability of cell compartments to regulate the redox levels of the molecules have to be considered.

COMPARTMENTATION OF ANTIOXIDANTS

The different cell compartments are not equal in terms of antioxidant concentrations (Zechmann, 2017) and redox state (Foyer and Noctor, 2016) and the main differences between cell compartments are discussed in this section. We also highlight some specific features related to the transport of these metabolites through intracellular membranes, which also contributes to the extent of antioxidant content and redox status in each compartment.

Apoplast

The apoplast comprises the cell wall and the fluid in the intercellular spaces as such constitutes the first barrier encountered by O_3 after entering the leaf through the stomata (Laisk et al., 1989). AsA contained in the apoplastic fluid was often considered as the first line of defense against O_3 and, consequently, its content may increase with the beginning of the exposure (Riikonen et al., 2009). In this context, it has been integrated in different models (Polle et al., 1995; Ranieri et al., 1996; Plöchl et al., 2000; Burkey and Eason, 2002; Conklin and Barth, 2004; Tuzet et al., 2011). In fact, in many species, the importance of apoplastic AsA regarding O_3 tolerance is still unclear (D'Haese et al., 2005; Booker et al., 2012; Dai et al., 2018). For example investigated poplar clones showed no relation between apoplastic AsA content and O_3 sensitivity of clones (Van Hove et al., 2001; Di Baccio et al., 2008). Moreover, the efficiency of apoplast detoxification by AsA depends on the export of the oxidized form to the cytoplasm where it then has to be regenerated (Luwe and Heber, 1995). Finally, despite an efficient transmembrane exchange between apoplast and symplasm, the AsA concentrations (around 0.2–1.5 mM) in the apoplast are 10–30 times lower than in the cytosol (Moldau et al., 1997; Plöchl et al., 2000; Van Hove et al., 2001) with higher oxidation rates (Booker et al., 2012). The transport proteins responsible for DHA uptake and ascorbate efflux have not yet been identified, even though the ascorbate efflux mechanism possibly occurs via an anion channel (Smirnoff, 2018). It should also be considered that the presence of ascorbate oxidase in the apoplast could maintain the AsA pool in a more oxidized state than the intracellular pool (Smirnoff, 2018).

There are furthermore other metabolites with antioxidant activity being present in the apoplast. Considering GSH, its content in the apoplast has been found to be very low (Zechmann, 2014), limiting its ability to scavenge ROS or contribute to ASA regeneration. Apoplastic GSH is therefore expected to be rather involved in signaling than in detoxification (Zechmann et al., 2008). Phenolic compounds (Grace, 2007) may be widespread in the apoplastic fluid of plants and in some cases were shown to increase in response to O_3 (Langebartels et al., 1991; Eckey-Kaltenbach et al., 1993; Booker et al., 2012). However this increase was considered to have little effectiveness in scavenging O_3 in *Arabidopsis* (Booker et al., 2012). Cell wall bound phenolics may also scavenge ROS (Vreeburg and Fry, 2007) but their contribution to O_3 detoxification is yet unknown. In the cell wall of foliar and stem cells, O_3 exposure resulted in an increase in lignin biosynthesis in a dose-dependent manner suggesting a role in detoxification (Cabane et al., 2012). The contribution of phenolics and more widely secondary metabolites in apoplastic O_3 detoxification has not been sufficiently studied so far and should be further investigated especially because of their species-specific diversity.

Cytosol

Cytosol is an important determinant in the antioxidant capacity of the cell, acting as a hub for the production/transportation to other cell compartments and between compartments (Zechmann, 2017). Using labeling techniques (Zechmann, 2011), showed that the highest concentration of AsA was found in this compartment (**Figure 1**). Moreover, isoenzymes related to HAF cycle localized in the cytosol seem to play an important role in O_3 tolerance (Yoshida et al., 2006; Di Baccio et al., 2008; Mhamdi et al., 2010a; Rahantaniaina et al., 2017; Dusart et al., 2019). A good example of the cytosol interface is the GSH biosynthesis taking place both in cytosol and chloroplast (Rausch et al., 2007). Interestingly, although chloroplasts synthesize GSH, this metabolite is also readily taken up by intact chloroplasts (Foyer et al., 2001). For the other compartments, unable to carry out GSH biosynthesis, transport from cytosol must also be efficient (Rausch et al., 2007). While these carriers are far from being characterized, their regulation under oxidative stress is fully unknown.

Vacuole

In vacuole, the AsA concentration is often considered not to exceed 2 mM, making it the lowest within the plant cells (**Figure 1**; Zechmann, 2017). However, its level was 2- and 4-times increased during drought and high light stress, respectively, which represents the strongest increase among all subcellular compartments (Rautenkranz et al., 1994; Zechmann, 2017). Changes in AsA concentration under O_3 are not known. This raises the question whether vacuolar AsA could significantly contribute to cell defense against oxidative stress. When facing stress conditions, a large amount of H_2O_2 is transported and accumulated in the vacuole, which might act as a sink for ROS (Michalak, 2006; Koffler et al., 2014).

It is expected that the increase in vacuolar AsA contributes to delocalize the detoxification of H_2O_2 and thus to avoid cytosol redox imbalance. AsA seems to contribute to ROS scavenging in the vacuole, either directly or by coupling with phenolics and phenol oxidase. In fact, vacuoles are also well-known to hold large amounts of polyphenols, especially anthocyanins, flavan-3-ol monomers, proanthocyanidins, and glycosylated flavonols. Vacuolar flavonols have been suggested to contribute to H_2O_2 detoxification in this compartment, by giving electrons to phenol peroxidases (POX) (Sakihama et al., 2002). Furthermore, it has been shown that vacuolar AsA can reduce phenoxy radicals produced by POX and then regenerate phenolic compounds (Takahama and Oniki, 1997). Therefore, an alternative AsA/phenolics/POX mechanism might efficiently contribute to the cellular defense arsenal against ROS, jointly to the "classic" HAF cycle. On this point, none or very little free GSH (lower than 0.5 mM) has ever been identified in the vacuole, limiting the potential regeneration of ascorbate by this way in this compartment (Zechmann et al., 2008; Zechmann, 2014). In addition, DHAR was reported in the vacuole (Zhang et al., 2015) but HAF cycle does not seem to be functioning due to the lack of glutathione reductase isoform in this compartment, therefore leading to glutathione disulphide (GSSG) accumulation (Queval et al., 2011). In any case, oxidized AsA (DHA and monodehydroascorbate) can cross the tonoplast to be regenerated in the cytoplasm (Rautenkranz et al., 1994). In case of oxidative stress, vacuoles also act as a sink for oxidized GSH or GSH conjugates formed in the cytosol and transferred to the vacuole via the action of one or more ABC transporters of the MRP (Multidrug Resistance associated Protein) subclass (Queval et al., 2011; Koffler et al., 2014). Despite extensive investigation of tonoplast transporters, the role of MRPs in the transport of GSSG to the vacuole is less clear (Bachhawat et al., 2013) as well as the final fate of this oxidized form in the vacuole.

Chloroplast

Within the chloroplast, the electron transport chain is, in addition to its role as major energy producer, one of the main sites of endogenous ROS generation (Asada, 2006; Tripathy and Oelmüller, 2012). Being triggered and increased by apoplastic ROS, the chloroplastic ROS function as amplifiers of signals from outer cell compartments to the nucleus where they modify the nuclear gene expression (Shapiguzov et al., 2012; Foyer and Noctor, 2016; Kleine and Leister, 2016). The presence of AsA (10 mM) and GSH (1 mM) has been previously reported in the chloroplast where they represent a significant part of the cell antioxidant pool (**Figure 1**; Queval et al., 2011; Zechmann, 2011). Interestingly, abiotic stresses lead to a major increase in AsA and GSH contents in the chloroplast (Heyneke et al., 2013). Furthermore, although lacking under normal conditions, both antioxidants also accumulated inside the thylakoid lumen under stress, thus, demonstrating the particular dependence of the chloroplast on these antioxidants when facing harmful abiotic stress (Heyneke et al., 2013). Concerning AsA and GSH transport, chloroplast and cytosol are tightly connected by the presence of many transporters. AsA uptake by chloroplasts is mediated by a member of a phosphate transporter family, named PHT4;4 (Fernie and Tóth, 2015; Miyaji et al., 2015). An active uptake of cytosolic GSH also occurred across the chloroplast envelope (Noctor et al., 2002), even though the molecular identity of the transporter(s) is still unknown (Bachhawat et al., 2013). In addition, three proteins belonging to the CRT (Chloroquine Resistance Transporter)-like transporter family were found to be chloroplastic and responsible for glutathione efflux from the chloroplast to the cytosol *in Arabidopsis* (Bachhawat et al., 2013).

At the same time, choroplasts contain large amounts of flavonoid-like ROS defense agents, which they are able to biosynthesize (Hernández et al., 2009; Pollastri and Tattini, 2011). Under severe light, flavonoids complete the scavenging role of the most abundant lipid-soluble antioxidants group(s), the carotenoids (and tocopherols), in chloroplasts (DellaPenna and Pogson, 2006). Due to their ability to remodel lipid membranes, flavonoids might preserve the integrity of the chloroplast envelope and therefore prevent oxidative stress-caused damage (Agati et al., 2012).

Mitochondria

An endogenous production of ROS takes place in mitochondria essentially at the level of the complexes I, II, and III of the respiratory chain which must not be neglected even though the contribution of this organelle to oxidative stress is rather low (Apel and Hirt, 2004; Rhoads et al., 2006; Bettini et al., 2008; Waszczak et al., 2018). Mitochondria are well-supplied with antioxidants and the enzymes of the HAF cycle are present (Jiménez et al., 1997; Foyer et al., 2001; Foyer and Noctor, 2011). Similar as chloroplast, a concentration of 10 mM AsA was determined in mitochondria (Zechmann, 2011; Zechmann et al., 2011). Considering that the last step of ascorbate biosynthesis can take place in the intermembrane space in contact with complex 1 (Millar et al., 2003), it is now seen that DHA is transported in the matrix to subsequently be reduced by the HAF cycle (Navrot et al., 2007). In this context, a high concentration of GSH (between 7 and 15 mM) has been determined in this organelle (Zechmann et al., 2008; Queval et al., 2011; Zechmann, 2014), despite it is considered to be devoid of GSH synthesis pathway. This implies an uptake of GSH from the cytosol assumed by different transporters (Chen and Lash, 1998). In addition, there is no work mentioning the accumulation of phenols in the mitochondria, these compounds been known as inhibitors of the respiratory activity (Demos et al., 1975). Finally, in spite of a quite large panel of antioxidants, the mitochondria have been pointed out as being more sensitive to O_3 than chloroplasts (Pellinen et al., 1999). Nevertheless, there is no consensus to validate this difference of sensitivity between organelles (Sutinen et al., 1990).

Peroxisome

Due to H_2O_2 production driven by photorespiration, the peroxisome is also provided with antioxidant systems (Corpas et al., 2019). To minimize H_2O_2 accumulation in this compartment, a significant catalase activity has been observed. In addition, the presence of DHAR isoform suggests a functioning HAF cycle (Jiménez et al., 1997) in the peroxisome. A high concentration of AsA (23 mM) was determined in the peroxisome (Zechmann, 2017) while GSH was also detected but at low level (4 mM) (Zechmann et al., 2008). O_3 increased catalase activity and enhanced the number of peroxisome in tolerant birch leaves (Oksanen et al., 2004). The increase of peroxisome number could be a response to an enhanced requirement for detoxification as photorespiration decreased (Booker et al., 1997; Bagard et al., 2008).

CONCLUSION

This article points out the great diversity of antioxidative systems, scattered in the different cellular compartments of leaves. The data so far published suggest that this diversity must be taken into account in O_3 risk assessment. However, under O_3, there is a lack of information regarding changes in the concentrations of the different antioxidants in each compartment under ozone treatment. As mentioned in previous works, and considering its occurrence in different cell compartments, it is obvious that the HAF cycle has a prominent role in cell detoxification. In addition, phenolic compounds in cell wall, vacuole and chloroplasts might also play a protective role. Subcellular immunocytochemical localization could allow a more precise identification of the respective contribution of each compartment to the global defense system. The next step would be to get an integrative scheme allowing to improve the modeling for the participation of detoxification to risk assessment. Recently, an attempt to integrate the vacuole in an H_2O_2 metabolism under oxidative constraint model appeared to be promising, especially since transporters were considered (Tuzet et al., 2019). Indeed, the transport of antioxidants between compartments during oxidative stress should be also studied to better understand the role of compartmentation.

AUTHOR CONTRIBUTIONS

All authors listed have made a substantial, direct and intellectual contribution to the work, and approved it for publication.

FUNDING

This laboratory was supported by the French National Research Agency through the Laboratory of Excellence ARBRE (ANR-12-LABXARBRE-01).

REFERENCES

Agati, G., Azzarello, E., Pollastri, S., and Tattini, M. (2012). Flavonoids as antioxidants in plants: location and functional significance. *Plant Sci.* 196, 67–76. doi: 10.1016/j.plantsci.2012.07.014

Apel, K., and Hirt, H. (2004). Reactive oxygen species: metabolism, oxidative stress, and signal transduction. *Annu. Rev. Plant Biol.* 55, 373–399. doi: 10.1146/annurev.arplant.55.031903.141701

Asada, K. (2006). Production and scavenging of reactive oxygen species in chloroplasts and their functions. *Plant Physiol.* 141, 391–396. doi: 10.1104/pp.106.082040

Bachhawat, A. K., Thakur, A., Kaur, J., and Zulkifli, M. (2013). Glutathione transporters. *Biochim. Biophys. Acta BBA-Gen. Subj.* 1830, 3154–3164. doi: 10.1016/j.bbagen.2012.11.018

Bagard, M., Le Thiec, D., Delacote, E., Hasenfratz-Sauder, M.-P., Banvoy, J., Gérard, J., et al. (2008). Ozone-induced changes in photosynthesis and photorespiration of hybrid poplar in relation to the developmental stage of the leaves. *Physiol. Plant.* 134, 559–574. doi: 10.1111/j.1399-3054.2008.01160.x

Bettini, P., Cosi, E., Bindi, D., and Buiatti, M. (2008). Reactive oxygen species metabolism in plants: production, detoxification and signaling in stress response. *Plant Stress* 2, 28–39.

Booker, F. L., Burkey, K. O., and Jones, A. M. (2012). Re-evaluating the role of ascorbic acid and phenolic glycosides in ozone scavenging in the leaf apoplast of *Arabidopsis thaliana* L. *Plant Cell Environ.* 35, 1456–1466. doi: 10.1111/j.1365-3040.2012.02502.x

Booker, F. L., Reid, C. D., Brunschon-Harti, S., Fiscus, E. L., and Miller, J. E. (1997). Photosynthesis and photorespiration in soybean [Glycine max (L.) Merr.] chronically exposed to elevated carbon dioxide and ozone. *J. Exp. Bot.* 48, 1843–1852.

Burkey, K. O., and Eason, G. (2002). Ozone tolerance in snap bean is associated with elevated ascorbic acid in the leaf apoplast. *Physiol. Plant.* 114, 387–394. doi: 10.1034/j.1399-3054.2002.1140308.x

Burkey, K. O., Wei, C., Eason, G., Ghosh, P., and Fenner, G. P. (2000). Antioxidant metabolite levels in ozone-sensitive and tolerant genotypes of snap bean. *Physiol. Plant.* 110, 195–200. doi: 10.1034/j.1399-3054.2000.110208.x

Cabane, M., Afif, D., and Hawkins, S. (2012). "Chapter 7–lignins and abiotic stresses," in *Advances in Botanical Research Lignins*, Vol. 61, eds L. Jouanin and C. Lapierre (Burlington: Academic Press), 219–262.

Chen, Z., and Lash, L. H. (1998). Evidence for mitochondrial uptake of glutathione by dicarboxylate and 2-oxoglutarate carriers. *J. Pharmacol. Exp. Ther.* 285, 608–618.

Conklin, P. L., and Barth, C. (2004). Ascorbic acid, a familiar small molecule intertwined in the response of plants to ozone, pathogens, and the onset of senescence. *Plant Cell Environ.* 27, 959–970. doi: 10.1111/j.1365-3040.2004.01203.x

Conklin, P. L., Saracco, S. A., Norris, S. R., and Last, R. L. (2000). Identification of ascorbic acid-deficient *Arabidopsis thaliana* mutants. *Genetics* 154, 847–856.

Conklin, P. L., Williams, E. H., and Last, R. L. (1996). Environmental stress sensitivity of an ascorbic acid-deficient *Arabidopsis* mutant. *Proc. Natl. Acad. Sci. U.S.A.* 93, 9970–9974. doi: 10.1073/pnas.93.18.9970

Corpas, F. J., del Río, L. A., and Palma, J. M. (2019). Impact of nitric oxide (NO) on the ROS metabolism of peroxisomes. *Plants* 8:37. doi: 10.3390/plants8020037

Dai, L., Feng, Z., Pan, X., Xu, Y., Li, P., Lefohn, A. S., et al. (2018). Increase of apoplastic ascorbate induced by ozone is insufficient to remove the negative effects in tobacco, soybean and poplar. *Environ. Pollut.* 245, 380–388. doi: 10.1016/j.envpol.2018.11.030

Das, K., and Roychoudhury, A. (2014). Reactive oxygen species (ROS) and response of antioxidants as ROS-scavengers during environmental stress in plants. *Front. Environ. Sci.* 2:53. doi: 10.3389/fenvs.2014.00053

DellaPenna, D., and Pogson, B. J. (2006). Vitamin synthesis in plants: tocopherols and carotenoids. *Annu. Rev. Plant Biol.* 57, 711–738. doi: 10.1146/annurev.arplant.56.032604.144301

Demos, E. K., Woolwine, M., Wilson, R. H., and McMillan, C. (1975). The effects of ten phenolics compoundds on hypocotyl growth and mitochondrial metabolism of mung bean. *Am. J. Bot.* 62, 97–102. doi: 10.1002/j.1537-2197.1975.tb12343.x

Dghim, A. A., Dumont, J., Hasenfratz-Sauder, M.-P., Dizengremel, P., Le Thiec, D., and Jolivet, Y. (2013). Capacity for NADPH regeneration in the leaves of two poplar genotypes differing in ozone sensitivity. *Physiol. Plant.* 148, 36–50. doi: 10.1111/j.1399-3054.2012.01686.x

D'Haese, D., Vandermeiren, K., Asard, H. A. N., and Horemans, N. (2005). Other factors than apoplastic ascorbate contribute to the differential ozone tolerance of two clones of *Trifolium repens* L. *Plant Cell Environ.* 28, 623–632. doi: 10.1111/j.1365-3040.2005.01308.x

Di Baccio, D., Castagna, A., Paoletti, E., Sebastiani, L., and Ranieri, A. (2008). Could the differences in O_3 sensitivity between two poplar clones be related to a difference in antioxidant defense and secondary metabolic response to O_3 influx? *Tree Physiol.* 28, 1761–1772. doi: 10.1093/treephys/28.12.1761

Dizengremel, P., Le Thiec, D., Bagard, M., and Jolivet, Y. (2008). Ozone risk assessment for plants: central role of metabolism-dependent changes in reducing power. *Environ. Pollut.* 156, 11–15. doi: 10.1016/j.envpol.2007.12.024

Dizengremel, P., Thiec, D. L., Hasenfratz-Sauder, M.-P., Vaultier, M.-N., Bagard, M., and Jolivet, Y. (2009). Metabolic-dependent changes in plant cell redox power after ozone exposure. *Plant Biol.* 11, 35–42. doi: 10.1111/j.1438-8677.2009.00261.x

Dos Santos, C. V., and Rey, P. (2006). Plant thioredoxins are key actors in the oxidative stress response. *Trends Plant Sci.* 11, 329–334. doi: 10.1016/j.tplants.2006.05.005

Dusart, N., Gérard, J., Le Thiec, D., Collignon, C., Jolivet, Y., and Vaultier, M.-N. (2019). Integrated analysis of the detoxification responses of two Euramerican poplar genotypes exposed to ozone and water deficit: focus on the ascorbate-glutathione cycle. *Sci. Total Environ.* 651, 2365–2379. doi: 10.1016/j.scitotenv.2018.09.367

Eckey-Kaltenbach, H., Heller, W., Sonnenbichler, J., Zetl, I., Schäfer, W., Ernst, D., et al. (1993). Oxidative stress and plant secondary metabolism: 6f two Euramerican poplar geno*Phytochemistry* 34, 687–691. doi: 10.1016/0031-9422(93)85340-W

Fernie, A. R., and Tóth, S. Z. (2015). Identification of the elusive chloroplast ascorbate transporter extends the substrate specificity of the PHT family. *Mol. Plant* 8, 674–676. doi: 10.1016/j.molp.2015.02.006

Foyer, C. H., and Noctor, G. (2011). Ascorbate and glutathione: the heart of the redox hub. *Plant Physiol.* 155, 2–18. doi: 10.1104/pp.110.167569

Foyer, C. H., and Noctor, G. (2016). Stress-triggered redox signalling: what's in pROSpect? *Plant Cell Environ.* 39, 951–964. doi: 10.1111/pce.12621

Foyer, C. H., Theodoulou, F. L., and Delrot, S. (2001). The functions of inter- and intracellular glutathione transport systems in plants. *Trends Plant Sci.* 6, 486–492. doi: 10.1016/S1360-1385(01)02086-6

Grace, S. C. (2007). "Phenolics as antioxidants," in *Antioxidants and Reactive Oxygen Species in Plants*, ed N. Smirnoff (Oxford: Blackwell Publishing Ltd), 141–168.

Hernández, I., Alegre, L., Van Breusegem, F., and Munné-Bosch, S. (2009). How relevant are flavonoids as antioxidants in plants? *Trends Plant Sci.* 14, 125–132. doi: 10.1016/j.tplants.2008.12.003

Heyneke, E., Luschin-Ebengreuth, N., Krajcer, I., Wolkinger, V., Müller, M., and Zechmann, B. (2013). Dynamic compartment specific changes in glutathione and ascorbate levels in *Arabidopsis* plants exposed to different light intensities. *BMC Plant Biol.* 13:104. doi: 10.1186/1471-2229-13-104

Jiménez, A., Hernández, J. A., del Rio, L. A., and Sevilla, F. (1997). Evidence for the presence of the ascorbate-glutathione cycle in mitochondria and peroxisomes of pea leaves. *Plant Physiol.* 114, 275–284. doi: 10.1104/pp.114.1.275

Jolivet, Y., Bagard, M., Caban, M., Vaultier, M.-N., Gandin, A., Afif, D., et al. (2016). Deciphering the ozone-induced changes in cellular processes: a prerequisite for ozone risk assessment at the tree and forest levels. *Ann. For. Sci.* 73, 923–943. doi: 10.1007/s13595-016-0580-3

Keunen, E. L. S., Peshev, D., Vangronsveld, J., Van Den Ende, W. I. M., and Cuypers, A. N. N. (2013). Plant sugars are crucial players in the oxidative challenge during abiotic stress: extending the traditional concept. *Plant Cell Environ.* 36, 1242–1255. doi: 10.1111/pce.12061

Kleine, T., and Leister, D. (2016). Retrograde signaling: organelles go networking. *Biochim. Biophys. Acta BBA-Bioenerg.* 1857, 1313–1325. doi: 10.1016/j.bbabio.2016.03.017

Koffler, B. E., Luschin-Ebengreuth, N., Stabentheiner, E., Müller, M., and Zechmann, B. (2014). Compartment specific response of antioxidants to drought stress in *Arabidopsis*. *Plant Sci.* 227, 133–144. doi: 10.1016/j.plantsci.2014.08.002

Laisk, A., Kull, O., and Moldau, H. (1989). Ozone concentration in leaf intercellular air spaces is close to zero. *Plant Physiol.* 90, 1163–1167. doi: 10.1104/pp.90.3.1163

Langebartels, C., Kerner, K., Leonardi, S., Schraudner, M., Trost, M., Heller, W., et al. (1991). Biochemical Plant Responses to Ozone. *Plant Physiol.* 95:8. doi: 10.1104/pp.95.3.882

Li, P., Feng, Z., Catalayud, V., Yuan, X., Xu, Y., and Paoletti, E. (2017). A meta-analysis on growth, physiological, and biochemical responses of woody species to ground-level ozone highlights the role of plant functional types. *Plant Cell Environ.* 40, 2369–2380. doi: 10.1111/pce.13043

Luwe, M., and Heber, U. (1995). Ozone detoxification in the apoplasm and symplasm of spinach, broad bean and beech leaves at ambient and elevated concentrations of ozone in air. *Planta* 197, 448–455. doi: 10.1007/BF00196666

Mhamdi, A., Hager, J., Chaouch, S., Queval, G., Han, Y., Taconnat, L., et al. (2010a). *Arabidopsis* glutathione reductase1 plays a crucial role in leaf responses to intracellular hydrogen peroxide and in ensuring appropriate gene expression through both salicylic acid and jasmonic acid signaling pathways. *Plant Physiol.* 153, 1144–1160. doi: 10.1104/pp.110.153767

Mhamdi, A., Queval, G., Chaouch, S., Vanderauwera, S., Breusegem, F. V., and Noctor, G. (2010b). Catalase function in plants: a focus on Arabidopsis mutants as stress-mimic models. *J. Exp. Bot.* 61, 4197–4220. doi: 10.1093/jxb/erq282

Michalak, A. (2006). Phenolic compounds and their antioxidant activity in plants growing under heavy metal stress. *Pol. J. Environ. Stud.* 15, 523–530.

Millar, A. H., Mittova, V., Kiddle, G., Heazlewood, J. L., Bartoli, C. G., Theodoulou, F. L., et al. (2003). Control of ascorbate synthesis by respiration and its implications for stress responses. *Plant Physiol.* 133, 443–447. doi: 10.1104/pp.103.028399

Miyaji, T., Kuromori, T., Takeuchi, Y., Yamaji, N., Yokosho, K., Shimazawa, A., et al. (2015). AtPHT4; 4 is a chloroplast-localized ascorbate transporter in *Arabidopsis*. *Nat. Commun.* 6:5928. doi: 10.1038/ncomms6928

Moldau, H., Padu, E., and Bichele, I. (1997). Quantification of ozone decay and requirement for ascorbate in *Phaseolus vulgaris* L. mesophyll cell walls. *Phyton Ann. Rei. Bot.* 37, 175–180.

Musselman, R. C., Lefohn, A. S., Massman, W. J., and Heath, R. L. (2006). A critical review and analysis of the use of exposure-and flux-based ozone indices for predicting vegetation effects. *Atmos. Environ.* 40, 1869–1888. doi: 10.1016/j.atmosenv.2005.10.064

Navrot, N., Rouhier, N., Gelhaye, E., and Jacquot, J.-P. (2007). Reactive oxygen species generation and antioxidant systems in plant mitochondria. *Physiol. Plant.* 129, 185–195. doi: 10.1111/j.1399-3054.2006.00777.x

Noctor, G., and Foyer, C. H. (2016). Intracellular redox compartmentation and ROS-related communication in regulation and signaling. *Plant Physiol.* 171, 1581–1592. doi: 10.1104/pp.16.00346

Noctor, G., Mhamdi, A., and Foyer, C. H. (2016). Oxidative stress and antioxidative systems: recipes for successful data collection and interpretation. *Plant Cell Environ.* 39, 1140–1160. doi: 10.1111/pce.12726

Noctor, G., Reichheld, J.-P., and Foyer, C. H. (2018). ROS-related redox regulation and signaling in plants. *Semin. Cell Dev. Biol.* 80, 3–12. doi: 10.1016/j.semcdb.2017.07.013

Noctor, G., Veljovic-Jovanovic, S., Driscoll, S., Novitskaya, L., and Foyer, C. H. (2002). Drought and oxidative load in the leaves of C3 plants: a predominant role for photorespiration? *Ann. Bot.* 89, 841–850. doi: 10.1093/aob/mcf096

Oksanen, E., Häikiö, E., Sober, J., and Karnosky, D. F. (2004). Ozone-induced H_2O_2 accumulation in field-grown aspen and birch is linked to foliar ultrastructure and peroxisomal activity. *New Phytol.* 161, 791–799. doi: 10.1111/j.1469-8137.2003.00981.x

Pellegrini, E., Hoshika, Y., Dusart, N., Cotrozzi, L., Gérard, J., Nali, C., et al. (2019). Antioxidative responses of three oak species under ozone and water stress conditions. *Sci. Total Environ.* 647, 390–399. doi: 10.1016/j.scitotenv.2018.07.413

Pellinen, R., Palva, T., and Kangasjärvi, J. (1999). Subcellular localization of ozone-induced hydrogen peroxide production in birch (*Betula pendula*) leaf cells. *Plant J.* 20, 349–356. doi: 10.1046/j.1365-313X.1999.00613.x

Plöchl, M., Lyons, T., Ollerenshaw, J., and Barnes, J. (2000). Simulating ozone detoxification in the leaf apoplast through the direct reaction with ascorbate. *Planta* 210, 454–467. doi: 10.1007/PL00008153

Pollastri, S., and Tattini, M. (2011). Flavonols: old compounds for old roles. *Ann. Bot.* 108, 1225–1233. doi: 10.1093/aob/mcr234

Polle, A., Wieser, G., and Havranek, W. M. (1995). Quantification of ozone influx and apoplastic ascorbate content in needles of Norway spruce trees (*Picea abies* L., Karst) at high altitude. *Plant Cell Environ.* 18, 681–688. doi: 10.1111/j.1365-3040.1995.tb00569.x

Queval, G., Jaillard, D., Zechmann, B., and Noctor, G. (2011). Increased intracellular H_2O_2 availability preferentially drives glutathione accumulation in vacuoles and chloroplasts. *Plant Cell Environ.* 34, 21–32. doi: 10.1111/j.1365-3040.2010.02222.x

Rahantaniaina, M.-S., Li, S., Chatel-Innocenti, G., Tuzet, A., Issakidis-Bourguet, E., Mhamdi, A., et al. (2017). Cytosolic and chloroplastic DHARs cooperate in oxidative stress-driven activation of the salicylic acid pathway. *Plant Physiol.* 174, 956–971. doi: 10.1104/pp.17.00317

Rahantaniaina, M.-S., Tuzet, A., Mhamdi, A., and Noctor, G. (2013). Missing links in understanding redox signaling via thiol/disulfide modulation: how is glutathione oxidized in plants? *Front. Plant Sci.* 4:477. doi: 10.3389/fpls.2013.00477

Ranieri, A., D'urso, G., Nali, C., Lorenzini, G., and Soldatini, G. F. (1996). Ozone stimulates apoplastic antioxidant systems in pumpkin leaves. *Physiol. Plant.* 97, 381–387. doi: 10.1034/j.1399-3054.1996.970224.x

Rausch, T., Gromes, R., Liedschulte, V., Müller, I., Bogs, J., Galovic, V., et al. (2007). Novel insight into the regulation of GSH biosynthesis in higher plants. *Plant Biol.* 9, 565–572. doi: 10.1055/s-2007-965580

Rautenkranz, A. A., Li, L., Machler, F., Martinoia, E., and Oertli, J. J. (1994). Transport of ascorbic and dehydroascorbic acids across protoplast and vacuole membranes isolated from barley (*Hordeum vulgare* L. cv Gerbel) leaves. *Plant Physiol.* 106, 187–193. doi: 10.1104/pp.106.1.187

Rhoads, D. M., Umbach, A. L., Subbaiah, C. C., and Siedow, J. N. (2006). Mitochondrial reactive oxygen species. Contribution to oxidative stress and interorganellar signaling. *Plant Physiol.* 141, 357–366. doi: 10.1104/pp.106.079129

Riikonen, J., Mäenpä, M., Alavillamo, M., Silfver, T., and Oksanen, E. (2009). Interactive effect of elevated temperature and O_3 on antioxidant capacity and gas exchange in *Betula pendula* saplings. *Planta* 230, 419–427. doi: 10.1007/s00425-009-0957-8

Rouhier, N., and Jacquot, J.-P. (2005). The plant multigenic family of thiol peroxidases. *Free Radic. Biol. Med.* 38, 1413–1421. doi: 10.1016/j.freeradbiomed.2004.07.037

Sakihama, Y., Cohen, M. F., Grace, S. C., and Yamasaki, H. (2002). Plant phenolic antioxidant and prooxidant activities: phenolics-induced oxidative damage mediated by metals in plants. *Toxicology* 177, 67–80. doi: 10.1016/S0300-483X(02)00196-8

Severino, J. F., Stich, K., and Soja, G. (2007). Ozone stress and antioxidant substances in *Trifolium repens* and *Centaurea jacea* leaves. *Environ. Pollut.* 146, 707–714. doi: 10.1016/j.envpol.2006.04.006

Shapiguzov, A., Vainonen, J., Wrzaczek, M., and Kangasjärvi, J. (2012). ROS-talk–how the apoplast, the chloroplast, and the nucleus get the message through. *Front. Plant Sci.* 3:292. doi: 10.3389/fpls.2012.00292

Smirnoff, N. (2018). Ascorbic acid metabolism and functions: a comparison of plants and mammals. *Free Radic. Biol. Med.* 122, 116–129. doi: 10.1016/j.freeradbiomed.2018.03.033

Sutinen, S., Skarby, L., Wallin, G., and Sellden, G. (1990). Long-term exposure of Norway spruce, *Picea abies* (L.) Karst., to ozone in open top chambers. II. Effects on the ultrastructure of needles. *New Phytol.* 115, 345–355. doi: 10.1111/j.1469-8137.1990.tb00461.x

Takahama, U., and Oniki, T. (1997). A peroxidase/phenolics/ascorbate system can scavenge hydrogen peroxide in plant cells. *Physiol. Plant.* 101, 845–852. doi: 10.1111/j.1399-3054.1997.tb01072.x

Tripathy, B. C., and Oelmüller, R. (2012). Reactive oxygen species generation and signaling in plants. *Plant Signal. Behav.* 7, 1621–1633. doi: 10.4161/psb.22455

Tuzet, A., Perrier, A., Loubet, B., and Cellier, P. (2011). Modelling ozone deposition fluxes: the relative roles of deposition and detoxification processes. *Agric. For. Meteorol.* 151, 480–492. doi: 10.1016/j.agrformet.2010.12.004

Tuzet, A., Rahantaniaina, M.-S., and Noctor, G. (2019). Analyzing the function of catalase and the ascorbate–glutathione pathway in H_2O_2 processing: insights from anexperimentally constrained kinetic model. *Antioxid. Redox Signal.* 30, 1238–1268. doi: 10.1089/ars.2018.7601

Van Hove, L. W. A., Bossen, M. E., San Gabino, B. G., and Sgreva, C. (2001). The ability of apoplastic ascorbate to protect poplar leaves against ambient ozone concentrations: a quantitative approach. *Environ. Pollut.* 114, 371–382. doi: 10.1016/S0269-7491(00)00237-2

Veljovic-Jovanovic, S., Noctor, G., and Foyer, C. H. (2002). Are leaf hydrogen peroxide concentrations commonly overestimated? The potential influence of artefactual interference by tissue phenolics and ascorbate. *Plant Physiol. Biochem.* 40, 501–507. doi: 10.1016/S0981-9428(02)01417-1

Vreeburg, R. A. M., and Fry, S. C. (2007). "Reactive oxygen species in cell walls," in *Antioxidants and Reactive Oxygen Species in Plants*, ed N. Smirnoff (Oxford: Blackwell Publishing Ltd), 215–249.

Waszczak, C., Carmody, M., and Kangasjarvi, J. (2018). Reactive oxygen species in plant signaling. *Annu. Rev. Plant Biol.* 69, 209–236. doi: 10.1146/annurev-arplant-042817-040322

Wittig, V. E., Ainsworth, E. A., Naidu, S. L., Karnosky, D. F., and Long, S. P. (2009). Quantifying the impact of current and future tropospheric ozone on tree biomass, growth, physiology and biochemistry: a quantitative meta-analysis. *Glob. Change Biol.* 15, 396–424. doi: 10.1111/j.1365-2486.2008.01774.x

Yoshida, S., Tamaoki, M., Shikano, T., Nakajima, N., Ogawa, D., Ioki, M., et al. (2006). Cytosolic dehydroascorbate reductase is important for ozone tolerance in *Arabidopsis thaliana*. *Plant Cell Physiol.* 47, 304–308. doi: 10.1093/pcp/pci246

Zechmann, B. (2011). Subcellular distribution of ascorbate in plants. *Plant Signal. Behav.* 6, 360–363. doi: 10.4161/psb.6.3.14342

Zechmann, B. (2014). Compartment-specific importance of glutathione during abiotic and biotic stress. *Front. Plant Sci.* 5:566. doi: 10.3389/fpls.2014.00566

Zechmann, B. (2017). Compartment-specific importance of ascorbate during environmental stress in plants. *Antioxid. Redox Signal.* 29, 1488–1501. doi: 10.1089/ars.2017.7232

Zechmann, B., Mauch, F., Sticher, L., and Müller, M. (2008). Subcellular immunocytochemical analysis detects the highest concentrations of glutathione in mitochondria and not in plastids. *J. Exp. Bot.* 59, 4017–4027. doi: 10.1093/jxb/ern243

Zechmann, B., Stumpe, M., and Mauch, F. (2011). Immunocytochemical determination of the subcellular distribution of ascorbate in plants. *Planta* 233, 1–12. doi: 10.1007/s00425-010-1275-x

Zhang, Y.-J., Wang, W., Yang, H.-L., Li, Y., Kang, X.-Y., Wang, X.-R., et al. (2015). Molecular properties and functional divergence of the dehydroascorbate reductase gene family in lower and higher plants. *PLoS ONE* 10:e0145038. doi: 10.1371/journal.pone.0145038

Zhao, J., and Dixon, R. A. (2009). MATE Transporters facilitate vacuolar uptake of epicatechin $3'$-O-glucoside for proanthocyanidin biosynthesis in *Medicago truncatula* and *Arabidopsis*. *Plant Cell Online* 21, 2323–2340. doi: 10.1105/tpc.109.067819

Conflict of Interest Statement: The authors declare that the research was conducted in the absence of any commercial or financial relationships that could be construed as a potential conflict of interest.

frontiers
in Forests and Global Change

REVIEW
published: 06 September 2019
doi: 10.3389/ffgc.2019.00050

The Interplay Between Ozone and Urban Vegetation—BVOC Emissions, Ozone Deposition, and Tree Ecophysiology

Anne Charlott Fitzky[1], *Hans Sandén*[1*], *Thomas Karl*[2], *Silvano Fares*[3], *Carlo Calfapietra*[4], *Rüdiger Grote*[5], *Amélie Saunier*[6] *and Boris Rewald*[1]

[1] Forest Ecology, Department of Forest and Soil Sciences, University of Natural Resources and Life Sciences Vienna (BOKU), Vienna, Austria, [2] Institute of Atmospheric and Cryospheric Sciences, University of Innsbruck, Innsbruck, Austria, [3] Research Centre for Forestry and Wood, Council for Agricultural Research and Economics (CREA), Rome, Italy, [4] National Research Council of Italy (CNR), Institute of Research on Terrestrial Ecosystems (IRET), Rome, Italy, [5] Institute of Meteorology and Climate Research, Atmospheric Environmental Research Division (IMK-IFU), Karlsruhe Institute of Technology, Garmisch-Partenkirchen, Germany, [6] Department of Environmental and Biological Sciences, University of Eastern Finland, Kuopio, Finland

OPEN ACCESS

Edited by:
Mark Potosnak,
DePaul University, United States

Reviewed by:
Xu Yue,
Nanjing University of Information Science and Technology, China
Dasa Gu,
Hong Kong University of Science and Technology, Hong Kong

***Correspondence:**
Hans Sandén
hans.sanden@boku.ac.at

Specialty section:
This article was submitted to Forests and the Atmosphere, a section of the journal Frontiers in Forests and Global Change

Received: *03 June 2019*
Accepted: *13 August 2019*
Published: *06 September 2019*

Citation:
Fitzky AC, Sandén H, Karl T, Fares S, Calfapietra C, Grote R, Saunier A and Rewald B (2019) The Interplay Between Ozone and Urban Vegetation—BVOC Emissions, Ozone Deposition, and Tree Ecophysiology. Front. For. Glob. Change 2:50. doi: 10.3389/ffgc.2019.00050

Tropospheric ozone (O_3) is one of the most prominent air pollution problems in Europe and other countries worldwide. Human health is affected by O_3 via the respiratory as well the cardiovascular systems. Even though trees are present in relatively low numbers in urban areas, they can be a dominant factor in the regulation of urban O_3 concentrations. Trees affect the O_3 concentration via emission of biogenic volatile organic compounds (BVOC), which can act as a precursor of O_3, and by O_3 deposition on leaves. The role of urban trees with regard to O_3 will gain further importance as NO_x concentrations continue declining and climate warming is progressing—rendering especially the urban ozone chemistry more sensitive to BVOC emissions. However, the role of urban vegetation on the local regulation of tropospheric O_3 concentrations is complex and largely influenced by species-specific emission rates of BVOCs and O_3 deposition rates, both highly modified by tree physiological status. In this review, we shed light on processes related to trees that affect tropospheric ozone concentrations in metropolitan areas from rural settings to urban centers, and discuss their importance under present and future conditions. After a brief overview on the mechanisms regulating O_3 concentrations in urban settings, we focus on effects of tree identity and tree physiological status, as affected by multiple stressors, influencing both BVOC emission and O_3 deposition rates. In addition, we highlight differences along the rural-urban gradient affecting tropospheric O_3 concentrations and current knowledge gaps with the potential to improve future models on tropospheric O_3 formation in metropolitan areas.

Keywords: biogenic volatile organic compounds, ozone formation and deposition, roadside trees, rural-urban gradient, stress, urban forest, urban trees

INTRODUCTION

Ground-level ozone (O_3, tropospheric ozone) is one of the most prominent air pollution problems in Europe and other countries worldwide. When taken-up by plants, O_3 irreversibly damages plant tissue-leading to reduced crop yields and forest growth (Mills et al., 2011). Human health is temporarily or chronically affected by O_3 via the respiratory as well the cardiovascular systems (WHO, 2006). The World Health Organization (WHO) has repeatedly released updated recommendations regarding ozone exposure limits. In order to avoid negative impacts on human health, the alert threshold for 8-h average O_3 exposure was lowered in 2005 from 120 $\mu g\ m^{-3}$ (60 ppb) to 100 $\mu g\ m^{-3}$ (50 ppb), and short-time concentrations should not exceed 160 $\mu g\ m^{-3}$ (80 ppb, WHO, 2006). However, many (supra-) national legislations incl. the European Unions' (EU) Air Quality Directive (EU, 2008) are allowing higher O_3 exposures (e.g., EU target value 120 $\mu g\ m^{-3}$ not to be exceeded on >25 days $year^{-1}$, averaged over 3 years). The set thresholds are frequently reached or exceeded in urban areas, especially during heat waves (Solberg et al., 2008; Holman et al., 2015). Recent data indicates that 95–99 % of the EU urban population were exposed to O_3 concentrations above WHO air quality guidelines in the period 2006–2016 (EEA, 2018a,b). However, within metropolitan areas large temporal and spatial heterogeneities of tropospheric O_3 levels exist (Paoletti et al., 2011; Calfapietra et al., 2016), which are influenced by a distinct rural-urban gradient and a broad range of abiotic and biotic factors (Sicard et al., 2013; Lahr et al., 2015; Hagenbjörk et al., 2017).

The recent literature on urban forests and greening ("green urban infrastructure") largely advocates the environmental services of trees such as air pollution mitigation (e.g., CO_2 sequestration, dry deposition), storm water interception, and heat mitigation (Escobedo et al., 2011; Connop et al., 2016; Livesley et al., 2016). In general, the substantial scientific evidence on many positive effects has led to a normative assertion by stakeholders that any increase in urban forests is desirable and will mitigate virtually all-kinds of environmental problems (Escobedo et al., 2011). However, the role of urban vegetation on the local regulation of tropospheric O_3 concentrations is complex. Among the different urban vegetation forms, trees are key as they can both remove (Hardin and Jensen, 2007) but also contribute significantly to O_3 formation (Jenkin et al., 2015). In addition, air chemistry reactions and thus O_3 formation are indirectly affected by the cooling and shading properties of vegetation (Yli-Pelkonen et al., 2018). The net effect of a tree on the O_3 concentration depends on tree species, its physiological status, environmental drivers of emission, as well as climate and air chemistry such as concentrations of volatile organic compounds (VOCs; see **Box 1** for glossary) and nitrogen oxides (NO_x). The emission of biogenic VOC (BVOC) by trees as source of tropospheric O_3, will gain further importance as climate change progresses (Peñuelas and Staudt, 2010; Trenberth et al., 2014). It is also expected that future urban NO_x concentrations will continue to decline by substituting combustion-powered vehicles, especially Diesel-powered models, with cleaner ones (O'Driscoll et al., 2018). Consequently, urban ozone chemistry might become more sensitive to BVOC emissions. While not all BVOCs will be equally effective and in some cases may actually contribute to a decomposition of O_3 (Bonn et al., 2018; Neirynck and Verstraeten, 2018), the combination of higher urban temperatures and lower levels of NO_x is generally thought to increase the importance of BVOCs as precursors of ozone in future urban environments (Chameides et al., 1988).

BOX 1 | Glossary of volatile organic compound classes

VOC	*Volatile organic compounds* encompass a broad range of gaseous compounds of (hydro-)carbons emitted into the atmosphere–containing alkanes, alkenes, aromatic hydrocarbons, oxygen-containing VOCs (e.g., methane), and nitrogen-containing VOCs. Sources of VOCs are e.g., plants, animals, microbes, and fungi, combustion by traffic, industry, biomass burning, and households.
NMVOC	*Non-methane volatile organic compounds* are VOCs not counting methane, which is mostly emitted by domestic ruminants, natural wetlands, landfills, biomass burning, and fossil-fuel emissions.
AVOC	*Anthropogenic VOCs* such as paraffin, olefins, and aromatics are predominantly emitted by combustion.
BVOC	*Biogenic VOCs* are biologic-originated VOCs. The vegetation emits isoprenoids as isoprene (C_5), monoterpenes (C_{10}), and sesquiterpenes (C_{15}), but also OVOCs and GLVs.
OVOC	*Oxygenated VOCs* are a heterogeneous group comprising various alcohols (e.g., methanol, ethanol), aldehydes (acetaldehyde, formaldehyde), ketones and specialized substances such as methyl jasmonates and dimethyl nonatriene. OVOCs are i.a. emitted by (stressed) plants and anthropogenic sources.
GLV	*Green leaf volatiles* are a part of BVOCs combining C_6 aldehydes and alcohols emitted by the vegetation during and after biotic and abiotic stress.

In this review, we summarize processes related to trees that affect tropospheric ozone concentrations in metropolitan areas from rural settings to urban centers, and discuss their importance under present and future conditions. Urban trees differ in their potential BVOC emission rates and are often exposed to a multiple and high stress environment, that is also particularly prone to climate change impacts; thus, we especially focus on tree species-specific effects and the physiological status as (potential) major factors influencing ground-level O_3 formation. In addition, the review will highlight knowledge gaps, e.g., concerning the spatial distribution of species and environmental factors along rural-urban gradients, with the potential to improve future models on tropospheric O_3 formation in metropolitan areas.

TROPOSPHERIC OZONE FORMATION AND SINKS

The O_3 forming process in the troposphere is generally catalyzed by nitrogen oxides in the presence of radiation, and fueled by methane, carbon monoxide and non-methane volatile organic compounds (NMVOC). The general pathways to tropospheric

O_3 formation are well understood (Brasseur et al., 1999), but the complexity of organic chemistry is still subject to intensive research (Fittschen et al., 2017). Ozone formation is always initiated by the photolysis of NO_2. The recycling of NO to NO_2 occurs after CO, methane or NMVOC react with OH and generate hydroxyl and peroxy radicals. These readily react with NO, regenerating NO_2. Thus, NO_x is recycled in what is referred to as the RO_x-NO_x cycle (**Figure 1**).

At low NO_x concentrations, O_3 formation becomes NO_x limited. At medium NO_x concentrations, OH recycling via the RO_x-NO_x cycle becomes efficient to sustain the oxidation of high levels of NMVOCs, which finally leads to a regime, where O_3 formation becomes VOC-limited (Carter, 1994). The O_3 forming potential also depends on the VOCs' reactivity, which differs among compounds. Isoprene, for example, is the most common BVOC and has a reactivity which is 22 times higher than that of the important anthropogenic VOC (AVOC) benzene (Carter, 1994; Wagner and Kuttler, 2014). The reaction rate constants of CO and methane with respect to OH are about 410 and 14,000 times lower than that of isoprene, which can therefore compete with their reactivity in many environments. For a more detailed description of the chemical reactions involved in tropospheric chemistry we refer to the specialized literature (Atkinson, 2000; Kirchner et al., 2001; Jenkin et al., 2015; Wang et al., 2017).

Recent measurements of OH reactivity (Kim et al., 2011; Kaiser et al., 2016; Nölscher et al., 2016; Williams et al., 2016) have suggested missing emission sources of reactive NMVOCs and missing secondary atmospheric reactions leading to reactive NMVOCs. This uncertainty is largely attributed to the complexity of organic chemistry and precursor emissions. On global and regional scales, BVOCs play a central role in tropospheric chemistry because of their reactivity with respect to OH (Guenther et al., 2012). While plants can release more than 30,000 different BVOCs (Trowbridge and Stoy, 2013), only a few are emitted in relatively large quantities and are highly reactive with atmospheric radicals (Atkinson and Arey, 2003). The most reactive classes of BVOC emitted by plants are isoprene (30%), monoterpenes and higher terpenoids (25 %; e.g., sesquiterpenes) whereas oxygenated VOCs (OVOC) are present in lower amounts and less reactive (Atkinson and Arey, 2003; Atkinson, 2007). Based on the maximum incremental reactivity scale (MIR), e.g., isoprene (MIR 10.6) reacts faster with ozone than monoterpenes (MIR 4.0) (Carter, 2000, 2010). Once in the atmosphere, isoprene is undergoing complex chemical cycling initiated by photochemistry, a fate all NMVOC have in common and are leading to a vast network of chemical reactions. Similar, higher molecular weight terpenes ($>C_{15}$) can also play a significant role in atmospheric chemistry due to their reactivity (Atkinson and Arey, 2003).

Once being produced, O_3 has several routes of removal. The most important ones include dry deposition and chemical loss (Monks et al., 2009; IPCC, 2014). On a global scale, the most important chemical loss term is the photolysis of O_3 in the atmosphere and subsequent reaction with water vapor (H_2O) leading to the production of OH radicals (Brasseur et al., 1999). Globally a gross chemical O_3 loss of $4{,}260 \pm 264$ Tg year^{-1} and a net chemical production of 633 ± 275 Tg year^{-1} was estimated (Lamarque et al., 2013). Under high NO_x emissions (e.g., in an urban context) another chemical conversion of O_3 is triggered by the reaction with NO, leading to a temporary production of excess NO_2. The reactions between NO, NO_2, and O_3 are often termed as the triad and represent a null cycle, where no net O_3 is produced or removed (**Figure 1**, NO_x cycle). Yet locally, O_3 is chemically converted to NO_2 and it can be speculated that O_3 deposition can also be facilitated via NO_2 uptake by plants. The second largest sink for O_3 is deposition on surfaces. Estimates of O_3 dry deposition are in the order of $1{,}094 \pm 309$ Tg year^{-1} (Young et al., 2013). Further, another sink of O_3 is the ozonolysis of VOCs forming secondary organic aerosols (SOAs), initiated by O_3 degrading C-C double bonds in alkenes and leading to the formation of energy-rich Criegee biradicals (Criegee, 1975; Pinto et al., 2010).

Whether the O_3 level increases or decreases by VOCs is depending on the chemical species and the relative concentrations of the involved compounds (Sillman and He, 2002). To implement effective mitigation strategies, the

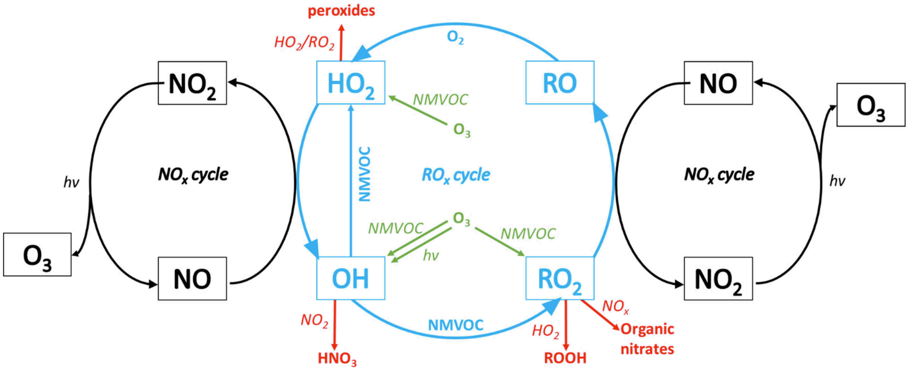

FIGURE 1 | Ozone formation via the interactions between the RO_X- (blue) and NO_X-cycles (black). Interfering with the RO_X-NO_X cycle are ozone degrading reactions (green) via NMVOCs (non-methane volatile organic compounds) as well as terminating reactions (red); $h\nu$, light. Methane and carbon monoxide are not displayed (modified after Wang et al., 2017 with permission).

relationship between the different reaction partners as well as their current absolute concentrations has to be considered.

IMPACT OF TREE SPECIES AND THEIR PHYSIOLOGICAL CONDITION ON THE OZONE DYNAMICS OF URBAN ENVIRONMENTS

Quantity and quality of BVOC emissions and O_3 removal by urban trees depends on community composition, and short- and long-term environmental conditions—affecting tree size and physiological status. In the following, an overview is given on key traits and stressors influencing O_3 removal and BVOC emission potential of urban tree vegetation—referring mainly to European examples to keep a manageable length and scope.

Species-Specific Effects

Community Composition

The sensitivity of plants to specific environmental conditions determines urban species composition, either by affecting mortality of established trees or by suggesting selection preferences to urban planners (Holmes et al., 2013). Three main locations of urban vegetation can be distinguished: street trees ("road-side" trees), parks and private gardens, and urban woodlands. Street trees are exposed to relatively high stress levels and the average lifespan of the trees is short, while trees in parks and private gardens are commonly exposed to less stress. Trees in urban woodland are subjected to relatively low stress levels and may reach a lifespan and size comparable to forests (Sæbø et al., 2005). The environmental conditions and the frequency of these different vegetation types, and thus species community composition, differs largely along rural-urban gradients as discussed below (section The Rural-Urban Gradient in Context of Tree-Ozone Interactions). However, despite an overall high number of species available for planning, only relatively few tree genera and species are highly abundant in streets and parks of northern and central European cities (Grote et al., 2016; Samson et al., 2017b). Common urban species in central to northern Europe are in particular: *Tilia* sp., *Platanus* sp., *Aesculus* sp., *Fraxinus* sp., *Quercus* sp., *Acer* sp., *Picea abies,* and *Pinus* sp. Additionally, *Fagus sylvatica* occurs frequently in parks, private gardens and urban woodlands. In southern Europe, a broader species pool is utilized but likewise dominated by a few tree genera and species: *Platanus* × *acerifolia, Quercus ilex, Robinia pseudoacacia, Celtis australis, Celtis occidentalis, Sophora japonica, Morus* sp., *Populus* sp., *Ulmus* sp., *Pinus* sp., and *Prunus* sp. (Pauleit et al., 2002; Grote et al., 2016). There is a general trend to introduce more exotic tree species that are supposed to withstand progressing "global warming" and diseases in urbanized areas better than their autochthonous counterparts (Youngsteadt et al., 2015). However, whether or not replacing native species with exotic species is still under debate as neophytes may disturb the ecological relationships between co-evolved species (Cornelis and Hermy, 2004; Kühn et al., 2004).

Under standard conditions, the contribution of an individual tree to either O_3 removal or BVOC emissions depends primarily on species-specific traits [e.g., high or low BVOC emission rates, (Samson et al., 2017a)], and gaseous exchange is proportional to the size of its canopy, as measured by its leaf mass or surface area (Harrison et al., 2013; Vos et al., 2013). Similar "size-symmetric"-effects of larger tree individuals have been found with regard to air pollution mitigation in particularly when the main removal process is surface deposition rather than stomatal adsorption (Grote et al., 2016). However, large and dense canopies, for example, may allow emitted BVOCs to react on leaf surfaces within the canopy before reacting with gases (Forkel et al., 1999); *vice versa* ozone deposition on leaf surfaces within dense canopies may be reduced due to a non-uniform distribution of ozone sources (Zhu et al., 2009)—attenuating "size-symmetric"-effects.

It should be furthermore considered that canopy size, shape, and density of street trees, despite being highly species/cultivar-specific, can largely be modified by management measures (Janhäll, 2015). Therefore, allometric relationships typically used in the forestry sector (e.g., to determine biomass and crown size from stem diameter and tree height) generally fail to predict tree attributes in the urban context. Surprisingly, closed canopies of trees may contribute to higher pollution in urban canyons by decreasing dispersion (Gromke and Ruck, 2009; Vos et al., 2013). However, this effect is beneficial for pedestrians and bikers when the lanes are located just on the external side of the road (outside the canyon).

Ozone Deposition Capacity

Vegetation plays a major role for the dry depositional sink of O_3. Dry deposition over lush vegetation is 40 times more efficient than over urban land according to common parameterizations in atmospheric models (Wesely, 1989). Deposition of O_3 to vegetation is modulated by a stomatal and a non-stomatal component. In either case, the removal of O_3 is ultimately driven by a chemical loss. Stomatal O_3 uptake triggers antioxidant reactions in the intercellular space and is largely dependent on stomatal conductance, which is driven by environmental conditions and varies among tree species (as discussed below). If the stomata are open, O_3 diffuses into the intercellular space from the atmosphere and is almost immediately deposited by reactions in the apoplast with membrane lipids, moisture and cell organelles; uptake increases with increasing outside concentrations (Wesely and Hicks, 2000). Non-stomatal O_3 deposition occurs on leaf surfaces by reactions with waxes, moisture and salts (Barnes et al., 1988; Altimir et al., 2006) and in the boundary layer with emitted BVOCs (see sections Tropospheric Ozone Formation, and Sinks and BVOC Emission Rates). Tree species featuring traits such as a large leaf area index, hairy leaves, leaf waxes and moist surfaces, and keeping their stomata longer open under stressed conditions (see below, section Plant Water Status), are depositing O_3 better than species without these traits (Barnes et al., 1988; Altimir et al., 2006; Cape et al., 2009). However, Calfapietra et al. (2016) showed that under standardized conditions, most common tree species in Rome, Italy had rather similar O_3 deposition rates per m^2 leaf area; however, photosynthetically very active trees like *Populus* × *euramericana* had higher and the gymnosperm *Pinus pinea* had lower O_3 deposition rates than the average. As similar plant traits are likely affecting fine particulate matter (PM2.5) and O_3 deposition rates, available rankings addressing the effectiveness of (deciduous) tree species for PM2.5 deposition (e.g., Yang et al., 2015) can probably be used as a guideline for ozone deposition capacity.

BVOC Emission Rates

The production and emission of BVOCs can serve as a protective mechanism of plants against O_3-induced tissue damage, for increasing thermotolerance, communicating with neighboring and interfering individuals and sometimes possibly just to get rid of surplus energy by releasing byproducts of physiological processes (Niinemets et al., 2013). The profiles of emitted BVOCs vary considerably among tree species (Courtois et al., 2009; Niinemets and Monson, 2013) and even genotypes (Blanch et al., 2012). **Figure 2** illustrates the available data on standard emission potentials of isoprene, monoterpene, sesquiterpenes and OVOCs of frequent tree species in European cities under non-stress conditions. **Isoprene** is known as the major BVOC emitted by trees globally (**Figure 2**) and also the one that has the highest potential contributing to tropospheric O_3 formation (Kamens et al., 1982; Loreto and Velikova, 2001; Xie et al., 2008). Among the most common city trees, *Populus nigra, P. tremula, Quercus robur* and *Q. pubescens* were identified as high isoprene emitters. **Monoterpenes** are emitted by conifers and several broad-leaved trees including *F. sylvatica*, which is dominant in forests of central Europe (Kramer et al., 2010), and thus may be important pre-cursors for particles and O_3 especially in rural-suburban transition zones. Common urban trees such as *Acer platanoides* and *Ulmus minor* are considered low emitters (Singh et al., 2007; Karl et al., 2009) while some as for example *Fraxinus excelsior,* and *Tilia platyphyllos* are generally assumed to be non-monoterpene and -isoprene emitters. **Sesquiterpenes** are mainly emitted in low quantities and have a similar O_3 formation potential than monoterpenes, although less than isoprene, and have thus a minor influence on ozone formation (Holopainen and Blande, 2013). Oxygenated VOCs (OVOCs) have different but generally minor ozone forming potentials. They are typically emitted as signaling compounds or as response to any kind of stressful conditions (Seco et al., 2007). As plant ontogeny can

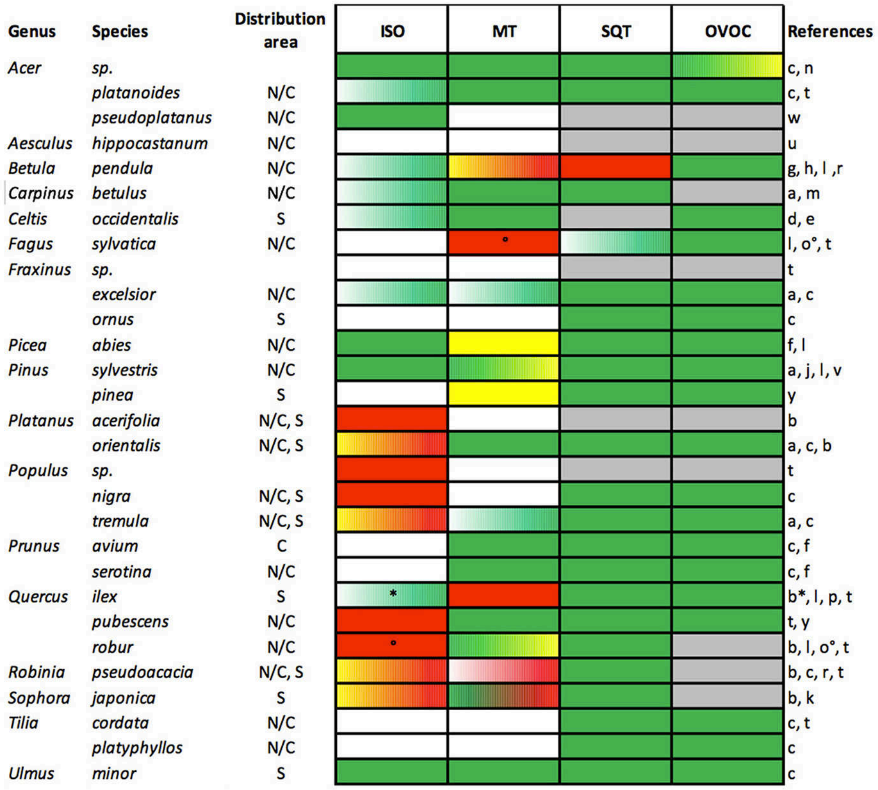

Genus	Species	Distribution area	ISO	MT	SQT	OVOC	References
Acer	*sp.*		🟩	🟩	🟩	🟩→🟨	c, n
	platanoides	N/C	⬜→🟩	🟩	🟩	🟩	c, t
	pseudoplatanus	N/C	🟩	⬜	▨	▨	w
Aesculus	*hippocastanum*	N/C	⬜	⬜	▨	▨	u
Betula	*pendula*	N/C	⬜→🟩	🟨→🟥	🟥	🟩	g, h, l ,r
Carpinus	*betulus*	N/C	⬜→🟩	🟩	🟩	▨	a, m
Celtis	*occidentalis*	S	⬜→🟩	🟩	▨	🟩	d, e
Fagus	*sylvatica*	N/C	⬜	🟥 °	⬜→🟩	🟩	l, o°, t
Fraxinus	*sp.*		⬜	⬜	▨	▨	t
	excelsior	N/C	⬜→🟩	⬜→🟩	🟩	🟩	a, c
	ornus	S	⬜	⬜	🟩	🟩	c
Picea	*abies*	N/C	🟩	🟨	🟩	🟩	f, l
Pinus	*sylvestris*	N/C	🟩	🟩→🟨	🟩	🟩	a, j, l, v
	pinea	S	⬜	🟨	🟩	🟩	y
Platanus	*acerifolia*	N/C, S	🟥	⬜	▨	▨	b
	orientalis	N/C, S	🟨→🟥	🟩	🟩	🟩	a, c, b
Populus	*sp.*		🟥	⬜	▨	▨	t
	nigra	N/C, S	🟥	⬜	🟩	🟩	c
	tremula	N/C, S	🟨→🟥	⬜→🟩	🟩	🟩	a, c
Prunus	*avium*	C	⬜	🟩	🟩	🟩	c, f
	serotina	N/C	⬜	🟩	🟩	🟩	c, f
Quercus	*ilex*	S	⬜→🟩 *	🟥	🟩	🟩	b*, l, p, t
	pubescens	N/C	🟥	🟩	🟩	🟩	t, y
	robur	N/C	🟥 °	🟩→🟨	🟩	▨	b, l, o°, t
Robinia	*pseudoacacia*	N/C, S	🟨→🟥	⬜→🟥	🟩	▨	b, c, r, t
Sophora	*japonica*	S	🟨→🟥	🟩→🟥	🟩	▨	b, k
Tilia	*cordata*	N/C	⬜	⬜	🟩	🟩	c, t
	platyphyllos	N/C	⬜	⬜	🟩	🟩	c
Ulmus	*minor*	S	🟩	🟩	🟩	🟩	c

FIGURE 2 | Standard emission potentials (μg g DW^{-1} h^{-1}; at 30°C leaf temperature and 1,000 μmol m^{-2} s^{-1} PPFD) of isoprene (ISO), monoterpene (MT), sesquiterpenes (SQT), and oxygenated VOC (OVOC) of frequent tree species in urban areas of northern/central (N/C) and southern (S) Europe. Potential emission rates are grouped in no (white), low (green), medium (yellow), and high (red) emission classes. ISO: low < 10, high > 30.1; MT and OVOC: low < 2, high > 5.1; SQT: low < 0.5, high > 1.1; with medium categories with values in-between. A color gradient indicates emission rates crossing the defined classes; gray indicates: "no data available." References: a (Aydin et al., 2014), b (Benjamin and Winer, 1998) *high ISO, c (EMEP/CORINAIR, 1999), d (Curtis et al., 2014), e (Geron et al., 1994), f (Grote et al., 2016), g (Hakola et al., 1998), h (Hakola et al., 2001), j (Hakola et al., 2006), k (Heinrich, 2007), l (Karl et al., 2009), m (König et al., 1995), n (Lamb et al., 1987), o (Meeningen et al., 2016) °low ISO, p (Owen et al., 1997), q (Paoletti et al., 2011), r (Préndez et al., 2013), s (Singh et al., 2007), t (Steinbrecher et al., 2009), u (Streiling and Matzarakis, 2003), v (Tarvainen et al., 2005), w (Tiwary et al., 2013), y (Veldt, 1989).

influence i.a. foliar defense metabolites (Goodger et al., 2013), it is likely that BVOC emission rates of tree species are changing along ontogenetic trajectories.

Other compounds are also occasionally reported as constitutive emissions from plants. Regarding trees in urban area, alkanes, aldehydes, alkenes, aromatic compounds, esters, and ketones have been determined to originate from *Ginkgo biloba* (Li et al., 2011). Their impact on air chemistry is generally assumed to be small since anthropogenic emissions are dominating the concentration of these compounds in urban areas by far (e.g., Costa and Baldasano, 1996; Cheng et al., 2010). However, alkanes and alkenes have been found as major emissions over many forests (Kourtchev et al., 2008; Halliday et al., 2015; Rhew et al., 2017); thus, at least the more reactive alkenes are assumed to play a significant role at larger to global levels (Goldstein et al., 1996; Rhew et al., 2017).

Looking at the community level, some general patterns in BVOC emissions can be identified among tree functional types (Dani et al., 2014). For example, trees featuring a high photosynthetic capacity are often also high monoterpene emitters. Deciduous trees are in general higher isoprene emitters and low monoterpene emitters whereas evergreen trees are low isoprene emitters and can be both low and high emitters of monoterpene (Dani et al., 2014). European forest biomes are generally thought to emit higher levels of monoterpenes relative to isoprene, compared to the continental US. For instance, *Quercus* sp. in the Mediterranean area are often evergreen and primarily monoterpene emitters in contrast to North-American *Quercus* sp., with relevant changes concerning the interaction of emitted isoprenoids with the atmosphere and air quality (Fares et al., 2013). As under normalized conditions the BVOC contribution of an individual plant is proportional to its BVOC emission rate (Kesselmeier and Staudt, 1999; Niinemets and Monson, 2013) and the size of its canopy (as discussed above), abundant and/or large species with high emission rates tend to dominate the BVOC emission inventory in a given landscape. Furthermore, plant phenology and ontogeny influence emission rates (Goodger et al., 2013; Jardine et al., 2016). However, as "standard conditions" rarely occur in urban settings, ozone removal capacities as well as BVOC emission rates are largely modified by stress as outlined below.

Stressors Modifying Species-Specific Effects via Tree Physiological Status

As urban plants are increasingly exposed to numerous stressors (Calfapietra et al., 2015), the vitality of street trees declined drastically over the last 3–4 decades (Bradshaw et al., 1995). While stress levels can vary considerable between urban centers and rural areas (see section The Rural-Urban Gradient in Context of Tree-Ozone Interactions), knowledge of the environmental physiology of trees in urban settings is key in order to understand the responses of trees to different stresses including feedback mechanisms on specific ecosystem services and/or disservices (Calfapietra et al., 2015).

Meteorological Factors and Air Composition

Higher temperatures and light intensities are often accompanied by increased formation of secondary air pollutants in the atmosphere including ozone (Chameides et al., 1988). Also, BVOC emissions are strongly positively correlated to temperature (Guenther et al., 1991; Niinemets and Monson, 2013; Guidolotti et al., 2019) as plants can use, for example, isoprene to stabilize the cell membrane during high temperatures (Singsaas et al., 1997). Behnke et al. (2013) showed that *Populus × canescens* leaves in which isoprene production was genetically removed were less heat resistant. However, the temperature sensitivity of BVOC emissions are highly species-specific, related to the emission traits that distinguish trees in isoprene or monoterpene emitters and, for the latter, in trees without and with isoprenoids pools (Niinemets et al., 2010; Grote et al., 2013). The direct effect of temperature on O_3 deposition is believed to be small; however, as high temperature increases evapotranspiration, and thus potentially drought stress levels, the indirect decrease in O_3 deposition by stomatal closure may be large (Morani et al., 2014). Another relevant but highly variable meteorological factor is wind. Ventilation of canopies increases evapotranspiration and cools down leaves (Drake et al., 1970). Cooler leaf temperatures lead to lower isoprene emissions in *Populus* sp. and *Quercus* sp. (Potosnak et al., 2014a). Further, strong wind gusts can damage trees—leading to the release of BVOCs (Loreto et al., 2006). For example, a burst of monoterpene emission has been measured at high wind speeds in Eucalypts, whose emissions are otherwise extremely low (Guidolotti et al., 2019). In contrast, higher wind speeds may render leaves within closed canopies more available for ozone deposition.

Urban areas are often characterized by higher concentrations of CO_2 and air pollutants (O'Driscoll et al., 2018). Estimating how these conditions will affect BVOC emissions from urban trees is, however, not easy as a number of factors are interrelated, including the chemical composition of the compound(s), the exposure, the concentration and the plant species. However, there is for example a consensus that an increase in CO_2 concentration will induce a reduction of isoprenoid emissions at least at leaf level (Rosenstiel et al., 2003; Calfapietra et al., 2008). On the other hand, an increase of O_3 concentration can have opposite effects depending on the length and level of exposure—with a general stimulation in the cases of acute exposures and a general inhibition under chronic exposures (Calfapietra et al., 2013). For example, Carriero et al. (2016) states an increase of monoterpene emissions under increased ozone concentrations by *B. pendula* whereas Vuorinen et al. (2005) observed no emission changes. Similar, OVOC emissions by *B. pendula* under elevated ozone exposure were found to decrease (Hartikainen et al., 2012) or increase (Carriero et al., 2016), and isoprene emissions under O_3 stress decreased in *P. tremuloides* (Calfapietra et al., 2008) but did not change for *P. tremula* (Hartikainen et al., 2009) and *P. tremula × tremuloides* (Blande et al., 2007). Despite the uncertainties, however, there are numerous publications that indicate a considerable induction of monoterpenes and various OVOCs by O_3 while the effect on isoprene is mostly negative—either because the biosynthesis pathway is very sensitive to ozone damages or more likely because precursors are directed toward protecting agents (Grote, 2019). Ozone deposition is normally negatively influenced by increased CO_2 and O_3 levels as both decrease stomatal conductivity and thereby stomatal O_3

deposition (Medlyn et al., 2001; Wittig et al., 2007). Globally, the increase of O_3 since the industrialization is estimated to have decreased stomatal conductance by 13% (Wittig et al., 2007)—with likely higher values in urban areas.

Plant Water Status

Urban vegetation can experience exceptional stresses from water scarcity to flooding, caused by extreme heat, drought, and rainfall events (Wissmar et al., 2004; Collier, 2006; Livesley et al., 2016).

With increasing drought stress the stomata close and the stomatal depletion of ozone decreases (Wissmar et al., 2004; Livesley et al., 2016), increasing tropospheric ozone levels by up to 10% (Anav et al., 2018). However, trees have evolved different strategies to deal with low water availability. Isohydric species maintain a constant midday leaf water potential by closing their stomata earlier, while anisohydric species keep their stomata open longer and allow the leaf water potential to drop (Sade et al., 2012). By keeping the stomata open during moderate drought, anisohydric tree species such as *Quercus* sp. and *Fagus* sp. can maintain stomatal ozone deposition on hot summer days when ozone levels may become high (Grote et al., 2016). In contrast, isohydric tree species such as *Acer* sp. and *Betula* sp. are more likely to survive severe droughts and remain thus available for O_3 deposition under post-stress conditions (Sade et al., 2012; Klein, 2014). Thus, in selecting tree species for maximizing urban ozone deposition there is a tradeoff between high stomatal deposition during moderate drought and survival during severe drought events.

BVOC emission rates under drought have been found increasing (Funk et al., 2004; Potosnak et al., 2014b), decreasing (Fortunati et al., 2008; Tiiva et al., 2009) or unaffected (Tingey et al., 1981; Pegoraro et al., 2006). Closing the stomata results in increasing leaf temperature as transpirational cooling decreases; this induces isoprene production in the short-term to increase the thermo-tolerance of tissue (Singsaas et al., 1997). Furthermore, when stomata close the supply of CO_2 decreases, whereas the photosynthetic electron transport rate (ETR) remains high. The emission of at least isoprene seems to be positively correlated to the ratio of ETR to net carbon assimilation rate [NAR; (Dani et al., 2015)]. The carbon used for isoprene production is believed to come from stored carbon and isoprene production can thus be maintained even though CO_2 assimilation decreases (de Souza et al., 2018). In contrast, closed stomata can lead also to decreased emissions of at least some BVOCs, which can less easily diffuse into the atmosphere (Saunier et al., 2017). The variable responses reported previously emphasize that BVOC emissions under drought are highly dependent on tree species (sensitivity) as well as the intensity and temporal extend of the stress events (Dani et al., 2015). Different effects are thus explained by species sensitivity as well as drought intensity (Niinemets, 2010; Klein, 2014; Saunier et al., 2018). For example, the same species can possess an increase of isoprene emissions under mild drought while severe drought decreases emissions (Brilli et al., 2007; Genard-Zielinski et al., 2014; Dani et al., 2015). Similar behavior has been observed for monoterpene emissions, with moderate stress suppressing photosynthesis but not BVOC emissions (Funk et al., 2004; Wu et al., 2015). Less is known on the effect of drought on highly volatile BVOC emissions such as methanol, formaldehyde or acetaldehyde (OVOC) or green leaf volatiles [GLV; (Vitale et al., 2007; Saunier et al., 2017)]. On the long term, drought stress is likely to decrease leaf biomass, which has a negative effect on both ozone deposition as well as BVOC emissions.

In snow-prone urban areas, de-icing salt (NaCl) ends up highly concentrated in street tree pits. De-icing salt has been found to have a negative effect on tree health (Czerniawska-Kusza et al., 2004; Munck et al., 2010; Rose and Webber, 2011; Ordóñez-Barona et al., 2018), by inducing water stress ("physiological drought"), with the effects describe above, but also malnutrition and accumulation of excess ions to potentially toxic levels (Ahmad et al., 2012). This is often decreasing leaf biomass & vitality (Shannon et al., 1999) and thereby the ozone deposition capacity. While emissions of isoprene and OVOC were found rather unaffected by mild salt stress (Loreto and Delfine, 2000; Teuber et al., 2008), it is currently unknown if the same holds true for severe salt stress.

Finally, flooding can also reduce stomatal conductance (Liao and Lin, 2001), and has consequently a negative effect on stomatal ozone deposition as described above (Chaves et al., 2003). Moreover, it has been observed that flooding can also increase methanol as well as GLV, but decrease isoprene emissions (Copolovici and Niinemets, 2010; Bourtsoukidis et al., 2013).

Nutrition Status

The urban ecosystem is highly heterogeneous in regard to nutrient availability; for example, some street trees have access only to the limited soil volume underneath the planting pit whereas others access nearby gardens and sewer pipes (Kopinga and Van den Burg, 1995; Day et al., 2010). Nutrients frequently limiting the growth of urban trees are potassium (K) and nitrogen (N), however, deficiencies of magnesium (Mg) and phosphorus (P) as well as micronutrients are common (Kopinga and Van den Burg, 1995; Sieghardt et al., 2005).

Deficient nutrition results in decreased growth and increased sensitivity to pests—leading to relatively reduced leaf area, affecting O_3 deposition negatively (Carriero et al., 2016; Hu et al., 2018). On a single leaf scale, N deficiency has been shown to cause a decrease in BVOC production due to a lower photosynthetic efficiency and thus less available carbon for secondary metabolites (Lerdau et al., 1995; Ormeño et al., 2008). Although direct studies are missing, it can be hypothesized that K and Mg deficiency, key elements of the photosynthetic system, cause similar effects (Lambers et al., 1998). P deficiency could eventually also lead to a decrease in energy-demanding BVOC production due to a shortage of P-rich ATP and NADPH (Ormeño and Fernandez, 2012). In contrast, increased BVOC emissions under warm temperatures, destabilizing the cell membrane and releasing GLVs, may be spurred under P deficiency (Siwko et al., 2007; Ormeño and Fernandez, 2012). Only recently, nutrient deficiency has also found leading to a shift of the emitted BVOC composition; for example, from terpenoids toward GLV in nitrogen-limited *Betula* sp. trees (Carriero et al., 2016). While it thus becomes increasingly clear that a shift in BVOC emissions via nutrient deficiency affects the formation and degradation of O_3 in the atmosphere, the contradictory results, i.e., either a positive or negative feedback of BVOC emissions due to malnutrition, may relate to reactions triggered on different timescales. Therefore, phenology and long-term allocation processes must be considered, combining the morphoanatomy of leaves with cell biochemistry and physiology (Lerdau et al., 1995, 1997; Ormeño and Fernandez, 2012).

Herbivores and Pathogens

Physical injuries by herbivores and pathogens frequently lead to increased GLV and monoterpene emissions (Gatehouse, 2002; Niinemets et al., 2013; Scala et al., 2013). These induced volatiles are emitted rapidly after the stress occurred (Ameye et al., 2018) and can account for 9 to 21-fold of the total emissions of damaged tissue (Ghimire et al., 2017). Fungal and pathogen infections of leaves also lead to increased emissions of GLV and monoterpene but often a decrease in isoprene emissions (Kesselmeier and Staudt, 1999; Steindel et al., 2005; Arimura et al., 2008; Jansen et al., 2009). Thus, even though isoprene decreases, the high monoterpene emission caused by herbivory and pathogens can, under high NO_x levels, contribute to ozone formation (Holopainen and Blande, 2013). The decrease in leaf biomass due to herbivory and pests decreases the ozone deposition on the leaves causing increasing ozone concentrations in the air (Kesselmeier and Staudt, 1999).

THE RURAL-URBAN GRADIENT IN CONTEXT OF TREE-OZONE INTERACTIONS

The commonly used terms "urban" and "rural" relate to a range of environmental conditions such as temperature, pollutant and CO_2 levels, and land cover types including the extension of sealed surfaces and housing densities, as well as changes in species composition and abundance of vegetation. In general, the availability of growing spaces tends to decrease along the rural-urban gradient (Zipperer et al., 1997). The differences between rural and urban are furthermore fueled by a gradient of human activities, such as emissions from traffic and industries but also vegetation management, that all affect the ozone forming potential and depletion, and thereby the (local) O_3 concentration.

Less abundant vegetation does not necessarily mean a low deposition capacity or BVOC emissions since both are strongly related to species, physiological state and stress severity as outlined above. It is therefore interesting that in many urban areas trees are predominantly deciduous (Grote et al., 2016) and in case of *Quercus* sp., *Salix* sp., and *Populus* sp. (and to some lesser degree *Platanus* sp. and *Robinia pseudoacacia*) belong to the topmost isoprene emitters. These high emitters contribute between 13% [Lancaster, UK; (Wolyniak and Elmendorf, 2011)] and 30% [Hamburg, Germany; (BUE, 2019)] of urban trees in Europe, and seem to have even higher shares in Asia [e.g., 30%, Beijing, China; (Ghirardo et al., 2016)] while US cities seem to have a bit less high emitters [11.4% in Chicago; (Nowak et al., 2010)]. In contrast, suburban and rural forests in northern and temperate regions are commonly formed by evergreen forests (Gallaun et al., 2010), which emit primarily monoterpenes that are far less effective regarding O_3 formation. Similar holds true for Mediterranean rural areas that are dominated by *Pinus* sp. and evergreen *Quercus* sp. (Sheffer, 2012).

Besides differences in species composition, trees' physiological status differs in urban compared to rural conditions because of changes in environmental conditions. Most prominently, urban centers are characterized by higher air temperatures as compared to suburbs which is the so called urban heat island (UHI) effect (Ajaaj et al., 2018; Saaroni et al., 2018). Higher temperatures in urban centers trigger higher BVOC emissions leading to higher ozone concentrations, an effect that is expected to increase with global warming (IPCC, 2014; Li et al., 2015). In contrast, higher CO_2 concentrations in urban areas do not only encourage growth but also tend to decrease BVOC emission capacity, particularly regarding isoprene (Gratani and Varone, 2014). The third effect on physiology that is not necessarily stress-related (if considering stress as damage that is not immediately reversible) is related to air humidity and soil moisture availability. Both are commonly lower in urban centers compared to urban woodlands and rural areas (Devakumar et al., 1999; Yang et al., 2017). Restricted water supply will decrease stomatal conductance and thereby stomatal ozone depletion and also modify BVOC emission rates as discussed above. Finally, urban trees, especially road-side trees, are more frequently stressed by drought (Clark and Kjelgren, 1990; Fahey et al., 2013; Bialecki et al., 2018), salt (Equiza et al., 2017), herbivores (Dale and Frank, 2014), and air pollution (Samson et al., 2017a). Stress-induced emissions are different from constitutively driven emissions in both intensity and composition. They are tightly linked to the intensity and duration of stress and thus depend for example on short-time ozone peaks. They also might eventually decrease if plants are substantially damaged although the necessary degree to reach this point is difficult to define. Indeed, considerable amounts of stress-related emission compounds have been found in metropolitan regions (Ghirardo et al., 2016).

In general, large uncertainty exists as to the effects of multiple factors, occurring in urban settings, on BVOC emissions (Holopainen and Gershenzon, 2010). They depend on species abundance and distribution, and furthermore interact with plant ecophysiological responses, such as stomatal regulation, and in particular stress responses, which are largely unknown for many urban species/ecotypes (Sjöman and Busse Nielsen, 2010). Studies show that the quota of ozone produced by BVOCs are up to 12% on average of the daily maximum 1-h O_3 concentration in Berlin but up to 60% on very warm days (Churkina et al., 2017), 50–75% during summer in Italy and Spain (Duane et al., 2002), and by a factor of 50 in Las Vegas, NV (Papiez et al., 2009). With increasing temperatures in the future, the heating effect is likely to override the suggested suppressive effect of higher CO_2 concentrations (Tingey et al., 1991; Lahr et al., 2015) and increase BVOC emissions in urban areas (Norton et al., 2015). It is therefore reasonable to speculate that combined effects will affect the emission by individual trees much more severely in the highly anthropogenic environment of city centers and suburbs than in rural areas. This assumption is supported by the fact that high temperatures and the occurrence of drought and ozone stress commonly occur in combination, which not only directly increases emissions but also decreases trees' resistance to pathogens and herbivores which then can lead to induction of further emissions (Holopainen, 2004; Loreto and Schnitzler, 2010). Indeed, several studies show that higher temperatures in urban areas in combination with drought stress increases insect herbivory (Meineke et al., 2013; Dale and Frank, 2014, 2017).

To calculate the effect of the diverging BVOC emission along the urban-rural gradient on the ozone concentration, it has to be set in relation to the NO_x concentration. In city centers and suburbs, the emissions of NO_x and AVOCs are high compared to rural areas. Toward the rural areas, NO_x and AVOC emissions decrease while BVOC emissions might increase due to an increasing leaf area or decrease depending on conditions discussed above. The emissions of AVOCs in Europe have dropped dramatically in the last 20 years (Stemmler et al., 2005; Dollard et al., 2007). Thus, on warm summer days the emission of BVOCs may be dominant relative to the contribution of AVOCs to O_3 formation (Wagner and Kuttler, 2014). In many other urban areas of the world (e.g., China), however, AVOCs are still the major driver of O_3 formation (Ran et al., 2011; Wang et al., 2017). With high NO_x concentrations within city boundaries, O_3 formation is usually small due to low VOC:NO_x ratios (Atkinson, 2000). With increasing distance from the urban center, however, NO_x concentrations decrease relative to BVOCs—resulting in an increase of the VOC:NO_x ratio and thereby a higher potential of O_3 formation in the suburbs and rural areas. An O_3 isopleth plot (**Figure 3**, dashed line) illustrates net O_3 production $P(O_3)$ as a function of BVOC and NO_2 reactivity giving data from Innsbruck, Austria as an example. A hypothetical trajectory from NO_x-rich urban conditions to BVOC-rich rural conditions is depicted along the red arrows—as NO_x is diluted, O_3 production increases until a ridge after which it decreases due to becoming NO_x-limited. This non-linear relationship of tropospheric O_3 production has important ramifications for air quality management across urban gradients, because strategies of O_3 mitigation will depend on the (local) interplay between NO_x and NMVOC (Sillman and He, 2002).

There is a strong societal demand on improving the air quality and comfort in cities. The focus is put on reducing gaseous and particulate pollution by reducing emissions from traffic, particularly of NO_x. In addition, mitigation strategies include measures to increase deposition of pollutants, including NO_x and ozone, which is preferably done by increasing leaf area (Taha et al., 2016; Tong et al., 2016). However, it should be noted that achieving reduction of NO_x by increasing deposition on leaves but simultaneously increasing BVOC emissions by selecting high emitting species can potentially increase the ozone forming potential particularly in the highly populated urban centers (**Figure 4**).

Considering future climate change scenarios with increasing temperatures, we hypothesize that ozone formation would expand toward the urban centers as with BVOC emissions increase, due to increasing temperatures, being the major driver. This effect would be enhanced if (exotic) species that are more tolerant against heat and drought but also have high BVOC emission potentials would be newly introduced in urban areas (Valkama et al., 2007; Himanen et al., 2009;

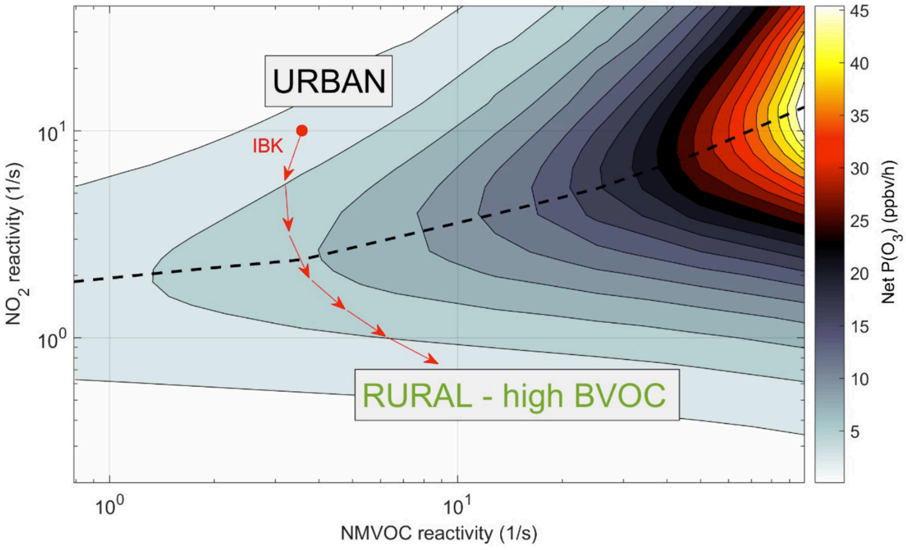

FIGURE 3 | Ozone isopleth showing urban (black) and rural (green) conditions of the relationship of NMVOC, NO_X, and O_3. Calculations are based on a model-measurement analysis for Innsbruck (Karl et al., 2017) based on the full chemistry MCM from Leeds (http://mcm.leeds.ac.uk/MCM/). Rural area conditions characterized by high BVOC emissions represent a typical range observed in the Southeast USA (Kaser et al., 2015). The trajectory to the rural end point was estimated based on a typical scenario (Ehlers et al., 2016). The MCM was implemented in Matlab (C) based on Wolfe and Thornton (2011). The red inset denotes a hypothetical trajectory from NO_X-rich urban conditions to BVOC-rich rural conditions in Innsbruck, Austria.

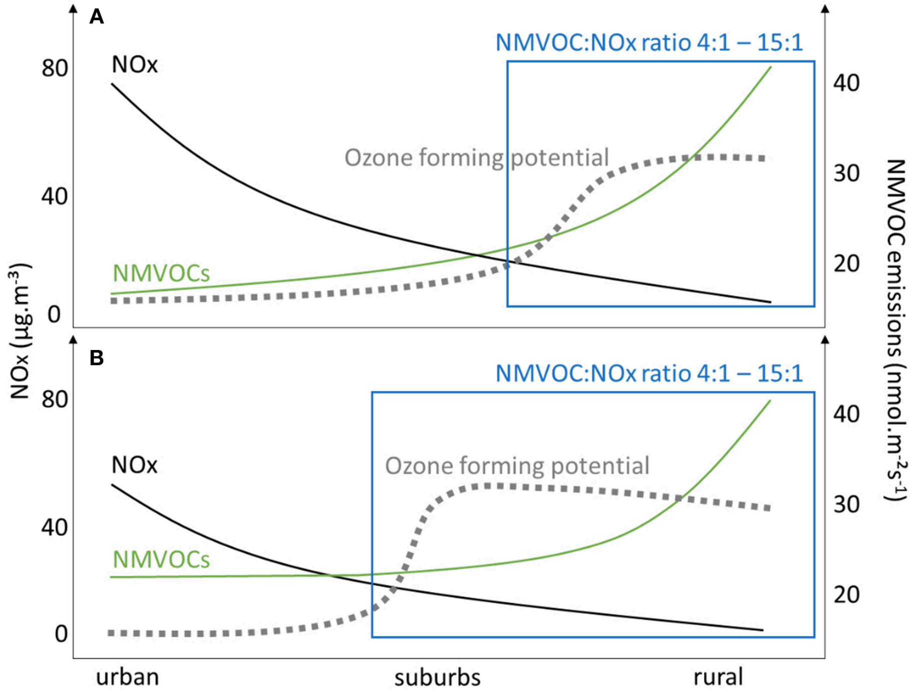

FIGURE 4 | A schematic display of current NO_X-VOC-O_3 relations (approximated from literature values) **(A)**, and a possible future scenario after decreasing NO_X pollution (black solid line) and increased non-methane hydrocarbons (NMVOCs, green solid line) in cities due to greening **(B)**. A left shift of the ozone forming potential curve (gray dotted line) indicates higher ozone pollution in suburbs, since the NMVOC:NO_X ratio reaches optimal values to form ozone (blue box).

Youngsteadt et al., 2015). Reduced emissions due to higher CO_2 concentrations and more frequent drought stress are not likely to reverse this trend, particularly since trees are often irrigated in arid and semiarid regions or during heat wave events in order to sustain their cooling function. However, estimating the net effect of urban trees on ozone concentrations, deposition would need to be taken into account as well, which would be enhanced by more trees. Ozone concentrations furthermore depend on temporal and spatial variations of biogenic and anthropogenic emissions as well as wind speed, and thus require elaborated air chemistry transport models. Approaches have been made to couple physiological models to such models of air chemistry, but the multitude of direct and indirect effects described here have not been considered (Baumgardner et al., 2012; Cabaraban et al., 2013).

OUTLOOK

Policies are strongly directed toward an improvement of air quality and an increase of resilience against climate change impacts in cities. Decisions need to be based on how these goals can be reached most efficiently while maintaining transport and other energy consuming functions. Obvious solutions are a reduction of emissions by introducing clean energy and transport concepts and providing green infrastructure for cooling and shading. Since a technological reduction of anthropogenic emissions will not immediately take place, an increase of green infrastructure is also supposed to enhance deposition and thus reduce air pollution. This is principally a valid and reasonable approach. However, the efficiency of vegetated urban area to fulfill these ecosystem services depends on various boundary conditions, cannot easily be evaluated, and potential ecosystem disservices, among which is the facilitation of ozone production via BVOC emissions, have to be considered. A general vote for a higher share of green infrastructure is thus difficult to implement and can eventually deliver results that might even be contradictory to expectations. It is thus of utmost importance to consider species properties, stress sensitivity, and physiological responses that can be expected under future environmental conditions. Achieving the goal to abate or at least not to increase ozone concentrations in cities, newly planted tree species would need the following requirements: (i) emit low or no BVOCs under current and future environmental conditions, (ii) have a large resistance to drought and biotic stresses, (iii) maximize biomass in terms of leaf area, and (iv) have a high photosynthetic capacity and therefore high stomatal conductance (and thus being high ozone sinks) (Nowak et al., 2018). This task is, however, complicated by the fact that the new plants will have a distinct effect on future urban environmental conditions.

The necessary efforts to enable such analyses will be substantial since our species-specific knowledge about stomatal responses as well as BVOC emission under various stress conditions is limited. The first requirement is therefore to refine our understanding of urban vegetation responses to local environmental conditions. A key knowledge gap is the response of BVOCs emissions to stressful conditions, which often lead to large increases that can potentially affect air quality (Grote et al., 2019). However, general responses to extreme heat and dry conditions that may trigger the death of the plant should also be evaluated in particular for urban tree species that might get more important in the future. Secondly, urban air quality needs to be investigated with integrated analyses considering climate, anthropogenic emissions, city structure as well as distribution and responses of vegetation, i.e., street and park trees. Current approaches are still suffering on coarse resolutions and missing climate-vegetation feedbacks but new developments are encouraging (Maronga et al., 2019). Finally, it should be considered that inventories of existing tree distributions are essential to evaluate any spatially explicit modeling approach. This also includes soil conditions and management that affects canopy dimension and physiology (e.g., pruning and irrigation). Only if this information is available, scenario analyses with varying climate, pollutant emissions, as well as vegetation abundance, composition and distribution can successfully be carried out. Thus, integrating ecosystem services and disservices into environmental quality strategies will therefore enable the identification of green infrastructure types, suitable species (combinations), as well as distribution and density of individuals in order to increase people's overall quality of life in a particular city at reasonable costs.

AUTHOR CONTRIBUTIONS

AF, HS, and BR contributed conception and design of the review. AF and TK composed the figures. AF, HS, TK, AS, CC, SF, and BR wrote the first draft of the manuscript. AF, HS, TK, SF, RG, and BR wrote sections of the manuscript and added to the tables. All authors contributed to manuscript revision, read, and approved the submitted version.

FUNDING

AF was funded by the project Urban trees and air pollution: Effect of drought and salt stress on the production of VOC and absorption of ozone by different city trees (UOzone) by the Vienna Science and Technology Fund (WWTF, project number: ESR17-027).

ACKNOWLEDGMENTS

The authors wish to thank the participants and organizers of the International Conference on Ozone and Plant Ecosystems, Florence, Italy (May 21–25, 2018), for impulses and intensive discussions. Two reviewers and the editor gave important inputs to revise an earlier version.

REFERENCES

Ahmad, P., Azooz, M. M., and Prasad, M. N. V. (2012). *Ecophysiology and Responses of Plants Under Salt Stress.* New York, NY: Springer.

Ajaaj, A. A., Mishra, A. K., and Khan, A. A. (2018). Urban and peri-urban precipitation and air temperature trends in mega cities of the world using multiple trend analysis methods. *Theor. Appl. Climatol.* 132, 403–418. doi: 10.1007/s00704-017-2096-7

Altimir, N., Kolari, P., Tuovinen, J.-P., Vesala, T., Bäck, J., Suni, T., et al. (2006). Foliage surface ozone deposition: a role for surface moisture? *Biogeosciences* 2, 1739–1793. doi: 10.5194/bgd-2-1739-2005

Ameye, M., Allmann, S., Verwaeren, J., Smagghe, G., Haesaert, G., Schuurink, R. C., et al. (2018). Green leaf volatile production by plants: a meta-analysis. *New Phytol.* 220, 666–683. doi: 10.1111/nph.14671

Anav, A., Proietti, C., Menut, L., Carnicelli, S., Marco, A. D., and Paoletti, E. (2018). Sensitivity of stomatal conductance to soil moisture: implications for tropospheric ozone. *Atmos. Chem. Phys.* 18, 5747–5763. doi: 10.5194/acp-18-5747-2018

Arimura, G., Köpke, S., Kunert, M., Volpe, V., David, A., Brand, P., et al. (2008). Effects of feeding *Spodoptera littoralis* on lima bean leaves: IV. Diurnal and nocturnal damage differentially initiate plant volatile emission. *Plant Physiol.* 146, 965–973. doi: 10.1104/pp.107.111088

Atkinson, R. (2000). Atmospheric chemistry of VOCs and NO_x. *Atmos. Environ.* 34, 2063–2101. doi: 10.1016/S1352-2310(99)00460-4

Atkinson, R. (2007). Gas-phase tropospheric chemistry of organic compounds: a review. *Atmos. Environ.* 41, 200–240. doi: 10.1016/j.atmosenv.2007.10.068

Atkinson, R., and Arey, J. (2003). Gas-phase tropospheric chemistry of biogenic volatile organic compounds: a review. *Atmos. Environ.* 37, 197–219. doi: 10.1016/S1352-2310(03)00391-1

Aydin, Y. M., Yaman, B., Koca, H., Dasdemir, O., Kara, M., Altiok, H., et al. (2014). Biogenic volatile organic compound (BVOC) emissions from forested areas in Turkey: Determination of specific emission rates for thirty-one tree species. *Sci. Total Environ.* 490, 239–253. doi: 10.1016/j.scitotenv.2014.04.132

Barnes, J., Davison, A., and Booth, T. (1988). Ozone accelerates structural degradation of epicuticular wax on Norway spruce needles. *New Phytol.* 110, 309–318. doi: 10.1111/j.1469-8137.1988.tb00267.x

Baumgardner, D., Varela, S., Escobedo, F. J., Chacalo, A., and Ochoa, C. (2012). The role of a peri-urban forest on air quality improvement in the Mexico City megalopolis. *Environ. Pollut.* 163, 174–183. doi: 10.1016/j.envpol.2011.12.016

Behnke, K., Ghirardo, A., Janz, D., Kanawati, B., Esperschütz, J., Zimmer, I., et al. (2013). Isoprene function in two contrasting poplars under salt and sunflecks. *Tree Physiol.* 33, 562–578. doi: 10.1093/treephys/tpt018

Benjamin, M. T., and Winer, A. M. (1998). Estimating the ozone-forming potential of urban trees and shrubs. *Atmos. Environ.* 32, 53–68. doi: 10.1016/S1352-2310(97)00176-3

Bialecki, M. B., Fahey, R. T., and Scharenbroch, B. (2018). Variation in urban forest productivity and response to extreme drought across a large metropolitan region. *Urban Ecosyst.* 21, 157–169. doi: 10.1007/s11252-017-0692-z

Blanch, J. S., Sampedro, L., Llusià, J., Moreira, X., Zas, R., and Peñuelas, J. (2012). Effects of phosphorus availability and genetic variation of leaf terpene content and emission rate in *Pinus pinaster* seedlings susceptible and resistant to the pine weevil, *Hylobius abietis*. *Plant Biol.* 14, 66–72. doi: 10.1111/j.1438-8677.2011.00492.x

Blande, J. D., Tiiva, P., Oksanen, E., and Holopainen, J. K. (2007). Emission of herbivore-induced volatile terpenoids from two hybrid aspen (*Populus tremula × tremuloides*) clones under ambient and elevated ozone concentrations in the field. *Glob. Change Biol.* 13, 2538–2550. doi: 10.1111/j.1365-2486.2007.01453.x

Bonn, B., von Schneidemesser, E., Butler, T., Churkina, G., Ehlers, C., Grote, R., et al. (2018). Impact of vegetative emissions on urban ozone and biogenic secondary organic aerosol: Box model study for Berlin, Germany. *J. Clean. Prod.* 176, 827–841. doi: 10.1016/j.jclepro.2017.12.164

Bourtsoukidis, E., Kawaletz, H., Radacki, D., Schütz, S., Hakola, H., Hellén, H., et al. (2013). *Impact of Flooding and Drought Conditions on the Emission of Volatile Organic Compounds of Quercus robur and Prunus serotina.* Berlin: Springer.

Bradshaw, A., Hunt, B., and Walmsley, T. (1995). *Trees in the Urban Landscape: Principles and Practice.* London; New York, NY: E & FN Spon.

Brasseur, G., Orlando, J. J., and Tyndall, G. S. (1999). *Atmospheric Chemistry and Global Change.* Oxford: Oxford University Press.

Brilli, F., Barta, C., Fortunati, A., Lerdau, M., Loreto, F., and Centritto, M. (2007). Response of isoprene emission and carbon metabolism to drought in white poplar (*Populus alba*) saplings. *New Phytol.* 175, 244–254. doi: 10.1111/j.1469-8137.2007.02094.x

BUE (2019). "Straßenbaumkataster Hamburg," in *Metaver.de* (Hamburg: Behörde für Umwelt und Energie).

Cabaraban, M. T., Kroll, C. N., Hirabayashi, S., and Nowak, D. J. (2013). Modeling of air pollutant removal by dry deposition to urban trees using a WRF/CMAQ/i-Tree Eco coupled system. *Environ. Pollut.* 176, 123–133. doi: 10.1016/j.envpol.2013.01.006

Calfapietra, C., Morani, A., Sgrigna, G., Di Giovanni, S., Muzzini, V., Pallozzi, E., et al. (2016). Removal of ozone by urban and peri-urban forests: evidence from laboratory, field, and modeling approaches. *J. Environ. Qual.* 45, 224–233. doi: 10.2134/jeq2015.01.0061

Calfapietra, C., Mugnozza, G. S., Karnosky, D. F., Loreto, F., and Sharkey, T. D. (2008). Isoprene emission rates under elevated CO_2 and O_3 in two field-grown aspen clones differing in their sensitivity to O_3. *New Phytol.* 179, 55–61. doi: 10.1111/j.1469-8137.2008.02493.x

Calfapietra, C., Pallozzi, E., Lusini, I., and Velikova, V. (2013). "Modification of BVOC emissions by changes in atmospheric $[CO_2]$ and air pollution," in *Biology, Controls and Models of Tree Volatile Organic Compound Emissions*. (Dotrecht: Springer), 253–284.

Calfapietra, C., Peñuelas, J., and Niinemets, U. (2015). Urban plant physiology: adaptation-mitigation strategies under permanent stress. *Trends Plant Sci.* 20, 72–75. doi: 10.1016/j.tplants.2014.11.001

Cape, J. N., Hamilton, R., and Heal, M. R. (2009). Reactive uptake of ozone at simulated leaf surfaces: Implications for 'non-stomatal' ozone flux. *Atmos. Environ.* 43, 1116–1123. doi: 10.1016/j.atmosenv.2008.11.007

Carriero, G., Brunetti, C., Fares, S., Hayes, F., Hoshika, Y., Mills, G., et al. (2016). BVOC responses to realistic nitrogen fertilization and ozone exposure in silver birch. *Environ. Pollut.* 213, 988–995. doi: 10.1016/j.envpol.2015.12.047

Carter, W. P. L. (1994). Development of ozone reactivity scales for volatile organic compounds. *J. Air Waste Manage.* 44, 881–899. doi: 10.1080/1073161X.1994.10467290

Carter, W. P. L. (2000). *Documentation of the SAPRC-99 Chemical Mechanism for VOC Reactivity Assessment*. Sacramento, CA: California Air Resources Board.

Carter, W. P. L. (2010). *Updated Maximum Incremental Reactivity Scale and Hydrocarbon Bin Reactivities for Regulatory Applications*. Sacramento, CA: California Air Resources Board.

Chameides, W. L., Lindsay, R. W., Richardson, J., and Kiang, C. S. (1988). The role of biogenic hydrocarbons in urban photochemical smog: Atlanta as a case study. *Science* 241, 1473–1475. doi: 10.1126/science.3420404

Chaves, M. M., Maroco, J. P., and Pereira, J. S. (2003). Understanding plant responses to drought—from genes to the whole plant. *Funct. Plant Biol.* 30, 239–264. doi: 10.1071/FP02076

Cheng, H. R., Guo, H., Saunders, S. M., Lam, S. H. M., Jiang, F., Wang, X. M., et al. (2010). Assessing photochemical ozone formation in the Pearl River Delta with a photochemical trajectory model. *Atmos. Environ.* 44, 4199–4208. doi: 10.1016/j.atmosenv.2010.07.019

Churkina, G., Kuik, F., Bonn, B., Lauer, A., Grote, R., Tomiak, K., et al. (2017). Effect of VOC emissions from vegetation on air quality in Berlin during a heatwave. *Environ. Sci. Technol.* 51, 6120–6130. doi: 10.1021/acs.est.6b06514

Clark, J. R., and Kjelgren, R. (1990). Water as a limiting factor in the development of urban trees. *J. Arboric.* 16, 203–208.

Collier, C. G. (2006). The impact of urban areas on weather. *Q. J. R. Meteor. Soc.* 132, 1–25. doi: 10.1256/qj.05.199

Connop, S., Vandergert, P., Eisenberg, B., Collier, M. J., Nash, C., Clough, J., et al. (2016). Renaturing cities using a regionally-focused biodiversity-led multifunctional benefits approach to urban green infrastructure. *Environ. Sci. Policy* 62, 99–111. doi: 10.1016/j.envsci.2016.01.013

Copolovici, L., and Niinemets, U. (2010). Flooding induced emissions of volatile signalling compounds in three tree species with differing waterlogging tolerance. *Plant Cell Environ.* 33, 1582–1594. doi: 10.1111/j.1365-3040.2010.02166.x

Cornelis, J., and Hermy, M. (2004). Biodiversity relationships in urban and suburban parks in Flanders. *Landsc. Urban Plan.* 69, 385–401. doi: 10.1016/j.landurbplan.2003.10.038

Costa, M., and Baldasano, J. M. (1996). Development of a source emission model for atmospheric pollutants in the Barcelona area. *Atmos. Environ.* 30, 309–318. doi: 10.1016/1352-2310(95)00221-J

Courtois, E. A., Paine, C. E., Blandinieres, P. A., Stien, D., Bessiere, J. M., Houel, E., et al. (2009). Diversity of the volatile organic compounds emitted by 55 species of tropical trees: a survey in French Guiana. *J. Chem. Ecol.* 35:1349. doi: 10.1007/s10886-009-9718-1

Criegee, R. (1975). Mechanism of ozonolysis. *Angew. Chem. Int. Edit.* 14, 745–752. doi: 10.1002/anie.197507451

Curtis, A. J., Helmig, D., Baroch, C., Daly, R., and Davis, S. (2014). Biogenic volatile organic compound emissions from nine tree species used in an urban tree-planting program. *Atmos. Environ.* 95, 634–643. doi: 10.1016/j.atmosenv.2014.06.035

Czerniawska-Kusza, I., Kusza, G., and Duzynski, M. (2004). Effect of deicing salts on urban soils and health status of roadside trees in the Opole region. *Environ. Toxicol.* 19, 296–301. doi: 10.1002/tox.20037

Dale, A. G., and Frank, S. D. (2014). The effects of urban warming on herbivore abundance and street tree condition. *PLoS ONE* 9:e102996. doi: 10.1371/journal.pone.0102996

Dale, A. G., and Frank, S. D. (2017). Warming and drought combine to increase pest insect fitness on urban trees. *PLoS ONE* 12:e0173844. doi: 10.1371/journal.pone.0173844

Dani, K. G., Jamie, I. M., Prentice, I. C., and Atwell, B. J. (2014). Evolution of isoprene emission capacity in plants. *Trends Plant Sci.* 19, 439–446. doi: 10.1016/j.tplants.2014.01.009

Dani, K. S., Jamie, I. M., Prentice, I. C., and Atwell, B. J. (2015). Species-specific photorespiratory rate, drought tolerance and isoprene emission rate in plants. *Plant Signal. Behav.* 10:e990830. doi: 10.4161/15592324.2014.990830

Day, S. D., Wiseman, P. E., Dickinson, S. B., and Harris, J. R. (2010). Contemporary concepts of root system architecture of urban trees. *Arboric Urban For* 36, 149–159. doi: 10.1016/j.atmosenv.2010.02.045

de Souza, V. F., Niinemets, Ü., Rasulov, B., Vickers, C. E., Júnior, S. D., Araújo, W. L., et al. (2018). Alternative carbon sources for isoprene emission. *Trends Plant Sci.* 23, 1081–1101. doi: 10.1016/j.tplants.2018.09.012

Devakumar, A., Prakash, P. G., Sathik, M., and Jacob, J. (1999). Drought alters the canopy architecture and micro-climate of *Hevea brasiliensis* trees. *Trees Struct. Funct.* 13, 161–167. doi: 10.1007/PL00009747

Dollard, G., Dumitrean, P., Telling, S., Dixon, J., and Derwent, R. (2007). Observed trends in ambient concentrations of C_2-C_8 hydrocarbons in the United Kingdom over the period from 1993 to 2004. *Atmos. Environ.* 41, 2559–2569. doi: 10.1016/j.atmosenv.2006.11.020

Drake, B. G., Raschke, K., and Salisbury, F. B. (1970). Temperature and transpiration resistances of *Xanthium* leaves as affected by air temperature, humidity, and wind speed. *Plant Physiol.* 46, 324–330. doi: 10.1104/pp.46.2.324

Duane, M., Poma, B., Rembges, D., Astorga, C., and Larsen, B. (2002). Isoprene and its degradation products as strong ozone precursors in Insubria, Northern Italy. *Atmos. Environ.* 36, 3867–3879. doi: 10.1016/S1352-2310(02)00359-X

EEA (2018a). *Air Quality in Europe—2018 Report*, EEA Report No 12/2018, EEA Reports. European Environment Agency, Copenhagen.

EEA (2018b). *Exceedance of Air Quality Standards in Urban Areas (CSI 004)*. 02 October 2018 ed. Copenhagen: European Environmental Agency.

Ehlers, C., Klemp, D., Rohrer, F., Mihelcic, D., Wegener, R., Kiendler-Scharr, A., et al. (2016). Twenty years of ambient observations of nitrogen oxides and specified hydrocarbons in air masses dominated by traffic emissions in Germany. *Faraday Dis.* 189, 407–437. doi: 10.1039/C5FD00180C

EMEP/CORINAIR (1999). *Atmospheric Emission Inventory Guidebook, 2nd Edn*. Copenhagen: European Environmental Agency.

Equiza, M., Calvo-Polanco, M., Cirelli, D., Senorans, J., Wartenbe, M., Saunders, C., et al. (2017). Long-term impact of road salt (NaCl) on soil and urban trees in Edmonton, Canada. *Urban Forest. Urban Green.* 21, 16–28. doi: 10.1016/j.ufug.2016.11.003

Escobedo, F. J., Kroeger, T., and Wagner, J. E. (2011). Urban forests and pollution mitigation: analyzing ecosystem services and disservices. *Environ. Pollut.* 159, 2078–2087. doi: 10.1016/j.envpol.2011.01.010

EU (2008). *Directive 2008/50/EC of the European Parliament and of the Council of 21 May 2008 on Ambient Air Quality and Cleaner Air for Europe* (OJ L 152, 11.6.2008). (Brussels: European Union), 1–44.

Fahey, R. T., Bialecki, M. B., and Carter, D. R. (2013). Tree growth and resilience to extreme drought across an urban land-use gradient. *Arboric. Urban Forest.* 39, 279–285. doi: 10.1007/s11104-012-1459-1

Fares, S., Schnitzhofer, R., Jiang, X., Guenther, A., Hansel, A., and Loreto, F. (2013). Observations of diurnal to weekly variations of monoterpene-dominated fluxes of volatile organic compounds from mediterranean forests: implications for regional modeling. *Environ. Sci. Technol.* 47, 11073–11082. doi: 10.1021/es4022156

Fittschen, C., Assaf, E., and Vereecken, L. (2017). Experimental and theoretical investigation of the reaction $NO + OH + O_2 \rightarrow HO_2 + NO_2$. *J. Phys. Chem. A* 121, 4652–4657. doi: 10.1021/acs.jpca.7b02499

Forkel, R., Stockwell, W. R., and Steinbrecher, R. (1999). Multilayer canopy/chemistry model to simulate the effect of in-canopy processes on the emission rates of biogenic VOCs. *WIT Trans. Ecol. Environ.* 28, 45–49.

Fortunati, A., Barta, C., Brilli, F., Centritto, M., Zimmer, I., Schnitzler, J. P., et al. (2008). Isoprene emission is not temperature-dependent during and after severe drought-stress: a physiological and biochemical analysis. *Plant J.* 55, 687–697. doi: 10.1111/j.1365-313X.2008.03538.x

Funk, J., Mak, J., and Lerdau, M. (2004). Stress-induced changes in carbon sources for isoprene production in Populus deltoides. *Plant Cell Environ.* 27, 747–755. doi: 10.1111/j.1365-3040.2004.01177.x

Gallaun, H., Zanchi, G., Nabuurs, G.-J., Hengeveld, G., Schardt, M., and Verkerk, P. J. (2010). EU-wide maps of growing stock and above-ground biomass in forests based on remote sensing and field measurements. *Forest Ecol. Manag.* 260, 252–261. doi: 10.1016/j.foreco.2009.10.011

Gatehouse, J. A. (2002). Plant resistance towards insect herbivores: a dynamic interaction. *New Phytol.* 156, 145–169. doi: 10.1046/j.1469-8137.2002.00519.x

Genard-Zielinski, A. C., Ormeno, E., Boissard, C., and Fernandez, C. (2014). Isoprene emissions from downy oak under water limitation during an entire growing season: what cost for growth? *PLoS ONE* 9:e112418. doi: 10.1371/journal.pone.0112418

Geron, C. D., Guenther, A. B., and Pierce, T. E. (1994). An improved model for estimating emissions of volatile organic compounds from forests in the eastern United States. *J. Geophys. Res. Atmos.* 99, 12773–12791. doi: 10.1029/94JD00246

Ghimire, R. P., Kivimäenpää, M., Kasurinen, A., Häikiö, E., Holopainen, T., and Holopainen, J. K. (2017). Herbivore-induced BVOC emissions of Scots pine under warming, elevated ozone and increased nitrogen availability in an open-field exposure. *Agric. Forest Meteorol.* 242, 21–32. doi: 10.1016/j.agrformet.2017.04.008

Ghirardo, A., Xie, J., Zheng, X., Wang, Y., Grote, R., Block, K., et al. (2016). Urban stress-induced biogenic VOC emissions and SOA-forming potentials in Beijing. *Atmos. Chem. Phys.* 16, 2901–2920. doi: 10.5194/acp-16-2901-2016

Goldstein, A. H., Fan, S. M., Goulden, M. L., Munger, J. W., and Wofsy, S. C. (1996). Emissions of ethene, propene and 1-butene by a midlatitude forest. *J. Geophys. Res.* 101, 9149–9157. doi: 10.1029/96JD00334

Goodger, J. Q., Heskes, A. M., and Woodrow, I. E. (2013). Contrasting ontogenetic trajectories for phenolic and terpenoid defences in *Eucalyptus froggattii*. *Ann. Bot.* 112, 651–659. doi: 10.1093/aob/mct010

Gratani, L., and Varone, L. (2014). Atmospheric carbon dioxide concentration variations in Rome: relationship with traffic level and urban park size. *Urban Ecosyst.* 17, 501–511. doi: 10.1007/s11252-013-0340-1

Gromke, C., and Ruck, B. (2009). On the impact of trees on dispersion processes of traffic emissions in street canyons. *Bound Lay Meteorol.* 131, 19–34. doi: 10.1007/s10546-008-9301-2

Grote, R. (2019). *Environmental Impacts on Biogenic Emissions of Volatile Organic Compounds (VOCs),* UBA-FB 002772/Eng. Dessau-Rosslau: Umweltbundesamt.

Grote, R., Monson, R. K., and Niinemets, Ü. (2013). "Leaf-level models of constitutive and stress-driven volatile organic compound emissions," in *Biology, Controls and Models of Tree Volatile Organic Compound Emissions*, eds Ü. Niinemets and R. K. Monson (Dordrecht: Springer), 315–355.

Grote, R., Samson, R., Alonso, R., Amorim, J. H., Cariñanos, P., Churkina, G., et al. (2016). Functional traits of urban trees: air pollution mitigation potential. *Front. Ecol. Environ.* 14, 543–550. doi: 10.1002/fee.1426

Grote, R., Sharma, M., Ghirardo, A., and Schnitzler, J. P. (2019). A new modelling approach for estimating abiotic and biotic stress-induced *de novo* emissions of biogenic volatile organic compounds from plants. *Front. Forest. Glob. Change.* 2:26. doi: 10.3389/ffgc.2019.00026

Guenther, A. B., Jiang, X., Heald, C. L., Sakulyanontvittaya, T., Duhl, T., Emmons, L. K., et al. (2012). The model of emissions of gases and aerosols from nature version 2.1 (MEGAN2.1): an extended and updated framework for modeling biogenic emissions. *Geosci. Model. Dev.* 5, 1471–1492. doi: 10.5194/gmd-5-1471-2012

Guenther, A. B., Monson, R. K., and Fall, R. (1991). Isoprene and monoterpene emission rate variability: observations with eucalyptus and emission rate algorithm development. *J. Geophys. Res. Atmos.* 96, 10799–10808. doi: 10.1029/91JD00960

Guidolotti, G., Pallozzi, E., Gavrichkova, O., Scartazza, A., Mattioni, M., Loreto, F., et al. (2019). Emission of constitutive isoprene, induced monoterpenes and other volatiles under high temperatures in *Eucalyptus camaldulensis*: a ^{13}C labelling study. *Plant Cell Environ.* 42, 1929–1938. doi: 10.1111/pce.13521

Hagenbjörk, A., Malmqvist, E., Mattisson, K., Sommar, N. J., and Modig, L. (2017). The spatial variation of O_3, NO, NO_2 and NO_x and the relation between them in two Swedish cities. *Environ. Monit. Assess.* 189:161. doi: 10.1007/s10661-017-5872-z

Hakola, H., Laurila, T., Lindfors, V., Hellén, H., Gaman, A., and Rinne, J. (2001). Variation of the VOC emission rates of birch species during the growing season. *Boreal. Environ. Res.* 6, 237–249.

Hakola, H., Rinne, J., and Laurila, T. (1998). The hydrocarbon emission rates of tea-leafed willow (*Salix phylicifolia*), silver birch (*Betula pendula*) and European aspen (*Populus tremula*). *Atmos. Environ.* 32, 1825–1833. doi: 10.1016/S1352-2310(97)00482-2

Hakola, H., Tarvainen, V., Bäck, J., Ranta, H., Bonn, B., Rinne, J., et al. (2006). Seasonal variation of mono-and sesquiterpene emission rates of Scots pine. *Biogeosciences* 3, 93–101. doi: 10.5194/bg-3-93-2006

Halliday, H. S., Thompson, A. M., Kollonige, D. W., and Martins, D. K. (2015). Reactivity and temporal variability of volatile organic compounds in the Baltimore/DC region in July 2011. *J. Atmos. Chem.* 72, 197–213. doi: 10.1007/s10874-015-9306-4

Hardin, P. J., and Jensen, R. R. (2007). The effect of urban leaf area on summertime urban surface kinetic temperatures: a Terre Haute case study. *Urban Forest. Urban Green.* 6, 63–72. doi: 10.1016/j.ufug.2007.01.005

Harrison, S. P., Morfopoulos, C., Dani, K. S., Prentice, I. C., Arneth, A., Atwell, B. J., et al. (2013). Volatile isoprenoid emissions from plastid to planet. *New Phytol.* 197, 49–57. doi: 10.1111/nph.12021

Hartikainen, K., Nerg, A.-M., Kivimäenpää, M., Kontunen-Soppela, S., Mäenpää, M., Oksanen, E., et al. (2009). Emissions of volatile organic compounds and leaf structural characteristics of European aspen (*Populus tremula*) grown under elevated ozone and temperature. *Tree Physiol.* 29, 1163–1173. doi: 10.1093/treephys/tpp033

Hartikainen, K., Riikonen, J., Nerg, A.-M., Kivimäenpää, M., Ahonen, V., Tervahauta, A., et al. (2012). Impact of elevated temperature and ozone on the emission of volatile organic compounds and gas exchange of silver birch (*Betula pendula* Roth). *Environ. Exp. Bot.* 84, 33–43. doi: 10.1016/j.envexpbot.2012.04.014

Heinrich, A. (2007). An estimate of biogenic emissions of volatile organic compounds during summertime in China. *Environ. Sci. Pollut. Res. Int.* 14, 69–75. doi: 10.1065/espr2007.02.376

Himanen, S. J., Nerg, A. M., Nissinen, A., Pinto, D. M., Stewart, C. N., Poppy, G. M., et al. (2009). Effects of elevated carbon dioxide and ozone on volatile terpenoid emissions and multitrophic communication of transgenic insecticidal oilseed rape (*Brassica napus*). *New Phytol.* 181, 174–186. doi: 10.1111/j.1469-8137.2008.02646.x

Holman, C., Harrison, R., and Querol, X. (2015). Review of the efficacy of low emission zones to improve urban air quality in European cities. *Atmos. Environ.* 111, 161–169. doi: 10.1016/j.atmosenv.2015.04.009

Holmes, K. R., Nelson, T. A., Coops, N. C., and Wulder, M. A. (2013). Biodiversity indicators show climate change will alter vegetation in parks and protected areas. *Diversity* 5, 352–373. doi: 10.3390/d5020352

Holopainen, J. K. (2004). Multiple functions of inducible plant volatiles. *Trends Plant Sci.* 9, 529–533. doi: 10.1016/j.tplants.2004.09.006

Holopainen, J. K., and Blande, J. D. (2013). Where do herbivore-induced plant volatiles go? *Front. Plant Sci.* 4:185. doi: 10.3389/fpls.2013.00185

Holopainen, J. K., and Gershenzon, J. (2010). Multiple stress factors and the emission of plant VOCs. *Trends Plant Sci.* 15, 176–184. doi: 10.1016/j.tplants.2010.01.006

Hu, B., Jarosch, A.-M., Gauder, M., Graeff-Hönninger, S., Schnitzler, J.-P., Grote, R., et al. (2018). VOC emissions and carbon balance of two bioenergy plantations in response to nitrogen fertilization: a comparison of Miscanthus and Salix. *Environ. Pollut.* 237, 205–217. doi: 10.1016/j.envpol.2018.02.034

IPCC (2014). "Climate change 2014: Impacts, adaptation, and vulnerability. Part A: Global and sectoral aspects," in *Contribution of Working Group II to the Fifth Assessment Report of the Intergovernmental Panel on Climate Change,* eds C. B. Field, V. R. Barros, D. J. Dokken, K. J. Mach, M. D. Mastrandrea, T. E. Bilir, et al. (Cambridge, UK; New York, NY: Cambridge University Press).

Janhäll, S. (2015). Review on urban vegetation and particle air pollution–deposition and dispersion. *Atmos. Environ.* 105, 130–137. doi: 10.1016/j.atmosenv.2015.01.052

Jansen, R. M., Miebach, M., Kleist, E., Van Henten, E. J., and Wildt, J. (2009). Release of lipoxygenase products and monoterpenes by tomato plants as an indicator of *Botrytis cinerea*-induced stress. *Plant Biol.* 11, 859–868. doi: 10.1111/j.1438-8677.2008.00183.x

Jardine, K. J., Jardine, A. B., Souza, V. F., Carneiro, V., Ceron, J. V., Gimenez, B. O., et al. (2016). Methanol and isoprene emissions from the fast growing tropical pioneer species *Vismia guianensis* (Aubl.) Pers. *(Hypericaceae)* in the central Amazon forest. *Atmos. Chem. Phys.* 16, 6441–6452. doi: 10.5194/acp-16-6441-2016

Jenkin, M., Young, J., and Rickard, A. (2015). The MCM v3. 3.1 degradation scheme for isoprene. *Atmos. Chem. Phys.* 15, 11433–11459. doi: 10.5194/acp-15-11433-2015

Kaiser, J., Skog, K. M., Baumann, K., Bertman, S. B., Brown, S. B., Brune, W. H., et al. (2016). Speciation of OH reactivity above the canopy of an isoprene-dominated forest. *Atmos. Chem. Phys.* 16, 9349–9359. doi: 10.5194/acp-16-9349-2016

Kamens, R. M., Gery, M. W., Jeffries, H. E., Jackson, M., and Cole, E. I. (1982). Ozone-isoprene reactions: Product formation and aerosol potential. *Int. J. Chem. Kinet.* 14, 955–975.

Karl, M., Guenther, A., Köble, R., Leip, A., and Seufert, G. (2009). A new European plant-specific emission inventory of biogenic volatile organic compounds for use in atmospheric transport models. *Biogeosciences* 6, 1059–1087. doi: 10.5194/bg-6-1059-2009

Karl, T., Graus, M., Striednig, M., Lamprecht, C., Hammerle, A., Wohlfahrt, G., et al. (2017). Urban eddy covariance measurements reveal significant missing NO_x emissions in Central Europe. *Sci. Rep. UK* 7:2536. doi: 10.1038/s41598-017-02699-9

Kaser, L., Karl, T., Yuan, B., Mauldin, R. L. III., Cantrell, C., Guenther, A. B., et al. (2015). Chemistry-turbulence interactions and mesoscale variability influence the cleansing efficiency of the atmosphere. *Geophys. Res. Lett.* 42,894–810; 903. doi: 10.1002/2015GL066641

Kesselmeier, J., and Staudt, M. (1999). Biogenic volatile organic compounds (VOC): an overview on emission, physiology and ecology. *J. Atmos. Chem.* 33, 23–88. doi: 10.1023/A:1006127516791

Kim, S., Guenther, A., Karl, T., and Greenberg, J. (2011). Contributions of primary and secondary biogenic VOC tototal OH reactivity during the CABINEX (Community Atmosphere-Biosphere INteractions Experiments)-09 field campaign. *Atmos. Chem. Phys.* 11, 8613–8623. doi: 10.5194/acp-11-8613-2011

Kirchner, F., Jeanneret, F., Clappier, A., Krüger, B., van den Bergh, H., and Calpini, B. (2001). Total VOC reactivity in the planetary boundary layer: 2. A new indicator for determining the sensitivity of the ozone production to VOC and NOx. *J. Geophys. Res. Atmos.* 106, 3095–3110. doi: 10.1029/2000JD900603

Klein, T. (2014). The variability of stomatal sensitivity to leaf water potential across tree species indicates a continuum between isohydric and anisohydric behaviours. *Funct. Ecol.* 28, 1313–1320. doi: 10.1111/1365-2435.12289

König, G., Brunda, M., Puxbaum, H., Hewitt, C. N., Duckham, S. C., and Rudolph, J. (1995). Relative contribution of oxygenated hydrocarbons to the total biogenic VOC emissions of selected mid-European agricultural and natural plant species. *Atmos. Environ.* 29, 861–874. doi: 10.1016/1352-2310(95)00026-U

Kopinga, J., and Van den Burg, J. (1995). Using soil and foliar analysis to diagnose the nutritional status of urban trees. *J. Arboric.* 21:17.

Kourtchev, I., Ruuskanen, T. M., Keronen, P., Sogacheva, L., Dal Maso, M., Reissell, A., et al. (2008). Determination of isoprene and alpha-/beta-pinene oxidation products in boreal forest aerosols from Hyytiälä, Finland: diel variations and possible link with particle formation events. *Plant Biol.* 10, 138–149. doi: 10.1055/s-2007-964945

Kramer, K., Degen, B., Buschbom, J., Hickler, T., Thuiller, W., Sykes, M. T., et al. (2010). Modelling exploration of the future of European beech (*Fagus sylvatica* L.) under climate change—range, abundance, genetic diversity and adaptive response. *Forest. Ecol. Manage.* 259, 2213–2222. doi: 10.1016/j.foreco.2009.12.023

Kühn, I., Brandl, R., and Klotz, S. (2004). The flora of German cities is naturally species rich. *Evol. Ecol. Res.* 6, 749–764.

Lahr, E. C., Schade, G. W., Crossett, C. C., and Watson, M. R. (2015). Photosynthesis and isoprene emission from trees along an urban-rural gradient in Texas. *Glob. Chang. Biol.* 21, 4221–4236. doi: 10.1111/gcb.13010

Lamarque, J.-F., Shindell, D. T., Josse, B., Young, P., Cionni, I., Eyring, V., et al. (2013). The atmospheric chemistry and climate model intercomparison project (ACCMIP): overview and description of models, simulations and climate diagnostics. *Geosci. Model. Dev.* 6, 179–206. doi: 10.5194/gmd-6-179-2013

Lamb, B., Guenther, A., Gay, D., and Westberg, H. (1987). A national inventory of biogenic hydrocarbon emissions. *Atmos. Environ.* 21, 1695–1705. doi: 10.1016/0004-6981(87)90108-9

Lambers, H., Chapin, III F. S., and Pons, T. L. (1998). *Plant Physiological Ecology.* New-York, NY: Springer.

Lerdau, M., Litvak, M., Palmer, P., and Monson, R. (1997). Controls over monoterpene emissions from boreal forest conifers. *Tree Physiol.* 17, 563–569. doi: 10.1093/treephys/17.8-9.563

Lerdau, M., Matson, P., Fall, R., and Monson, R. (1995). Ecological controls over monoterpene emissions from Douglas-fir (*Pseudotsuga menziesii*). *Ecology* 76, 2640–2647. doi: 10.2307/2265834

Li, D., Sun, T., Liu, M., Yang, L., Wang, L., and Gao, Z. (2015). Contrasting responses of urban and rural surface energy budgets to heat waves explain synergies between urban heat islands and heat waves. *Environ. Res. Lett.* 10:054009. doi: 10.1088/1748-9326/10/5/054009

Li, D. W., Shi, Y., He, X. Y., and Chi, G. Y. (2011). Seasonal variations of BVOCs emission from *Ginkgo biloba* linn in urban area. *Appl. Mech. Mater.* 71–78, 2891–2894. doi: 10.4028/www.scientific.net/AMM.71-78.2891

Liao, C.-T., and Lin, C.-H. (2001). Physiological adaptation of crop plants to flooding stress. *Proc. Natl. Sci. Counc. Repub. China B* 25, 148–157.

Livesley, S. J., McPherson, G. M., and Calfapietra, C. (2016). The urban forest and ecosystem services: impacts on urban water, heat, and pollution cycles at the tree, street, and city scale. *J. Environ. Qual.* 45, 119–124. doi: 10.2134/jeq2015.11.0567

Loreto, F., Barta, C., Brilli, F., and Nogues, I. (2006). On the induction of volatile organic compound emissions by plants as consequence of wounding or fluctuations of light and temperature. *Plant Cell Environ.* 29, 1820–1828. doi: 10.1111/j.1365-3040.2006.01561.x

Loreto, F., and Delfine, S. (2000). Emission of isoprene from salt-stressed *Eucalyptus globulus* leaves. *Plant Physiol.* 123, 1605–1610. doi: 10.1104/pp.123.4.1605

Loreto, F., and Schnitzler, J.-P. (2010). Abiotic stresses and induced BVOCs. *Trends Plant Sci.* 15, 154–166. doi: 10.1016/j.tplants.2009.12.006

Loreto, F., and Velikova, V. (2001). Isoprene produced by leaves protects the photosynthetic apparatus against ozone damage, quenches ozone products, and reduces lipid peroxidation of cellular membranes. *Plant Physiol.* 127, 1781–1787. doi: 10.1104/pp.010497

Maronga, B., Gross, G., Raasch, S., Banzhaf, S., Forkel, R., Heldens, W., et al. (2019). Development of a new urban climate model based on the model PALM–Project overview, planned work, and first achievements. *Meteorol. Z.* 28, 105–119. doi: 10.1127/metz/2019/0909

Medlyn, B. E., Barton, C. V. M., Broadmeadow, M. S. J., Ceulemans, R., De Angelis, P., Forstreuter, M., et al. (2001). Stomatal conductance of forest species after long-term exposure to elevated CO2 concentration: a synthesis. *New Phytol.* 149, 247–264. doi: 10.1046/j.1469-8137.2001.00028.x

Meeningen, Y. V., Schurgers, G., Rinnan, R., and Holst, T. (2016). BVOC emissions from English oak (*Quercus robur*) and European beech (*Fagus sylvatica*) along a latitudinal gradient. *Biogeosciences* 13, 6067–6080. doi: 10.5194/bg-13-6067-2016

Meineke, E. K., Dunn, R. R., Sexton, J. O., and Frank, S. D. (2013). Urban warming drives insect pest abundance on street trees. *PLoS ONE* 8:e59687. doi: 10.1371/journal.pone.0059687

Mills, G., Hayes, F., Simpson, D., Emberson, L., Norris, D., Harmens, H., et al. (2011). Evidence of widespread effects of ozone on crops and (semi-)natural vegetation in Europe (1990–2006) in relation to AOT40- and flux-based risk maps. *Glob. Change Biol.* 17, 592–613. doi: 10.1111/j.1365-2486.2010.02217.x

Monks, P., Granier, C., Fuzzi, S., Stohl, A., Williams, M., Akimoto, H., et al. (2009). Atmospheric composition change–global and regional air quality. *Atmos. Environ.* 43, 5268–5350. doi: 10.1016/j.atmosenv.2009.08.021

Morani, A., Nowak, D., Hirabayashi, S., Guidolotti, G., Medori, M., Muzzini, V., et al. (2014). Comparing i-Tree modeled ozone deposition with field measurements in a periurban Mediterranean forest. *Environ. Pollut.* 195, 202–209. doi: 10.1016/j.envpol.2014.08.031

Munck, I. A., Bennett, C. M., Camilli, K. S., and Nowak, R. S. (2010). Long-term impact of de-icing salts on tree health in the Lake Tahoe Basin: environmental influences and interactions with insects and diseases. *Forest. Ecol. Manage.* 260, 1218–1229. doi: 10.1016/j.foreco.2010.07.015

Neirynck, J., and Verstraeten, A. (2018). Variability of ozone deposition velocity over a mixed suburban temperate forest. *Front. Environ. Sci.* 6:82. doi: 10.3389/fenvs.2018.00082

Niinemets, Ü. (2010). Mild versus severe stress and BVOCs: thresholds, priming and consequences. *Trends Plant Sci.* 15, 145–153. doi: 10.1016/j.tplants.2009.11.008

Niinemets, Ü., Arneth, A., Kuhn, U., Monson, R., Peñuelas, J., and Staudt, M. (2010). The emission factor of volatile isoprenoids: stress, acclimation, and developmental responses. *Biogeosciences* 7, 2203–2223. doi: 10.5194/bg-7-2203-2010

Niinemets, Ü., Kännaste, A., and Copolovici, L. (2013). Quantitative patterns between plant volatile emissions induced by biotic stresses and the degree of damage. *Front. Plant Sci.* 4:262. doi: 10.3389/fpls.2013.00262

Niinemets, Ü., and Monson, R. K. (2013). *Biology, Controls and Models of Tree Volatile Organic Compound Emissions*. Dordrecht: Springer. doi: 10.1007/978-94-007-6606-8

Nölscher, A. C., Yanez-Serrano, A. M., Wolff, S., De Araujo, A. C., Lavrič, J. V., Kesselmeier, J., et al. (2016). Unexpected seasonality in quantity and composition of Amazon rainforest air reactivity. *Nat. Commun.* 7:10383. doi: 10.1038/ncomms 10383

Norton, B. A., Coutts, A. M., Livesley, S. J., Harris, R. J., Hunter, A. M., and Williams, N. S. (2015). Planning for cooler cities: a framework to prioritise green infrastructure to mitigate high temperatures in urban landscapes. *Landsc. Urban Plan.* 134, 127–138. doi: 10.1016/j.landurbplan.2014.10.018

Nowak, D. J., Hirabayashi, S., Doyle, M., McGovern, M., and Pasher, J. (2018). Air pollution removal by urban forests in Canada and its effect on air quality and human health. *Urban Forest. Urban Green.* 29, 40–48. doi: 10.1016/j.ufug.2017.10.019

Nowak, D. J., Hoehn, R. E. III., Crane, D. E., Stevens, J. C., and Fisher, C. L. (2010). Assessing urban forest effects and values, Chicago's urban forest. *Resour. Bull.* 37, 1–27. doi: 10.2737/NRS-RB-37

O'Driscoll, R., Stettler, M. E., Molden, N., Oxley, T., and ApSimon, H. M. (2018). Real world CO_2 and NO_x emissions from 149 Euro 5 and 6 diesel, gasoline and hybrid passenger cars. *Sci. Total Environ.* 621, 282–290. doi: 10.1016/j.scitotenv.2017.11.271

Ordóñez-Barona, C., Sabetski, V., Millward, A. A., and Steenberg, J. (2018). De-icing salt contamination reduces urban tree performance in structural soil cells. *Environ. Pollut.* 234, 562–571. doi: 10.1016/j.envpol.2017.11.101

Ormeño, E., Baldy, V., Ballini, C., and Fernandez, C. (2008). Production and diversity of volatile terpenes from plants on calcareous and siliceous soils: effect of soil nutrients. *J. Chem. Ecol.* 34:1219. doi: 10.1007/s10886-008-9515-2

Ormeño, E., and Fernandez, C. (2012). Effect of soil nutrient on production and diversity of volatile terpenoids from plants. *Curr. Bioact. Comp.* 8, 71–79. doi: 10.2174/157340712799828188

Owen, S., Boissard, C., Street, R., Duckham, S., Csiky, O., and Hewitt, C. (1997). Screening of 18 Mediterranean plant species for volatile organic compound emissions. *Atmos. Environ.* 31, 101–117. doi: 10.1016/S1352-2310(97)00078-2

Paoletti, E., Bardelli, T., Giovannini, G., and Pecchioli, L. (2011). Air quality impact of an urban park over time. *Procedia Environ. Sci.* 4, 10–16. doi: 10.1016/j.proenv.2011.03.002

Papiez, M. R., Potosnak, M. J., Goliff, W. S., Guenther, A. B., Matsunaga, S. N., and Stockwell, W. R. (2009). The impacts of reactive terpene emissions from plants on air quality in Las Vegas, Nevada. *Atmos. Environ.* 43, 4109–4123. doi: 10.1016/j.atmosenv.2009.05.048

Pauleit, S., Jones, N., Garcia-Martin, G., Garcia-Valdecantos, J. L., Rivière, L. M., Vidal-Beaudet, L., et al. (2002). Tree establishment practice in towns and cities–Results from a European survey. *Urban Forest. Urban Green.* 1, 83–96. doi: 10.1078/1618-8667-00009

Pegoraro, E., Rey, A. N. A., Abrell, L., Haren, J., and Lin, G. (2006). Drought effect on isoprene production and consumption in Biosphere 2 tropical rainforest. *Glob. Change Biol.* 12, 456–469. doi: 10.1111/j.1365-2486.2006.01112.x

Peñuelas, J., and Staudt, M. (2010). BVOCs and global change. *Trends Plant Sci.* 15, 133–144. doi: 10.1016/j.tplants.2009.12.005

Pinto, D. M., Blande, J. D., Souza, S. R., Nerg, A. M., and Holopainen, J. K. (2010). Plant volatile organic compounds (VOCs) in ozone (O_3) polluted atmospheres: the ecological effects. *J. Chem. Ecol.* 36, 22–34. doi: 10.1007/s10886-009-9732-3

Potosnak, M. J., LeStourgeon, L., and Nunez, O. (2014a). Increasing leaf temperature reduces the suppression of isoprene emission by elevated CO_2 concentration. *Sci. Total Environ.* 481, 352–359. doi: 10.1016/j.scitotenv.2014.02.065

Potosnak, M. J., LeStourgeon, L., Pallardy, S. G., Hosman, K. P., Gu, L., Karl, T., et al. (2014b). Observed and modeled ecosystem isoprene fluxes from an oak-dominated temperate forest and the influence of drought stress. *Atmos. Environ.* 84, 314–322. doi: 10.1016/j.atmosenv.2013.11.055

Préndez, M., Carvajal, V., Corada, K., Morales, J., Alarcón, F., and Peralta, H. (2013). Biogenic volatile organic compounds from the urban forest of the Metropolitan Region, Chile. *Environ. Pollut.* 183, 143–150. doi: 10.1016/j.envpol.2013.04.003

Ran, L., Zhao, C. S., Xu, W. Y., Lu, X. Q., Han, M., Lin, W. L., et al. (2011). VOC reactivity and its effect on ozone production during the HaChi summer campaign. *Atmos. Chem. Phys.* 11, 4657–4667. doi: 10.5194/acp-11-4657-2011

Rhew, R. C., Deventer, M. J., Turnipseed, A. A., Warneke, C., Ortega, J., Shen, S., et al. (2017). Ethene, propene, butene and isoprene emissions from a ponderosa pine forest measured by Relaxed Eddy Accumulation. *Atmos. Chem. Phys.* 17, 13417–13438. doi: 10.5194/acp-17-13417-2017

Rose, D., and Webber, J. (2011). *De-Icing Salt Damage to Trees.* Pathology Advisory Note 11, Forest Research. Edinburgh: Forestry Commission.

Rosenstiel, T. N., Potosnak, M. J., Griffin, K. L., Fall, R., and Monson, R. K. (2003). Increased CO_2 uncouples growth from isoprene emission in an agriforest ecosystem. *Nature* 421:256. doi: 10.1038/nature01312

Sæbø, A., Borzan, Ž., Ducatillion, C., Hatzistathis, A., Lagerström, T., Supuka, J., et al. (2005). "The selection of plant materials for street trees, park trees and urban woodland," in *Urban Forests and Trees,* eds C. Konijnendijk, K. Nilsson, T. Randrup and J. Schipperijn. (Berlin; Heidelberg: Springer), 257–280. doi: 10.1007/3-540-27684-X_11

Saaroni, H., Amorim, J. H., Hiemstra, J., and Pearlmutter, D. (2018). Urban Green Infrastructure as a tool for urban heat mitigation: Survey of research methodologies and findings across different climatic regions. *Urban Clim.* 24, 94–110. doi: 10.1016/j.uclim.2018.02.001

Sade, N., Gebremedhin, A., and Moshelion, M. (2012). Risk-taking plants: anisohydric behavior as a stress-resistance trait. *Plant Signal. Behav.* 7, 767–770. doi: 10.4161/psb.20505

Samson, R., Grote, R., Calfapietra, C., Cariñanos, P., Fares, S., Paoletti, E., et al. (2017a). "Urban trees and their relation to air pollution," in *The Urban Forest: Cultivating Green Infrastructure for People and the Environment,* eds D. Pearlmutter, C. Calfapietra, R. Samson, L. O'Brien, S. Krajter Ostoić, G. Sanesi et al. (Cham: Springer International Publishing), 21–30.

Samson, R., Ningal, T. F., Tiwary, A., Grote, R., Fares, S., Saaroni, H., et al. (2017b). "Species-specific information for enhancing ecosystem services," in *The Urban Forest,* eds D. Pearlmutter, C. Calfapietra, R. Samson, L. O'Brien, S. Krajter Ostoić, G. Sanesi, and R. Alonso del Amo (Cham: Springer), 111–144.

Saunier, A., Ormeño, E., Boissard, C., Wortham, H., Temime-Roussel, B., Lecareux, C., et al. (2017). Effect of mid-term drought on *Quercus pubescens*; BVOCs' emission seasonality and their dependency on light and/or temperature. *Atmos. Chem. Phys.* 17, 7555–7566. doi: 10.5194/acp-17-7555-2017

Saunier, A., Ormeno, E., Havaux, M., Wortham, H., Ksas, B., Temime-Roussel, B., et al. (2018). Resistance of native oak to recurrent drought conditions simulating predicted climatic changes in the Mediterranean region. *Plant Cell Environ.* 41, 2299–2312. doi: 10.1111/pce.13331

Scala, A., Allmann, S., Mirabella, R., Haring, M., and Schuurink, R. (2013). Green leaf volatiles: a plant's multifunctional weapon against herbivores and pathogens. *Int. J. Mol. Sci.* 14, 17781–17811. doi: 10.3390/ijms140917781

Seco, R., Peñuelas, J., and Filella, I. (2007). Short-chain oxygenated VOCs: Emission and uptake by plants and atmospheric sources, sinks, and concentrations. *Atmos. Environ.* 41, 2477–2499. doi: 10.1016/j.atmosenv.2006.11.029

Shannon, M., Banuelos, G., Draper, J., Ajwa, H., Jordahl, J., and Licht, L. (1999). Tolerance of hybrid poplar (*Populus*) trees irrigated with varied levels of salt, selenium, and boron. *Int. J. Phytoremediat.* 1, 273–288. doi: 10.1080/15226519908500020

Sheffer, E. (2012). A review of the development of Mediterranean pine–oak ecosystems after land abandonment and afforestation: are they novel ecosystems? *Ann. Forest. Sci.* 69, 429–443. doi: 10.1007/s13595-011-0181-0

Sicard, P., De Marco, A., Troussier, F., Renou, C., Vas, N., and Paoletti, E. (2013). Decrease in surface ozone concentrations at Mediterranean remote sites and increase in the cities. *Atmos. Environ.* 79, 705–715. doi: 10.1016/j.atmosenv.2013.07.042

Sieghardt, M., Mursch-Radlgruber, E., Paoletti, E., Couenberg, E., Dimitrakopoulus, A., Rego, F., et al. (2005). "The abiotic urban environment: impact of urban growing conditions on urban vegetation," in *Urban Forests and Trees,* eds C. Konijnendijk, K. Nilsson, T. Randrup, and J. Schipperijn (Cham: Springer), 281–323. doi: 10.1007/3-540-27684-X_12

Sillman, S., and He, D. (2002). Some theoretical results concerning O_3-NO_x-VOC chemistry and NO_x-VOC indicators. *J. Geophys. Res.* D22:4659 doi: 10.1029/2001JD001123

Singh, A. P., Varshney, C. K., and Singh, U. K. (2007). Seasonal variations in isoprene emission from tropical deciduous tree species. *Environ. Monit. Assess.* 131, 231–235. doi: 10.1007/s10661-006-9471-7

Singsaas, E. L., Lerdau, M., Winter, K., and Sharkey, T. D. (1997). Isoprene increases thermotolerance of isoprene-emitting species. *Plant Physiol.* 115, 1413–1420. doi: 10.1104/pp.115.4.1413

Siwko, M. E., Marrink, S. J., de Vries, A. H., Kozubek, A., Uiterkamp, A. J. S., and Mark, A. E. (2007). Does isoprene protect plant membranes from thermal shock? A molecular dynamics study. *Biochim. Biophys. Acta Biomembr.* 1768, 198–206. doi: 10.1016/j.bbamem.2006.09.023

Sjöman, H., and Busse Nielsen, A. (2010). Selecting trees for urban paved sites in Scandinavia – a review of information on stress tolerance and its relation to the requirements of tree planners. *Urban Forest. Urban Green.* 9, 281–293. doi: 10.1016/j.ufug.2010.04.001

Solberg, S., Hov, Ø., Søvde, A., Isaksen, I. S. A., Coddeville, P., De Backer, H., et al. (2008). European surface ozone in the extreme summer 2003. *J. Geophys. Res. Atmos.* 113:D07307. doi: 10.1029/2007JD009098

Steinbrecher, R., Smiatek, G., Köble, R., Seufert, G., Theloke, J., Hauff, K., et al. (2009). Intra-and inter-annual variability of VOC emissions from natural and semi-natural vegetation in Europe and neighbouring countries. *Atmos. Environ.* 43, 1380–1391. doi: 10.1016/j.atmosenv.2008.09.072

Steindel, F., Beauchamp, J., Hansel, A., Kesselmeier, J., Kleist, E., Kuhn, U., et al. (2005). "Stress induced VOC emissions from mildew infested oak," in *Geophysical Research Abstract* 7 EGU05-A-03010.

Stemmler, K., Bugmann, S., Buchmann, B., Reimann, S., and Staehelin, J. (2005). Large decrease of VOC emissions of Switzerland's car fleet during the past decade: results from a highway tunnel study. *Atmos. Environ.* 39, 1009–1018. doi: 10.1016/j.atmosenv.2004.10.010

Streiling, S., and Matzarakis, A. (2003). Influence of single and small clusters of trees on the bioclimate of a city: a case study. *J. Arboric.* 29, 309–316.

Taha, H., Wilkinson, J., Bornstein, R., Xiao, Q., McPherson, G., Simpson, J., et al. (2016). An urban-forest control measure for ozone in the Sacramento, CA Federal Non-Attainment Area (SFNA). *Sustain. Cities Soc.* 21, 51–65. doi: 10.1016/j.scs.2015.11.004

Tarvainen, V., Hakola, H., Hellén, H., Bäck, J., Hari, P., and Kulmala, M. (2005). Temperature and light dependence of the VOC emissions of Scots pine. *Atmos. Chem. Phys.* 5, 989–998. doi: 10.5194/acp-5-989-2005

Teuber, M., Zimmer, I., Kreuzwieser, J., Ache, P., Polle, A., Rennenberg, H., et al. (2008). VOC emissions of Grey poplar leaves as affected by salt stress and different N sources. *Plant Biol.* 10, 86–96. doi: 10.1111/j.1438-8677.2007.00015.x

Tiiva, P., Faubert, P., Räty, S., Holopainen, J. K., Holopainen, T., and Rinnan, R. (2009). Contribution of vegetation and water table on isoprene emission from boreal peatland microcosms. *Atmos. Environ.* 43, 5469–5475. doi: 10.1016/j.atmosenv.2009.07.026

Tingey, D., Turner, D., and Weber, J. (1991). "Factors controlling the emissions of monoterpenes and other volatile organic compounds," in *Trace Gas Emission by Plants,* eds T. D. Sharkey, E. A. Holland, and H. A. Mooney (Academic Press), 93—119.

Tingey, D. T., Evans, R., and Gumpertz, M. (1981). Effects of environmental conditions on isoprene emission from live oak. *Planta* 152, 565–570. doi: 10.1007/BF00380829

Tiwary, A., Namdeo, A., Fuentes, J., Dore, A., Hu, X.-M., and Bell, M. (2013). Systems scale assessment of the sustainability implications of emerging green initiatives. *Environ. Pollut.* 183, 213–223. doi: 10.1016/j.envpol.2013.03.049

Tong, Z., Baldauf, R. W., Isakov, V., Deshmukh, P., and Max Zhang, K. (2016). Roadside vegetation barrier designs to mitigate near-road air pollution impacts. *Sci. Total Environ.* 541, 920–927. doi: 10.1016/j.scitotenv.2015.09.067

Trenberth, K. E., Dai, A., Van Der Schrier, G., Jones, P. D., Barichivich, J., Briffa, K. R., et al. (2014). Global warming and changes in drought. *Nat. Clim. Change* 4, 17–22. doi: 10.1038/nclimate2067

Trowbridge, A. M., and Stoy, P. C. (2013). "BVOC-mediated plant-herbivore interactions," in *Biology, Controls and Models of Tree Volatile Organic Compound Emissions,* Ü. Niinemets and R. K. Monson (Dordrecht: Springer), 21–46.

Valkama, E., Koricheva, J., and Oksanen, E. (2007). Effects of elevated O_3, alone and in combination with elevated CO_2, on tree leaf chemistry and insect herbivore performance: a meta-analysis. *Glob. Chang. Biol.* 13, 184–201. doi: 10.1111/j.1365-2486.2006.01284.x

Veldt, C. (1989). *Leaf Biomass Data for the Estimation of Biogenic VOC Emissions.* Apeldoorn: MTO-TNO Report 99–306.

Vitale, M., Salvatori, E., Loreto, F., Fares, S., and Manes, F. (2007). Physiological responses of *Quercus ilex* leaves to water stress and acute ozone exposure under controlled conditions. *Water Air Soil Pollut.* 189, 113–125. doi: 10.1007/s11270-007-9560-4

Vos, P. E., Maiheu, B., Vankerkom, J., and Janssen, S. (2013). Improving local air quality in cities: to tree or not to tree? *Environ. Pollut.* 183, 113–122. doi: 10.1016/j.envpol.2012.10.021

Vuorinen, T., Nerg, A.-M., Vapaavuori, E., and Holopainen, J. K. (2005). Emission of volatile organic compounds from two silver birch (*Betula pendula* Roth) clones grown under ambient and elevated CO_2 and different O_3 concentrations. *Atmos. Environ.* 39, 1185–1197. doi: 10.1016/j.atmosenv.2004.09.077

Wagner, P., and Kuttler, W. (2014). Biogenic and anthropogenic isoprene in the near-surface urban atmosphere—a case study in Essen, Germany. *Sci. Total Environ.* 475, 104–115. doi: 10.1016/j.scitotenv.2013.12.026

Wang, T., Xue, L., Brimblecombe, P., Lam, Y. F., Li, L., and Zhang, L. (2017). Ozone pollution in China: a review of concentrations, meteorological influences, chemical precursors, and effects. *Sci. Total Environ.* 575, 1582–1596. doi: 10.1016/j.scitotenv.2016.10.081

Wesely, M. (1989). Parameterization of surface resistances to gaseous dry deposition in regional-scale numerical models. *Atmos. Environ.* 23, 1293–1304. doi: 10.1016/0004-6981(89)90153-4

Wesely, M., and Hicks, B. (2000). A review of the current status of knowledge on dry deposition. *Atmos. Environ.* 34, 2261–2282. doi: 10.1016/S1352-2310(99)00467-7

WHO (2006). *Who Air Quality Guidelines for Particulate Matter, Ozone, Nitrogen Dioxide and Sulfur Dioxide: Global Update 2005: Summary of Risk Assessment* (No. WHO/SDE/PHE/OEH/06.02). Geneva: World Health Organization.

Williams, J., Kessel, S. U., Nölscher, A. C., Yang, Y. D., Lee, Y., Yanez-Serrano, A. M., et al. (2016). Opposite OH reactivity and ozone cycles in the Amazon rainforest and megacity Beijing: subversion of biospheric oxidant control by anthropogenic emissions. *Atmos. Environ.* 125, 112–118. doi: 10.1016/j.atmosenv.2015.11.007

Wissmar, R. C., Timm, R. K., and Logsdon, M. G. (2004). Effects of changing forest and impervious land covers on discharge characteristics of watersheds. *Environ. Manage.* 34, 91–98. doi: 10.1007/s00267-004-0224-5

Wittig, V. E., Ainsworth, E. A., and Long, S. P. (2007). To what extent do current and projected increases in surface ozone affect photosynthesis and stomatal conductance of trees? A meta-analytic review of the last 3 decades of experiments. *Plant Cell Environ.* 30, 1150–1162. doi: 10.1111/j.1365-3040.2007.01717.x

Wolfe, G., and Thornton, J. (2011). The chemistry of atmosphere-forest exchange (CAFÉ) model–Part 1: model description and characterization. *Atmos. Chem. Phys.* 11, 77–101. doi: 10.5194/acp-11-77-2011

Wolyniak, B., and Elmendorf, W. F. (2011). *Lancaster City Tree Inventory: Summary Report.* Penn State School of Forest Resources.

Wu, C., Pullinen, I., Andres, S., Carriero, G., Fares, S., Goldbach, H., et al. (2015). Impacts of soil moisture on *de novo* monoterpene emissions from European beech, Holm oak, Scots pine, and Norway spruce. *Biogeosciences* 12, 177–191. doi: 10.5194/bg-12-177-2015

Xie, X., Shao, M., Liu, Y., Lu, S., Chang, C.-C., and Chen, Z.-M. (2008). Estimate of initial isoprene contribution to ozone formation potential in Beijing, China. *Atmos. Environ.* 42, 6000–6010. doi: 10.1016/j.atmosenv.2008.03.035

Yang, J., Chang, Y., and Yan, P. (2015). Ranking the suitability of common urban tree species for controlling $PM_{2.5}$ pollution. *Atmos. Pollut. Res.* 6, 267–277. doi: 10.5094/APR.2015.031

Yang, P., Ren, G., and Hou, W. (2017). Temporal–spatial patterns of relative humidity and the urban dryness Island effect in Beijing City. *J. Appl. Meteorol. Climatol.* 56, 2221–2237. doi: 10.1175/JAMC-D-16-0338.1

Yli-Pelkonen, V., Viippola, V., Rantalainen, A.-L., Zheng, J., and Setälä, H. (2018). The impact of urban trees on concentrations of PAHs and other gaseous air pollutants in Yanji, northeast China. *Atmos. Environ.* 192, 151–159. doi: 10.1016/j.atmosenv.2018.08.061

Young, P. J., Archibald, A. T., Bowman, K. W., Lamarque, J. F., Naik, V., Stevenson, D. S., et al. (2013). Pre-industrial to end 21st century projections of tropospheric ozone from the Atmospheric Chemistry and Climate Model Intercomparison Project (ACCMIP). *Atmos. Chem. Phys.* 13, 2063–2090. doi: 10.5194/acp-13-2063-2013

Youngsteadt, E., Dale, A. G., Terando, A. J., Dunn, R. R., and Frank, S. D. (2015). Do cities simulate climate change? A comparison of herbivore response to urban and global warming. *Glob. Chang. Biol.* 21, 97–105. doi: 10.1111/gcb.12692

Zhu, Z., Tsokankunku, A., Plake, D., Falge, E., Foken, T., and Meixner, F. (2009). "Multi-level eddy covariance measurements for ozone fluxes above, within and below spruce forest canopy," in *Proceedings of the International Conference of Atmospheric Transport and Chemistry in Forest Ecosystems* (Thurnau, Bayreuth University; Abteilung Mikrometeorologie).

Zipperer, W. C., Sisinni, S. M., Pouyat, R. V., and Foresman, T. W. (1997). Urban tree cover: an ecological perspective. *Urban Ecosyst.* 1, 229–246. doi: 10.1023/A:1018587830636

Conflict of Interest Statement: The authors declare that the research was conducted in the absence of any commercial or financial relationships that could be construed as a potential conflict of interest.

frontiers
in Forests and Global Change

ORIGINAL RESEARCH
published: 18 September 2019
doi: 10.3389/ffgc.2019.00053

Salt Stress Reduced the Seedling Growth of Two Larch Species Under Elevated Ozone

Tetsuto Sugai[1†], *Wang Yannan*[2†‡], *Toshihiro Watanabe*[1*], *Fuyuki Satoh*[3], *Laiye Qu*[4,5*] and *Takayoshi Koike*[1,4]

[1] *Plant Nutrition Laboratory, Research Faculty of Agriculture, Hokkaido University, Sapporo, Japan,* [2] *Forest Ecology and Silviculture Laboratory, Graduate School of Agriculture, Hokkaido University, Sapporo, Japan,* [3] *Field Science Center for Northern Biosphere, Hokkaido University, Sapporo, Japan,* [4] *State Key Laboratory of Urban and Regional Ecology, Research Center for Eco-Environmental Science, Chinese Academy of Sciences, Beijing, China,* [5] *University of Chinese Academy of Sciences, College of Resources and Environment, Beijing, China*

Edited by:
Elena Paoletti,
Italian National Research Council (CNR), Italy

Reviewed by:
Lina Fusaro,
Sapienza University of Rome, Italy
Antonella Calzone,
University of Pisa, Italy

***Correspondence:**
Toshihiro Watanabe
nabe@chem.agr.hokudai.ac.jp
Laiye Qu
lyqu@rcees.ac.cn

[†] *These authors have contributed equally to this work*

[‡] Present address:
Wang Yannan,
Jiangxi Academy of Forestry, Nanchang, China

Specialty section:
This article was submitted to Forests and the Atmosphere, a section of the journal Frontiers in Forests and Global Change

Received: *25 June 2019*
Accepted: *27 August 2019*
Published: *18 September 2019*

Citation:
Sugai T, Yannan W, Watanabe T, Satoh F, Qu L and Koike T (2019) Salt Stress Reduced the Seedling Growth of Two Larch Species Under Elevated Ozone. Front. For. Glob. Change 2:53. doi: 10.3389/ffgc.2019.00053

The effect of elevated ozone (eO_3) and soil salinization with alkaline salts in northeastern (NE) China is a serious concern affecting the success of the national replanting project. As planted areas exceed 4 million hectares in China, we must consider future afforestation efforts after thinning and harvesting. Here, we investigated eO_3 and salt stress on Dahurian larch (*Larix gmelinii* var. *japonica*; DL) and Japanese larch (*L. kaempferi*; JL) seedlings. The seedlings were exposed to eO_3 (~70 nmol mol^{-1}) and ambient ozone (aO_3) (~25~40 nmol mol^{-1}) for one growing season in an open top chamber (OTC) system with simulated salinity in NE China (alkaline salt, $NaHCO_3$:NaCl = 9:1, 20mM Na^+). The seedlings under salt-free treatment received tap water. Although the effects of eO_3 on DL were not significant, eO_3 significantly increased total dry mass and total leaf area index of JL. There was no significant reduction in total dry mass under salt stress in both species. The relationship between needle Na and other mineral contents indicated that both species maintained K contents even with excess Na contents in needles. DL showed relatively lower reduction of other mineral contents, indicating higher salt tolerance of needle element homeostasis than JL. Contrary to our hypothesis, there were no interaction effects of eO_3 and salt stress on both species. These results indicated that DL seedlings may be more suitable than JL seedlings as a future afforestation species under eO_3 levels of <70 nmol mol^{-1} at saline soil condition.

Keywords: combined effect, salt stress, larch, interspecific differences, homeostasis

INTRODUCTION

Ground-level ozone (O_3) is the most harmful air pollutant to forest ecosystems on both local and global scales (Paoletti et al., 2007, 2010; Matyssek et al., 2012; Sicard and Dalstein-Richier, 2015; Sicard et al., 2016). Ozone suppresses plant growth, accelerates leaf senescence, changes carbon allocation to roots, and induces nutritional imbalances in leaves (Matyssek et al., 2012; Agathokleous et al., 2015; Shi et al., 2017). Effects of elevated O_3 (eO_3) on forest ecosystems are a concern in northeast (NE) Asia (Koike et al., 2013; Akimoto et al., 2015). In China, the annual daily maximum O_3 concentration in some regions often reaches 60 nmol mol^{-1} (Gaudel et al., 2018). Recent studies have predicted that the annual mean change in surface O_3 concentrations in Asia will rise to ∼8 nmol mol^{-1} by 2050 (Lee et al., 2015; Turnock et al., 2018). The current eO_3 level is high enough to suppress tree growth and degrade ecosystem health (Chen et al., 2015; Feng et al., 2015). Thus, the conservation of forests in China is an issue of increasing interest in regions that face multiple environmental stresses, such as eO_3, nitrogen deposition, and drought (Reilly et al., 2007; Fang et al., 2014; Hu et al., 2015; Yuan et al., 2016).

Several regions of China have begun reforestation because of the intensive thinning and harvesting that has persisted since the Grain for Green Project began in 1999 (Zhang et al., 2000; Feng et al., 2005; Xu, 2011). However, in NE China, where forestry practices have been active, not all afforestation is well established cause to the soil salinization that occurs with low precipitation and high temperature (e.g., Feng et al., 2005; Sakai, 2012). Saline soil occupies ∼99,000 km^2 of China's land area (Zhang et al., 2010; Xu, 2011; Li et al., 2014). The frequency of extreme high temperatures in summer has been increasing in China over 60-fold since the 1950s (Sun et al., 2014). The relative drought conditions may increase the potential for salinization stresses (Polle and Chen, 2015). Especially in NE China, soil salinization often occurs with low precipitation and high temperature (Ma and Fu, 2006; Zhou et al., 2011; Sakai, 2012). Excess salinity causes physiological and metabolic imbalance in plants via ionic stresses (Marschner, 2012; Polle and Chen, 2015; Wungrampha et al., 2018). The effects of salinity on plants have been investigated with sodium chloride (NaCl), which are known to cause ionic imbalance and inhibit mineral ion uptake of potassium (K) and calcium (Ca) (Gerosa et al., 2014; Guidi et al., 2016; Plesa et al., 2018). Since arid and semi-arid lands contain chlorides and carbonates of several minerals, including Na, Ca, and magnesium (Mg), the severe effects of alkaline salt accumulation on plants and trees have received increased attention (Yang et al., 2008; Liu and Shi, 2010; Wang et al., 2013). For example, in the Songnen plain of Heilongjiang Province, 3.2 million ha are influenced by alkaline salt accumulation, and continues to expand by 20,000 ha per year (Wang et al., 2009). Thus, for forest conservation in NE China, we should investigate the combined stresses of eO_3 and salts on forest growth and health.

The combined effects of eO_3 and salt have largely been described in Mediterranean areas. For example, metabolic responses in pomegranate (*Punica granatum* L.) have indicated eco-physiological adaptation up to 50 mM NaCl stress, but did not mitigate O_3-induced oxidative stresses (Calzone et al., 2019). Holm oaks (*Quercus ilex* L.) treated under 150 mM NaCl treatments did not show significant photosynthetic depression by eO_3 (Guidi et al., 2016). In addition, previous studies have reported that salt stresses mitigated negative effects of eO_3 via stomatal closure (Gerosa et al., 2014), and its effects were exacerbated under salt stresses (Calzone et al., 2019), or no interaction between eO_3 and salt stresses (Guidi et al., 2016). Thus, the views of the combined effects of eO_3 and salt stresses are still inconsistent.

Larch (*Larix* sp.) has a higher tolerance to harsh conditions and is widely planted throughout northern hemisphere (Gower and Richards, 1990; Zhang et al., 2000; Ryu et al., 2009; Mao et al., 2010). For examples, Dahurian larch (*Larix gmelinii*) has a higher expectation as an afforestation species in NE China (Zhang et al., 2000; Shi et al., 2010). Japanese larch (*L. kaempferi*, JL) has been planted in the Korean peninsula and northern Japan (Lee et al., 2004; Ryu et al., 2009). The current larch forests occupy over 40 % of the total carbon growing stock in Eurasian boreal forests, including NE China (Alexeyev et al., 2000; Wang et al., 2001). Based on the Chinese policy of replantation since 1999, increased afforestation has raised concerns regarding low species diversity in forests and poor ecological functions, such as material cycling and habitat provision (Xu and Wilkes, 2004; Zhang and Zhang, 2007). Thus, the effects of eO_3 and salt should be investigated on *Larix* sp. (Zhang et al., 2000; Chazdon, 2008; Ryu et al., 2009) as well as exciting afforestation species, such as *Populus* sp.

The purpose of this study was to evaluate the effects of eO_3 and alkaline salt on Dahurian larch (DL) and Japanese larch (JL) seedlings. Koike et al. (2012) reported the O_3 suppressed photosynthesis rate of only DL but not of JL. While many studies have reported that O_3-induce inhibition can be determined by absorbed O_3 amount (Matyssek et al., 2004; Hu et al., 2015), there were no significant differences in stomatal conductance between DL and JL seedlings (Koike et al., 2012). These results indicate that O_3 sensitivity differences between these two larch species can be caused by non-stomatal factors, which may be evaluated through PSII photochemical systems (Gielen et al., 2006; Guidi et al., 2016) and the leaf nutritional status (e.g., Barnes et al., 1995; Shang et al., 2018).

We expected that the inhibitions of eO_3 and salt could be evaluated via nutrient imbalance status. It was reported that the nutrient concentrations in plants, such as N and P, were increased by eO_3, which may be adaptive strategy against eO_3 (Cao et al., 2016; Shang et al., 2018). Besides, Larch may have specific salt tolerance to the K homeostasis (Renault, 2005; Plesa et al., 2018). It was reported that NaCl treatment did not inhibit K absorption in larch saplings; rather, the saplings took up more K even with NaCl treatment compared to the control condition (Renault, 2005; Plesa et al., 2018). K homeostasis is one of the salt tolerances and it has been considered as secondary importance in many published literatures (Tester and Davenport, 2003; Marschner, 2012). There are several other mechanisms to manage excess Na contents such as the exclusion of Na and osmotic regulation by compatible solutes (Flowers, 2004; Munns et al., 2006). However, it has reported that the practical outcomes of these approaches were not effective on improving salt tolerance of plants under filed conditions (Shabala and Cuin, 2007; Wang et al., 2013; Anschütz et al., 2014).

Increasing K contents could induce the homeostasis of photosynthesis and metabolic activity, and the osmotic adjustment (Volkov et al., 2003; Shabala and Cuin, 2007). In fact, an optimal K status can be index for stress resistance when plants are exposed to abiotic stresses (Marschner, 2012; Wang et al., 2014). It was reported that a K fertilization compensated the O_3 effects on potted Norway spruce (*Picea abies*) seedlings although there were genetic-specific responses (Keller and Matyssek, 1990; Barnes et al., 1995), suggesting that the species with relatively higher K content may show insights for the O_3 tolerance. Furthermore, several studies have investigated the mineral homeostasis under eO_3 (Alcántara et al., 2006; Agathokleous et al., 2018). These studies suggest that the homeostatic adjustment in leaf element content can mitigate physiological inhibitions of eO_3 although they focused on the homeostasis of other mineral element such as iron and P.

Here, we firstly expected that (i) O_3 would suppress growth of DL but not of JL as Koike et al. (2012) reported. However, we hypothesized (ii) DL is more tolerant relative to JL since it is more adapted to salty soils due to its ecological distribution (Abaimov, 2010; Mao et al., 2010; Mamet et al., 2019), where soil salinization often occurs (Shi et al., 2010; Zhou et al., 2011), and thus salt treatment would not inhibit K absorption in DL. This comparison of salt responses between the two larches may provide novel insights on the eco-physiology to understand how larch acquires the adaptive capacity to salt stress. Further, it has reported that the reduction of K content in salt-tolerant wheat was lower than in salt-sensitive wheat at combined effect of eO_3 and salt treatment (Zheng et al., 2014). Hence, given that DL can maintain higher K contents than JL under eO_3 and salt treatment, (iii) DL may show higher tolerance to the synergic effect than JL. Based on our results, we assessed the possibility of future candidate afforestation species in northeast Asian regions.

MATERIALS AND METHODS

Study Site and Materials

Experiments were conducted at the experimental nursery of the Sapporo Experimental Forest, Hokkaido University in northern Japan (43° 04' N, 141° 20' E 15 m a. s. l.). Two-year-old Dahurian larch (*Larix gmelinii* var. *japonica*; DL) and Japanese larch (*Larix kaempferi*; JL) seedlings were cultivated from seeds in the nursery of the Hokkaido Forestry Research Organization (HRO), Forestry Research Institute in Bibai city near Sapporo. The seedlings were transplanted into 1-L pots (Height: 114 mm, top diameter: 135 mm, bottom diameter: 95 mm) in early May 2017 before buds opened. The initial stem diameter means ± standard deviations were 1.13 ± 0.23 mm for DL and 1.32 ± 0.31 mm for JL, and the height was 8.83 ± 1.35 cm for DL and 8.55 ± 1.73 cm for JL, respectively. Soils underneath the seedlings were removed just before transplantation, with well-weathered volcanic ash soil (Kanuma and Akadama soil, 1:1, v/v) used as cultivation soil in pots. To measure the original nutrient status of the soil, ∼10 g of soil and 25 ml ultrapure water were mixed and shaken for 1 h. The samples were poured through filter paper (110 mm mesh, ADVANTEC, Tokyo, Japan) and the filtrate was centrifuged at 2,000 G for 20 min. The supernatant fluid was mixed with 61% nitric acid and adjusted for the concentration of 2% nitric acid. Mineral elements contents of K, Ca, Mg, and Na were measured by ICP-MS (ELAN, DRC-e; Perkin Elmer, Waltham, MA, USA). The Na adsorption rate of this soil medium was also measured. The three levels of NaCl dissolved in demineralized water were loaded on the pot soil, which contained approximately 1,200 g of soil without seedlings, seven times during 3 weeks (110, 190, and 240 mmol Na in total). There were no leaks from the pot after each loading. After completing Na loading, the soil sample was obtained from the well-mixed and dried soil. Na content of the sample was measured by the same method described above. Na adsorption rate was calculated as the difference between total loaded Na and the water extracted Na amount. Results of the original nutrient status and the Na adsorption rate were summarized in **Supplemental Data**. Until treatments started, irrigation was manually carried out in the morning once every 3 or 4 days to avoid soil drying. Balanced liquid fertilizer (200 ml, 1/2,000, v/v, HYPONEX, Japan; 36.2 mg N L^{-1}, 142 mg P L^{-1}, 47.1 mg K L^{-1}) was applied once every week to ensure nutrient balance (four times in total).

Experimental Design

Four treatments were totally established in this study: ambient O_3 and tap water irrigation as the control (aO_3+CW), elevated O_3 and control water irrigation (eO_3+CW), ambient O_3 and salt water irrigation (aO_3+SW), and elevated O_3 and salt water irrigation (eO_3+SW), respectively. All treatments were conducted from June 27 to September 25, 2017 before the winter season. The mean temperature was 19.6°C and precipitation was 127.38 mm during the experimental period. The open top chamber (OTC; 1.2 × 1.2 × 1.2 m) system was adopted to control the O_3 concentration levels in each treatment. Seedlings were grown in OTC surrounded by a polyvinyl chloride film (Noh-bi Co. Ltd., Sapporo, Japan), such that approximately 88% sunlight could be transmitted without UVB and UVC radiation. The O_3 concentration monitored is described in **Table 1**. More detailed descriptions of the methodology of the O_3 exposure system in OTCs were provided in Sugai et al. (2019). Plants in the salt treatment were watered with 200 ml of saline water. Control plants were maintained by watering with 200 ml of tap water. The applications were performed at 3- or 4-day intervals for a total of 20 times. Mixed salt composed of alkaline salt ($NaHCO_3$) and neutral salt (NaCl) was used to imitate the realistic extant salt-alkaline soil condition of NE China (Ge and Li, 1990; Sakai, 2012). The two salts were mixed $NaHCO_3$:NaCl = 9:1 to make 20 mM Na^+ saline water. To prevent salt leaching, rainfall was excluded by plastic shelters over the top of the OTC only during rainy days. During the final experimental period when the seedlings were harvested, 10 g of fresh soil samples were taken from the surface and bottom soils in the pots of all treatments to measure soil pH. The depth of soil sampling was set at approximately 2 cm from both the surface and bottom. The soil was shaken for 1 h, with 25 ml ion-exchanged water as soon as possible after sampling. The soil pH was measured by a portable pH meter (M-12, Horiba, Japan). All treatments were replicated four times with 16 OTCs, with a split-plot completely randomized design with four seedlings in each OTC (totally 128 seedlings).

Growth, Leaf Mass Area, and Total Leaf Area Index

Sixty four seedlings for each species were harvested and washed with tap water. After washing, needles, branches, stems, and roots were separated. Each sample was oven dried at 70°C until a constant weight was achieved, and then weighed.

Mature needle leaves were sampled at the same shoot position near the crown in each seedling at the end of September 2017. Part of the needle samples was used to measure the leaf mass area

TABLE 1 | Summary of the mean concentration at ambient (aO_3) and elevated ozone (eO_3) for daytime (06:00–18:00) and over 24 h in the OTC from June to September 2017, and pH in the surface and bottom soil (~2 cm layer) of Dahurian larch (DL) and Japanese larch (JL) seedlings under all treatments: ambient O_3 and tap water irrigation (aO_3+CW) as the control, elevated O_3 and control water irrigation (eO_3+CW), ambient O_3 and salt water irrigation (aO_3+SW), and elevated O_3 and salt water irrigation (eO_3+SW) in September 2017.

		O_3 concentration (nmol mol^{-1})	
		Daytime average	**24 h average**
aO_3	June	43.99 ± 0.79	39.28 ± 0.62
	July	43.59 ± 0.82	36.99 ± 0.61
	August	40.09 ± 1.48	32.24 ± 0.94
	September	34.02 ± 1.00	27.11 ± 0.89
eO_3	June	71.91 ± 1.29	50.28 ± 1.39
	July	71.13 ± 1.12	47.38 ± 1.28
	August	70.64 ± 1.44	46.60 ± 1.62
	September	70.39 ± 1.19	46.17 ± 1.87
		Soil pH	
		Surface soil	**Bottom soil**
DL	aO_3+CW	6.37 ± 0.01	6.05 ± 0.03
	eO_3+CW	6.52 ± 0.04	6.08 ± 0.03
	aO_3+SW	7.96 ± 0.11	7.19 ± 0.01
	eO_3+SW	8.17 ± 0.13	6.93 ± 0.01
JL	aO_3+CW	6.37 ± 0.03	6.04 ± 0.04
	eO_3+CW	6.37 ± 0.02	6.11 ± 0.02
	aO_3+SW	7.92 ± 0.07	7.21 ± 0.07
	eO_3+SW	8.10 ± 0.02	7.29 ± 0.04

All values are means ± SE.

(LMA) and the other part was used to measure the contents of several nutrient elements (see below). The projected area of fresh needles was measured by an image scanner (LIDE 200, Canon, Japan). After the projection measurement, the needle dry mass was measured by the same method as above. LMA was calculated as dry weight divided by the needle area projected.

As a species difference between two studied larches, the lower needle proportion of DL than JL has been reported (Harayama et al., 2013; Dong-Gyu et al., 2015). To evaluate these differences under eO_3 and salt stress, we calculated needle dry mass divided by total dry mass as the needle ratio. While larch species have both short and long needles (Gower and Richards, 1990), the ratio of mature short needles dry mass is relatively lower than the mature long needles at a seedling stage (Powell, 1988). Based on this characteristic, we estimated the leaf area at the whole plant level as a total leaf area index (TLA) by LMA of mature needle leaves times needle dry mass per a seedling.

Maximal Photochemical Efficiency of Photosystem II

The maximal photochemical efficiency of photosystem II (F_v/F_m) was measured with a portable fluorometer (PAM-2000, Walz, Effeltrich, Germany) in September 2017. The measurement was conducted after an overnight dark adaptation to evaluate the chronic photoinhibition (Krause et al., 1995; Kitao et al., 2003). F_v/F_m was calculated with the following parameters and formula: F_0 for the steady state yields, F_m for the maximum yields measured under irradiance of approximately 5,000 μmol m^{-2} s^{-1} photon flux density for 1 s, and $F_v/F_m = (F_m\text{-}F_0)/F_m$ as defined by Schreiber et al. (1986).

Nutrition and Chlorophyll Contents in Needles

Approximately 15 mg powder samples obtained from mature needles sampled at the end of September 2017 were weighed and used to measure nitrogen (N) content with a NC analyzer (Elementar, Vario EL III, Japan). Approximately 50 mg of powder samples were weighed and digested with 2 ml of 61% nitric acid (Kanto Chemical, Tokyo, Japan) at 110°C for ~2 h. A 0.5 ml solution of hydrogen peroxide was added and the sample was heated continuously at 110°C for 20 min. After cooling to room temperature, 10 ml of 2% nitric acid were added. The concentration of K, Ca, Mg, and Na in these samples was measured by ICP-MS (ELan, DRC-e; PerkinElmer, Waltham, MA, U.S.A.). Element contents were calculated as the dry weight unit and converted as the leaf area unit by LMA.

Samples were stored at −75°C after sampling and weighing. Needles were immersed in 2 ml dimethyl sulfoxide and incubated at 65°C in the dark to extract chlorophyll (Chl). Then, the extracts were measured with a spectrophotometer (Gen spec III, Hitachi, Tokyo, Japan) with two waves; 665 nm (A_{665}) and 648 nm (A_{648}). Chl-a and Chl-b contents were calculated according to Barnes et al. (1992) and Shinano et al. (1996). The total Chl (i.e., Chl a+b) and Chl a/b were also calculated. We also obtained ratio of total Chl/needle N content (Chl/N) as an index of allocation in foliar nitrogen (Kitaoka and Koike, 2004).

Statistical Analyses

Statistical analyses were conducted using R (R Core Team, 2017). All the data of response variables were set as the four mean values per treatment, which were obtained from four seedlings per species in each chamber ($n = 4$). The effects of eO_3 and salt stress were determined by analysis of variance in each species (Two-way ANOVA). The relationships between needle Na and mineral element contents at all treatments in both species were analyzed using a generalized linear mix model (GLMM, $n = 32$). The random effect was set as the experimental unit. When species differences and their interactions were significant, correlation analysis was performed in each species ($n = 16$). Relationships between TLA and content of each element in needles were analyzed by the same GLMM. In each model, explanatory variables (= fixed effects) were set with each mineral element, species, and its interaction, whereas the response variables were the mean values at all treatments in both species. In all the linear analyses, the coefficient of determination (R^2), P-value, and the *Akaike*'s information criterion were calculated (AIC, Akaike, 1974). AIC is one of the most popular criterion for linear model identification and the optimal model is selected when AIC is minimized.

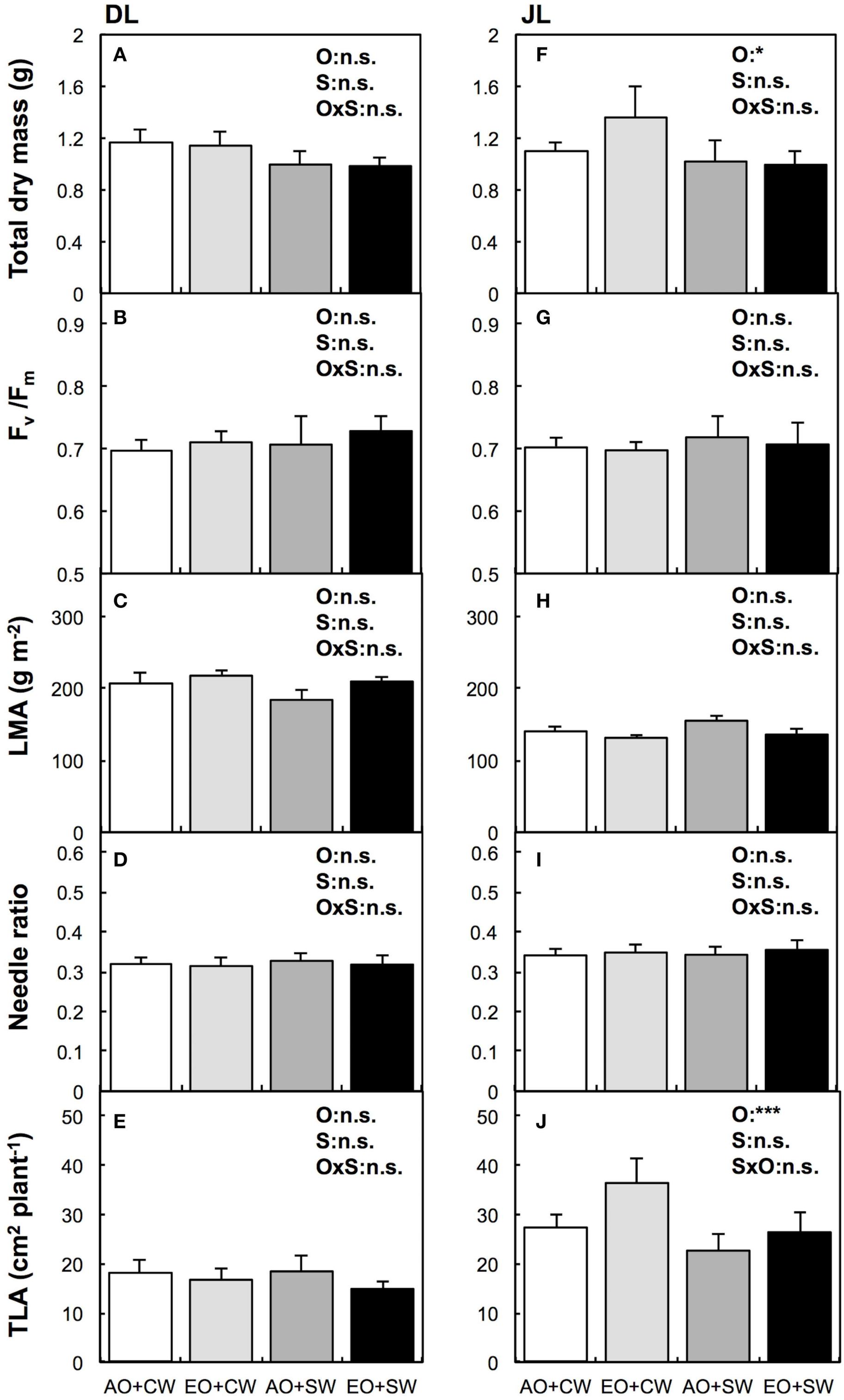

FIGURE 1 | Biometric responses to salt treatment and elevated ozone (O_3) in Dahurian larch [DL, *Larix gmelinii*, **(A–E)**] and Japanese larch [JL, *Larix kaempferi*, **(F–J)**]. White bar means ambient ozone (O_3) and control tap water (aO_3+CW), light gray bar means elevated O_3 and control tap water (eO_3+CW), dark gray bar means ambient O_3 and salt water (aO_3+SW), and black bar means elevated O_3 and salt water (eO_3+SW). The explanatory variables were set as elevated O_3 (O), salt treatment (S), and its interaction (OxS). Results of Two-way ANOVA ($n = 4$) with statistical significant difference are shown as: $^{***}P < 0.001$, $^{*}P < 0.05$, and n.s. $P \geq 0.05$. F_V/F_m, the maximal photochemical efficiency of photosystem II; LMA, leaf mass area; Needle ratio, needle dry mass to total dry mass; TLA, total leaf area index.

RESULTS

Response to Elevated O_3 and Salt Stress

No significant effects of elevated O_3 (eO_3) were observed on the total dry mass of DL. We did not observe significant inhibition of O_3 on F_v/F_m between both larch species. However, O_3 significantly increased total dry mass and TLA of only JL ($P < 0.05$, **Figure 1**). The mean value of total dry mass and TLA at eO_3 were ∼23 and 34% higher than at the ambient O_3 condition, respectively. No significant effects of O_3 were observed in other biometric (i.e., needle ratio and LMA, **Figure 1**) and biochemical parameters (i.e., element contents and chlorophyll in needles, **Table 2**).

While salt stress had also no significant effects on all biometric and physiological parameters of the two species, several element contents in needles were significantly changed (**Table 2**). Needle Na contents were significantly increased under salt stresses in both larches. In the dry mass unit, needle Na content of DL with salt treatment was approximately eight times greater than in the salt-free condition ($P < 0.05$) whereas Na of JL with salt treatment was at least 13 times greater ($P < 0.001$). Salt stress increased Chl ratio only in DL, which showed an ∼14% increase in average values ($P < 0.01$). In contrast, salt stress significantly reduced K, Ca, and Mg contents of JL. In the dry mass unit, the K, Ca, and Mg contents of DL decreased ∼17% under salt treatment ($P < 0.05$), 36% ($P < 0.001$), and 34% ($P < 0.001$), respectively. In the needle area unit, however, the increment of N content was observed in only JL ($P < 0.05$).

Relationship Between Needle Na and Other Elements

The overall relationship between Na and K contents was not significant in the larch seedlings (**Figure 2**). However, a significant relationship between Na and K contents was observed in JL ($R^2 = 0.2$, $P < 0.05$, AIC = 48.6) but not in DL ($R^2 = 0.02$, $P = 0.33$, AIC = 47.1). A significant relationship between Ca and Mg were observed in both larch species, as was a significant relationship between Na and Mg content (DL; $R^2 = 0.35$, $P < 0.01$, AIC = −10.22, JL; $R^2 = 0.23$, $P < 0.05$, AIC = −4.63). On the contrary, there were species differences in the relationship between Na and Ca content ($P < 0.05$, **Figure 3**). The coefficient value of Na on Ca content was ∼1.8 times higher in JL than DL (**Table 3**). All the relationships between Na and N contents in both and each larch species were not significant (**Figure 2**, **Table 3**).

Relationship Between TLA and Needle Mineral Elements

Table 3 shows the summary of model formulas to explain TLA by each element in needles. The best model to explain TLA of both larches determined by AIC was constructed with N ($R^2 = 0.54$, $P < 0.001$, AIC = 211). This significant relationship was also observed within each species (DL; $R^2 = 0.35$, $P < 0.01$, AIC = 94, JL; $R^2 = 0.23$, $P < 0.05$, AIC = 116) whereas the highest R^2 in model of DL was performed by K ($R^2 = 0.36$, $P < 0.01$, AIC = 94) although AIC was the same value with N (**Figure 3**). The

TABLE 2 | Summary of the biochemical needle traits; mineral element contents, total chlorophyll (Chl) contents, Chl a, Chl b, the ratio of Chl a/b, and the ratio of total Chl/needle N contents in Dahurian larch (DL) and Japanese larch (JL) seedlings at all the treatments.

Species	Factor	Treatments				Two-way ANOVA		
		aO_3+CW	eO_3+CW	aO_3+SW	eO_3+SW	O_3	Salt	O_3 × Salt
DL	Na (mg g^{-1})	0.64 ± 0.27	0.29 ± 0.10	3.13 ± 0.62	4.50 ± 1.21	n.s.	*	n.s.
	K (mg g^{-1})	4.10 ± 0.42	4.97 ± 0.54	4.09 ± 0.51	4.84 ± 0.28	n.s.	n.s.	n.s.
	Ca (mg g^{-1})	2.61 ± 0.22	2.71 ± 0.18	2.16 ± 0.05	2.07 ± 0.16	n.s.	n.s.	n.s.
	Mg (mg g^{-1})	1.45 ± 0.06	1.54 ± 0.13	1.24 ± 0.05	1.22 ± 0.10	n.s.	n.s.	n.s.
	N (mg g^{-1})	13.8 ± 0.38	13.0 ± 0.58	15.7 ± 0.55	15.6 ± 1.19	n.s.	n.s.	n.s.
	Total Chl (mg g FW^{-1})	8.75 ± 0.39	10.09 ± 1.10	9.24 ± 1.49	7.78 ± 0.97	n.s.	n.s.	n.s.
	Chl-a (mg g FW^{-1})	6.87 ± 0.29	7.83 ± 0.76	7.58 ± 1.25	6.18 ± 0.82	n.s.	n.s.	n.s.
	Chl-b (mg g FW^{-1})	1.88 ± 0.11	2.26 ± 0.36	1.67 ± 0.24	1.60 ± 0.15	n.s.	n.s.	n.s.
	Chl a/b	3.62 ± 0.16	3.60 ± 0.25	4.46 ± 0.18	3.78 ± 0.14	n.s.	**	n.s.
	Chl/N (mg mg^{-1})	0.63 ± 0.02	0.79 ± 0.11	0.59 ± 0.11	0.50 ± 0.03	n.s.	n.s.	n.s.
JL	Na (mg g^{-1})	0.28 ± 0.04	0.08 ± 0.02	3.82 ± 0.43	4.55 ± 0.49	n.s.	***	n.s.
	K (mg g^{-1})	5.05 ± 0.46	5.23 ± 0.51	3.95 ± 0.41	4.63 ± 0.66	n.s.	*	n.s.
	Ca (mg g^{-1})	3.01 ± 0.12	2.97 ± 0.22	1.89 ± 0.09	1.95 ± 0.05	n.s.	***	n.s.
	Mg (mg g^{-1})	1.58 ± 0.02	1.60 ± 0.09	1.00 ± 0.06	1.12 ± 0.09	n.s.	***	n.s.
	N (mg g^{-1})	12.5 ± 1.08	12.5 ± 1.06	14.5 ± 0.45	13.8 ± 0.98	n.s.	n.s.	n.s.
	Total Chl (mg g FW^{-1})	8.41 ± 0.68	9.21 ± 0.99	7.64 ± 0.99	8.04 ± 1.49	n.s.	n.s.	n.s.
	Chl-a (mg g FW^{-1})	6.44 ± 0.53	7.11 ± 0.75	5.95 ± 0.77	6.32 ± 1.30	n.s.	n.s.	n.s.
	Chl-b (mg g FW^{-1})	1.97 ± 0.16	2.10 ± 0.24	1.69 ± 0.25	1.72 ± 0.20	n.s.	n.s.	n.s.
	Chl a/b	3.28 ± 0.16	3.38 ± 0.05	3.61 ± 0.25	3.55 ± 0.32	n.s.	n.s.	n.s.
	Chl/N (mg mg^{-1})	0.68 ± 0.07	0.74 ± 0.02	0.52 ± 0.06	0.57 ± 0.06	n.s.	n.s.	n.s.

*All the values are shown as the mean ± SE with the results of two-way ANOVA (n = 4). Statistical significant differences are shown as: ***$P < 0.001$, **$P < 0.01$, *$P < 0.05$, and n.s., $P \geq 0.05$.*

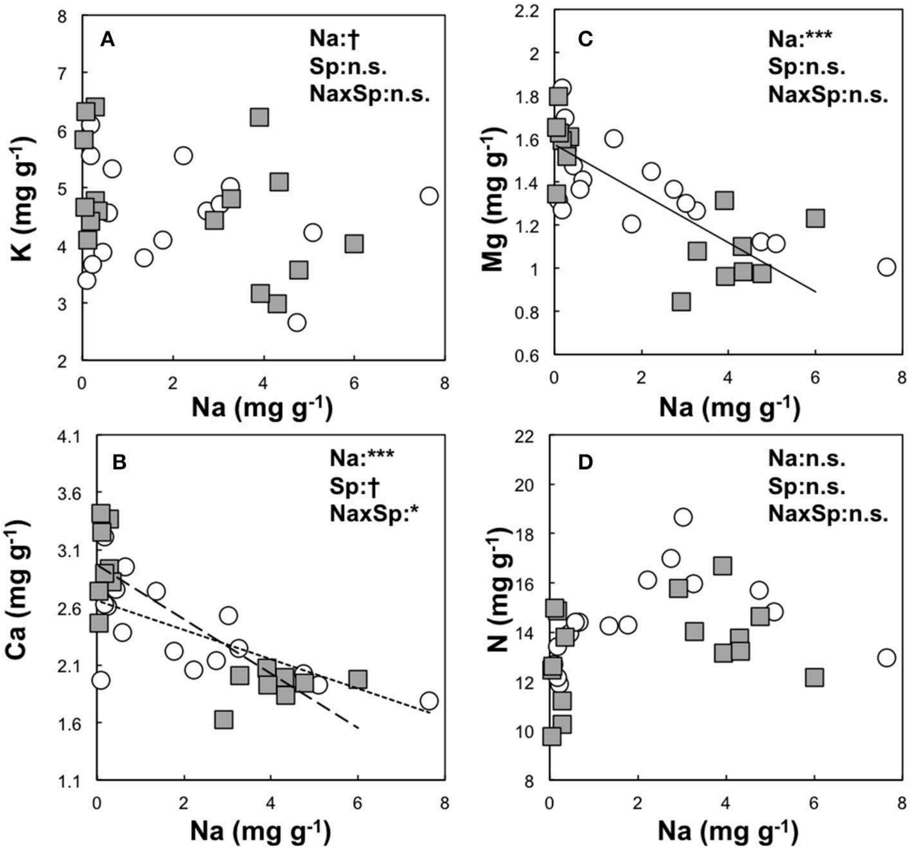

FIGURE 2 | Relationship between the needle Na content and other element contents (K and Na: **A**, Ca and Na: **B**, Mg and Na: **C**, N and Na: **D**) of mass based unit (mg g^{-1}) in Dahurian larch (DL, white circle) and Japanese larch (JL, gray square) were analyzed by GLMM with statistical significant difference are shown as: ***$P <$ 0.001, *$P < 0.05$, and n.s. $P \geq 0.05$. The explanatory variables were set as needle Na content (Na), species (Sp), and its interaction (NaxSp). The relationships between needle Na content and other element contents are shown as solid lines for both species, a fine dotted line for DL, and a heavy dotted line for JL.

second best model of both larches was constructed with K ($R^2 = 0.28$, $P < 0.01$, AIC = 225) while the third models contained almost equal R^2 and AIC values (Ca; $R^2 = 0.20$, $P < 0.01$, AIC = 229, Mg; $R^2 = 0.20$, $P < 0.01$, AIC = 229). However, no significant relationships between TLA and K, Ca, and Mg content were observed in JL (**Table 4**). Although needle Na content was significantly correlated with TLA in both larch species ($P < 0.05$), the result of GLMM showed a species difference in TLA ($P < 0.001$). When the effects of Na contents on TLA were analyzed in each species, the significant relationship was observed only in JL ($R^2 = 0.20$, $P < 0.05$, AIC = 116) but not in DL ($R^2 = 0.02$, $P = 0.28$, AIC = 101).

DISCUSSION

We evaluated initial growth of Dahurian larch (DL) and Japanese larch (JL) seedlings treated with the simulated eO_3 and alkaline salt stress. In contrast to our expectations, eO_3 did not suppress the total dry mass of both larch species. Moreover, eO_3 did not induce significant nutritional imbalance in needles even with salt stress (**Table 2**). Elevated O_3 significantly increased the dry mass of JL while we did not observe any significant inhibitions of biometric and physiological parameters, except for TLA. In fact, the similar results indicated that JL can show hormetic responses of photosynthesis rates and dry mass to mild O_3 stress (Dong-Gyu et al., 2015; Sugai et al., 2018). Since leaf quantity as well as photosynthetic capacity are related to plant growth (Poorter, 1989), the dry mass increment might be related to the TLA response (**Figure 1**).

The best factor explaining variables of TLA was needle N contents. The results of negative correlation between TLA and N contents suggests that DL originally may not produce TLA regardless of any growth conditions as relatively higher N contents per needle area, while JL may be able to adjust producing TLA as relatively lower N contents. This result suggests that the N use efficiency in forming needles may vary between the two larches, and DL may have adaptive abilities for harsh conditions, such as low temperature and limited soil nutrient availability more than JL (Gower and Richards, 1990). Koike et al. (2012) reported that the photosynthetic N use efficiency of DL was higher (over 20%) compared to JL. Instead of these higher abilities in a needle scale, DL may be inferior to adjust TLA along with abiotic environments (Abaimov, 2010; Polezhaeva et al., 2010; Mamet et al., 2019).

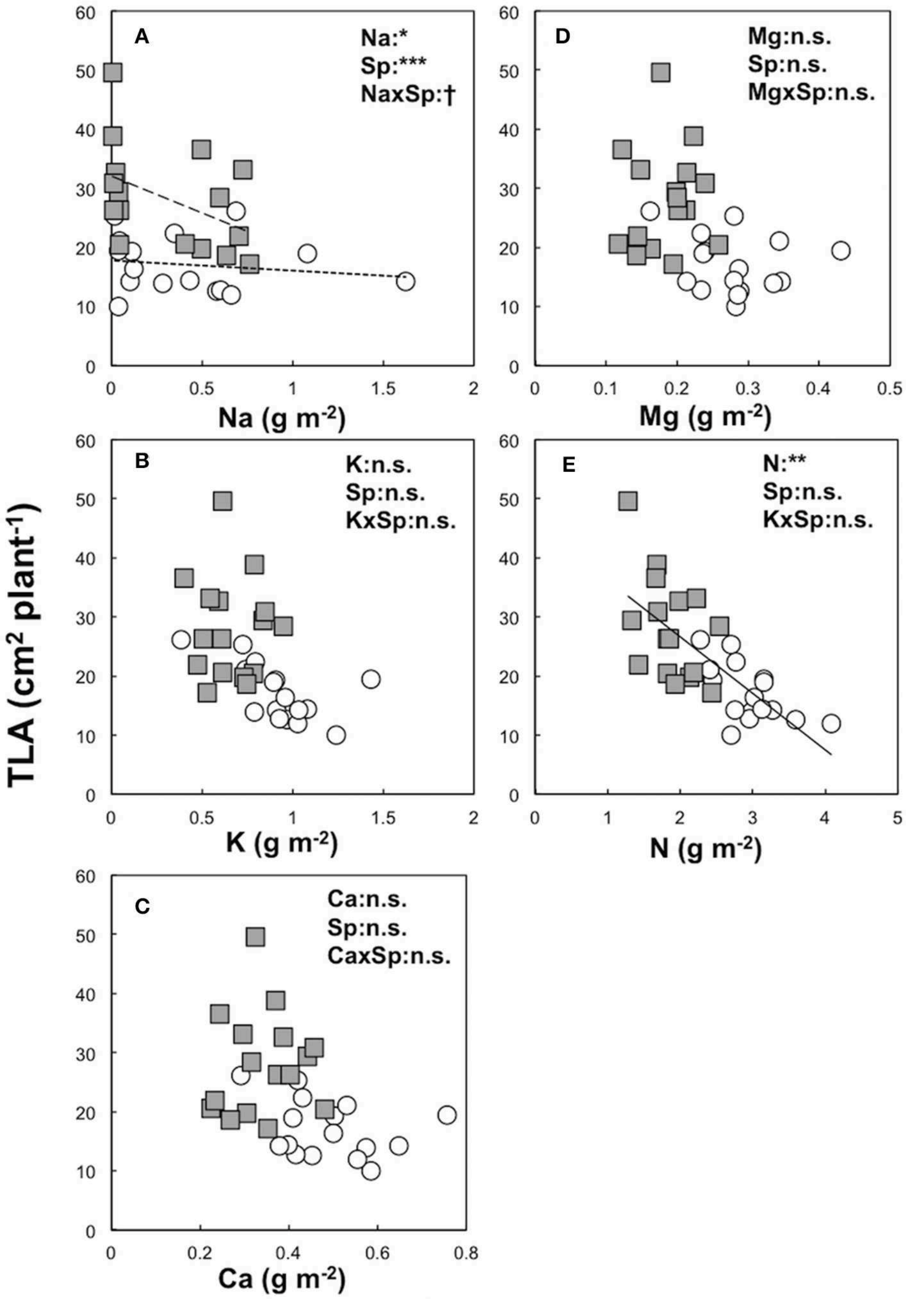

FIGURE 3 | Relationship between the total leaf area index (TLA, cm^2 plant^{-1}) and needle element contents (TLA and Na: **A**, TLA and K: **B**, TLA and Ca: **C**, TLA and Mg: **D**, TLA and N: **E**) of leaf area-based unit (g m^{-2}) in Dahurian larch (DL, white circle) and Japanese larch (JL, gray square) were analyzed by GLMM with statistical significant difference are shown as: ***$P < 0.001$, **$P < 0.01$, *$P < 0.05$, and n.s. $P \geq 0.05$. The explanatory variables were set as each needle element content, species (Sp), and its interaction. The relationships between TLA and each element content are shown as solid lines for both species, a fine dotted line for DL, and a heavy dotted line for JL.

In a previous study, 1-month-old saplings of European larch (*Larix decidua* Mill) showed a 16% lower dry mass at 150 mM NaCl compared to controls (Plesa et al., 2018). While salt treatment showed no significant suppression in any initial growth, we observed significant biochemical responses in needles (i.e., several element contents, **Table 2**). As expected, DL showed a relatively lower degree of needle Na content under salt stress compared to JL. The increased degree based on mean values was up to 3.5 times, indicating that the capacity to accumulate Na into needles may be higher in JL. Furthermore, DL showed no change in K contents under salt stress as compared with JL. High Na concentration can have negative effects on

TABLE 3 | Results of the generalized liner mixed models (GLMM) to describe the relationship between needle Na and other element contents in Dahurian larch (DL) and Japanese larch (JL).

Model formula	R^2	*P*-value	AIC
Both larch species			
K = −0.13 Na + 4.90	0.087	0.057	91.43
Ca = −0.18 Na + 2.81	0.586	<0.001	24.14
Mg = −0.09 Na + 1.54	0.577	<0.001	−17.68
N = 0.28 Na + 13.3	0.099	0.954	134.36
DL			
K = −0.05 Na + 4.61	0.015	0.326	47.05
Ca = −0.13 Na + 2.66	0.467	<0.01	11.61
Mg = −0.07 Na + 1.52	0.521	<0.001	−10.22
N = 0.27 Na + 14.0	0.107	0.891	67.51
JL			
K = −0.22 Na + 5.19	0.202	<0.05	48.63
Ca = −0.24 Na + 2.97	0.723	<0.001	13.59
Mg = −0.11 Na + 1.57	0.654	<0.001	−4.63
N = 0.30 Na + 12.7	0.118	0.904	68.89

All the values of element content were mass based unit (mg g^{-1}). R^2, the coefficient of determination; AIC, Akaike's information criterion.

TABLE 4 | Results of the generalized liner mixed models (GLMM) to describe the relationship between total leaf area (TLA, cm^2) and needle mineral element contents in Dahurian larch (DL) and Japanese larch (JL).

Model formula	R^2	*P*-value	AIC
Both larch species			
TLA = −7.31 Na + 25.3	0.097	<0.05	232
TLA = −19.9 K + 38.5	0.278	<0.01	225
TLA = −32.2 Ca + 36.0	0.196	<0.01	229
TLA = −56.5 Mg + 35.8	0.204	<0.01	229
TLA = −9.57 N + 45.8	0.535	<0.001	211
DL			
TLA = −1.71 Na + 17.8	0.024	0.282	101
TLA = −12.5 K + 28.7	0.355	<0.01	94
TLA = −13.5 Ca + 23.7	0.101	0.115	99
TLA = −15.5 Mg + 21.4	0.041	0.227	100
TLA = −6.30 N + 35.7	0.346	<0.01	94
JL			
TLA = −12.5 Na + 32.1	0.198	<0.05	116
TLA = −2.50 K + 29.8	0.002	0.435	120
TLA = 7.55 Ca + 25.6	0.005	0.600	120
TLA = 15.5 Mg + 25.3	0.005	0.607	120
TLA = −11.5 N + 49.8	0.232	<0.05	116

All the values of element content were area-based unit (g m^{-2}).

physiological functions due to the inhibition of enzyme activities and K uptakes (Marschner, 2012; Polle and Chen, 2015). K has an outstanding role in plant-water relations, contributing to the osmotic potential of cells and tissues (Marschner, 2012). Reductions of K contents under salt stress in JL, therefore, supported this competitive absorption with Na. However, the salt effect on needle K content was not significant in DL. Previous studies have also reported stable values of K of other *Larix* species (e.g., *Larix laricina* Du Roi; Renault, 2005, *L. decidua* Mill; Plesa et al., 2018). The K homeostasis can be accomplished by cation selectivity in uptake systems from the cytoplasm into vacuoles. Plesa et al. (2018) have pointed out that needle K content of *L. decidua* increased under salt treatment. Since we did not observe any increments of K contents across all treatments, future investigations should compare the specific mechanism differences of K homeostasis within the genus *Larix*.

We observed homeostasis of other mineral contents. Regression analysis showed negative correlations between needle Na and Ca, and between Na and Mg contents in both larches and each larch seedlings (**Figure 2**), while significant salt effects were only observed in JL (**Table 2**). In particular, we observed significant species differences regarding the relationship between needle Na and Ca contents, suggesting that the Na sensitivity to needle Ca contents was higher in JL than DL. Ca plays an important role in the cell membrane, cell wall stabilization, signaling functions, and the mitigation of salinity (Köster et al., 2019). These results supported our hypothesis that salt tolerance would be greater in DL, and that mineral homeostasis was related to other mineral elements apart from K. DL may obtain the adaptive capacity to salt stress as the original distribution of the species where the primary salinization is likely to occur cause to drought condition (Polezhaeva et al., 2010; Mamet et al., 2019). In contrast, JL is naturally distributed in central Japan. Species differences in adaptive traits, including salt tolerance, may be induced by the geographical isolation from other continental *Larix* species in the interglacial period (Polezhaeva et al., 2010)

While we hypothesized that the increment of N content via the synergy with K^+ uptake would be either a species specific responses or related to osmotic regulations, we did not observe significant changes in needle N content, except for the area-based value of JL (**Table 2**). However, we observed higher Chl a/b under salt stress in DL, but not in JL. In tamarack saplings (*L. laricina* Du Roi), 60 mM NaCl reduced the total Chl and the Chl a/b (Renault, 2005). However, in *L. decidua*, 150 mM NaCl reduced the total Chl, while the Chl a/b did not change (Plesa et al., 2018). A high value of Chl a/b under salt treatment was previously reported in herbaceous plants, including sunflower (*Helianthus annuus* L., Liu and Shi, 2010) and wheat (*Triticum aestivum*, Yang et al., 2008), while a lower Chl a/b was reported in poplar (*Populus alba* x *P. berolinensis*, Wang et al., 2013). Given the preferential reduction in Chl-b than Chl-a under salt stresses, it may act to protect the reaction center core more than the light harvesting capacity related to Chl-b. Future studies should continue to investigate N metabolism, with the consideration that this process may be related closely to Chl metabolic regulation (e.g., Yang et al., 2008).

Irrespective of our hypothesis, we observed no clear combined effect of eO_3 and salt stress on physiological parameters in larch seedlings (**Table 2**). Therefore, even if we employ these larch species to manage soil salinization under eO_3, their initial growth may not be suppressed by eO_3 and salinity stress. Non-significant changes of needle element contents indicated that the element variables were maintained even under the combined effect. These results suggested that eO_3 may not inhibit the element homeostasis of larch species, especially in DL. This may be attributed to non-significant changes of the total dry mass in DL treated with single O_3 and the combined effect. It was reported that the stable P and iron (Fe) contents in leaves implied homeostatic readjustment, contributing to preventing physiological inhibition of eO_3 (Agathokleous et al., 2018). It is possible that the combined effect, and even single O_3 effect, were not detected due to the physiological status of seedlings, which were shown in F_v/F_m (**Figure 1**). In all treatments, F_v/F_m showed almost the same value from 0.70 to 0.72, which were significantly lower than the standard normal value of health condition ranged between 0.81 and 0.83 (Schreiber et al., 1986).

We conclude that the effects of eO_3 and alkaline salt stress did not suppress the total dry mass of both larch species. Although we did not find any specific factors explaining species difference in O_3 sensitivities between species, TLA may be involved. Stress adaptive capacity to salt was higher in DL than JL, suggesting that salt treatment did not reduce needle K content in DL, and DL also maintained Ca and Mg contents in needles. Specifically, DL may show the greater salt tolerance to the mineral homeostatic capacity even under eO_3. Further study should evaluate the relationship between the stomatal responses and K homeostasis under eO_3 and salt stress, which may reveal how larch achieves the optimal nutrient balance for these stress resistances. Our results suggest that *L. gmelinii* seedlings may be future candidates for afforestation, even under eO_3 condition at saline soils.

DATA AVAILABILITY

All datasets generated for this study are included in the manuscript/**Supplementary Files**.

AUTHOR CONTRIBUTIONS

TS and WY were the same contribution to the planning and working. TS primarily worked on drafting and editing the manuscript with figures and tables. WY performed cultivation and measurements at the field. FS had responsible for managing the experimental fields. All other co-authors (TW, LQ, and TK) equally contributed to funding, manuscript writing, and revision.

FUNDING

This work *Ecological impacts of ozone pollution: monitoring, assessment, and mitigation* was supported by the National Key Research and Development Program of China (2017YFE0127700), JST-SICORP-No. 10 and JSPS KAKENHI Grant no. 18J2031908.

ACKNOWLEDGMENTS

We thank Dr. K. Kita of the Forestry Research Institute for providing planting stocks of three larch species seedlings. We gratefully acknowledge late Mr. K. Ichikawa and the staff of Hokkaido University Forests for planning and maintaining the free air O_3 fumigation system.

SUPPLEMENTARY MATERIAL

The Supplementary Material for this article can be found online at: https://www.frontiersin.org/articles/10.3389/ffgc.2019.00053/full#supplementary-material

REFERENCES

Abaimov, A. P. (2010). “Geographical distribution and genetics of Siberian larch species,” in *Permafrost Ecosystems*, eds A. Osawa, O. A. Zyryanova, Y. Matsuura, T, Kajimoto, and R. W. Wein (Dordrecht: Springer), 41–58.

Agathokleous, E., Kitao, M., Qingnan, C., Saitanis, C. J., Paoletti, E., Manning, W. J., et al. (2018). Effects of ozone (O_3) and ethylenediurea (EDU) on the ecological stoichiometry of a willow grown in a free-air exposure system. *Environ. Pollut.* 238, 663–676. doi: 10.1016/j.envpol.2018.03.061

Agathokleous, E., Saitanis, C. J., and Koike, T. (2015). Tropospheric O_3, the nightmare of wild plants: a review study. *J. Agric. Meteor.* 71, 142–152. doi: 10.2480/agrmet.D-14-00008

Akaike, H. (1974). “A new look at the statistical model identification,” in *Selected Papers of Hirotugu Akaike. Springer Series in Statistics (Perspectives in Statistics)*, eds E. Parzen, K. Tanabe, and G. Kitagawa (New York, NY: Springer), 215–222.

Akimoto, H., Mori, Y., Sasaki, K., Nakanishi, H., Ohizumi, T., and Itano, Y. (2015). Analysis of monitoring data of ground-level ozone in Japan for long-term trend during 1990–2010: causes of temporal and spatial variation. *Atmos. Environ.* 102, 302–310. doi: 10.1016/j.atmosenv.2014.12.001

Alcántara, E., de la Guardia, M. D., Montilla, I., and Romera, F. J. (2006). Interaction between ozone exposure and iron nutrition in two tobacco cultivars. *J. Plant. Nutr.* 29, 2245–2255. doi: 10.1080/01904160600975228

Alexeyev, V. A., Birdsey, R. A., Stakanov, V. D., and Korotkov, I. A. (2000). “Carbon storage in the Asian boreal forests of Russia,” in *Fire, Climate Change, and Carbon Cycling in the Boreal Forest,* eds S. E. Kasischke and J. B. Stocks (Springer), 239–257.

Anschütz, U., Becker, D., and Shabala, S. (2014). Going beyond nutrition: regulation of potassium homeostasis as a common denominator of plant adaptive responses o environment. *J. Plant. Physiol.* 171, 670–687. doi: 10.1016/j.jplph.2014.01.009

Barnes, J. D., Balaguer, L., Manrique, E., Elvira, S., and Davison, A. W. (1992). A reappraisal of the use of DMSO for the extraction and determination of chlorophylls a and b in lichens and higher plants. *Environ. Exp. Bot.* 32, 85–100. doi: 10.1016/0098-8472(92)90034-Y

Barnes, J. D., Pfirrmann, T., Steiner, K., Lütz, C., Busch, U., Küchenhoff, H., et al. (1995). Effects of elevated CO_2, elevated O_3 and potassium deficiency on Norway spruce [*Picea abies* (L) Karst.]: seasonal changes in photosynthesis and non-structural carbohydrate content. *Plant Cell Environ.* 18, 1345–1457. doi: 10.1111/j.1365-3040.1995.tb00195.x

Calzone, A., Podda, A., Lorenzini, G., Maserti, B. E., Carrari, E., Deleanu, E., et al. (2019). Cross-talk between physiological and biochemical adjustments by *Punica granatum* cv. Dente di cavallo mitigates the effects of salinity and ozone stress. *Sci. Total. Environ.* 656, 589–597. doi: 10.1016/j.scitotenv.2018.11.402

Cao, J., Shang, H., Chen, Z., Tian, Y., and Yu, H. (2016). Effects of elevated ozone on stoichiometry and nutrient pools of *Phoebe bournei* (Hemsl.) Yang and *Phoebe zhennan* S. Lee et FN Wei seedlings in subtropical China. *Forests* 7:78. doi: 10.3390/f7040078

Chazdon, R. L. (2008). Beyond deforestation: restoring forests and ecosystem services on degraded lands. *Science* 320, 1458–1460. doi: 10.1126/science.1155365

Chen, W., Tang, H. Z., and Zhao, H. M. (2015). Diurnal, weekly and monthly spatial variations of air pollutants and air quality of Beijing. *Atmos. Environ.* 119, 21–34. doi: 10.1016/j.atmosenv.2015.08.040

Dong-Gyu, K., Shi, C., Watanabe, M., Kita, K., Satoh, F., and Koike, T. (2015). Growth of Japanese and hybrid larch seedlings grown under free-air O_3fumigation—an initial assessment of the effects of adequate and excessive nitrogen. *J. Agr. Met.* 71, 239–244. doi: 10.2480/agrmet.D-14-00029

Fang, J. Y., Guo, Z. D., Hu, H. F., Kato, T., Muraoka, H., and Son, Y. (2014). Forest biomass carbon sinks in East Asia, with special reference to the relative contributions of forest expansion and forest growth. *Glob. Change Biol.* 20, 2019–2030. doi: 10.1111/gcb.12512

Feng, Z., Yang, Y., Zhang, Y., Zhang, P., and Li, Y. (2005). Grain-for-green policy and its impacts on grain supply in West China. *Land Use Policy* 22, 301–312. doi: 10.1016/j.landusepol.2004.05.004

Feng, Z. Z., Paoletti, E., Bytnerowicz, A., and Harmens, H. (2015). Ozone and plants. *Environ. Pollut.* 202, 215–216. doi: 10.1016/j.envpol.2015.02.004

Flowers, T. J. (2004). Improving crop salt tolerance. *J. Exp. Bot.* 55, 307–319. doi: 10.1093/jxb/erh003

Gaudel, A., Cooper, O. R., Ancellet, G., Barret, B., Boynard, A., Burrows, J. P., et al. (2018). Tropospheric Ozone Assessment Report: Present-day distribution and trends of tropospheric ozone relevant to climate and global atmospheric chemistry model evaluation. *Sci. Anthropocene* 6, 1–58. doi: 10.1525/elementa.291

Ge, Y., and Li, J. D. (1990). A preliminary study on the effects of halophytes on salt accumulation and desalination in the soil of Songnen Plain, Northeast China. *Acta. Pratacult. Sinica* 1, 70–76.

Gerosa, G., Marzuoli, R., Finco, A., Monga, R., Fusaro, I., and Faoro, F. (2014). Contrasting effects of water salinity and ozone concentration on two cultivars of durum wheat (*Triticum durum* Desf.) in Mediterranean conditions. *Environ. Pollut.* 193, 13–21. doi: 10.1016/j.envpol.2014.05.027

Gielen, B., Löw, M., Deckmyn, G., Metzger, U., Franck, F., Heerdt, C., et al. (2006). Chronic ozone exposure affects leaf senescence of adult beech trees: a chlorophyll fluorescence approach. *J. Exp. Bot.* 58, 785–795. doi: 10.1093/jxb/erl222

Gower, S. T., and Richards, J. H. (1990). Larches: deciduous conifers in an evergreen world. *BioScience* 40, 818–826. doi: 10.2307/1311484

Guidi, L., Remorini, D., Cotrozzi, L., Giordani, T., Lorenzini, G., Massai, R., et al. (2016). The harsh life of an urban tree: the effect of a single pulse of ozone in salt-stressed *Quercus ilex* saplings. *Tree Physiol.* 37, 246–260. doi: 10.1093/treephys/tpw103

Harayama, H., Ohno, Y., Uemura, A., Kitaoka, S., Utsugi, H., and Kita, K. (2013). Seasonal variations in photosynthetic properties in saplings of three *Larix* spp. *Boreal. For. Soc.* 61, 57–58. doi: 10.24494/jfsh.61.0_57

Hu, E., Gao, F., Xin, Y., Jia, H., Li, K., Hu, J., et al. (2015). Concentration-and flux-based ozone dose–response relationships for five poplar clones grown in North China. *Environ. Pollut.* 207, 21–30. doi: 10.1016/j.envpol.2015.08.034

Keller, T., and Matyssek, R. (1990). Limited compensation of ozone stress by potassium in Norway spruce. *Environ. Pollut.* 67, 1–14. doi: 10.1016/0269-7491(90)90168-C

Kitao, M., Utsugi, H., Kuramoto, S., Tabuchi, R., Fujimoto, K., and Lihpai, S. (2003). Light-dependent photosynthetic characteristics indicated by chlorophyll fluorescence in five mangrove species native to Pohnpei Island, Micronesia. *Physiol. Plant.* 117, 376–382. doi: 10.1034/j.1399-3054.2003.00042.x

Kitaoka, S., and Koike, T. (2004). Invasion of broad-leaf tree species into a larch plantation: seasonal light environment, photosynthesis and nitrogen allocation. *Physiol. Plant.* 121, 604–611. doi: 10.1111/j.1399-3054.2004.00359.x

Koike, T., Mao, Q., Inada, N., Kawaguchi, K., Hoshika, Y., Kita, K., et al. (2012). Growth and photosynthetic responses of cuttings of a hybrid larch (*Larix gmelinii* var. *japonica* x *L. kaempferi*) to elevated ozone and/or carbon dioxide. *Asian. J. Atmos. Environ.* 6, 104–110. doi: 10.5572/ajae.2012.6.2.104

Koike, T., Watanabe, M., Hoshika, Y., Kitao, M., Matsumura, H., Funada, R., et al. (2013). Effects of ozone on forest ecosystems in East and Southeast Asia. *Dev. Environ. Sci.* 13, 371–390. doi: 10.1016/B978-0-08-098349-3.00017-7

Köster, P., Wallrad, L., Edel, K. H., Faisal, M., Alatar, A. A., and Kudla, J. (2019). The battle of two ions: Ca_2^+ signalling against Na^+ stress. *Plant Bio.* 21, 39–48. doi: 10.1111/plb.12704

Krause, G. H., Virgo, A., and Winter, K. (1995). High susceptibility to photoinhibition of young leaves of tropical forest trees. *Planta* 197, 583–591. doi: 10.1007/BF00191564

Lee, D. K., Kang, H. S., and Park, Y. D. (2004). Natural restoration of deforested woodlots in South Korea. *For. Ecol. Manag.* 201, 23–32. doi: 10.1016/j.foreco.2004.06.019

Lee, J. B., Cha, J. S., Hong, S. C., Choi, J. Y., Myoung, J. S., Park, R. J., et al. (2015). Projections of summertime ozone concentration over East Asia under multiple IPCC SRES emission scenarios. *Atmos. Environ.* 106, 335–346. doi: 10.1016/j.atmosenv.2015.02.019

Li, J., Pu, L., Han, M., Zhu, M., Zhang, R., and Xiang, Y. (2014). Soil salinization research in China: advances and prospects. *J. Geographic. Sci.* 24, 943–960. doi: 10.1007/s11442-014-1130-2

Liu, J., and Shi, D. C. (2010). Photosynthesis, chlorophyll fluorescence, inorganic ion and organic acid accumulations of sunflower in responses to salt and salt-alkaline mixed stress. *Photosynthetica* 48, 127–134. doi: 10.1007/s11099-010-0017-4

Ma, Z., and Fu, C. (2006). Some evidence of drying trend over northern China from 1951 to 2004. *Chin. Sci. Bull.* 51, 2913–2925. doi: 10.1007/s11434-006-2159-0

Mamet, S. D., Brown, C. D., Trant, A. J., and Laroque, C. P. (2019). Shifting global *Larix* distributions: northern expansion and southern retraction as species respond to changing climate. *J. Biogeogr.* 46, 30–44. doi: 10.1111/jbi.13465

Mao, Q., Watanabe, M., and Koike, T. (2010). Growth characteristics of two promising tree species for afforestation, birch and larch in the northeastern part of Asia. *Eurasian J. For. Res.* 13, 69–76. Available online at: http://hdl.handle.net/2115/44672

Marschner, H. (2012). "Adaptation of plants to adverse chemical soil conditions," in *Marschner's Mineral Nutrition of Higher Plants, 3rd Edn*, ed P. Marschner (San Diego, CA: Academic Press), 455–472.

Matyssek, R., Wieser, G., Calfapietra, C., De Vries, W., Dizengremel, P., Ernst, D., et al. (2012). Forests under climate change and air pollution: gaps in understanding and future directions for research. *Environ. Pollut.* 160, 57–65. doi: 10.1016/j.envpol.2011.07.007

Matyssek, R., Wieser, G., Nunn, A. J., Kozovits, A. R., Reiter, I. M., Heerdt, C., et al. (2004). Comparison between AOT40 and ozone uptake in forest trees of different species, age and site conditions. *Atmos. Environ.* 38, 2271–2281. doi: 10.1016/j.atmosenv.2003.09.078

Munns, R., James, R. A., and Läuchli, A. (2006). Approaches toincreasing the salt tolerance of wheat and other cereals. *J. Exp. Bot.* 57, 1025–1043. doi: 10.1093/jxb/erj100

Paoletti, E., Bytnerowicz, A., Andersen, C., Augustaitis, A., Ferretti, M., Grulke, N., et al. (2007). Impacts of air pollution and climate change on forest ecosystems—emerging research needs. *ScientificWorldJournal* 7, 1–8. doi: 10.1100/tsw.2007.52

Paoletti, E., Schaub, M., Matyssek, R., Wieser, G., Augustaitis, A., Bastrup-Birk, A. M., et al. (2010). Advances of air pollution science: from forest decline to multiple-stress effects on forest ecosystem services. *Environ. Pollut.* 158, 1986–1989. doi: 10.1016/j.envpol.2009.11.023

Plesa, I., González-Orenga, S., Al Hassan, M., Sestras, A., Vicente, O., Prohens, J., et al. (2018). Effects of drought and salinity on European Larch (*Larix decidua* Mill.) seedlings. *Forests* 9:320. doi: 10.3390/f9060320

Polezhaeva, M. A., Lascoux, M., and Semerikov, V. L. (2010). Cytoplasmic DNA variation and biogeography of *Larix Mill.* in Northeast Asia. *Mol. Eco.* 19, 1239–1252. doi: 10.1111/j.1365-294X.2010.04552.x

Polle, A., and Chen, S. (2015). On the salty side of life: molecular, physiological and anatomical adaptation and acclimation of trees to extreme habitats. *Plant. Cell Environ.* 38, 1794–1816. doi: 10.1111/pce.12440

Poorter, H. (1989). Plant growth analysis: towards a synthesis of the classical and the functional approach. *Physiol. Plant.* 75, 237–244. doi: 10.1111/j.1399-3054.1989.tb06175.x

Powell, G. R. (1988). Shoot elongation, leaf demography and bud formation in relation to branch position on *Larix laricina* saplings. *Trees* 2, 150–164. doi: 10.1007/BF00196020

R Core Team (2017). *R: A Statistical Computing*. Available online at: https://www.R-project.org (accessed August 10, 2019).

Reilly, J., Paltsev, S., Felzer, B., Wang, X., Kicklighter, D., Melillo, J., et al. (2007). Global economic effects of changes in crops, pasture, and forests due to changing climate, carbon dioxide, and ozone. *Energy Policy* 35, 5370–5383. doi: 10.1016/j.enpol.2006.01.040

Renault, S. (2005). Tamarack response to salinity: effects of sodium chloride on growth and ion, pigment, and soluble carbohydrate levels. *Can. J. For. Res.* 35, 2806–2812. doi: 10.1139/x05-194

Ryu, K., Watanabe, M., Shibata, H., Takagi, K., Nomura, M., and Koike, T. (2009). Ecophysiological responses of the larch species in northern Japan to environmental changes as a base of afforestation. *Landsc. Ecol. Eng.* 5, 99–106. doi: 10.1007/s11355-009-0063-x

Sakai, Y. (2012). Approach for salt-affected soil amelioration by desulfurization of by-products in China and its future perspectives. *Bull. Soc. Sea Water Sci. Jpn.* 66, 66–73. doi: 10.11457/swsj.66.66

Schreiber, U., Schliwa, U., and Bilger, W. (1986). Continuous recording of photochemical and non-photochemical chlorophyll fluorescence quenching with a new type of modulation fluorometer. *Photosyn. Res.* 10, 51–62. doi: 10.1007/BF00024185

Shabala, S., and Cuin, T. A. (2007). Potassium transport and plant salt tolerance. *Physiol. Plant.* 133, 651–669. doi: 10.1111/j.1399-3054.2007.01008.x

Shang, B., Feng, Z., Li, P., and Calatayud, V. (2018). Elevated ozone affects C, N and P ecological stoichiometry and nutrient resorption of two poplar clones. *Environ. Pollut.* 234, 136–144. doi: 10.1016/j.envpol.2017.11.056

Shi, C., Watanabe, T., and Koike, T. (2017). Leaf stoichiometry of deciduous tree species in different soils exposed to free-air O_3 enrichment over two growing seasons. *Environ. Exp. Bot.* 138, 148–163. doi: 10.1016/j.envexpbot.2017.03.012

Shi, F., Sasa, K., and Koike, T. (2010). "Characteristics of larch forests in Daxingan mountains, Northeast China," *Permafrost Ecosystems*, eds. A. Osawa, O. A. Zyryanova, Y. Matsuura, T, Kajimoto, and R. W. Wein (Dordrecht: Springer), 367–383.

Shinano, T., Lei, T. T., Kawamukai, T., Inoue, M. T., Koike, T., and Tadano, T. (1996). Dimethyl sulfoxide method for the extraction of chlorophylls a and b from the leaves of wheat, field bean, dwarf bamboo, and oak. *Photosynthetica* 32, 409–415.

Sicard, P., Augustaitis, A., Belyazid, S., Calfapietra, C., de Marco, A., Fenn, M., et al. (2016). Global topics and novel approaches in the study of air pollution, climate change and forest ecosystems. *Environ. Pollut.* 213, 977–987. doi: 10.1016/j.envpol.2016.01.075

Sicard, P., and Dalstein-Richier, L. (2015). Health and vitality assessment of two common pine species in the context of climate change in southern Europe. *Environ. Res.* 137, 235–245. doi: 10.1016/j.envres.2014.12.025

Sugai, T., Kam, D. G., Agathokleous, E., Watanabe, M., Kita, K., and Koike, T. (2018). Growth and photosynthetic response of two larches exposed to O_3 mixing ratios ranging from preindustrial to near future. *Photosynthetica* 56, 901–910. doi: 10.1007/s11099-017-0747-7

Sugai, T., Watanabe, T., Kita, K., and Koike, T. (2019). Nitrogen loading increases the ozone sensitivity of larch seedlings with higher sensitivity to nitrogen loading. *Sci. Total. Environ.* 663, 587–595. doi: 10.1016/j.scitotenv.2019.01.292

Sun, Y., Zhang, X., Zwiers, F. W., Song, L., Wan, H., and Hu, T. (2014). Rapid increase in the risk of extreme summer heat in Eastern China. *Nat. Clim. Change* 4, 1082–1085. doi: 10.1038/nclimate2410

Tester, M., and Davenport, R. (2003). Na1tolerance and Na1transport in higher plants. *Ann. Bot.* 91, 503–527. doi: 10.1093/aob/mcg058

Turnock, S. T., Wild, O., Dentener, F. J., Davila, Y., Emmons, L. K., Flemming, J., et al. (2018). The impact of future emission policies on tropospheric ozone using a parameterized approach. *Atmos. Chem. Phys.* 18, 8953–8978. doi: 10.5194/acp-18-8953-2018

Volkov, V., Wang, B., Dominy, P. J., Fricke, W., and Amtmann, A. (2003). *Thellungiella halophila*, a salt-tolerant relative of *Arabidopsis thaliana*, possesses effective mechanisms to discriminate between potassium and sodium. *Plant. Cell Environ.* 27, 1–14. doi: 10.1046/j.0016-8025.2003.01116.x

Wang, C., Gower, S. T., Wang, Y., Zhao, H., Yan, P., and Bond-Lamberty, B. P. (2001). The influence of fire on carbon distribution and net primary production of boreal *Larix gmelinii* forests in north-eastern China. *Glob. Change Biol.* 7, 719–730. doi: 10.1046/j.1354-1013.2001.00441.x

Wang, H. M., Wang, W. J., Wang, H. Z., Wang, Y., Xu, H. N., and Zu, Y. G. (2013). Effect of inland salt-alkaline stress on C_4 enzymes, pigments, antioxidant enzymes, and photosynthesis in leaf, bark, and branch chlorenchyma of poplars. *Photosynthetica* 51, 115–126. doi: 10.1007/s11099-013-0008-3

Wang, L., Seki, K., Miyazaki, T., and Ishihama, Y. (2009). The causes of soil alkalinization in the Songnen Plain of Northeast China. *Paddy Water Environ.* 7, 259–270. doi: 10.1007/s10333-009-0166-x

Wang, M., Zheng, Q., Shen, Q., and Guo, S. (2014). The critical role of potassium in plant stress response. *Int. J. Mol. Sci.* 14, 7370–7390. doi: 10.3390/ijms14047370

Wungrampha, S., Joshi, R., Singla-Pareek, S. L., and Pareek, A. (2018). Photosynthesis and salinity: are these mutually exclusive? *Photosynthetica* 56, 366–381. doi: 10.1007/s11099-017-0763-7

Xu, J. (2011). China's new forests aren't as green as they seem. *Nat. News* 477, 371–371. doi: 10.1038/477371a

Xu, J., and Wilkes, A. (2004). Biodiversity impact analysis in northwest Yunnan, southwest China. *Biodivers. Conserv.* 13, 959–983. doi: 10.1023/B:BIOC.0000014464.80847.02

Yang, C. W., Wang, P., Li, C. Y., Shi, D. C., and Wang, D. L. (2008). Comparison of effects of salt and alkali stresses on the growth and photosynthesis of wheat. *Photosynthetica* 46, 107–114. doi: 10.1007/s11099-008-0018-8

Yuan, X., Calatayud, V., Gao, F., Fares, S., Paoletti, E., Tian, Y., et al. (2016). Interaction of drought and ozone exposure on isoprene emission from extensively cultivated poplar. *Plant. Cell Environ.* 39, 2276–2287. doi: 10.1111/pce.12798

Zhang, J. T., and Zhang, F. (2007). Diversity and composition of plant functional groups in mountain forests of the Lishan Nature Reserve, North China. *Bot. Stud.* 48, 339–348. Available online at: http://www.airitilibrary.com/Publication/alDetailedMesh?docid=1817406X-200707-48-3-339-348-a

Zhang, P., Shao, G., Zhao, G., Le Master, D. C., Parker, G. R., Dunning, J. B., et al. (2000). China's forest policy for the 21st century. *Science* 288, 2135–2136. doi: 10.1126/science.288.5474.2135

Zhang, S. W., Yang, J. C., Li, Y., Zhang, Y. Z., and Chang, L. P. (2010). Changes of saline-alkali land in Northeast China and its causes since the mid-1950s. *J. Nat. Res.* 125, 435–442. doi: 10.11849/zrzyxb.2010.03.009

Zheng, Y., Cheng, D., and Simmons, M. (2014). Ozone pollution effects on gas exchange, growth and biomass yield of salinity-treated winter wheat cultivars. *Sci. Total Environ.* 499, 18–26. doi: 10.1016/j.scitotenv.2014.08.049

Zhou, X., Zhao, P., Liu, G., and Zhou, T. (2011). Characteristics of decadal-centennial-scale changes in East Asian summer monsoon circulation and precipitation during the Medieval Warm Period and Little Ice Age and in the present day. *Chine. Sci. Bull.* 56:3003. doi: 10.1007/s11434-011-4651-4

Conflict of Interest Statement: The authors declare that the research was conducted in the absence of any commercial or financial relationships that could be construed as a potential conflict of interest.

frontiers
in Forests and Global Change

ORIGINAL RESEARCH
published: 09 April 2020
doi: 10.3389/ffgc.2020.00042

Neural Network Analysis to Evaluate Ozone Damage to Vegetation Under Different Climatic Conditions

Flavia Savi[1]*, Eiko Nemitz[2]*, Mhairi Coyle[2,3], Matt Aitkenhead[3], Kfa Frumau[4], Giacomo Gerosa[5], Angelo Finco[5], Carten Gruening[6], Ignacio Goded[6], Benjamin Loubet[7], Patrick Stella[8], Taaina Ruuskanen[9], T. Weidinger[10], L. Horvath[11,12], Terenzio Zenone[13] and Silvano Fares[1,14]*

[1] Council for Agricultural Research and Economics (CREA) – Research Centre for Forestry and Wood, Rome, Italy, [2] Centre for Ecology and Hydrology (CEH), Bush Estate, Penicuik, United Kingdom, [3] The James Hutton Institute, Aberdeen, United Kingdom, [4] Energy Research Centre of the Netherlands, Petten, Netherlands, [5] Department of Mathematics and Physics "Niccolò Tartaglia", Università Cattolica del Sacro Cuore, Brescia, Italy, [6] European Commission, Joint Research Centre, Ispra, Italy, [7] INRA, UMR INRA-AgroParisTech ECOSYS, Université Paris-Saclay, Thiverval-Grignon, France, [8] UMR SAD-APT, AgroParisTech, INRA, Université Paris-Saclay, Paris, France, [9] Institute for Atmospheric and Earth System Research/Physics, Faculty of Science, University of Helsinki, Helsinki, Finland, [10] Department of Meteorology, Eötvös Loránd University, Budapest, Hungary, [11] Hungarian Meteorological Service, Budapest, Hungary, [12] MTA-SZIE Plant Ecology Research Group, Szent István University, Gödöllõ, Hungary, [13] College of Life and Environmental Sciences, University of Exeter, Exeter, United Kingdom, [14] National Research Council, Institute for BioEconomy, Rome, Italy

OPEN ACCESS

Edited by:
Alex B. Guenther,
University of California, Irvine,
United States

Reviewed by:
Lina Fusaro,
Sapienza University of Rome, Italy
Steffen M. Noe,
Estonian University of Life Sciences,
Estonia

***Correspondence:**
Flavia Savi
flav.savi@gmail.com;
flavia.savi@crea.gov.it
Eiko Nemitz
en@ceh.ac.uk
Silvano Fares
silvano.fares@cnr.it

Specialty section:
This article was submitted to Forests and the Atmosphere, a section of the journal Frontiers in Forests and Global Change

Received: *15 January 2020*
Accepted: *20 March 2020*
Published: *09 April 2020*

Citation:
Savi F, Nemitz E, Coyle M, Aitkenhead M, Frumau K, Gerosa G, Finco A, Gruening C, Goded I, Loubet B, Stella P, Ruuskanen T, Weidinger T, Horvath L, Zenone T and Fares S (2020) Neural Network Analysis to Evaluate Ozone Damage to Vegetation Under Different Climatic Conditions.
Front. For. Glob. Change 3:42.
doi: 10.3389/ffgc.2020.00042

Tropospheric ozone (O_3) is probably the air pollutant most damaging to vegetation. Understanding how plants respond to O_3 pollution under different climate conditions is of central importance for predicting the interactions between climate change, ozone impact and vegetation. This work analyses the effect of O_3 fluxes on net ecosystem productivity (NEP), measured directly at the ecosystem level with the eddy covariance (EC) technique. The relationship was explored with artificial neural networks (ANNs), which were used to model NEP using environmental and phenological variables as inputs in addition to stomatal O_3 uptake in Spring and Summer, when O_3 pollution is expected to be highest. A sensitivity analysis allowed us to isolate the effect of O_3, visualize the shape of the O_3-NEP functional relationship and explore how climatic variables affect NEP response to O_3. This approach has been applied to eleven ecosystems covering a range of climatic areas. The analysis highlighted that O_3 effects over NEP are highly non-linear and site-specific. A significant but small NEP reduction was found during Spring in a Scottish shrubland (−0.67%), in two Italian forests (up to −1.37%) and during Summer in a Californian orange orchard (−1.25%). Although the overall seasonal effect of O_3 on NEP was not found to be negative for the other sites, with episodic O_3 detrimental effect still identified. These episodes were correlated with meteorological variables showing that O_3 damage depends on weather conditions. By identifying O_3 damage under field conditions and the environmental factors influencing to that damage, this work provides an insight into O_3 pollution, climate and weather conditions.

Keywords: net ecosystem exchange, european forest, stomatal deposition, tropospheric ozone, artificial neural networks, climate change

INTRODUCTION

Tropospheric ozone (O_3) is a harmful air pollutant which affects human health (Ainsworth et al., 2012), damages vegetation, including natural ecosystems and crops (The Royal Society, 2008), and contributes to climate change, being a greenhouse gas with a radiative forcing of 0.35–0.37 W m^{-2} (Shindell et al., 2009). It is a secondary pollutant, mainly produced through photochemical reactions of methane, carbon monoxide and volatile organic compounds in the presence of nitrogen oxides (Monks et al., 2015).

Although O_3 is a natural component of the troposphere, its concentration has been increasing since the pre-industrial era as a result of anthropogenic emission of its precursors (Ainsworth et al., 2012). Nowadays, the background O_3 mixing ratio of the northern hemisphere is 30 to 40 ppb (Parrish et al., 2012), although large regional differences are recorded due to the strong influence of weather, which promotes O_3 formation in warm, dry and sunny conditions (see **Table 2** for mean O_3 mixing ratio at our study sites).

Following chemical destruction, the second most important sink of tropospheric O_3 is the dry deposition on land surfaces, primarily controlled by vegetation, which contributes to O_3 removal through stomatal uptake, deposition onto the surface, and in-canopy chemistry (Stevenson et al., 2006). Major O_3 uptake occurs at leaf level, controlled by stomatal absorption (Cieslik, 2004; Fowler et al., 2009). Entering the leaves through stomata, O_3 sets off a chain of oxidative reactions within the apoplast, damaging cell metabolism (Wohlgemuth et al., 2002). The main detrimental effect is a reduction in carbon assimilation, which represents the first evidence of O_3 impact over vegetation, before the occurrence of visible injuries.

Manipulation experiments have been widely used to assess the impact of O_3 over vegetation carbon assimilation capacity (Karlsson et al., 2000; Manning, 2005; Gerosa et al., 2015). While this approach has been useful in understanding vegetation behavior in standard conditions and to derive dose-response functions, it may be inadequate to provide the complete picture, since plants are often exposed to unrealistic concentrations, the approach is often limited to young plants, and the experimental facilities alter the microclimate.

An ecosystem approach is thus of primary importance for understanding how O_3 pollution affects CO_2 uptake by vegetation and to assess the validity of extrapolating the effect (Sitch et al., 2007). Eddy covariance (EC) towers, from which the carbon flux is measured with a wide range of meteorological variables at high temporal resolution, provide large datasets which can be used to extrapolate information about ecosystem responses to O_3 pollution (Fares et al., 2018).

A useful tool for investigating functional relationships between site characteristics and environmental factors such as climate and other atmospheric conditions is Artificial Neural Network (ANN) modeling (Aitkenhead and Coull, 2016). ANNs are very powerful in analyzing and modeling non-linear relationships owing to their capacity to learn from examples and generalize, allowing them to explore relationships without making assumptions about the shape of these relations (such as are made by other approaches such as multiple linear regression) (Olden and Jackson, 2002; Moffat et al., 2010). Although ANNs are primarily used in the building of predictive models, methods for quantifying the independent variable contributions within networks have also been developed (Olden et al., 2004), allowing researchers to use them to understand how climate variables drive ecosystem responses (Moffat et al., 2010).

In this work, feed-forward ANNs were used to test the hypothesis that current O_3 concentration affect vegetation photosynthetic CO_2 assimilation under field condition by isolating the effect of O_3 on the net ecosystem productivity (NEP) of eleven ecosystems, characterized by different climatic condition and O_3 concentration, taking into account the influence of other NEP climatic drivers (solar radiation, air temperature, vapor pressure deficit, soil water content) and stomatal conductance. This approach is fully empirical and avoids *a priori* assumption on the functional relationships between the study variables, which are measured directly. The analysis was conducted using daytime eddy covariance (EC) data directly measured over: eight northern hemisphere open tree canopies; one moorland; one grassland and one cropland. We had the following aims: (1) to determine if current O_3 concentrations affect vegetation photosynthetic CO_2 assimilation under field condition; (2) to quantify potential CO_2 assimilation decrease due to O_3; (3) to evaluate how O_3 effects change according to other environmental factors variations. Understanding how O_3 effect over NEP is linked to environmental factors variation would help understanding vegetation behavior in the context of a changing climate.

MATERIALS AND METHODS

Study Sites

Eleven sites from three eddy covariance flux measurement networks were selected to test the effect of O_3 pollution on NEP different type of vegetation: four semi-natural forests, three planted forests, one orange orchard, one moorland, one grassland and one cropland. The study sites are spread across five different Köppen climatic areas: Oceanic (Auchencorth Moss, Grignon, Lochristi, Speulderbos), Semi-arid-Continental (Bugac), Subartic (Hyytiälä), Humid-Subtropical (Bosco Fontana, Ispra) and Mediterranean (Castelporziano, Blodgett, Lindcove). Information about site location and ecosystem type can be found in **Table 1** and a map showing the ECLAIRE site locations can be found in Fares et al. (2018).

Datasets

Data used in the development of the ANNs was recorded continuously from EC towers, at half-hour intervals, from January 2012 to December 2013 for all sites, except for: (1) Blodgett where data was collected from January 2001 to December 2007; (2) Lindcove which operated from 2009 to 2010; (3) Castelporziano for which data were collected from 2013 to 2015 and (4) Grignon, where only the dataset with rapeseed was used (31 August 2012 to 15 August 2013). Only relevant data for detecting O_3 effect over NEP were considered in the study.

TABLE 1 | Brief description of location and ecosystem type for the study sites.

Acronym	Site name	Country	Ecosystem type	Main species	Location	Network	References
Au	Auchencorth Moss	United Kingdom	Moorland	*Sphagnum, Deschampsia flexuosa*, *Eriophorum vaginatum, Juncus effusus*	55°47′33″N, 3°14′36″W	ECLAIRE	Flechard and Fowler, 1998; Helfter et al., 2015
Bu	Bugac	HU	Grassland		46°41′31″N, 19°36′06″E	ECLAIRE	Villányi et al., 2008
Gr	Grignon	FR	Crop	*Brassica napus*	48°51′N, 1°58′E	ECLAIRE	Loubet et al., 2011
Hy	Hyytiälä	FL	Boreal Scots pine forest	*Pinus sylvestris*	61°51′N, 24°17′E	ECLAIRE	Rannik et al., 2009
Sp	Speulderbos	NL	Douglas fir plantation	*Pseudotsuga menziesii*	52°15′4″N, 5°41′24″E	ECLAIRE	Erisman et al., 1997; Copeland et al., 2014
Lo	Lochristi	BG	Poplar plantation	*Populus* spp.	51°06′44″N, 3°51′ 02″E		Zenone et al., 2016
BF	Bosco Fontana	IT	Mixed forest	*Carpinus betulus, Quercus robur, Quercus cerris, Quercus rubra*	45°11′51″N, 10°44′ 31″E	ECLAIRE	Acton et al., 2016
Is	Ispra	IT	Mixed forest	*Quercus robur, Alnus glutinosa, Populus alba, Carpinus betulus*	45°45′81″N, 8°63′40″E	ECLAIRE	Jensen et al., 2018
CPZ	Castelporziano	IT	Holm oak forest	*Quercus ilex*	41°70′42″N, 12°35′72″E	ECLAIRE	Savi et al., 2016
BL	Blodgett	United States	Pine plantation	*Pinus ponderosa*	38°53′42″N, 120°37′57″W	AMERIFLUX	Fares et al., 2013
Ci	Lindcove	United States	Orange orchard	*Lindcove sinensis*	36°21′23″N, 119°5′32″W	AMERIFLUX	Fares et al., 2013

Last column indicates references where a detailed description of the sites is available.

Since damage occurs due to O_3 stomatal absorption (Reich and Amundson, 1985; Biswas et al., 2007; Broschè et al., 2010), we reduced the dataset to daytime data (10:00 – 18:00 UTC time) from the Spring and Summer seasons, when stomata are open and O_3 levels in the atmosphere are high. A summary of data used in this study is given in **Table 2**.

Although data coverage was incomplete over the measured period at each site, interpolation of large gaps was avoided in order to make sure that the functional relationships captured by ANNs were unbiased. Small gaps (less of 50% of missing data over 10:00–18:00 period in a day) were replaced by the mean of correspondent half-hour data of adjacent days (Falge et al., 2001).

Stomatal conductance to H_2O (G_{st}, m s^{-1}) was calculated as the inverse of stomatal resistance (R_s), derived from measured latent heat flux (E, kg m^{-2} s^{-1}) using the evaporative/resistance method (Monteith, 1981):

$$R_s = \frac{cp\ \ \rho\ \ (q_a - q_s(z_0))}{\gamma\ \lambda\ E} \tag{1}$$

where cp is the specific heat capacity of air (J kg^{-1} K^{-1}), ρ is the density of the dry air (kg m^{-3}) q_a is the vapor pressure at measurement height (Pa), q_s is the saturation mass fraction (Pa) of H_2O at air temperature and roughness length z_0, γ is the psychrometric constant (67 Pa K^{-1}) and λ is the vaporization heat for H_2O (2.5×10^6 J kg^{-1}).

The use of E to calculate R_s is valid only if transpiration is the only significant source of water vapor from the ecosystem and thus only data recorded during dry-daylight conditions were used. Data were discarded if they met any of the following criteria: net solar radiation <20 W m^{-2}, relative humidity > 80%, rainy days (daily rainfall > 2 mm day^{-1}) or the day after a rain event. Discarded data are mainly located when R_s is also large, hence little influence on overall dose is expected. Percentages of data discarded by this procedure are as follow: 25% for Auchencorth Moss (Au), 11% for Bugac (Bu), 24% for Grignon (Gr), 18% for Hyytiälä (Hy), 19% for Speulderbos (Sp), 31% for Lochristi (Lo), 15% for Bosco Fontana (BF), 18% for Ispra (Is), 15% for Castelporziano (CPZ), 6% for Blodgett (BL) and 11% for Lindcove (Ci).

O_3 stomatal uptake ($FO3_{sto}$, nmol m^{-2} s^{-1}) was calculated as:

$$FO3_{sto} = G_{st} * 0.61 * [O_3]_{canopy}\,, \tag{2}$$

where 0.61 is the ratio of diffusivity between O_3 and H_2O (Marrero and Mason, 1972) and $[O_3]_{\text{canopy}}$ is the O_3 concentration at the canopy level. The latter was calculated following the standard resistance analogy (Hicks et al., 1987).

TABLE 2 | Mean ± standard deviation of the data recorded during daytime (10:00 – 18:00) of Spring and Summer seasons.

Site		**NEP** $\mathbf{mmol\ m^{-2}s^{-1}}$	***St*** $\mathbf{W\ m^{-2}}$	***T*** **°C**	***vpd*** **kPa**	***swc*** **%**	$\mathbf{G_{st}}$ $\mathbf{m\ s^{-1}}$	$\mathbf{FO_{3sto}}$ $\mathbf{nmol\ m^{-2}\ s^{-1}}$	$\mathbf{[O_3]_{canopy}}$ **ppb**
Au	SP	1.61 ± 1.22	345.62 ± 161.88	7.09 ± 3.51	0.39 ± 0.16	80.30 ± 0.27	0.32 ± 0.15	−6.72 ± 3.15	34.53 ± 6.38
	S	4.60 ± 2.08	472.74 ± 193.24	16.25 ± 3.71	0.76 ± 0.35	77.46 ± 2.95	0.17 ± 0.09	−2.73 ± 1.29	27.46 ± 6.45
Bu	SP	6.22 ± 4.29	463.2 ± 276.95	19.00 ± 8.00	1.34 ± 0.77	7.94 ± 2.93	0.20 ± 0.10	−4.71 ± 2.49	38.69 ± 10.03
	S	−0.25 ± 1.44	477.68 ± 271.36	27.35 ± 5.02	2.52 ± 1.12	4.68 ± 0.54	0.04 ± 0.03	−1.05 ± 0.73	48.16 ± 14.21
Gr	SP	10.66 ± 8.03	421.20 ± 222.53	11.46 ± 5.16	0.62 ± 0.34	25.69 ± 3.65	0.29 ± 0.11	−5.77 ± 2.50	32.38 ± 8.46
	S	4.55 ± 8.46	554.58 ± 218.16	21.18 ± 4.66	1.26 ± 0.64	26.37 ± 3.17	0.21 ± 0.15	−4.16 ± 2.94	35.25 ± 12.13
Hy	SP	2.68 ± 3.26	393.11 ± 176.89	5.38 ± 7.53	0.55 ± 0.31	38.48 ± 4.00	0.13 ± 0.07	−3.10 ± 1.77	40.71 ± 5.11
	S	10.68 ± 5.02	377.21 ± 183.58	16.42 ± 3.93	0.85 ± 0.43	32.01 ± 3.88	0.26 ± 0.11	−3.85 ± 1.82	25.98 ± 9.67
Sp	SP	5.59 ± 4.86	378.06 ± 197.00	9.26 ± 5.52	0.54 ± 0.28	13.57 ± 0.94	0.14 ± 0.12	−2.41 ± 2.40	29.15 ± 9.64
	S	13.00 ± 6.72	465.47 ± 200.74	19.18 ± 3.97	0.97 ± 0.44	11.38 ± 1.10	0.22 ± 0.12	−2.74 ± 1.88	22.34 ± 11.23
Lo	SP	6.41 ± 5.76	489.82 ± 209.20	14.64 ± 3.70	0.76 ± 0.36	0.29 ± 0.03	0.20 ± 0.06	−3.94 ± 1.94	32.52 ± 11.32
	S	12.51 ± 5.65	474.82 ± 202.04	20.33 ± 3.84	1.03 ± 0.49	0.21 ± 0.09	0.34 ± 0.15	−5.60 ± 3.41	27.70 ± 13.53
BF	SP	3.59 ± 5.68	413.58 ± 185.12	17.32 ± 5.28	0.99 ± 0.51	29.46 ± 0.71	0.12 ± 0.08	−2.39 ± 1.41	36.20 ± 15.01
	S	10.07 ± 5.83	522.51 ± 152.80	27.05 ± 3.70	1.89 ± 0.62	23.42 ± 3.53	0.17 ± 0.07	−4.44 ± 2.14	46.59 ± 18.08
Is	SP	3.81 ± 7.08	511.90 ± 268.05	16.13 ± 5.44	1.06 ± 0.54	26.98 ± 4.62	0.11 ± 0.07	−1.97 ± 1.36	33.53 ± 15.99
	S	16.18 ± 7.99	619.54 ± 218.26	24.74 ± 4.12	1.75 ± 0.62	22.70 ± 4.43	0.24 ± 0.11	−4.12 ± 2.46	30.73 ± 17.27
CPZ	SP	8.78 ± 5.32	541.90 ± 248.77	17.98 ± 2.00	0.72 ± 0.28	12.27 ± 3.92	0.17 ± 0.08	−4.40 ± 2.06	44.82 ± 9.67
	S	6.27 ± 5.15	576.44 ± 236.35	25.70 ± 3.03	1.14 ± 0.43	6.12 ± 1.79	0.12 ± 0.07	−3.69 ± 2.32	49.13 ± 11.57
BL	SP	7.24 ± 4.47	558.01 ± 266.41	14.71 ± 5.26	1.04 ± 0.55	n.a.	0.18 ± 0.13	−3.94 ± 2.84	36.97 ± 9.95
	S	7.26 ± 4.71	675.20 ± 236.97	22.82 ± 4.20	1.96 ± 0.68	n.a.	0.09 ± 0.06	−2.00 ± 1.23	39.64 ± 13.88
Ci	SP	1.42 ± 3.53	616.90 ± 281.93	19.52 ± 4.20	1.44 ± 0.62	21.57 ± 2.43	0.16 ± 0.10	−3.29 ± 1.68	37.13 ± 10.59
	S	1.89 ± 3.71	676.44 ± 268.21	27.47 ± 4.95	2.70 ± 1.02	22.64 ± 4.74	0.12 ± 0.07	−3.14 ± 1.50	50.81 ± 16.01

Net ecosystem productivity (NEP), used as output in ANN modeling and data used as inputs in ANN modeling: net solar radiation (St), air temperature (T), vapor pressure deficit (vpd), soil water content (swc), stomatal conductance to H_2O (G_{st}), stomatal O_3 fluxes (FO_{3sto}) and O_3 mixing ratio at canopy level ($[O_3]_{canopy}$). Explanation of acronyms of the site names can be found in ***Table 1****.*

A detailed explanation of the calculation can be found in **Supplementary Appendix 1**.

Artificial Neural Network Modeling

Artificial neural networks (ANNs) were used to model the NEP. An ANN can be defined as a large series of simultaneous equations with each variable equivalent to a simple processing element (node) connected to each other by connection weights. Appropriate values within the connection weights provide the network with the ability to store knowledge about some modeled system. A supervised learning algorithm (i.e. with predefine input and output values within the training data) adjusts the connection weights, randomly assigned at the beginning, to approximate relationships that are present in the data.

Three ANN model runs were conducted, trained using three different groups of input variables. The three cases were used to test the hypothesis that O_3 influences NEP:

> *Case 1*. ANNs were trained using solar radiation (*St*, W m^{-2}), air temperature (*T*,°C), vapor pressure deficit (*vpd*, kPa), soil water content measured between 10 and 30 cm depth (*swc*,%, not available for BL) and stomatal conductance to H_2O (G_{st}, m s^{-1}).
>
> *Case 2*. Included all *Case 1* input variables plus O_3 stomatal uptake (FO_{3sto}, nmol m^{-2} s^{-1}). The latter was included in the analysis under the assumption that, if O_3 has a detrimental effect on vegetation (and thus on NEP), it would be caused by the O_3 entering the leaves. If O_3 absorbed through stomata affects NEP, the ANN model's ability to predict NEP would be improved.
>
> *Case 3*. consisted of *Case 1* input variables plus the O_3 dose absorbed through stomata integrated over 3 h before the measure time (FO_{3cum}, μmol s m^{-2}). This case was used to test if accumulated O_3 entering the stomata was a better predictor of NEP damage than instantaneous O_3 stomatal uptake, under the assumption that antioxidants are consumed by O_3 during the day and a longer exposition to high O_3 level reduces the leaf capacity to detoxify O_3 entering the stomata due to fast scavenging of antioxidant defense in the intercellular spaces. The 3-h interval was chosen because it was the longest interval which permitted us to not include the night-time data (i.e. at 10 am, FO_{3cum} integrated measurements between 7 am and 9 am).

In Case 1, O_3 variables were not considered so that, if the model performance was better using Case 1 rather than Case 2 or 3, O_3 had no effect on NEP.

All input variables and NEP values within the dataset were normalized by scaling between 0 and 1, to ensure that no variables had an inherently greater effect than others. The dataset was split into two subsets, Spring (from 21st of March to 20th of June) and Summer (from 21st of June to 22nd of September), and ANNs were trained separately for each subset, with the aim of highlighting the seasonal variability of the response of NEP to O_3. Feed forward ANNs with a sigmoid activation function were used.

The feed-forward ANN was made of three layers: one input layer, a single hidden layer and an output layer. In a feed-forward ANN the information flows only in a forward direction, from the input to the output through the hidden layer. Layers are composed of nodes, with nodes in adjacent layers fully interconnected by weights which are determined by a supervised learning algorithm appropriate for non-linear regression (backpropagation algorithm, Rumelhart, 1986). In this work, the hidden layer consisted of 8 nodes. The number of nodes of the hidden layer war chosen by comparing the performance of different networks, with 1 to 10 hidden nodes, and choosing the number that produced the best network performance (Gevrey et al., 2003; Olden et al., 2004).

For each group, ANN training was repeated 100 times, because different ANNs trained with the same dataset may return different connection weights, depending on the training procedure and initially randomized connection weights. A common criticism of ANN modeling is "overfitting," which is the case that ANN memorizes the training data but may fail to fit new data (Chan et al., 2006). Overfitting occurs when the model is parameterized to give the best possible fit to the training data, rather than to the "global dataset" possible from all possible examples of the system being studied. While this is a risk of all data mining or statistical regression approaches, the same solution can be applied as here: datasets were split randomly into three subsets: training (70% of dataset), test (15% of dataset) and validation (15% of dataset). The training subset was used to compute the weights of the network's nodes and the test subset for stopping the training process and checking the model generalization ability. The validation subset was used to validate the model and prove the ANN's ability to generalize beyond the training dataset.

Artificial neural network development and training was carried out using Neural Network Toolbox (Matlab 2010, Natick, MA, United States).

Performance of ANNs

One-way analysis of variance (ANOVA, confidence interval 95%) was used to determine whether there were any statistically significant differences between the means of the original measured NEP and the 100 modeled NEP values derived from ANN simulations of each case. If a statistical difference was found, a *post hoc* test was performed to detect which specific simulation differed from measured NEP, in order to discard that simulation and train the ANN again. The coefficient of determination (r^2) was used as a measure of goodness of fit, and as an indicator to evaluate if the inclusion of O_3 parameters into ANN models improved the model ability to simulate NEP, thus suggesting an effect of O_3 over NEP.

Artificial neural network model was compared with a linear statistical approach, Multiple Linear Regression (MLR). MLR model is used to explore the relationship between a dependent variable and independent variables, under the assumption that each independent variable has a linear relationship with the dependent variable (Civelekoglu et al., 2008). In this work, MLR was used to model the linear relationship between NEP and the three groups of input variables (case 1, case 2 and case 3, see above) which were the same input variables of ANN modeling. The MLR r^2 was calculated and compared with ANN r^2, in order to evaluate if the ANN approach better performed than the linear approach in predicting NEP behavior.

Analysis Tools for Quantifying O_3 Contributions as NEP Driver in ANN Modeling

The integrated information gathered from ANNs can be decomposed to disentangle the effects of different inputs on the output values, to improve understanding of how each input variable affects the predictions. Gevrey et al. (2003) and Olden et al. (2004) provided a comparison of the different existing methods for estimating variables importance in ANN applications. In this work, the partial derivative method (Dimopoulos et al., 1995) was used to isolate the effect of O_3 over NEP estimated by ANN modeling.

The partial derivative method produces a profile of the output variations for unit change of selected input variable. The link between the modification of the input, x_j, and the variation of the output, $y_j = f(x_j)$, is the partial derivative of each activation function with respect to its input (d_j), with $j = 1,\ldots,N$ and N the total number of observations.

Given an ANN with n inputs i ($i = 1,\ldots,n$), one hidden layer with m_h nodes h ($h = 1,\ldots,m_h$) where the logistic sigmoid function is used for activation, the partial derivative of y_j with respect to x_i is d_{ji} (Dimopoulos et al., 1999; Gevrey et al., 2003):

$$d_{ji} = S_j * \sum_{h=1}^{m_h} w_{ho} * I_{hj} \left(1 - I_{hj}\right) * w_{ih} \tag{3}$$

where S_j is the derivative of the output with respect to its input, I_{hj} is the response of the h hidden node, w_{ho} is the weight between the output node and h, w_{ih} is the weight between h and the input node (n_i).

Partial derivatives were calculated for each of the ANN runs and averaged to calculate the mean absolute change of NEP associated with O_3. To get information about positive and negative change of NEP, positive and negative fraction of the partial derivatives were averaged separately (Moffat et al., 2010).

The weather influence on O_3 down-regulating effect was tested using Spearman partial correlation. This is a non-parametric measure of rank correlation that assesses monotonic relationships of two variables whilst controlling for other, potentially confounding variables. The negative fraction of partial derivative associated with O_3 (FO_{3st} or FO_{3cum}) was correlated with environmental factors such as solar radiation, air temperature, vapor pressure deficit, soil water content and O_3 concentration at canopy level. The latter was included in the analysis with the aim of controlling the confounding effect it may have on correlation coefficients, since O_3 concentration strongly depends on weather (Monks et al., 2015). All environmental factors were transformed between 0 and 1 to avoid scale effects.

TABLE 3 | Mean r^2 ± standard deviation of the 100 ANN simulations trained with Spring and Summer data.

Site	r^2						# of observation	
	Case 1		Case 2		Case 3			
	Spring	Summer	Spring	Summer	Spring	Summer	Spring	Summer
Au	0.77 ± 0.00	**0.76 ± 0.00**	**0.78 ± 0.00**	0.76 ± 0.00	0.78 ± 0.00	0.76 ± 0.00	311	340
Bu	0.91 ± 0.00	0.48 ± 0.00	**0.92 ± 0.00**	0.51 ± 0.01	0.92 ± 0.00	**0.52 ± 0.01**	662	1197
Gr	**0.94 ± 0.00**	0.85 ± 0.00	0.94 ± 0.00	**0.86 ± 0.00**	0.94 ± 0.00	0.85 ± 0.00	1262	2274
Hy	**0.93 ± 0.00**	**0.77 ± 0.00**	0.93 ± 0.00	0.76 ± 0.00	0.93 ± 0.00	0.77 ± 0.00	368	705
Sp	0.64 ± 0.00	0.54 ± 0.00	0.63 ± 0.01	0.53 ± 0.00	**0.66 ± 0.00**	**0.57 ± 0.00**	359	950
Lo	**0.87 ± 0.00**	0.55 ± 0.00	0.87 ± 0.00	**0.57 ± 0.00**	0.84 ± 0.00	0.57 ± 0.00	342	736
BF	0.68 ± 0.00	0.36 ± 0.00	0.7 ± 0.00	0.37 ± 0.00	**0.71 ± 0.00**	**0.4 ± 0.00**	404	1265
Is	0.51 ± 0.00	**0.5 ± 0.00**	0.51 ± 0.00	0.5 ± 0.00	**0.52 ± 0.00**	0.5 ± 0.00	600	2315
CPZ	0.54 ± 0.00	0.49 ± 0.00	**0.55 ± 0.00**	**0.5 ± 0.00**	0.55 ± 0.00	0.5 ± 0.00	816	2545
BL	0.36 ± 0.00	**0.52 ± 0.00**	0.36 ± 0.00	0.52 ± 0.00	**0.39 ± 0.00**	0.52 ± 0.00	3341	10509
Ci	0.41 ± 0.00	0.52 ± 0.00	0.41 ± 0.00	**0.53 ± 0.00**	**0.43 ± 0.00**	0.53 ± 0.00	953	1581

*Case 1: Artificial neural networks were trained using solar radiation (W m^{-2}), air temperature (°C), vapor pressure deficit (vpd, kPa), soil water content measured between 10 and 30 cm depth (swc,%, not available for BL) and stomatal conductance to H_2O (Gst, m s^{-1}). Case 2: Included all Case 1 input variables plus O_3 stomatal uptake (FO_3sto, nmol m^{-2} s^{-1}). Case 3: consisted of Case 1 input variables plus O_3 dose absorbed through stomata during 3 h before the measurement time. Last column reports the number of half-hour measurements available for the analysis at each site. Bold numbers indicate the case with the highest r^2. Explanation of acronyms of the site names can be found in **Table 1**.*

RESULTS

Performance of ANNs

The ANOVA test highlighted that there are no statistically significant differences between the means of the original measured NEP and the 100 modeled NEP derived from ANN simulations (confidence interval 95%). The r^2 values (**Table 3**) attested the data mining capability of the ANNs: the best performances were obtained for the northern sites, especially Grignon and Hyytiälä (0.93 and 0.94, respectively), while the lowest r^2 values were from the Blodgett and Bosco Fontana sites (0.39 and 0.40, respectively).

Multiple linear regression modeling produced poorer r^2 values (**Table 4**) in comparison to ANN modeling (**Table 3**) in every single case. MLR modeling r^2 are on average 0,16 ± 0,06 points lower that ANN r^2.

TABLE 4 | r^2 derived from MLR modeling of NEP calculated separately for Spring and Summer from three combination of independent variables: Case 1: solar radiation (W m^{-2}), air temperature (°C), vapor pressure deficit (*vpd*, kPa), soil water content measured between 10 and 30 cm depth (*swc*,%, not available for BL) and stomatal conductance to H_2O (Gst, m s^{-1}).

Site	r^2					
	Case 1		Case 2		Case 3	
	Spring	Summer	Spring	Summer	Spring	Summer
Au	0.62	0.49	0.62	0.49	0.62	0.49
Bu	0.84	0.21	0.84	0.22	0.84	0.21
Gr	0.81	0.64	0.81	0.64	0.81	0.64
Hy	0.76	0.64	0.76	0.64	0.76	0.64
Sp	0.42	0.35	0.42	0.35	0.44	0.37
Lo	0.77	0.36	0.77	0.37	0.78	0.37
BF	0.54	0.20	0.54	0.21	0.53	0.22
Is	0.34	0.43	0.34	0.43	0.34	0.43
CPZ	0.36	0.36	0.36	0.37	0.36	0.36
BL	0.17	0.41	0.17	0.41	0.17	0.42
Ci	0.29	0.46	0.29	0.46	0.29	0.46

*Case 2: Included all Case 1 input variables plus O_3 stomatal uptake (FO_3sto, nmol m^{-2} s^{-1}). Case 3: consisted of Case 1 input variables plus O_3 dose absorbed through stomata during 3 h before the measurement time. Half-hour measurements available for the analysis at each site are the same as in **Table 3**. Explanation of acronyms of the site names can be found in **Table 1**.*

Do Current O_3 Levels Affect NEP?

The inclusion of O_3 stomatal uptake in the ANN simulation did not change ANN performance (i.e. no impact of O_3) in some cases, and in others it improved the ANN performance (i.e. O_3 had an impact). In particular, the results suggest that O_3 damage does not occur in most of the northern sites which are less exposed to O_3 pollution, while in the other ecosystems a limited effect was observed.

Artificial neural networks trained with Spring data (**Table 3**) showed no O_3 effect on NEP for Hyytiälä, Grignon and Lochristi sites, where the *Case 1* model run returned the highest r^2. For the same period, we detected an effect of O_3 on NEP for Auchencorth Moss, Bugac and Castelporziano sites, where the inclusion of O_3 stomatal flux in the model (*Case 2*) resulted in an r^2 increase compared with the *Case 1* model. For Speulderbos, Bosco Fontana, Ispra, Blodgett and Lindcove the best ANN performance was achieved for *Case 3,* (inclusion in the model of 3-h O_3 dose), indicating that the preceding O_3 dose to which vegetation is exposed is the best predictor of O_3 effects over NEP for these sites.

Different results were achieved by training the ANNs with Summer data (**Table 3**). No O_3 effect was found for Hyytiälä,

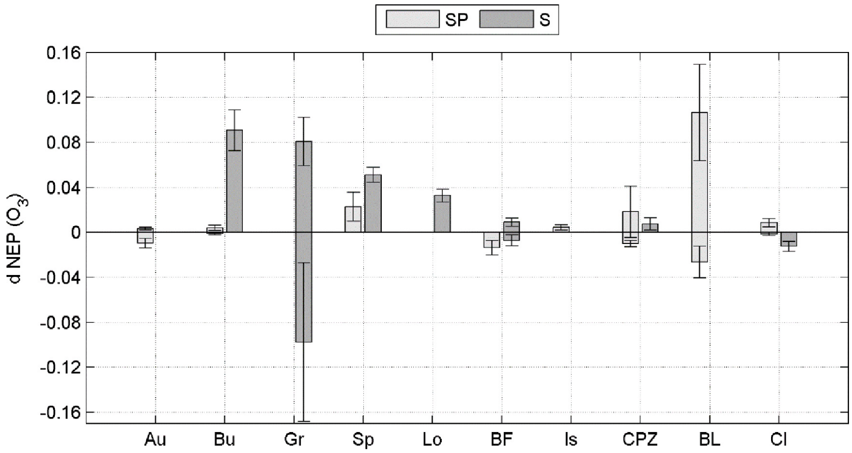

FIGURE 1 | Positive and negative sensitivity of the NEP response to FO_{3st} or FO_{3CUM} (d NEP (O_3), presented separately for Spring (SP) and Summer (S) seasons. Bars represent standard deviations.

Auchencorth Moss, Ispra and Blodgett, while an O_3 effect was detected for Grignon, Lochristi, Castelporziano and Lindcove, where the instantaneous stomatal O_3 flux was the better predictor for the O_3 effect on NEP. For Bugac, Speulderbos and Bosco Fontana, the cumulative O_3 dose was the best predictor.

Since the 3-h O_3 dose was calculated from cumulated instantaneous O_3 stomatal fluxes, r^2 between the two parameters was calculated at each site to verify the degree of independence of the two variables. They were shown to be fully independent (r^2 = 0.00) for Lindcove, Blodgett, Castelporziano, Bosco Fontana, Speulderbos and Hyytiälä. An r^2 value of 0.00 was also found for Auchencorth Moss and Ispra in Summer, while in Spring r^2 were 0.10 and 0.25, respectively. Higher r^2 were found for Grignon (0.45 and 0.73 for Spring and Summer, respectively), Bugac (0.37 and 0.42 for Spring and Summer, respectively), and Lochristi (0.25 and 0.48 for Spring and Summer, respectively).

Assessing the Sensitivity of NEP to Current O_3 Levels

Partial derivatives represent NEP rate of change with respect to O_3 (FO_{3st} or FO_{3cum}). If this rate is negative, then the NEP will tend to decrease as FO_{3st} or FO_{3cum} increases while if the rate is positive, NEP will tend to increase. Partial derivatives were calculated for each half hour observation. Partial derivatives calculated with respect to one predictor can be positive for some half hours and negative for other half hours. This means that a predictor has not always a positive or negative effect on NEP, and that it depends on the combination of all ANN predictors values occurring at that time.

Averaging separately positive and negative partial derivatives helps to discern when O_3 has a negative effect over NEP. **Figure 1** shows that, although the O_3 variables were significant factors for predicting NEP in the ANN model runs, they did not always lead to a reduction in NEP. Reduction of NEP related to O_3 was detected at Auchencorth Moss, Bugac, Grignon, Bosco Fontana, Castelporziano, Blodgett and Lindcove in Spring, Grignon, Bosco Fontana and Lindcove in Summer (**Figure 1**), with values ranging from 0.15 to 2.64% average NEP loss due to O_3 (**Table 5**).

In a few cases the response is only negative, indicating that current O_3 concentration level consistently reduces NEP during Spring or Summer, for all combinations of the other predictors. This is the case of Bosco Fontana in Spring and Lindcove in Summer. In other cases, the ANN did not always determine O_3 to be a damaging factor for NEP. To highlight how the rate of change of NEP responds to different levels of O_3 entering the stomata, a profile of the NEP partial derivative versus O_3 input (FO_{3st} or FO_{3cum} depending on the case) was plotted (**Figures 2**, **3**).

The relationships shown in **Figures 2**, **3** are highly non-linear and present different behaviors at each site: at Auchencorth Moss site (**Figure 2A**) a down-regulating effect was found in Spring for FO_{3sto} below the 40th percentile (−0.27 nmol m^2 s^{-1}), peaking around 23rd percentile (−0.20 nmol m^2 s^{-1}). The same trend was observed at the Castelporziano site (**Figure 2C**) during Spring, where FO_{3sto} below the 33rd percentile (−0.13 nmol m^2 s^{-1}) negatively affected NEP. At the Bugac site (**Figure 2B**), the FO_{3sto} effect on NEP was almost linear, and the effect turned negative above the 52nd percentile (−0.19 nmol m^2 s^{-1}). At the Blodgett site, during Spring (**Figure 2E**), FO_{3cum} negatively affected NEP in a range between 29th (68.33 μmol m^{-2}) and 49th (91.23 μmol m^{-2} percentile, peaking at the 40th (80.67 μmol m^{-2}) percentile.

At the Bosco Fontana site the ANN analysis predicted a consistently negative effect of FO_{3cum} flux for the Spring data (**Figure 2D**), although the largest effect was recorded for the smallest doses (below 20th percentile, 43.68 μmol m^{-2}). During Summer (**Figure 3C**), a depressing effect of FO_{3cum} over NEP was observed only below the 26th percentile (70.72 μmol m^{-2}). At the Lindcove site, during Spring (**Figure 2F**), only low doses of FO_{3cum} had a negative effect on NEP (below 7th, 45.42 μmol m^{-2}, and above 95th percentile, 151.02 μmol m^{-2}), whilst during Summer (**Figure 3A**), all FO_{3st} values induced a decrease in NEP, peaking at 88th percentile (0.19 nmol m^{-2} s^{-1}). At the Grignon site, the

TABLE 5 | Average NEP loss due to O_3 in Spring and Summer seasons. Explanation of acronyms of the site names can be found in **Table 1**.

Site	**Average NEP loss due to O_3 (%)**	
	Spring	**Summer**
Au	0.97 ± 0.04	0
Bu	0.12 ± 0.09	0
Gr	0	0.1 ± 7.03
Hy	0	0
Sp	0	0
Lo	0	0
BF	1.37 ± 0.65	0.72 ± 0.49
Is	0	0
CPZ	1.02 ± 0.27	0
BL	2.64 ± 1.39	0
Ci	0.15 ± 0.16	1.25 ± 0.44

FO_{3st} effect on NEP during Summer seemed to fluctuate, peaking at 48th and 82st percentiles (nmol m^{-2} s^{-1} and nmol m^{-2} s^{-1}, respectively).

The negative fraction of dNEP(O_3) was transformed between 0 and 1 (where 1 is the maximum negative effect of O_3 over NEP) and averaged as a function of time of day. This was done with the aim of identifying diurnal dynamics in the NEP decrease due to O_3 (**Figures 4**, **5**). During the Spring season, the average dNEP(O_3) followed a pronounced bell-shape curve at the Lindcove site, where the maximum effect of O_3 was observed during the middle hours of the day, coinciding with FO_{3cum} peak (**Figure 4F**). The same pattern was found for Bugac (**Figure 4B**) sites, although the bell-shape was slightly accentuated. At Auchencorth (**Figure 4A**) and Castelporziano (**Figure 4C**) larger effects of FO_{3st} were recorded at the end of the afternoon. The damaging effect of instantaneous O_3 followed an exponential decrease during the day at Bosco Fontana site (**Figure 4D**), opposite to the shape of the response to FO_{3cum}. The damaging effect of O_3 peaked at 10:00 h, when FO_{3cum} was still low. At Blodgett (**Figure 4E**) no significant variations were found during the day.

For the Summer season, average dNEP(O_3) showed a bell-shape curve which follows the FO_{3st} trend at Grignon and Lindcove (**Figures 5A,B**, respectively), while at Bosco Fontana (**Figure 5C**) the dNEP (FO_{3cum}) presents the same pattern as during the Spring season.

How O_3 Reduces NEP According to Other Environmental Factors

For the sites where a negative effect of O_3 over NEP was found (Au, Bu, Gr, BF, CPZ, Bl and Ci), the correlation between the negative fraction of dNEP(FO_{3st}) or dNEP(FO_{3cum}) and the other environmental variables was tested through Spearman partial correlation (**Table 6**).

No correlation was found for Auchencorth Moss, where no values were statistically significant. Solar radiation enhanced O_3 detrimental effect at Bugac, Bosco Fontana and Blodgett during Spring and at Lindcove during Summer, while it had the opposite effect at Castelporziano during Spring and at Bosco Fontana during Summer. The correlation between air temperature and dNEP(O_3) was significant only at Blodgett, where air temperature decreased O_3 damage during Spring. The increase of *vpd* depressed O_3 damage at Bosco Fontana and Castelporziano during Spring, and at Lindcove during Summer. Increasing *swc* reduced O_3 damage at Bugac and Bosco Fontana during Spring, and increased O_3 damage at Lindcove during both Spring and Summer. The O_3 concentration at canopy level increased O_3 damage at Bugac, Grignon, Blodgett and Lindcove whilst it had an opposite effect on Castelporziano and Bosco Fontana vegetation.

DISCUSSION

How O_3 pollution alters vegetation carbon sequestration capacity is considered an important component of global change (Ashmore and Bell, 1991), but few studies have quantified its impact over ecosystems. Some of them confirm a detrimental effect of O_3 over vegetation occurring in sites where ambient O_3 concentrations are typically high (Zapletal et al., 2011; Fares et al., 2013), while others did not find any effect of high levels of tropospheric ozone concentrations (Zona et al., 2014; Verryckt et al., 2017). Results of these studies are difficult to interpret in the context of ozone/plant interactions because of the great variability among site characteristics, vegetation type and methodological approaches (Cailleret et al., 2018).

This work demonstrates that ANN modeling is a useful tool to understand O_3 – NEP correlation considering other co-varying environmental factors. r^2 values produced by ANN were found higher than r^2 values produced by MLR, indicating that a non-linear statistical data modeling approach as ANN is more appropriate in modeling complex relationships such the dependence of NEP from co-varying environmental factors. Our results are in line with other ecological studies in literature which compared the two methods and found ANN models more accurate than MLR (e.g. Lek et al., 1996; Paruelo and Tomasel, 1997; Brion et al., 2005). The strength of ANN lies in its fully inductive approach, which allows multidimensional relationships to be investigated without *a priori* knowledge of the shape of these relations. Coupling ANN analysis with EC provided a picture of the current status of O_3 pollution effects over ecosystems.

Although overfitting was controlled in this work, high r^2 values calculated between simulations and measured data (**Table 3**) indicates that the possibility of overfitting from ANN exists.

We did not carry out an assessment of whether the model accuracy was significantly better for the training or test subsets than for the final validation subset in each case, and so cannot provide an indication of whether or not the model was actually overfitted to the training data. However, in this work, the power and flexibility of ANN in fitting the data is an advantage and not a limitation, indeed the aim was not to find a general model for NEP, but to evaluate the influence of a variable (O_3) in each single study site.

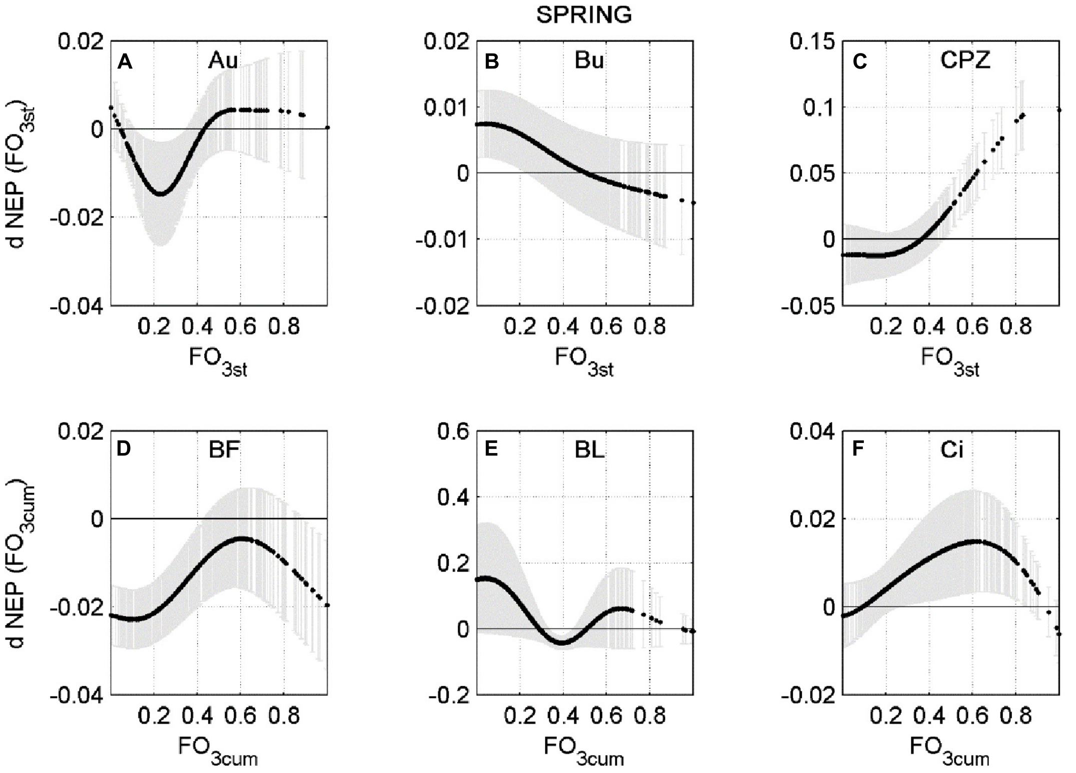

FIGURE 2 | Averaged partial derivative of NEP (dNEP) with respect to the corresponding input variable (FO_{3st} or FO_{3CUM}) ± standard deviation, calculated using Spring data. **(A)** Auchencorth Moss (Au), **(B)** Bugac (Bu), **(C)** Castelporziano (CPZ), **(D)** Bosco Fontana (BF), **(E)** Blodgett (BL), **(F)** Lindcove (Ci).

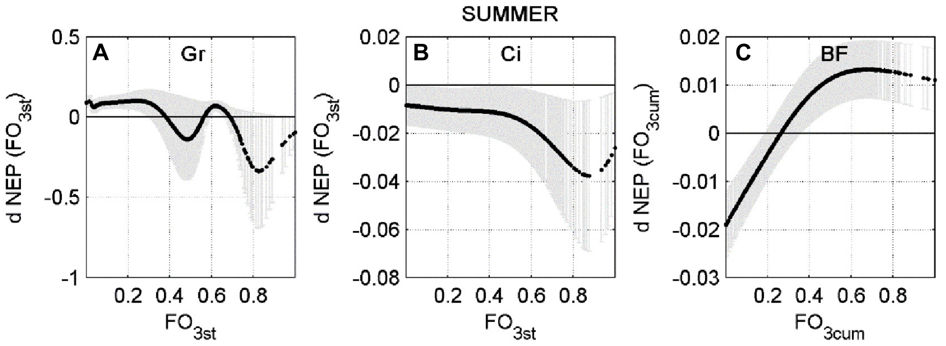

FIGURE 3 | Average partial derivative of NEP (dNEP) with respect to the corresponding input variable (FO_{3st} or FO_{3CUM}) ± standard deviation, calculated using Summer data. **(A)** Grignon (Gr), **(B)** Lindcove (Ci), **(C)** Bosco Fontana (BF).

Artificial neural network performance analysis found that both FO_{3st} and FO_{3cum} are suitable indicators for predicting NEP reduction, depending on season and type of vegetation. Since FO_{3cum} is obtained from cumulated values of FO_{3st}, an analysis of correlation between the two variables was performed with the aims of verifying the degree of dependence of the two variables. None or low correlation was found for most of the study sites. That may suggest that the O_3 dose entering the stomata is discontinuous and that vegetation is subjected to O_3 pulses rather than a constant flux. However, we did not find any relation between the degree of correlation between the two variables and the selection of ANN model best predictor, which means that the most suitable predictor was selected for each site and season regardless of how discontinuous the O_3 fluxes were, and it probably depends on vegetation type and climate conditions.

Of the eleven sites tested, four ecosystems were free from O_3 damage. These sites were the Finnish Scots pine forest (Hyytiälä), the Dutch Douglas fir plantation (Speulderbos), the Belgian poplar plantation (Lochristi) and the Italian

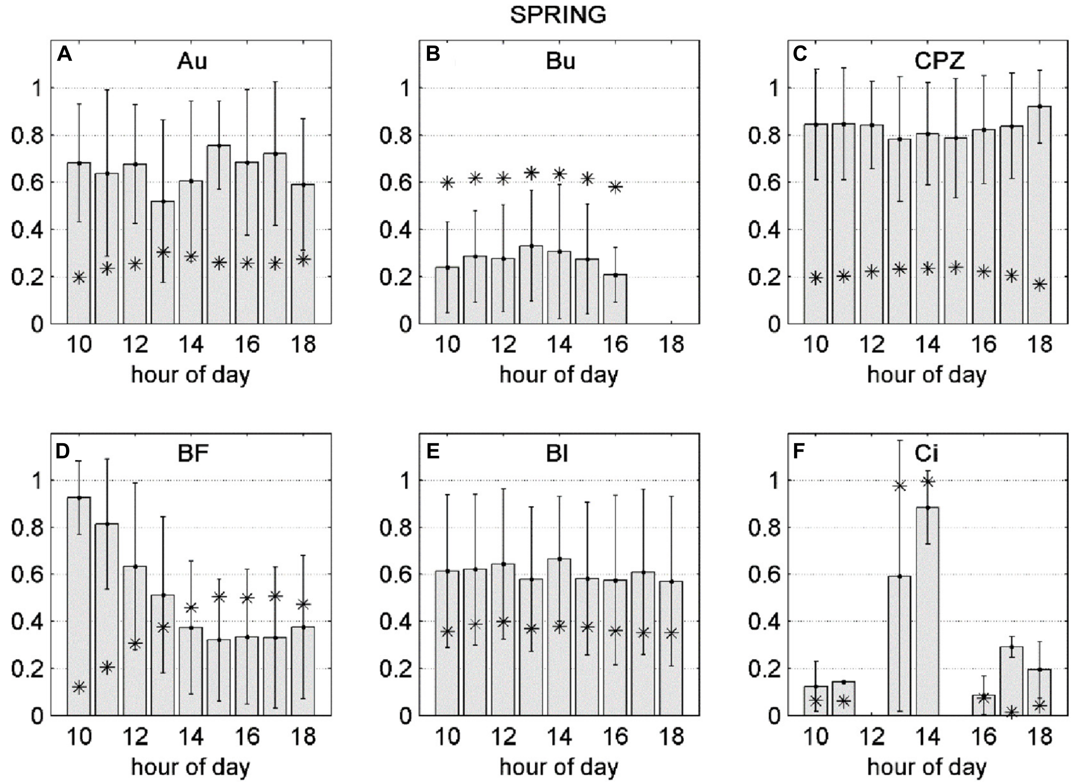

FIGURE 4 | Gray bars: negative fraction of partial derivative of NEP with respect to FO_{3st} **(A–C)** or FO_{3CUM} **(D–F)** averaged over hours of day, ± standard deviations. Asterisks: FO_{3st} **(A–C)** or FO_{3CUM} **(D–F)** averaged over hours of day. All variables presented in this figure were transformed between 0 and 1.

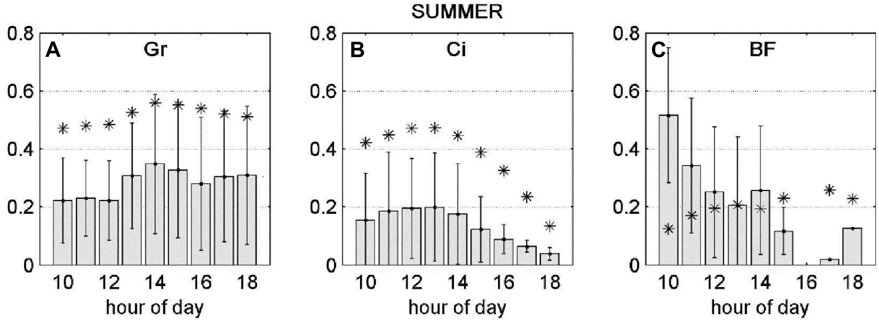

FIGURE 5 | Gray bars: negative fraction of partial derivative of NEP with respect to FO_{3st} **(A,B)** or FO_{3CUM} **(C)** averaged over hours of day, ±standard deviations. Asterisks: FO_{3st} **(A,B)** or FO_{3CUM} **(C)** averaged over hours of day. All variables presented in this figure were transformed between 0 and 1.

mixed forest (Ispra). These results are in line with Zona et al. (2014), who did not find a negative relationship between O_3 and net ecosystem exchange at Lochristi. All of these ecosystems are located in northern areas with the exception of Ispra, where O_3 concentrations are not particularly high compared with typical high ozone-prone Mediterranean sites (**Table 2**) and this may support the hypothesis that low to moderate ozone concentrations and therefore lower stomatal ozone fluxes may generate cumulative exposure to ozone far below possible critical levels in northern ecosystems.

Seven ecosystems showed a significant but limited NEP loss due to O_3 entering the stomata: the United Kingdom shrubland (Auchencorth Moss), the Hungarian grassland (Bugac), the Italian Holm oak forest (Castelporziano), the Californian pine plantation (Blodgett) during the Spring season, the French cropland (Grignon) during Summer, the Italian mixed forest (Bosco Fontana) and the Californian Citrus orchard (Lindcove) during both Spring and Summer seasons. Mean NEP loss was estimated at between 0.15 and 2.64%.

These values are low compared with other studies: for example Fares et al. (2013) adopted more traditional

TABLE 6 | Spearman partial correlation coefficients of the negative partial derivative of dNEP(O_3) (FO_{3sto} for Au, Bu, Gr, CPZ and Ci in Summer; FO_{3cum} for BF, Bl and Ci in Spring) with respect to solar radiation (rad), air temperature (t), vapor pressure deficit (*vpd*), soil water content (*swc*) and O_3 concentration at canopy level([O_3]).

Site	Season	rad	*t*	*vpd*	*swc*	[O_3]
Au	SP	–0.01	0.04	–0.01	0.01	0.00
Bu	SP	–**0.29**	0.14	–0.02	**0.29**	–**0.20**
Gr	S	0.01	0.09	–0.03	0.04	–**0.14**
BF	SP	–**0.16**	–0.09	**0.12**	**0.49**	**0.38**
	S	**0.25**	0.02	0.06	0.09	**0.34**
CPZ	SP	**0.10**	–0.04	**0.18**	0.06	**0.19**
BL	SP	–**0.16**	**0.32**	–0.02	n.a.	–**0.32**
Ci	SP	0.26	0.30	–0.24	–**0.40**	–0.08
	S	–**0.58**	–0.11	**0.23**	–**0.27**	–**0.26**

Bold numbers indicate statistically significant correlations ($p < 0.05$). Note that, since dNEP is negative, positive coefficients indicate that the negative effect of O_3 on NEP decreases when the other variable increases, while negative coefficients indicate that the negative effect of O_3 is further exacerbated by an increase in the other variable. Explanation of acronyms of the site names can be found in ***Table 1****.*

statistical methods based on step-wise regression analysis and multivariate analysis and found up to 12–19% of the carbon assimilation reduction in Blodgett and Lindcove sites explained by O_3 entering the stomata. Such results suggest that either our approach is extremely conservative and does not appropriately attribute O_3 effect, or statistical methods adopted in earlier studies may have overestimated O_3 effects by including the effects of covariates in the predictive model of NEP. It should be noted, however, that both approaches focus on the quantification of the instantaneous or near-instantaneous effect of O_3 on NEP, and capture neither the effect of this NEP reduction on biomass reduction which may further reduce NEP in the future nor the long-term effects of leaf injury.

Among the northern sites affected by O_3, Auchencorth Moss showed higher sensitivity to O_3 damage. This was despite non-stomatal deposition being the principal sink of O_3 at this site, representing 70% of the overall O_3 flux (Fowler et al., 2001), and where moorland mosses like *Sphagnum* are relatively tolerant to elevated O_3 concentrations (Rinnan et al., 2003). The reason of the depression of NEP linked to O_3 entering the stomata can be attributed to the increase of the plant respiration rate, as already observed by Niemi et al. (2002) for moorland vegetation, as a result of the plants repairing O_3 damaged tissues (Williamson et al., 2015).

Partial derivative results indicate that the O_3 effects on NEP are highly non-linear and site-specific. In almost all study sites, positive relationships between stomatal O_3 flux and NEP were found. Both are controlled by stomatal conductance and thus, in the absence of O_3 damage, stomatal O_3 fluxes positively correlated with NEP, as already observed by Proietti et al. (2016). This also implies that a limited effect of ozone on stomatal closure may still take place, as this matches with a moderate reduction in NEP.

Episodes in which O_3 detrimental effect occurred were identified from the models using partial derivative analysis. These episodes were correlated to climatic variables showing that O_3 damage dependence on weather varies with the climate. O_3 damage occurred primarily during Spring, especially for those sites where stomatal conductance decreases in Summer as affected by water availability (see **Table 2**). Partial correlation analysis showed that *swc* decreases the O_3 negative effect for those sites where no drought stress occurred (Blodgett and Bosco Fontana).

In Mediterranean regions, drought periods (which coincide with high O_3 levels) limit stomatal conductance, protecting vegetation from O_3 oxidative stress (Paoletti, 2006). At Lindcove, a well irrigated Mediterranean citrus plantation as previously reported by Fares et al. (2012), O_3 detrimental effects were observed both during Spring and Summer and positively correlate with *swc*. In these warm periods, with O_3 concentrations often exceeding 80 ppb, the mean stomatal O_3 fluxes were 3.29 and 3.19 nmol $m^{-2}s^{-1}$ during the central hours of the day during Spring and Summer, respectively. *swc* was not a significant predictor of O_3 damage at Castelporziano, a Mediterranean Holm oak forest, where the high water table (Bucci, 2006) protected trees from water stress, although during Spring high stomatal fluxes were associated with high levels of precipitations (Savi and Fares, 2014).

The inclusion of O_3 concentration at canopy level in the partial correlation analysis showed that NEP damage does not always occur at peak O_3 concentrations, as the case of the Italian sites of Bosco Fontana and Castelporziano. It must be noted that being photochemically produced, O_3 concentrations tend to peak when solar radiation is high and that BVOC emitted by some tree species can contribute to ozone formation (Monks et al., 2015). When radiation increases, *vpd* also increases, causing stomatal closure and leading to a protective effect against O_3 entering the leaves (Mereu et al., 2009; Fares et al., 2010b, 2014). For the same sites, partial correlation analysis highlights that when solar radiation and *vpd* increase, O_3 impact on NEP decreases. We do not exclude that to some minor extend high reactive terpenoid emissions at Castelporziano and Bosco Fontana in the central hours of the day [documented by Fares et al. (2013) and Acton et al. (2016)] may be responsible for ozone scavenging in the gas phase, thus reducing the amount of ozone entering stomata. This phenomenon of mid-day exclusion of O_3 damage does not happen in the Mediterranean Ponderosa pine plantation at Blodgett, this species being relatively insensitive to *vpd* when drought is not a limiting factor (Panek and Goldstein, 2001). At this site, air temperature was found to be a limiting factor for O_3 damage during Spring, when high temperature constrained gas exchange (Panek and Goldstein, 2001) and helped reduce O_3 oxidative stress.

At Auchencorth Moss, the relation of O_3 damage to weather remains unclear, although a significant negative effect of O_3 on NEP was found. O_3 damage estimates were averaged over the course of the day, with the aim of highlighting hourly patterns. For some sites (Lindcove, Bugac and Grignon), the detrimental effect of O_3 followed a bell-shaped curve, thus suggesting that most of damage to photosynthetic apparatus occurred rapidly during hours of maximum O_3 absorption. Interestingly, for Auchencorth Moss and Castelporziano, major damage was observed at the end of the afternoon, indicating that: (1) high *vpd* reduces stomatal conductance, and therefore O_3 damage, during the central hours of the day; and (2) to some extent plants may be able to detoxify O_3 during hours of maximum exposure to the pollutant, while at the end of the day detoxification capacity of leaves decreases. While there is evidence of a mid-day depression of stomatal conductance in those sites (Fares et al., 2010a, 2014), the second hypothesis is highly speculative and deserves further investigation. However, the possibility of changes in reducing power during the day has been previously described by Dizengremel et al. (2008) who showed decreasing foliar level of antioxidants during the afternoon hours in response to oxidative stress. Conversely, O_3 damaging effect and O_3 absorption were completely decoupled at Bosco Fontana, where the O_3 damaging effect peaks in the morning, under low O_3 concentrations, suggesting the occurrence of species-specific acclimatization phenomena along the day which we cannot explain in this study.

CONCLUSION

This work clearly suggests that long-term datasets are required to identify O_3 damage to vegetation under field conditions. We found that O_3 has a detrimental effect on NEP, although damage can be sporadic and is driven by specific weather conditions and in general, has lower magnitude compared with observations carried out through manipulative experiments or in the field using traditional statistical methods. Our results suggest that vegetation response to O_3 depends not only on pollution level but also on how the ecosystems respond to climate variables. Future climate changes may therefore either expose ecosystems to further O_3 damage by increasing temperatures or rather lead to a reduction in ozone damage in drought-prone ecosystems.

DATA AVAILABILITY STATEMENT

The datasets generated for this study are available on request to the corresponding author.

AUTHOR CONTRIBUTIONS

All authors contributed providing experimental data and/or supporting the preparation of the manuscript.

FUNDING

We want to thank the ÉCLAIRE project (Effects of Climate Change on Air Pollution and Response Strategies for European Ecosystems) funded by the EU's Seventh Framework Program for Research and Technological Development (FP7), which supported the flux measurements at the sites Au, Bu, Gr, Hy, Sp, Lo, BF, and Is. The CREA team wants to acknowledge the LIFE financial instruments of the European Union (LIFE15 ENV/IT/000183 – LIFE18 PRE IT 003) in the framework of the projects MOTTLES ("Monitoring ozone injury for setting new critical levels") and VEG-GAP ("Vegetation for Urban Green Air Quality Plans") LIFE18 PRE IT 003 and the General Secretariat of the Presidency of Italian Republic for financing the CASTEL4 project and the Directorate of Castelporziano Estate. The CEH measurement sites were supported by National Capability funding from the United Kingdom Natural Environment Research Council. The ECOSYS team acknowledge INGOS (grant agreement 284274), the French ANR project ANAEE, and ICOS France.

ACKNOWLEDGMENTS

We acknowledge the director of the AgroParsiTech Farm Dominique Tristan for allowing access to the field. We also thanks to K. Pintér and Z. Nagy, Szent István University, Gödöllõ, Hungary for contribution in EC measurements.

SUPPLEMENTARY MATERIAL

The Supplementary Material for this article can be found online at: https://www.frontiersin.org/articles/10.3389/ffgc.2020.00042/full#supplementary-material

REFERENCES

Acton, W. J. F., Schallhart, S., Langford, B., Valach, A., Rantala, P., Fares, S., et al. (2016). Canopy-scale flux measurements and bottom-up emission estimates of volatile organic compounds from a mixed oak and hornbeam forest in northern Italy. *Atmos. Chem. Phys.* 16, 7149–7170. doi: 10.5194/acp-16-7149-2016

Ainsworth, E. A., Yendrek, C. R., Sitch, S., Collins, W. J., and Emberson, L. D. (2012). The effects of tropospheric ozone on net primary productivity and implications for climate change. *Annu. Rev. Plant Biol.* 63, 637–661. doi: 10.1146/annurev-arplant-042110-103829

Aitkenhead, M. J., and Coull, M. C. (2016). Mapping soil carbon stocks across Scotland using a neural network model. *Geoderma* 262, 187–198. doi: 10.1016/j.geoderma.2015.08.034

Ashmore, R., and Bell, J. N. B. (1991). The role of ozone in global change. *Ann. Bot.* 67, 39–48.

Biswas, D. K., Xu, H., Li, Y. G., Sun, J. Z., Wang, X. Z., Han, X. G., et al. (2007). Genotypic differences in leaf biochemical, physiological and growth responses to ozone in 20 winter wheat cultivars released over the past 60 years. *Glob. Chang. Biol.* 14, 46–59. doi: 10.1111/j.1365-2486.2007.01477.x

Brion, G., Viswanathan, C., Neelakantan, T. R., Lingireddy, S., Girones, R., Lees, D., et al. (2005). Artificial neural network prediction of viruses in shellfish. *Appl. Environ. Microbiol.* 71, 5244–5253. doi: 10.1128/AEM.71.9.5244-5253.2005

Broschè, M., Merilo, E., Mayer, F., Pechter, P., Puzõrjova, I., Brader, G., et al. (2010). Natural variation in ozone sensitivity among *Arabidopsis thaliana* accessions and its relation to stomatal conductance. *Plant. Cell Environ.* 33, 914–925. doi: 10.1111/j.1365-3040.2010.02116.x

Bucci, M. (2006). *The state of Water Resources, in: Ricerche Sulla Complessità Di Un Ecosistema Forestale Costiero Mediterraneo*. Rome: Accademia Nazionale delle Scienze detta dei XL.

Cailleret, M., Ferretti, M., Gessler, A., Rigling, A., and Schaub, M. (2018). Ozone effects on European forest growth-Towards an integrative approach. *J. Ecol.* 106, 1377–1389. doi: 10.1111/1365-2745.12941

Chan, Z. S. H., Ngan, H. W., Rad, A. B., David, A. K., and Kasabov, N. (2006). Short-term ANN load forecasting from limited data using generalization learning strategies. *Neurocomputing* 70, 409–419. doi: 10.1016/J.NEUCOM.2005.12.131

Cieslik, S. A. (2004). Ozone uptake by various surface types: a comparison between dose and exposure. *Atmos. Environ.* 38, 2409–2420. doi: 10.1016/j.atmosenv.2003.10.063

Civelekoglu, G., Yigit, N. O., Diamadopoulos, E., and Kitis, M. (2008). Prediction of bromate formation using multi-linear regression and artificial neural networks. *J. Int. Oz. Assoc.* 29, 353–362. doi: 10.1080/01919510701549327

Copeland, N., Cape, J. N., Nemitz, E., and Heal, M. R. (2014). Volatile organic compound speciation above and within a Douglas fir forest. *Atmos. Environ.* 94, 86–95. doi: 10.1016/J.ATMOSENV.2014.04.035

Dimopoulos, I., Chronopoulos, J., Chronopoulou-Sereli, A., and Lek, S. (1999). Neural network models to study relationships between lead concentration in grasses and permanent urban descriptors in Athens city (Greece). *Ecol. Modell.* 120, 157–165. doi: 10.1016/S0304-3800(99)00099-X

Dimopoulos, Y., Bourret, P., and Lek, S. (1995). Use of some sensitivity criteria for choosing networks with good generalization ability. *Neural Process. Lett.* 2, 1–4. doi: 10.1007/BF02309007

Dizengremel, P., Le Thiec, D., Bagard, M., and Jolivet, Y. (2008). Ozone risk assessment for plants: central role of metabolism-dependent changes in reducing power. *Environ. Pollut.* 156, 11–15. doi: 10.1016/J.ENVPOL.2007.12.024

Erisman, J. W., Draaijers, G., Duyzer, J., Hofschreuder, P., Leeuwen, N., Van Römer, F., et al. (1997). The aerosol project: introduction and some background information. *Atmos. Environ.* 31, 315–319. doi: 10.1016/S1352-2310(96)00186-0

Falge, E., Baldocchi, D., Olson, R., Anthoni, P., Aubinet, M., Bernhofer, C., et al. (2001). Gap filling strategies for defensible annual sums of net ecosystem exchange. *Agric. For. Meteorol.* 107, 43–69. doi: 10.1016/S0168-1923(00)00225-2

Fares, S., Conte, A., and Chabbi, A. (2018). Ozone flux in plant ecosystems: new opportunities for long-term monitoring networks to deliver ozone-risk assessments. *Environ. Sci. Pollut. Re.* 25, 8240–8248. doi: 10.1007/s11356-017-0352-0

Fares, S., Goldstein, A., and Loreto, F. (2010a). Determinants of ozone fluxes and metrics for ozone risk assessment in plants. *J. Exp. Bot.* 61, 629–633. doi: 10.1093/jxb/erp336

Fares, S., McKay, M., Holzinger, R., and Goldstein, A. H. (2010b). Ozone fluxes in a Pinus ponderosa ecosystem are dominated by non-stomatal processes: evidence from long-term continuous measurements. *Agric. For. Meteorol.* 150, 420–431. doi: 10.1016/j.agrformet.2010.01.007

Fares, S., Savi, F., Muller, J., Matteucci, G., and Paoletti, E. (2014). Simultaneous measurements of above and below canopy ozone fluxes help partitioning ozone deposition between its various sinks in a Mediterranean Oak Forest. *Agric. For. Meteorol* 198–199, 181–191. doi: 10.1016/j.agrformet.2014.08.014

Fares, S., Vargas, R., Detto, M., Goldstein, A. H., Karlik, J., Paoletti, E., et al. (2013). Tropospheric ozone reduces carbon assimilation in trees: estimates from analysis of continuous flux measurements. *Glob. Chang. Biol.* 19, 2427–2443. doi: 10.1111/gcb.12222

Fares, S., Weber, R., Park, J.-H., Gentner, D., Karlik, J., and Goldstein, A. H. (2012). Ozone deposition to an orange orchard: partitioning between stomatal and non-stomatal sinks. *Environ. Pollut.* 169, 258–266. doi: 10.1016/j.envpol.2012.01.030

Flechard, C. R., and Fowler, D. (1998). Atmospheric ammonia at a moorland site. I: the meteorological control of ambient ammonia concentrations and the influence of local sources. *Q. J. R. Meteorol. Soc.* 124, 733–757. doi: 10.1002/qj.49712454705

Fowler, D., Flechard, C., Cape, J. N., Storeton-West, R. L., and Coyle, M. (2001). Measurements of ozone deposition to vegetation quantifying the flux, the stomatal and non-stomatal components. *Water. Air. Soil Pollut.* 130, 63–74. doi: 10.1023/A:1012243317471

Fowler, D., Pilegaard, K., Sutton, M. A., Ambus, P., Raivonen, M., Duyzer, J., et al. (2009). Atmospheric composition change: ecosystems-atmosphere interactions. *Atmos. Environ.* 43, 5193–5267. doi: 10.1016/j.atmosenv.2009.07.068

Gerosa, G., Fusaro, L., Monga, R., Finco, A., Fares, S., Manes, F., et al. (2015). A flux-based assessment of above and below ground biomass of Holm oak (*Quercus ilex* L.) seedlings after one season of exposure to high ozone concentrations. *Atmos. Environ.* 113, 41–49. doi: 10.1016/J.ATMOSENV.2015.04.066

Gevrey, M., Dimopoulos, I., and Lek, S. (2003). Review and comparison of methods to study the contribution of variables in artificial neural network models. *Ecol. Modell.* 160, 249–264. doi: 10.1016/S0304-3800(02)00257-0

Helfter, C., Campbell, C., Dinsmore, K. J., Drewer, J., Coyle, M., Anderson, M., et al. (2015). Drivers of long-term variability in CO2 net ecosystem exchange in a temperate peatland. *Biogeosciences* 12, 1799–1811. doi: 10.5194/bg-12-1799-2015

Hicks, B. B., Baldocchi, D. D., Meyers, T. P., Hosker, R. P., and Matt, D. R. (1987). A preliminary multiple resistance routine for deriving dry deposition velocities from measured quantities. *Water. Air. Soil Pollut.* 36, 311–330. doi: 10.1007/BF00229675

Jensen, N. R., Gruening, C., Goded, I., Müller, M., Hjorth, J., and Wisthaler, A. (2018). Eddy-covariance flux measurements in an Italian deciduous forest using PTR-ToF-MS, PTR-QMS and FIS. *Int. J. Environ. Anal. Chem.* 98, 758–788. doi: 10.1080/03067319.2018.1502758

Karlsson, P. E., Pleijel, H., Pihl Karlsson, G., Medin, E. L., and Skärby, L. (2000). Simulations of stomatal conductance and ozone uptake to Norway spruce saplings in open-top chambers. *Environ. Pollut.* 109, 443–451. doi: 10.1016/S0269-7491(00)00047-6

Lek, S., Delacoste, M., Baran, P., Dimopoulus, I., Lauga, J., and Aulagnier, S. (1996). Application of neural networks to modellingnon-linear relationship in ecology. *Ecol. Modell.* 90, 39–52.

Loubet, B., Laville, P., Lehuger, S., Larmanou, E., Fléchard, C., Mascher, N., et al. (2011). Carbon, nitrogen and Greenhouse gases budgets over a four years crop rotation in northern France. *Plant Soil* 343:109–137. doi: 10.1007/s11104-011-0751-9

Manning, W. J. (2005). Establishing a cause and effect relationship for ambient ozone exposure and tree growth in the forest: progress and an experimental approach. *Environ. Pollut.* 137, 443–454. doi: 10.1016/j.envpol.2005.01.031

Marrero, T. R., and Mason, E. A. (1972). Gaseous diffusion coefficients. *J. Phys. Chem. Ref. Data* 1, 3–118. doi: 10.1063/1.3253094

Mereu, S., Salvatori, E., Fusaro, L., Gerosa, G., Muys, B., and Manes, F. (2009). An integrated approach shows different use of water resources from *Mediterranean maquis* species in a coastal dune ecosystem. *Biogeosciences* 6, 2599–2610. doi: 10.5194/bg-6-2599-2009

Moffat, A. M., Beckstein, C., Churkina, G., Mund, M., and Heimann, M. (2010). Characterization of ecosystem responses to climatic controls using artificial neural networks. *Glob. Chang. Biol.* 16, 2737–2749. doi: 10.1111/j.1365-2486.2010.02171.x

Monks, P. S., Archibald, A. T., Colette, A., Cooper, O., Coyle, M., Derwent, R., et al. (2015). Tropospheric ozone and its precursors from the urban to the global scale from air quality to short-lived climate forcer. *Atmos. Chem. Phys.* 15, 8889–8973. doi: 10.5194/acp-15-8889-2015

Monteith, J. L. (1981). Evaporation and surface temperature. *Q. J. R. Meteorol. Soc.* 107, 1–27. doi: 10.1002/qj.49710745102

Niemi, R., Martikainen, P. J., Silvola, J., and Holopainen, T. (2002). Ozone effects on Sphagnum mosses, carbon dioxide exchange and methane emission in boreal peatland microcosms. *Sci. Total Environ.* 289, 1–12. doi: 10.1016/S0048-9697(01)01012-9

Olden, J. D., and Jackson, D. A. (2002). Illuminating the "black box": a randomization approach for understanding variable contributions in artificial neural networks. *Ecol. Modell.* 154, 135–150. doi: 10.1016/S0304-3800(02)00064-9

Olden, J. D., Joy, M. K., and Death, R. G. (2004). An accurate comparison of methods for quantifying variable importance in artificial neural networks using simulated data. *Ecol. Modell.* 178, 389–397. doi: 10.1016/j.ecolmodel.2004.03.013

Panek, J. A., and Goldstein, A. H. (2001). Response of stomatal conductance to drought in ponderosa pine: implications for carbon and ozone uptake. *Tree Physiol.* 21, 337–344. doi: 10.1093/treephys/21.5.337

Paoletti, E. (2006). Impact of ozone on mediterranean forests: a review. *Environ. Pollut.* 144, 463–474. doi: 10.1016/j.envpol.2005.12.051

Parrish, D. D., Law, K. S., Staehelin, J., Derwent, R., Cooper, O. R., Tanimoto, H., et al. (2012). Long-term changes in lower tropospheric baseline ozone concentrations at northern mid-latitudes. *Atmos. Chem. Phys.* 12, 11485–11504. doi: 10.5194/acp-12-11485-2012

Paruelo, J. M., and Tomasel, F. (1997). Prediction of functional charac-teristics of ecosystems: a comparison of artificial neural net-works and regression models. *Ecol. Modell.* 98, 173–186. doi: 10.1016/s0304-3800(96)01913-8

Proietti, C., Anav, A., Marco, A., De, Sicard, P., and Vitale, M. (2016). A multi-sites analysis on the ozone effects on gross primary production of European forests. *Sci. Total Environ.* 556, 1–11. doi: 10.1016/j.scitotenv.2016.02.187

Rannik, U., Mammarella, I., Keronen, P., and Vesala, T. (2009). Vertical advection and nocturnal deposition of ozone over a boreal pine fores. *Atmos. Chem. Phys.* 9, 2089–2095. doi: 10.5194/acp-9-2089-2009

Reich, P., and Amundson, R. (1985). Ambient levels of ozone reduce net photosynthesis in tree and crop species. *Science* 230, 566–570. doi: 10.1126/science.230.4725.566

Rinnan, R., Impio, M., Silvola, J., Holopainen, T., and Martikainen, P. J. (2003). Carbon dioxide and methane fluxes in boreal peatland microcosms with different vegetation cover?effects of ozone or ultraviolet-B exposure. *Oecologia* 137, 475–483. doi: 10.1007/s00442-003-1366-5

Rumelhart, D. (1986). "Learning by error backpropagation," in *Parallel Distributed Processing*, eds D. E. Rumelhart and J. L. McClelland (Chicago, IL: Encyclopædia Britannica, Inc.).

Savi, F., and Fares, S. (2014). Ozone dynamics in a Mediterranean Holm oak forest : comparison among transition periods characterized by different amounts of precipitation. *Ann. Silvicultural Res.* 38, 1–6. doi: 10.12899/asr-801

Savi, F., Di Bene, C., Canfora, L., Mondini, C., and Fares, S. (2016). Environmental and biological controls on CH4 exchange over an evergreen mediterranean forest. *Agric. For. Meteorol.* 226–227, 67–79. doi: 10.1016/j.agrformet.2016.05.014

Shindell, D. T., Faluvegi, G., Koch, D. M., Schmidt, G. A., Unger, N., and Bauer, S. E. (2009). Improved attribution of climate forcing to emissions. *Science* 326, 716–718. doi: 10.1126/science.1174760

Sitch, S., Cox, P. M., Collins, W. J., and Huntingford, C. (2007). Indirect radiative forcing of climate change through ozone effects on the land-carbon sink. *Nature* 448, 791–794. doi: 10.1038/nature06059

Stevenson, D. S., Dentener, F. J., Schultz, M. G., Ellingsen, K., van Noije, T. P. C., Wild, O., et al. (2006). Multimodel ensemble simulations of present-day and near-future tropospheric ozone. *J. Geophys. Res.* 111:D08301. doi: 10.1029/2005JD006338

The Royal Society (2008). *Ground-Level Ozone in the 21st Century: Future Trends, Impacts and Policy Implications*. London: The Royal Society, 132.

Verryckt, L. T., Op, De Beeck, M., Neirynck, J., Gielen, B., Roland, M., et al. (2017). No impact of tropospheric ozone on the gross primary productivity of a Belgian pine forest. *Biogeosciences* 14, 1839–1855. doi: 10.5194/bg-14-1839-2017

Villányi, V., Ürmös, Z., Balogh, J., Horváth, L., Csintalan, Z., and Tuba, Z. (2008). Ozone biomonitoring at mountainous and lowland areas in Hungary. *Acta Biol. Szeged* 52, 209–212.

Williamson, J. L., Mills, G., Hayes, F., Jones, T., and Freeman, C. (2015). How do increasing background concentrations of tropospheric ozone affect peatland 1 plant growth and carbon gas exchange? *Atmos. Environ.* 127, 133–138. doi: 10.1016/j.atmosenv.2015.12.004

Wohlgemuth, H., Mittelstrass, K., Kschieschan, S., Bender, J., Weigel, H.-J., Overmyer, K., et al. (2002). Activation of an oxidative burst is a general feature of sensitive plants exposed to the air pollutant ozone. *Plant, Cell Environ.* 25, 717–726. doi: 10.1046/j.1365-3040.2002.00859.x

Zapletal, M., Cudlin, P., Chroust, P., Urban, O., Pokorny, R., Edwards-Jonsova, M., et al. (2011). Ozone flux over a Norway spruce forest and correlation with net ecosystem production. *Environ. Pollut.* 159, 1024–1034. doi: 10.1016/j.envpol.2010.11.037

Zenone, T., Zona, D., Gelfand, I., Gielen, B., Camino-Serrano, M., and Ceulemans, R. (2016). CO2 uptake is offset by CH4 and N2O emissions in a poplar short-rotation coppice. *GCB Bioenergy* 8, 524–538. doi: 10.1111/gcbb.12269

Zona, D., Gioli, B., Fares, S., De Groote, T., Pilegaard, K., Ibrom, A., et al. (2014).). Environmental controls on ozone fluxes in a poplar plantation in Western Europe. *Environ. Pollut.* 184, 201–210. doi: 10.1016/j.envpol.2013.08.032

Conflict of Interest: The authors declare that the research was conducted in the absence of any commercial or financial relationships that could be construed as a potential conflict of interest.

frontiers
in Forests and Global Change

ORIGINAL RESEARCH
published: 12 May 2020
doi: 10.3389/ffgc.2020.00045

Developing Ozone Risk Assessment for Larch Species

Yasutomo Hoshika[1], Elena Paoletti[1], Evgenios Agathokleous[2]*, Tetsuto Sugai[3] and Takayoshi Koike[3]*

[1] IRET-CNR, Firenze, Italy, [2] Institute of Ecology, Key Laboratory of Agrometeorology of Jiangsu Province, School of Applied Meteorology, Nanjing, China, [3] Research Faculty of Agriculture, School of Agriculture, Hokkaido University, Sapporo, Japan

Ozone (O_3) risk assessment for the protection of forests requires species-specific critical levels (CLs), based on either O_3 concentrations (AOT40) or stomatal uptake (PODY) accumulation over the growing season. Larch (*Larix* sp.) is a genus with O_3-susceptible species, widely distributed in the northern hemisphere and with global economic importance. We analyzed published and unpublished data of Japanese larch (*Larix kaempferi*) and its hybrid F_1 (*Larix gmelinii* var. *japonica* × *L. kaempferi*) stomatal responses for developing a parameterization of stomatal conductance model and estimating PODY-based CLs with two *Y* thresholds, that is, 0 and 1 nmol m^{-2} s^{-1} projected leaf area (PLA). In parallel, we estimated AOT40-based CLs. The results show that the AOT40-based CLs for a 2% and 4% biomass loss in Japanese larch were 5.79 and 11.59 ppm h, that is, higher than those in hybrid larch F_1 (2.18 and 4.36 ppm h AOT40), suggesting a higher O_3 susceptibility of the hybrid. However, the use of PODY reconciled the species-specific differences, because the CLs were similar, that is, 9.40 and 12.00 mmol m^{-2} POD0 and 2.21 and 4.31 mmol m^{-2} POD1 in Japanese larch versus 10.44 and 12.38 mmol m^{-2} POD0 and 2.45 and 4.19 mmol m^{-2} POD1 in the hybrid, for 2% and 4% biomass loss, respectively. Overall, the CLs were lower than those in other forest species, which suggests a relatively high susceptibility of these larches. These results will inform environmental policy-makers and modelers about larch susceptibility to O_3.

Keywords: critical level, DO$_3$SE model, forest, larch, parameterization, tropospheric ozone

OPEN ACCESS

Edited by:
Armin Hansel,
University of Innsbruck, Austria

Reviewed by:
Juha-Pekka Tuovinen,
Finnish Meteorological Institute, Finland
Steffen M. Noe,
Estonian University of Life Sciences, Estonia
Rüdiger Grote,
Karlsruhe Institute of Technology (KIT), Germany

****Correspondence:***
Elena Paoletti
elena.paoletti@cnr.it
Evgenios Agathokleous
evgenios_ag@hotmail.com

Specialty section:
This article was submitted to Forests and the Atmosphere, a section of the journal Frontiers in Forests and Global Change

Received: *19 December 2019*
Accepted: *25 March 2020*
Published: *12 May 2020*

Citation:
Hoshika Y, Paoletti E, Agathokleous E, Sugai T and Koike T (2020) Developing Ozone Risk Assessment for Larch Species. Front. For. Glob. Change 3:45. doi: 10.3389/ffgc.2020.00045

INTRODUCTION

Tropospheric ozone (O_3) is the most widespread phytotoxic air pollutant (Mills et al., 2018). In the period 1995–2014, control measures were effective in North America and Europe, as indicated by a decrease of O_3 concentrations, while a significant increase in O_3 concentrations occurred in East Asia (Chang et al., 2017; Mills et al., 2018). Ozone has a strong oxidative capacity and may cause severe injury to forests (Paoletti, 2007; Li et al., 2017). To assess O_3 risk to forests, different metrics have been developed (Lefohn et al., 2018). One of the most common metrics is AOT40, that is, the accumulated exposure over an hourly threshold of 40 ppb during the growing season, although there is a general consensus that the accumulated stomatal O_3 flux – or phytotoxic ozone dose (POD) – is more biologically meaningful as it estimates the amount of O_3 actually entering the plants through the stomata (Paoletti and Manning, 2007). A flux threshold *Y* below which O_3 uptake is not expected to be injurious to plants has been postulated. For all tree species, a uniform threshold of $Y = 1$ nmol m^{-2} s^{-1} projected leaf area (PLA) was recommended by the

Convention on Long-Range Transboundary Air Pollution (CLRTAP, 2017) based on Büker et al. (2015). For easier calculation, a Y threshold of 0 nmol m^{-2} s^{-1} PLA was also recommended, if we assume that all O_3 molecules induce a physiological reaction after uptake (De Marco et al., 2015, 2016; Anav et al., 2016), which is a plausible assumption in the light of low-dose *adaptive responses* (Agathokleous et al., 2019).

For the protection of susceptible vegetation from O_3, critical levels (CLs) are recommended, defined as the "concentration, cumulative exposure or cumulative stomatal flux of atmospheric pollutants above which direct adverse effects on susceptible vegetation may occur according to present knowledge" (CLRTAP, 2017). CLs are derived for either a 2% (Norway spruce) reduction or a 4% (beech/birch, Mediterranean deciduous and evergreen species) reduction in annual new growth (based on aboveground, root, or whole-tree biomass) of young trees up to 10 years old. AOT40-based CLs for tree biomass loss (5%) are available for *Fagus sylvatica* and *Betula pendula* in a previous version of the ICP Vegetation manual (CLRTAP, 2014; AOT40-based CLs are not included in the latest version) and for some other species in the literature (e.g., 18 Japanese species including two larch species, Yamaguchi et al., 2011; *Populus deltoides* cv. "55/56" × *P. deltoides* cv. "Imperial" and *Populus euramericana* cv. "74/76," Shang et al., 2017). Stomatal flux-based CLs are available for *F. sylvatica*, *B. pendula*, *Picea abies*, *Quercus faginea*, *Quercus pyrenaica*, *Quercus robur*, *Quercus ilex*, *Ceratonia siliqua*, and *Pinus halepensis* in the ICP Vegetation manual (CLRTAP, 2017) and for few other species in the literature (*Zelkova serrata*, Hoshika et al., 2012; *Quercus pubescens*, Hoshika et al., 2018b; *Pinus pinea*, Hoshika et al., 2017; hybrid poplars, Zhang et al., 2018; Feng et al., 2019b; *Fagus crenata*, *Quercus serrata*, *Quercus mongolica* var. *crispula*, and *Betula platyphylla* var. *japonica*, Yamaguchi et al., 2019). For estimating PODY (phytotoxic ozone dose above a threshold Y nmol m^{-2} s^{-1})-based CLs, a species-specific parameterization of the stomatal flux or DO_3SE model is required (Emberson et al., 2000; Büker et al., 2012). There is a need of more species-specific CLs for biomass loss in forest species, especially for forest species in Asia, where elevated O_3 pollution levels are a serious risk for forests at present (Li et al., 2017; Mills et al., 2018; Feng et al., 2019a).

Larch (*Larix* sp.) is a widely distributed genus (*Pinaceae* family) with global economic importance, which includes some of the few deciduous conifer species. Larch is among the dominant tree species of northern hemisphere boreal forests. Hence, its natural distribution range is very wide and spans from Siberia to Canada, passing through Europe, mountainous China, and Japan. Larches provide high-quality wood and are commercially valuable (Bardak et al., 2019). As any pioneer species, larches have a relatively high growth rate and stomatal conductance (Streit et al., 2014; Agathokleous et al., 2017; Hoshika et al., 2018c). Although their susceptibility to O_3 has been investigated in several papers (Wieser and Havranek, 1996; Matsumura, 2001; Watanabe et al., 2006; Koike et al., 2012; Agathokleous et al., 2017; Sugai et al., 2018, 2019), a comprehensive risk assessment including parameterization of the stomatal conductance model and definition of CLs for biomass losses is missing. Previous studies focused on the biomass responses to O_3 of Japanese larch (*Larix kaempferi*) and its hybrid F_1 (*Larix gmelinii* var. *japonica* × *L. kaempferi*). Hybrid F_1 displays heterosis and is important for timber production and afforestation due to more desirable characteristics compared to its parents, with a significant superiority in terms of growth rates (Ryu et al., 2009; Kita et al., 2009; Agathokleous et al., 2017; Sugai et al., 2018). A question arises whether hybrid clones, selected for fast-growing capacities, are representative of natural forest responses to O_3 when used in manipulative experiments (e.g., Di Baccio et al., 2008; Hu et al., 2015; Dusart et al., 2019; Podda et al., 2019).

Our aim was to collate published and unpublished data from previous experiments for developing a parameterization of the DO_3SE model for Japanese larch and its hybrid F_1 and estimating the CLs not to be exceeded for the protection of these larch species from O_3. Based on published research documenting a higher O_3 susceptibility of the faster-growing hybrid F_1 than the slower-growing Japanese larch (Agathokleous et al., 2017; Sugai et al., 2018), we hypothesized that the CLs of hybrid F_1 have a lower susceptibility than that of the wild Japanese larch.

MATERIALS AND METHODS

A literature survey was conducted in Web of Science (9 December 2019), with the keywords "ozone" and "larch" or "larix" (search method: Topic). All the identified papers (n = 33 and 36 for each combination; most were duplicates) were reviewed for relevance, including whether they reported O_3 and biomass data. Finally, data on O_3 concentrations, exposure duration, and total biomass were collected from six published experiments carried out in open-top chambers (OTCs) (**Table 1**: Matsumura, 2001; Watanabe et al., 2006; Koike et al., 2012; Wang et al., 2015; Sugai et al., 2018, 2019) and used to calculate AOT40 and percentage losses of biomass relative to controls in low-O_3 air. Data from combined experiments, such as O_3 with either fertilization or CO_2, were not included. Data of Dahurian larch (*L. gmelinii* var. *japonica*) from the same experiments were not included because of scarcity, thus being insufficient for analysis.

Individual measurements of stomatal conductance across a range of environmental conditions were obtained from the authors Sugai et al. (2018, 2019) and Agathokleous (unpublished). Measurements by Agathokleous (unpublished) were carried out in field-grown 2-year-old larch seedlings at the Sapporo experimental forest, Hokkaido University, in Japan (**Table 1**). All measurements were carried out by means of Li-Cor 6400 gas analyzers (Li-Cor Inc., Lincoln, NE, United States). As soil water content measurements were missing, we used the following simplified formula for the estimation of the stomatal conductance g_{sto} in the DO_3SE model (CLRTAP, 2017):

$$g_{sto} = g_{max} * f_{light} * \max\{f_{min}, (f_{temp} * f_{VPD})\} \quad (1)$$

where g_{max} is the maximum stomatal conductance of either Japanese larch or its hybrid F_1, f_{min} is the species-specific minimum stomatal conductance, and f_{light}, f_{temp}, and f_{VPD} account for the effects of photosynthetic photon flux density (PPFD), air temperature (T), and vapor pressure deficit (VPD),

TABLE 1 | Details of experiments from which data were obtained for the analysis (PODY, AOT40, and Gs model).

References	Species	Experimental setup	Duration	Exposure level	Other treatments	Type of assessment
Koike et al. (2012)	*Larix kaempferi*	OTC	June–September 2010	CF, NF60	Elevated CO_2	PODY/AOT40
	Larix gmelinii var. *japonica*	OTC	June–September 2010	CF, NF60	Elevated CO_2	PODY/AOT40
	F1 (*L. gmelinii* var. *japonica* × *L. kaempferi*)	OTC	June–September 2010	CF, NF60	Elevated CO_2	PODY/AOT40
Matsumura (2001)	*L. kaempferi*	OTC	June 1993–September 1995	CF, NF	n.a.	AOT40
Sugai et al. (2018)	*L. kaempferi*	OTC	June 2013–September 2014	CF, NF, NF40, NF60	n.a.	PODY/AOT40/Gs model
	F_1 (*L. gmelinii* var. *japonica* × *L. kaempferi*)	OTC	June 2013–September 2014	CF, NF, NF40, NF60	n.a.	PODY/AOT40/Gs model
Sugai et al. (2019)	*L. kaempferi*	OTC	June 2015–August 2016	CF, NF60	Nitrogen addition	PODY/AOT40/Gs model
	F_1 (*L. gmelinii* var. *japonica* × *L. kaempferi*)	OTC	June 2015–August 2016	CF, NF60	Nitrogen addition	PODY/AOT40/Gs model
Wang et al. (2015)	F_1 (*L. gmelinii* var. *japonica* × *L. kaempferi*)	OTC	July 2011–September 2012	CF, NF60	n.a.	PODY/AOT40
Watanabe et al. (2006)	*L. kaempferi*	OTC	April 2004–September 2005	CF, AA, 1.5AA, 2.0AA	Nitrogen addition	AOT40
Agathokleous (unpublished)	*L. kaempferi*	Field	June–August 2015	n.a.	n.a.	Gs model
	F_1 (*L. gmelinii* var. *japonica* × *L. kaempferi*)	Field	August 2017	n.a.	n.a.	Gs model

OTC, open-top chamber; CF, charcoal-filtered air; NF, non-filtered air; NF40, 40 ppb O_3; NF60, 60 ppb O_3; AA, ambient O_3 concentration; 1.5AA, 1.5 times ambient O_3 concentration; 2.0AA, twice ambient O_3 concentration; n.a., not available.

respectively, on stomata. Parameterization was carried out using a boundary line analysis (Alonso et al., 2008; Braun et al., 2010; Hoshika et al., 2012). First, the g_{sto} data were divided into classes with the following stepwise increases for each variable: 200 μmol photons m^{-2} s^{-1} for PPFD (when the values were less than 200 μmol photons m^{-2} s^{-1}, PPFD classes at 50 μmol photons m^{-2} s^{-1} steps were adopted), 2°C for T, and 0.2 kPa for VPD. A function was fitted against each model variable based on 95th percentile values per class of environmental factors. Values of g_{max} and f_{min} were calculated as the 95th percentile and 5th percentile, respectively (Hoshika et al., 2012; Bičárová et al., 2019). For details of f_{light}, f_{temp}, and f_{VPD}, see CLRTAP (2017).

Stomatal O_3 uptake (F_{st}; nmol m^{-2} s^{-1}) was calculated as follows:

$$F_{st} = [O_3] \cdot g_{sto} \cdot \frac{r_c}{r_b + r_c} \tag{2}$$

where r_c is the leaf surface resistance [= $1/(g_{sto} + g_{ext})$; s m^{-1}] and g_{ext} is the external leaf or cuticular conductance (= 0.0004 m s^{-1}, CLRTAP, 2017). The standard DO3SE model considers the leaf boundary layer resistance (r_b):

$$r_b = 1.3 \cdot 150 \cdot (L_d/u)^{0.5} \tag{3}$$

where the factor 1.3 accounts for the difference in diffusivity between heat and O_3, 150 is the empirical constant, L_d is the cross-wind leaf dimension (0.008 m for conifers, CLRTAP, 2017), and u is the wind speed. The wind speed data were not available in collected literatures. However, in OTCs, since a constant ventilation from the blowers is realized, r_b is less important compared with stomatal resistance (r_{sto}) (Unsworth et al., 1984; Uddling et al., 2004; Tuovinen et al., 2009). This is supported by the fact that the r_b/r_c ratio was small in the present study when assuming that r_{sto} was r_{sto_min} (= $1/g_{max}$) and wind speed was constant inside a chamber (r_b/r_c = 0.07 and 0.06 at 1 m s^{-1} and 0.05 and 0.04 at 2 m s^{-1} of wind speed in hybrid and Japanese larch, respectively). Here, we assumed that r_b was negligible for the calculation of F_{st}.

PODY (mmol m^{-2}) was estimated from hourly data as follows:

$$PODY = \sum_{i=1}^{n} (F_{st,i} - Y) \cdot \Delta t \tag{4}$$

where Y is a species-specific threshold of stomatal O_3 uptake (nmol m^{-2} s^{-1}) and Δt = 1 h is the averaging period. $F_{st,i}$ is the ith hourly stomatal O_3 uptake (nmol m^{-2} s^{-1}), and n is the number of hours included in the calculation period. Y is subtracted from each $F_{st,i}$ when $F_{st,i} > Y$. PODY was then estimated based on hourly data of air temperature, solar photosynthetic active radiation, and VPD as registered locally and accumulated over the duration of the experiments from the six papers (**Table 1**). Data from Matsumura (2001) and Watanabe et al. (2006) were excluded from this analysis because of missing meteorological data.

To establish PODY-based dose–response relationships, two representative values of Y (= 0 or 1 nmol m^{-2} s^{-1}) were tested. This is because CLRTAP (2017) suggested POD1 to be suitable for biomass assessment in elevated O_3 while several studies reported a better performance of POD0 rather than POD1 for O_3 risk assessment (e.g., Sicard et al., 2016). CLs were estimated for a total biomass reduction of both 2% as suggested for deciduous species and 4% as suggested for non-Mediterranean conifer species (CLRTAP, 2017). In addition, since CLRTAP (2017) provided an AOT40-based CL corresponding to a 5% biomass reduction for forests, the CLs for the 5% biomass reduction were also shown. For PODY, CLs were calculated, referring to a "REF10" PODY calculated at a constant O_3 concentration of 10 ppb referring to a "pre-industrial" O_3 concentration, as recommended by CLRTAP (2017).

Simple linear regression analyses were used to assess the relationships between O_3 indices (AOT40, POD0, and POD1) and relative biomass. In addition, to compare the g_{max} values between the two larches, Student's t-test was performed on values within the top five percentile in g_{sto} data. Results were considered significant at $p < 0.05$. All the analyses were performed using R 3.5.1 (R Core Team, 2018).

TABLE 2 | DO3SE model parameters for Japanese larch and hybrid F_1, where g_{max} is maximum stomatal conductance; f_{min} is minimum stomatal conductance; f_{light_a} is a parameter determining the shape of the hyperbolic relationship of stomatal response to light; T_{max}, T_{opt}, and T_{min} are the maximum, optimal, and minimum temperatures, respectively, for calculating the function f_{temp} that expresses the variation of g_{sto} with temperature; VPD_{min} and VPD_{max} are the vapor pressure deficit for attaining minimum and maximum stomatal aperture, respectively (f_{VPD}).

Parameter	Japanese larch	Hybrid F_1
g_{max}, mmol O_3 m^{-2} PLA s^{-1}	120 [95% CI: 103–188]	140 [95% CI: 110–225]
f_{min}, fraction	0.16	0.09
f_{light_a}, μmol^{-1} m^{-2} s^{-1}	0.0097	0.0096
T_{min}, °C	5	5
T_{opt}, °C	25	25
T_{max}, °C	40	40
VPD_{max}, kPa	1.6	1.6
VPD_{min}, kPa	4.0	4.2

CI denotes confidence interval.

RESULTS

The parameterization of the stomatal conductance model (**Figure 1**) resulted in very similar values for Japanese larch and its hybrid F_1 (**Table 2**). The g_{max} in hybrid larch was slightly higher than that in Japanese larch although g_{max} values in the two larches were not statistically different ($p = 0.48$, Student's t-test for the values within the top five percentile in g_{sto}, data not shown). On

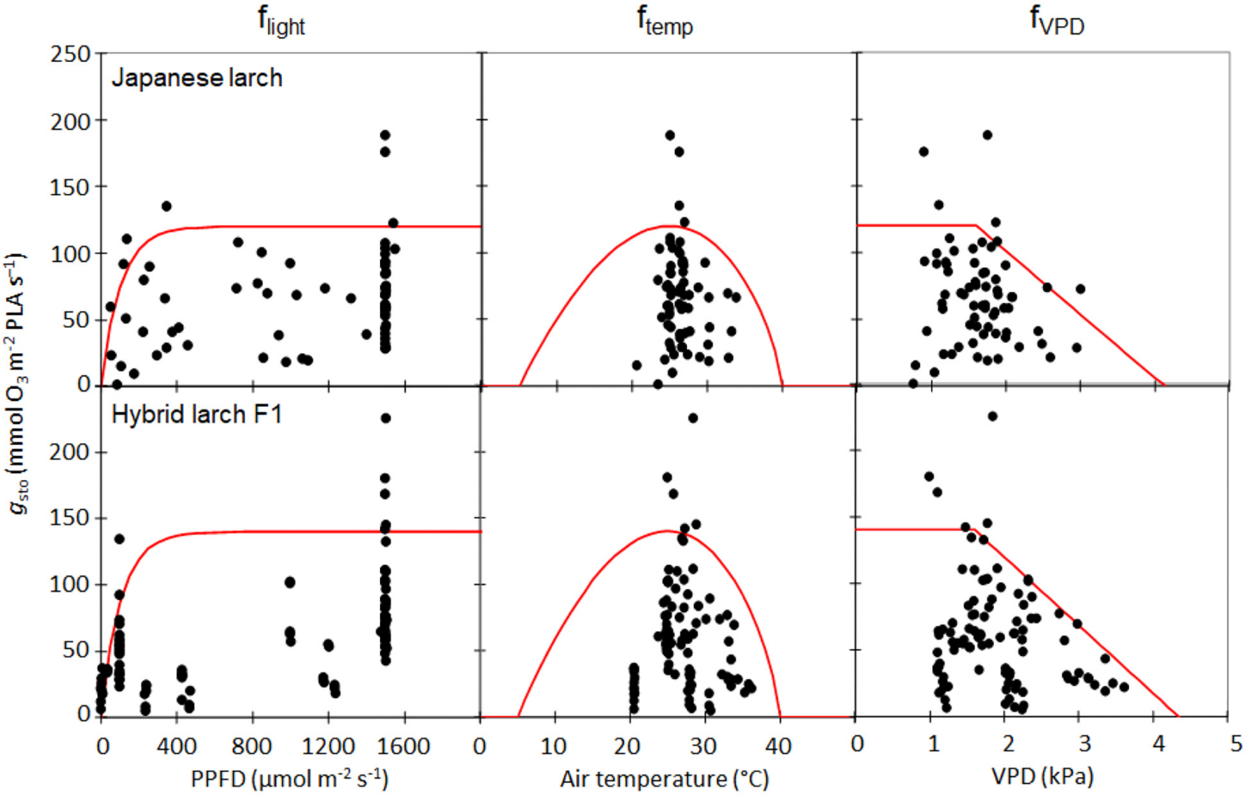

FIGURE 1 | Parameterization of the stomatal conductance (g_{sto}) model for Japanese larch (above) and its hybrid F_1 (below), where f_{light}, f_{temp}, and f_{VPD} are functions of photosynthetically photon flux density (μmol photons m^{-2} s^{-1}), air temperature (T, °C), and vapor pressure deficit (VPD, kPa), respectively. The results of the boundary line analysis are shown in red.

the other hand, $f_{\min}$ was slightly higher in Japanese larch than in hybrid larch F_1.

All the dose–response relationships were significant. When AOT40 was applied, in particular, a higher slope was found for hybrid larch F_1 than for Japanese larch (**Figure 2**).

The CLs calculated on the basis of these dose–response relationships were 2.7 times higher in Japanese larch than in its hybrid F_1 when AOT40 was used, while PODY-based CLs were similar between the two species when using either no *Y* threshold or a *Y* threshold of 1 nmol m^{-2} s^{-1} PLA (**Table 3**).

DISCUSSION

The boreal area in the northern hemisphere where larches are widely distributed is at risk of changes due to the

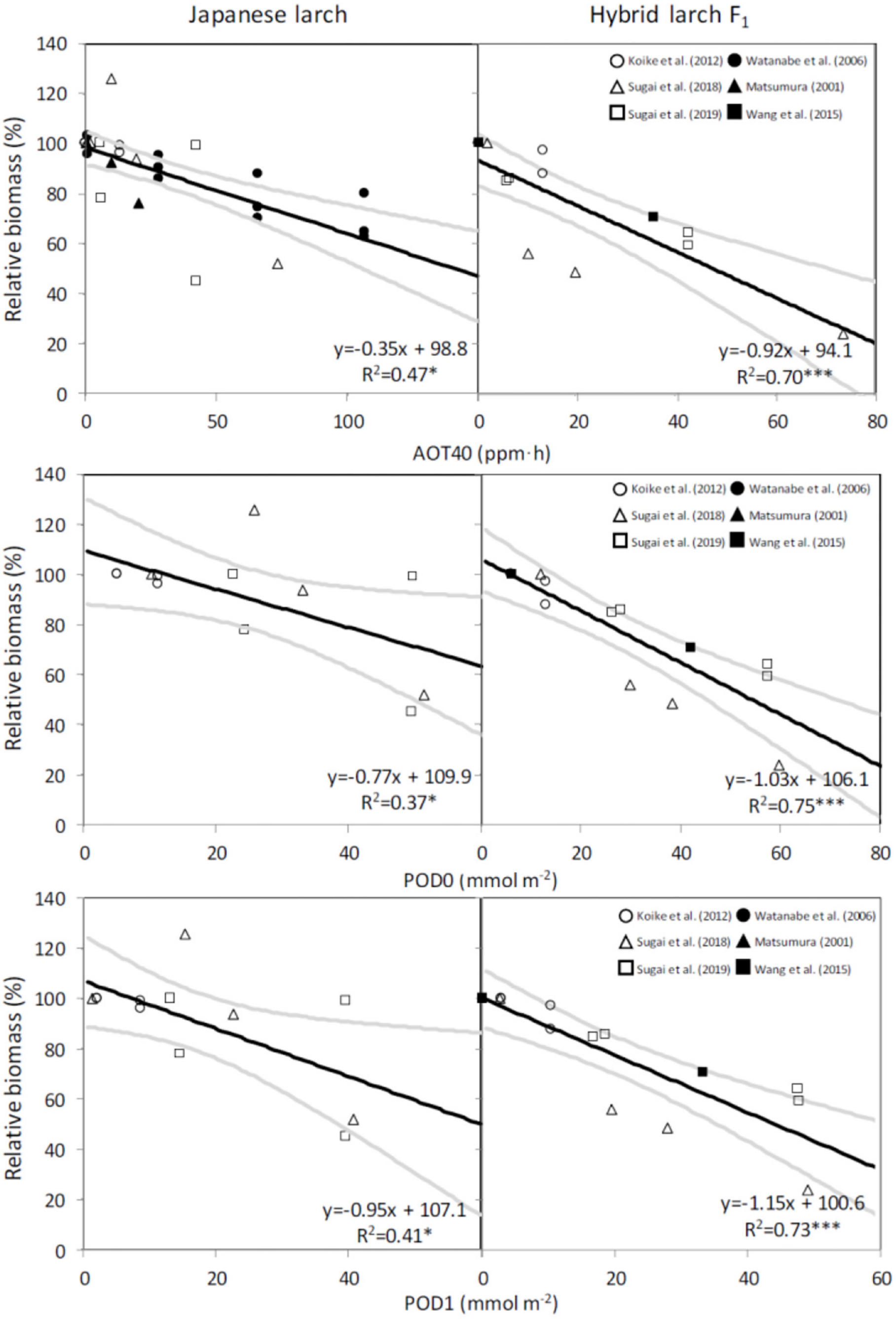

FIGURE 2 | Dose–response relationships for total biomass losses in two species of larch seedlings on the basis of AOT40, POD0, or POD1 in different experiments. Black lines denote the regressions, and gray lines denote the 95% confidence intervals. Asterisks show the level of significance: $^{***}p \leq 0.001$; $^{*}p \leq 0.05$.

TABLE 3 | Critical levels for larch protection from ozone corresponding to a total biomass loss of 2%, 4%, or 5% and based on the dose–response relationships in **Figure 2**.

	Japanese larch			**Hybrid larch F_1**		
	2%	**4%**	**5%**	**2%**	**4%**	**5%**
AOT40 based, ppm h	5.79	11.59	14.48	2.18	4.36	5.45
POD0 based, mmol m^{-2}	9.40	12.00	13.29	10.44	12.38	13.35
POD1 based, mmol m^{-2}	2.21	4.31	5.36	2.45	4.19	5.06

potential O_3 impact on photosynthetic carbon assimilation (Sicard et al., 2017), as estimated by several global atmospheric chemistry transport models and representative concentration pathways emission scenarios. For a realistic estimate of O_3 risks to forests, CLs should be developed for the major forest species or types. Even though natural areas and plantations for larch trees are very wide and larch is a major genus of the forest category defined as boreal deciduous species, PODY-based CLs were not yet available for larch and are suggested here for the first time.

Organismic "sensitivity" may be defined as "the response of an organism (i.e., biological deviation) above or below a homeostatic state (control) of a set of biological traits, after sensing some environmental stress-inducing agents" (Agathokleous and Saitanis, 2020). However, "the organismal predisposition to be inhibited or adversely affected by or die of a xenobiotic," as expressed by "negative (inhibitory or adverse) effects induced by diseases or environmental challenges," is termed susceptibility (Agathokleous and Saitanis, 2020). Hence, organismic susceptibility can be assessed by studying dose/exposure–response relationships and, in particular, by comparing CLs among organisms (Agathokleous and Saitanis, 2020). Since the CLs are affected by the O_3 metric used to develop dose/exposure–response relationships, susceptibility rankings can be different depending on the O_3 metric used (Agathokleous et al., 2019).

So far, CLs have been estimated for a total biomass reduction in either deciduous broadleaf and Mediterranean conifer species (recommended biomass loss: 2%) or non-Mediterranean evergreen conifer species (recommended biomass loss: 4%) (CLRTAP, 2017). As larch is both a deciduous species and a non-Mediterranean conifer species, we decided to calculate the CLs for both the loss thresholds of 2% and 4%. We decided also to calculate the CLs for AOT40, although this metric is known for not being able to assess how much O_3 enters the leaf through the stomata (Paoletti and Manning, 2007). However, it is still the legislative standard in Europe (Directive 2008/50), is used in many other continents (e.g., Agathokleous et al., 2018; Pleijel et al., 2019) because it is simple to calculate, and helps in the comparison with other results in the literature. The AOT40-based CL suggested so far for O_3-susceptible deciduous broadleaves (*F. sylvatica* and *B. pendula*, 5 ppm h for a 5% biomass loss; CLRTAP, 2014, 2017) is similar to that of hybrid larch F_1 (5.45 ppm h for 5% biomass loss), while Japanese larch showed a markedly higher AOT40-based CL corresponding to 5% loss (i.e., 14.48 ppm h). Based on a reanalysis of only two of the papers investigated here (Matsumura, 2001; Watanabe et al., 2006), Yamaguchi et al. (2011) had already suggested high O_3 susceptibility for Japanese larch. In fact, the AOT40-based CLs that they recommended were consistent with those found in our work (i.e., 8–15 ppm h). In addition, our results would suggest a higher susceptibility to O_3 of the hybrid and confirm previous studies where ecophysiological responses of the hybrid were more severely affected by O_3 exposure than those of Japanese larch (Koike et al., 2012; Sugai et al., 2019).

An accurate parameterization of stomatal conductance model is essential for the flux-based O_3 risk assessments (Emberson et al., 2000). For larch, the information of leaf-level g_{sto} parameters was limited, although some studies tried to estimate O_3 uptake at stand level by sap-flow measurements (Nunn et al., 2007) and at forest level by eddy covariance (Finco et al., 2017). Wieser and Havranek (1995) previously reported just stomatal VPD responses to estimate stomatal O_3 uptake in European larch (*Larix decidua*). Our study is the first one to achieve a proper leaf-level parameterization (g_{max}, f_{min}, f_{light}, f_{temp}, and f_{VPD}) in larch trees to develop a flux-based approach. The maximum value of g_{sto} in European larch by Wieser and Havranek (1995) was 150 mmol O_3 m^{-2} PLA s^{-1}, which was comparable to the g_{max} values in our findings. Interestingly, hybrid larch F_1 showed a slightly higher g_{max} (140 vs. 120 mmol O_3 m^{-2} PLA s^{-1} in Japanese larch). As g_{max} is known to play the most important role in determining PODY (Tuovinen et al., 2007), the small difference in g_{max} between the two species translated into a higher stomatal uptake of O_3 by the hybrid at similar AOT40 levels; that is, the higher susceptibility of the hybrid under similar O_3 exposures was due to a higher stomatal uptake. It is well known that fast-growing species with high stomatal conductance are susceptible to O_3 because of an elevated stomatal uptake (Feng et al., 2018; Hoshika et al., 2018a). When the CLs are calculated on a PODY basis, in fact, the two species showed surprisingly similar CLs: 9.40 and 12.00 mmol m^{-2} POD0 and 2.21 and 4.31 mmol m^{-2} POD1 in Japanese larch versus 10.44 and 12.38 mmol m^{-2} POD0 and 2.45 and 4.19 mmol m^{-2} POD1 in the hybrid, for 2% and 4% biomass loss, respectively. These POD1-based values are below the CL recommended for non-Mediterranean trees (5.7 mmol m^{-2}; CLRTAP, 2017), suggesting that these larches are more susceptible to O_3 even when evaluated on the basis of stomatal flux. Different susceptibilities to O_3 injury in the two larch species may be also due to different antioxidant capacities (Di Baccio et al., 2008). Although monoterpene emissions from leaves were preliminarily studied (Mochizuki et al., 2017), the role of antioxidants, secondary metabolites, and other leaf defensive molecules in the response of these two species to O_3 remains elusive.

CONCLUSION

Based on a reanalysis of literature results and new measurements, we conclude that Japanese larch and its hybrid F_1 should be classified as species with considerable O_3 susceptibility as compared to the CLs available so far for other forest species. We also found that AOT40 and PODY can give very different results when assessing a species' susceptibility to O_3. While AOT40 suggested a higher susceptibility of hybrid F_1, PODY did not highlight marked differences between the two species. Future research should clarify the O_3 susceptibility of hybrid clones versus their wild forest species and increase the number of forest species with a species-specific parameterization and PODY-based CLs, especially in the Asian continent. This kind of information is needed for improving our modeling capacities, assessing O_3 risks to local-to-global forests, and transferring this knowledge to environmental policy-makers.

DATA AVAILABILITY STATEMENT

Basic raw data are available with YH (Italy) or TK (Japan).

AUTHOR CONTRIBUTIONS

EP conceptualized the work and wrote the manuscript. EA, TS, and TK provided the data. YH analyzed the data. All authors reviewed the manuscript.

ACKNOWLEDGMENTS

This study is partly supported by the LIFE15 ENV/IT/000183 project MOTTLES and JST-2019 (Grant No. JPMJSC18HB).

REFERENCES

Agathokleous, E., Belz, R. G., Calatayud, V., De Marco, A., Hoshika, Y., Kitao, M., et al. (2019). Predicting the effect of ozone on vegetation via the linear non-threshold (LNT), threshold and hormetic dose-response models. *Sci. Total Environ.* 649, 61–74. doi: 10.1016/j.scitotenv.2018.08.264

Agathokleous, E., Kitao, M., and Kinose, Y. (2018). A review study on O3 phytotoxicity metrics for setting critical levels in Asia. *Asian J. Atmos. Environ.* 12, 1–16. doi: 10.5572/ajae.2018.12.1.001

Agathokleous, E., and Saitanis, C. J. (2020). Plant susceptibility to ozone: a tower of babel? *Sci. Total Environ.* 703:134962. doi: 10.1016/j.scitotenv.2019.134962

Agathokleous, E., Vanderstock, A., Kita, K., and Koike, T. (2017). Stem and crown growth of Japanese larch and its hybrid F_1 grown in two soils and exposed to two free-air O3 regimes. *Environ. Sci. Pollut. Res.* 24, 6634–6647. doi: 10.1007/s11356-017-8401-2

Alonso, R., Elvira, S., Sanz, M. J., Gerosa, G., Emberson, L. D., Bermejo, B., et al. (2008). Sensitivity analysis of a parameterization of the stomatal component of the DO3SE model for *Quercus ilex* to estimate ozone fluxes. *Environ. Pollut.* 155, 473–480. doi: 10.1016/j.envpol.2008.01.032

Anav, A., De Marco, A., Proietti, C., Alessandri, A., Dell'Aquila, A., Cionni, I., et al. (2016). Comparing concentration-based (AOT40) and stomatal uptake (PODy) metrics for ozone risk assessment to European forests. *Glob. Change Biol.* 22, 1608–1627. doi: 10.1111/gcb.13138

Bardak, S., Nemli, G., and Bardak, T. (2019). The quality comparison of particleboards produced from heartwood and sapwood of European Larch. *Maderas* 21:19.

Bičárová, S., Sitková, Z., Pavlendová, H., Fleisher, P. Jr., Fleisher, P. Sr., and Bytnerowicz, A. (2019). The role of environmental factors in ozone uptake of *Pinus mugo* Turra. *Atmos. Pollut. Res.* 10, 283–293. doi: 10.1016/j.apr.2018.08.003

Braun, S., Schindler, C., and Leuzinger, S. (2010). Use of sap flow measurements to validate stomatal functions for mature beech (*Fagus sylvatica*) in view of ozone uptake calculations. *Environ. Pollut.* 158, 2954–2963. doi: 10.1016/j.envpol.2010.05.028

Büker, P., Feng, Z., Uddling, J., Briolat, A., Alonso, R., Braun, S., et al. (2015). New flux based dose-response relationships for ozone for European forest tree species. *Environ. Pollut.* 206, 163–174. doi: 10.1016/j.envpol.2015.06.033

Büker, P., Morrissey, T., Briolat, A., Falk, R., Simpson, D., Tuovinen, J.-P., et al. (2012). DO3SE modelling of soil moisture to determine ozone effects to forest trees. *Atmos. Chem. Phys.* 12, 5537–5562. doi: 10.5194/acp-12-5537-2012

Chang, K.-L., Petropavlovskikh, I., Cooper, O. R., Schultz, M. G., and Wang, T. (2017). Regional trend analysis of surface ozone observations from monitoring networks in eastern North America, Europe and East Asia. *Elementa Sci. Anthropocene* 5:50. doi: 10.1525/elementa.243

CLRTAP, (2014). *Mapping Critical Levels for Vegetation, Chapter III of Manual on Methodologies and Criteria for Modelling and Mapping Critical Loads and Levels and Air Pollution Effects, Risks and Trends*. Geneva: UNECE.

CLRTAP, (2017). *Mapping Critical Levels for Vegetation, Chapter III of Manual on Methodologies and Criteria for Modelling and Mapping Critical Loads and Levels and Air Pollution Effects, Risks and Trends*. Geneva: UNECE.

De Marco, A., Sicard, P., Fares, S., Tuovinen, J.-P., Anav, A., and Paoletti, E. (2016). Assessing the role of soil water limitation in determining the Phytotoxic Ozone Dose (PODY) thresholds. *Atmos. Environ.* 147, 88–97. doi: 10.1016/j.atmosenv.2016.09.066

De Marco, A., Sicard, P., Vitale, M., Carriero, G., Renou, C., and Paoletti, E. (2015). Metrics of ozone risk assessment for Southern European forests: canopy moisture content as a potential plant response indicator. *Atmos. Environ.* 120, 182–190. doi: 10.1016/j.atmosenv.2015.08.071

Di Baccio, D., Castagna, A., Paoletti, E., Sebastiani, L., and Ranieri, A. (2008). Could the differences in O_3 sensitivity between two poplar clones be related to a difference in antioxidant defense and secondary metabolic response to O3 influx? *Tree Physiol.* 28, 1761–1772. doi: 10.1093/treephys/28.12.1761

Dusart, N., Gérard, J., Le Thiec, D., Collignon, C., Jolivet, Y., and Vaultier, M. N. (2019). Integrated analysis of the detoxification responses of two Euramerican poplar genotypes exposed to ozone and water deficit: focus on the ascorbate-glutathione cycle. *Sci. Total Environ.* 651, 2365–2379. doi: 10.1016/j.scitotenv.2018.09.367

Emberson, L. D., Ashmore, M. R., Cambridge, H. M., Simpson, D., and Tuovinen, J. P. (2000). Modelling stomatal ozone flux across Europe. *Environ. Pollut.* 109, 403–413.

Feng, Z., Büker, P., Pleijel, H., Emberson, L., Karlsson, P. E., and Uddling, J. (2018). A unifying explanation for variation in ozone sensitivity among woody plants. *Glob. Change Biol.* 24, 78–84. doi: 10.1111/gcb.13824

Feng, Z., De Marco, A., Anav, A., Gualtieri, M., Sicard, P., Tian, H., et al. (2019a). Economic losses due to ozone impacts on human health, forest productivity and crop yield across China. *Environ. Int.* 131:104966. doi: 10.1016/j.envint.2019.104966

Feng, Z., Shang, B., Gao, F., and Calatayud, V. (2019b). Current ambient and elevated ozone effects on poplar: a global meta-analysis and response relationships. *Sci. Total Environ.* 654, 832–840. doi: 10.1016/j.scitotenv.2018.11.179

Finco, A., Marzuoli, R., Chiesa, M., and Gerosa, G. (2017). Ozone risk assessment for an Alpine larch forest in two vegetative seasons with different approaches: comparison of POD1 and AOT40. *Environ. Sci. Pollut. Res.* 24, 26238–26248. doi: 10.1007/s11356-017-9301-1

Hoshika, Y., Carrari, E., Zhang, L., Carriero, G., Pignatelli, S., Fasano, G., et al. (2018a). Testing a ratio of photosynthesis to O_3 uptake as an index for assessing O3-induced foliar visible injury in poplar trees. *Environ. Sci. Pollut. Res.* 25, 8113–8124. doi: 10.1007/s11356-017-9475-6

Hoshika, Y., Fares, S., Gruening, C., Goded, I., De Marco, A., Sicard, P., et al. (2017). Stomatal conductance models for ozone risk assessment at canopy level in two Mediterranean evergreen forests. *Agric. Forest Meteorol.* 234, 212–221. doi: 10.1016/j.agrformet.2017.01.005

Hoshika, Y., Moura, B. B., and Paoletti, E. (2018b). Ozone risk assessment in three oak species as affected by soil water availability. *Environ. Sci. Pollut. Res.* 25, 8125–8136. doi: 10.1007/s11356-017-9786-7

Hoshika, Y., Osada, Y., De Marco, A., Penuelas, J., and Paoletti, E. (2018c). Global diurnal and nocturnal parameters of stomatal conductance in woody plants and major crops. *Glob. Ecol. Biogeogr.* 27, 257–275. doi: 10.1111/geb.12681

Hoshika, Y., Paoletti, E., and Omasa, K. (2012). Parameterization of *Zelkova serrata* stomatal conductance model to estimate stomatal ozone uptake in Japan. *Atmos. Environ.* 55, 271–278.

Hu, E., Gao, F., Xin, Y., Jia, H., Li, K., Hu, J., et al. (2015). Concentration- and flux-based ozone dose-response relationships for five poplar clones grown in North China. *Environ. Pollut.* 207, 21–30. doi: 10.1016/j.envpol.2015.08.034

Kita, K., Fujimoto, T., Uchiyama, K., Kuromaru, M., and Akutsu, H. (2009). Estimated amount of carbon accumulation of hybrid larch in three 31-year-old progeny test plantations. *J. Wood Sci.* 55, 425–434. doi: 10.1007/s10086-009-1064-y

Koike, T., Mao, Q., Inada, N., Kawaguchi, K., Hoshika, Y., Kita, K., et al. (2012). Growth and photosynthetic responses of cuttings of a hybrid larch (*Larix gmelinii* var. *japonica* x *L. kaempferi*) to elevated ozone and/or carbon dioxide. *Asian J. Atmos. Environ.* 2, 104–110.

Lefohn, A. S., Malley, C. S., Smith, L., Wells, B., Hazucha, M., Simon, H., et al. (2018). Tropospheric ozone assessment report: global ozone metrics for climate change, human health, and crop/ecosystem research. *Elementa* 6:28. doi: 10.1525/elementa.279

Li, P., Feng, Z., Catalayud, V., Yuan, X., Xu, Y., and Paoletti, E. (2017). A meta-analysis on growth, physiological, and biochemical responses of woody species to ground-level ozone highlights the role of plant functional types. *Plant Cell Environ.* 40, 2369–2380. doi: 10.1111/pce.13043

Matsumura, H. (2001). Impacts of ambient ozone and/or acid mist on the growth of 14 tree species: an open-top chamber study conducted in Japan. *Water Air Soil Pollut.* 130, 959–964. doi: 10.1007/978-94-007-0810-5_7

Mills, G., Pleijel, H., Malley, C. S., Sinha, B., Cooper, O. R., Schultz, M. G., et al. (2018). Tropospheric ozone assessment report: present-day tropospheric ozone distribution and trends relevant to vegetation. *Elementa* 6:47. doi: 10.1525/elementa.302

Mochizuki, T., Watanabe, M., Koike, T., and Tani, A. (2017). Monoterpene emissions from needles of hybrid larch F_1 (*Larix gmelinii* var. *japonica* × *Larix kaempferi*) grown under elevated carbon dioxide and ozone. *Atmos. Environ.* 148, 197–202. doi: 10.1016/j.atmosenv.2016.10.041

Nunn, A. J., Wieser, G., Metzger, U., Löw, M., Wipfler, P., Häberle, K. H., et al. (2007). Exemplifying whole-plant ozone uptake in adult forest trees of contrasting species and site conditions. *Environ. Pollut.* 146, 629–639. doi: 10.1016/j.envpol.2006.06.015

Paoletti, E. (2007). Ozone impacts on forests. *CAB Rev.* 2:68.

Paoletti, E., and Manning, W. J. (2007). Toward a biologically significant and usable standard for ozone that will also protect plants. *Environ. Pollut.* 150, 85–95. doi: 10.1016/j.envpol.2007.06.037

Pleijel, H., Broberg, M. C., and Uddling, J. (2019). Ozone impact on wheat in Europe, Asia and North America – A comparison. *Sci. Total Environ.* 664, 908–914. doi: 10.1016/j.scitotenv.2019.02.089

Podda, A., Pisuttu, C., Hoshika, Y., Pellegrini, E., Carrari, E., Lorenzini, G., et al. (2019). Can nutrient fertilization mitigate the effects of ozone exposure on an ozone-sensitive poplar clone? *Sci. Total Environ.* 657, 340–350. doi: 10.1016/j.scitotenv.2018.11.459

R Core Team (2018). *R: A Language and Environment for Statistical Computing*. Vienna: R Foundation for Statistical Computing. Available online at: https://www.R-project.org/

Ryu, K., Watanabe, M., Shibata, H., Takagi, K., Nomura, M., and Koike, T. (2009). Ecophysiological responses of the larch species in northern Japan to environmental changes as a base of afforestation. *Landsc. Ecol. Eng.* 5, 99–106. doi: 10.1007/s11355-009-0063-x

Shang, B., Feng, Z., Li, P., Yuan, X., Xu, Y., and Calatayud, V. (2017). Ozone exposure- and flux-based response relationships with photosynthesis, leaf morphology and biomass in two poplar clones. *Sci. Total Environ.* 603-604, 185–195. doi: 10.1016/j.scitotenv.2017.06.083

Sicard, P., Anav, A., De Marco, A., and Paoletti, E. (2017). Projected global tropospheric ozone impacts on vegetation under different emission and climate scenarios. *Atmos. Chem. Phys.* 17, 12177–12196. doi: 10.5194/acp-17-12177-2017

Sicard, P., De Marco, A., Dalstein-Richier, L., Tagliaferro, F., Renou, C., and Paoletti, E. (2016). An epidemiological assessment of stomatal ozone flux-based critical levels for visible ozone injury in Southern European forests. *Sci. Total Environ.* 541, 729–741. doi: 10.1016/j.scitotenv.2015.09.113

Streit, K., Siegwolf, R. T. W., Hagedorn, F., Schaub, M., and Buchman, N. (2014). Lack of photosynthetic or stomatal regulation after 9 years of elevated [CO_2] and 4 years of soil warming in two conifer species at the alpine treeline. *Plant Cell Environ.* 37, 315–326. doi: 10.1111/pce.12197

Sugai, T., Kam, D.-G., Agathokleous, E., Watanabe, M., Kita, K., and Koike, T. (2018). Growth and photosynthetic response of two larches exposed to O_3 mixing ratios ranging from preindustrial to near future. *Photosynthetica* 56, 901–910. doi: 10.1007/s11099-017-0747-7

Sugai, T., Watanabe, T., Kita, K., and Koike, T. (2019). Nitrogen loading increases the ozone sensitivity of larch seedlings with higher sensitivity to nitrogen loading. *Sci. Total Environ.* 663, 587–595. doi: 10.1016/j.scitotenv.2019.01.292

Tuovinen, J.-P., Emberson, L., and Simpson, D. (2009). Modelling ozone fluxes to forests for risk assessment: status and prospects. *Ann. For. Sci.* 66:401. doi: 10.1051/forest/2009024

Tuovinen, J.-P., Simpson, D., Emberson, L., Ashmore, M., and Gerosa, G. (2007). Robustness of modelled ozone exposures and doses. *Environ. Pollut.* 146, 578–586. doi: 10.1016/j.envpol.2006.03.011

Uddling, J., Günthardt-Goerg, M. S., Matyssek, R., Oksanen, E., Pleijel, H., Selldén, G., et al. (2004). Biomass reduction of juvenile birch is more strongly related to stomatal uptake of ozone than to indices based on external exposure. *Atmos. Environ.* 38, 4709–4719. doi: 10.1016/j.atmosenv.2004.05.026

Unsworth, M. H., Heagle, A. S., and Heck, W. W. (1984). Gas exchange in open-top field chambers—II. Resistances to ozone uptake by soybeans. *Atmos. Environ.* 18, 381–385. doi: 10.1016/0004-6981(84)90112-4

Wang, X., Qu, L., Mao, Q., Watanabe, M., Hoshika, Y., Koyama, A., et al. (2015). Ectomycorrhizal colonization and growth of the hybrid larch F_1 under elevated CO_2 and O_3. *Environ. Pollut.* 197, 116–126. doi: 10.1016/j.envpol.2014.11.031

Watanabe, M., Yamaguchi, M., Iwasaki, M., Matsuo, N., Naba, J., Tabe, C., et al. (2006). Effects of ozone and/ or nitrogen load on the growth of *Larix kaempferi*, *Pinus densiflora* and *Cryptomeria japonica* seedlings. *J. Jpn. Soc. Atmos. Environ.* 41, 320–334.

Wieser, G., and Havranek, W. M. (1995). Environmental control of ozone uptake in *Larix decidua* Mill.: a comparison between different altitudes. *Tree Physiol.* 15, 253–258. doi: 10.1093/treephys/15.4.253

Wieser, G., and Havranek, W. M. (1996). Evaluation of ozone impact on mature spruce and larch in the field. *J. Plant Physiol.* 148, 189–194. doi: 10.1016/S0176-1617(96)80313-0

Yamaguchi, M., Kinose, Y., Matsumura, H., and Izuta, T. (2019). Evaluation of O_3 effects on cumulative photosynthetic CO_2 uptake in seedlings of four Japanese deciduous broad-leaved forest tree species based on stomatal O_3 uptake. *Forests* 10:556. doi: 10.3390/f10070556

Yamaguchi, M., Watanabe, M., Matsumura, H., Kohno, Y., and Izuta, T. (2011). Experimental studies on the effects of ozone on growth and photosynthetic activity of Japanese forest tree species. *Asian J. Atmos. Environ.* 5, 65–78. doi: 10.5572/ajae.2011.5.2.065

Zhang, L., Hoshika, Y., Carrari, E., Badea, O., and Paoletti, E. (2018). Ozone risk assessment is affected by nutrient availability: evidence from a simulation experiment under free air controlled exposure (FACE). *Environ. Pollut.* 328, 812–822. doi: 10.1016/j.envpol.2018.03.102

Conflict of Interest: The authors declare that the research was conducted in the absence of any commercial or financial relationships that could be construed as a potential conflict of interest.